UNCLASSIFIED

## AD NUMBER

AD341065

## CLASSIFICATION CHANGES

TO: unclassified

FROM: secret

## LIMITATION CHANGES

TO:

Approved for public release, distribution unlimited

FROM:

Distribution: DoD only: others to Director, Defense Nuclear Agency, Attn: STTI. Washington, DC 20305.

## AUTHORITY

DTRA ltr, 2 Mar 2001; Same.

THIS PAGE IS UNCLASSIFIED

SECRET
RESTRICTED DATA

AD 341065L

DEFENSE DOCUMENTATION CENTER
FOR
SCIENTIFIC AND TECHNICAL INFORMATION
CAMERON STATION, ALEXANDRIA, VIRGINIA

RESTRICTED DATA
SECRET

NOTICE: When government or other drawings, specifications or other data are used for any purpose other than in connection with a definitely related government procurement operation, the U. S. Government thereby incurs no responsibility, nor any obligation whatsoever; and the fact that the Government may have formulated, furnished, or in any way supplied the said drawings, specifications, or other data is not to be regarded by implication or otherwise as in any manner licensing the holder or any other person or corporation, or conveying any rights or permission to manufacture, use or sell any patented invention that may in any way be related thereto.

NOTICE:

THIS DOCUMENT CONTAINS INFORMATION AFFECTING THE NATIONAL DEFENSE OF THE UNITED STATES WITHIN THE MEANING OF THE ESPIONAGE LAWS, TITLE 18, U.S.C., SECTIONS 793 and 794. THE TRANSMISSION OR THE REVELATION OF ITS CONTENTS IN ANY MANNER TO AN UNAUTHORIZED PERSON IS PROHIBITED BY LAW.

341065D

AD NO. 341065

DDC FILE COPY

AIR FORCE
BALLISTIC MISSILE DIVISION
TECHNICAL LIBRARY
Document No. K-507
Copy No. 1

(4) NA

(5) 104 500

SECRET
RESTRICTED DATA

(18) DASA
(19) Rpt. No. WT-1301
(21) Report on
OPERATION REDWING—PROJECT 1.1 [U]

# (6) GROUND SURFACE AIR-BLAST PRESSURE VERSUS DISTANCE (U) (9)

(7) NA
(9) Rpt. for May-Jul 64,

(10) by C.N. Kingery,
C.H. Hoover,
J.H. Keefer.

Ballistic Research Laboratories
Aberdeen Proving Ground, Maryland

(11) 6 May 60,
(12) 114 p.
(13-14) NA
(15-17) NA

"This document contains information affecting the National Defense of the United States within the meaning of the Espionage Laws, Title 18, U. S. C., Section 793 and 794. Its transmission or the revelation of its contents in any manner to an unauthorized person is prohibited by law."

(20) S-RD

RESTRICTED DATA

This document contains restricted data as defined in the Atomic Energy Act of 1954. Its transmittal or the disclosure of its contents in any manner to an unauthorized person is prohibited.

EXCLUDED FROM AUTOMATIC REGRADING: DOD DIR 5200.10 DOES NOT APPLY



SECRET
RESTRICTED DATA

RESTRICTED DATA
SECRET

# FOREWORD

This report presents the final results of one of the projects participating in the military-effect programs of Operation Redwing. Overall information about this and the other military-effect projects can be obtained from WT-1344, the "Summary Report of the Commander, Task Unit 3." This technical summary includes: (1) tables listing each detonation with its yield, type, environment, meteorological conditions, etc.; (2) maps showing shot locations; (3) discussions of results by programs; (4) summaries of objectives, procedures, results, etc., for all projects; and (5) a listing of project reports for the military-effect programs.

RESTRICTED DATA
SECRET

# ABSTRACT

Project 1.1 participated in five shots during Operation Redwing. Participation consisted of the measurement of overpressure and dynamic pressure versus time, with specific objectives for each shot. The self-recording air-blast gages and self-recording dynamic pressure gages developed by the Ballistic Research Laboratories (BRL) were used to measure and record the phenomenon.

Shot Lacrosse afforded an opportunity to instrument a medium yield (37.8 kt) surface burst. Ground surface air-blast gages recorded a precursor type shock wave at a station 1,180 feet from ground zero and a clean or classical type wave at a station 1,950 feet from ground zero. Correlation of air-blast data with Projects 1.2 and 30.2 of Sandia Corporation (SC) electronically recorded blast measurements was excellent.

Shot Cherokee was a high yield (3.8 Mt) air burst. It had the largest instrumentation participation of the series, but unfortunately the device did not detonate over the intended ground zero. This caused the loss of many records and a reduction of the accuracy of many because the range of the pressure transducers at some stations was as much as 40 times greater than the actual pressure measured. A difference in the overpressure and wave shape was noted on records obtained from the man-made islands and those obtained from the reef stations east of Site Charlie. Scaled models of these stations were fired on in the BRL shock tube and, based on these experiments, the difference in wave shape and 20 percent or more degradation in pressure may be attributed to the type gage mount used for the reef stations.

Shot Zuni was the first high yield (3.53 Mt) surface burst that afforded a land-surface blast line from ground zero to the gages. Two blast lines, approximately 180 degrees apart, were instrumented for this shot. One blast line was along the Tare Complex where nonideal (precursor type) shock waves were recorded out as far as 8,300 feet. The second blast line was on Site Uncle where nonideal shock waves were recorded as far out as 9,880 feet.

Participation in Shot Yuma gave an opportunity to record air-blast data from a fractional kiloton (0.188 kt) device detonated from a tower. Basic blast data were recorded which will be used to validate or modify the height of burst curves for use with fractional-kiloton yields.

Shot Inca was the last shot in which Project 1.1 participated. Two blast lines were instrumented on the same island, one over a cleared area and the other over a vegetated area. Records were obtained from both blast lines, but some accuracy was lost because the actual yield (14.8 kt) was more than double the predicted yield (7 kt), and some of the pressure-sensing capsules were overstressed beyond their intended range.

# PREFACE

The excellent advice and guidance of C.W. Lampson, E.E. Minor, and J.J. Meszaros of BRL and of Major H.T. Bingham, Director, Program 1, Weapons Effects Test Division, Field Command, AFSWP, is gratefully acknowledged.

Acknowledgment is extended to: J.I. Randall, Chief of the Instrument Development Section, Explosions Kinetics Branch, and Raymond Blackmer and MSGT E.O. Engel for the design, development and construction of the present transistorized photo initiation circuit and time pulse circuit; D.P. Lefevre for design and supervision of the construction of the modified $p_t$ gage, and Dale Polley for assistance in the above; Frank Clevenger and Bill Campbell for the rehabilitation of the q gages; Ed Wilkes and John Schmidt for the experimental work carried on in developing the prototype differential q gage; and Roger Anderson for his investigation of the sensitivity of the drive motor to shock and establishing a correction for the lag inherent in the start-up time of the motors.

Personnel of the Explosion Kinetics Branch, Terminal Ballistic Laboratory, BRL, who served in a supervisory capacity in the preparation, field operation and data analysis included; C.N. Kingery, Project Officer; C.H. Hoover, Deputy Project Officer; J.J. Meszaros, Administrative Officer; J.H. Keefer, Technical Group Leader; D.P. Lefevre, Technical Group Leader; R.F. Blackmer, Technical Group Leader; R.E. Anderson, Technical Group; and T.F. Stipa, Technical Group.

The primary assignments of certain enlisted military personnel retained at these laboratories included: E.O. Engel, USAF, Electronics; A.F. Clevenger, USA, q gage; and B.S. Campbell, USA, q gage.

# CONTENTS

FOREWORD ---- 4

ABSTRACT ---- 5

PREFACE ---- 6

CHAPTER 1 INTRODUCTION ---- 11

1.1 Objectives ---- 11
1.2 Background ---- 11
1.3 Dynamic Pressure Corrections ---- 12

CHAPTER 2 PROCEDURE ---- 13

2.1 Operations ---- 13
2.2 Instrument Stations ---- 13
2.2.1 Gage Station Types ---- 13
2.2.2 Station Locations ---- 14
2.3 Instrumentation ---- 14
2.3.1 The BRL Pressure-Time ($p_t$) Gage ---- 14
2.3.2 BRL Dynamic-Pressure (q) Gage ---- 15
2.3.3 Blast Line Layouts ---- 16
2.3.4 Method of Calibration ---- 18
2.4 Data Requirements ---- 18

CHAPTER 3 RESULTS ---- 21

3.1 Scaling ---- 21
3.2 Shot Lacrosse ---- 21
3.2.1 Gage Performance ---- 21
3.2.2 Air-Blast Pressure Versus Time ---- 22
3.2.3 Dynamic Pressure ---- 22
3.2.4 Arrival Time, Duration and Impulse ---- 22
3.3 Shot Cherokee ---- 25
3.3.1 Gage Performance ---- 25
3.3.2 Air-Blast Pressure Versus Time ---- 25
3.3.3 Dynamic Pressure ---- 27
3.3.4 Arrival Time, Duration and Impulse ---- 27
3.4 Shot Zuni ---- 27
3.4.1 Gage Performance ---- 31
3.4.2 Air-Blast Pressure Versus Time ---- 32
3.4.3 Dynamic Pressure ---- 32
3.4.4 Arrival Time, Duration and Impulse ---- 35
3.5 Shot Yuma ---- 36
3.5.1 Gage Performance ---- 36
3.5.2 Surface Air-Blast Pressures ---- 36
3.5.3 Dynamic Pressure Measurements ---- 36

3.5.4 Arrival Time, Duration and Impulse ---- 36
3.6 Shot Inca ---- 36
3.6.1 Gage Performance ---- 38
3.6.2 Surface Air-Blast Pressures ---- 39
3.6.3 Dynamic Pressure Measurements ---- 43
3.6.4 Arrival Time, Positive Duration and Total Impulse ---- 43
3.6.5 Orientation Effect on the BRL q Gage ---- 43

CHAPTER 4 DISCUSSION ---- 44

4.1 Surface Air-Blast Data ---- 44
4.1.1 Surface Bursts, Shots Lacrosse and Zuni ---- 44
4.1.2 Air Bursts, Shots Cherokee, Yuma and Inca ---- 44
4.2 Dynamic Pressure Measurements ---- 48
4.2.1 Dynamic Pressure from Surface Bursts, Shots Lacrosse, and Zuni ---- 49
4.2.2 Dynamic Pressure Measurements from Air Bursts, Shots Yuma, Cherokee and Inca ---- 49
4.3 Time of Arrival Measurements ---- 49
4.4 Duration Measurements ---- 49
4.5 Positive Impulse Measurements ---- 52

CHAPTER 5 CONCLUSIONS AND RECOMMENDATIONS ---- 53

5.1 Instrumentation ---- 53
5.2 Air-Blast Parameters ---- 53
5.2.1 Precursors ---- 54
5.2.2 Yield Determination ---- 54
5.2.3 1.6 W Concept ---- 54
5.3 Recommendations ---- 54

APPENDIX A INSTRUMENTATION DESIGN ---- 55

A.1 Introduction ---- 55
A.2 Pressure-Sensing Elements ---- 55
A.2.1 Calibration ---- 55
A.2.2 Recording Blanks ---- 55
A.2.3 Drive Motor ---- 56
A.3 Pressure-Time Gage ---- 58
A.3.1 Mechanical Construction ---- 58
A.3.2 Thermal Initiation ---- 58
A.3.3 Photoelectric Initiation ---- 58
A.3.4 Timing ---- 62
A.3.5 Calibration ---- 63
A.4 Dynamic-Pressure Gage ---- 63
A.5 Gage Performance ---- 63
A.6 Post Operation Gage Examination ---- 65
A.6.1 Record Check ---- 65
A.6.2 Capsule Examination ---- 65
A.6.3 Protective Screen ---- 65
A.6.4 Thermal Initiation Tests ---- 65
A.6.5 Electronic Circuit Tests ---- 66
A.6.6 Drive Motor Tests ---- 66
A.6.7 Motor Start-Up Time ---- 66

APPENDIX B PRESSURE-TIME RECORDS ---- 68

APPENDIX C ISLAND DIFFRACTION RECORDS ---- 109

C.1 Introduction ---- 109
C.2 Scaled Model Studies ---- 109
C.3 Island Configuration ---- 109
C.4 Data Presentation ---- 109

REFERENCES ---- 113

FIGURES

2.1 Type 113 reef station ---- 17
2.2 Type 113 man-made island station ---- 17
2.3 Shot Lacrosse blast-line layout ---- 18
2.4 Shot Cherokee blast-line layout ---- 18
2.5 Shot Zuni blast-line layout ---- 19
2.6 Shot Yuma blast-line layout ---- 19
2.7 Shot Inca blast-line layout ---- 20
2.8 Shot Lacrosse blast-line obstructions ---- 20
3.1 Pressure versus distance, Shot Lacrosse ---- 24
3.2 Dynamic pressure versus distance, Shot Lacrosse ---- 24
3.3 Arrival time and positive duration versus distance, Shot Lacrosse ---- 24
3.4 Impulse versus distance, Shot Lacrosse ---- 24
3.5 Pressure versus distance, Shot Cherokee ---- 26
3.6 Plot of Stations 113.06 and 113.07 ---- 26
3.7 Plot of shock tube record with and without baffle ---- 26
3.8 Comparison of records of pressure versus time from three gages at Station 113.09 ---- 30
3.9 Impulse, arrival time, duration versus distance, Shot Cherokee ---- 31
3.10 Peak overpressure versus distance, Shot Zuni ---- 34
3.11 Corrected peak dynamic pressure versus distance, Shot Zuni ---- 34
3.12 Arrival time and positive duration versus distance, Shot Zuni ---- 35
3.13 Total impulse versus distance, Shot Zuni ---- 35
3.14 Peak overpressure and corrected dynamic pressure, Shot Yuma ---- 38
3.15 Arrival time and positive duration versus distance, Shot Yuma ---- 38
3.16 Impulse versus distance, Shot Yuma ---- 38
3.17 Peak overpressure versus distance, Shot Inca ---- 39
3.18 Corrected peak dynamic pressure versus distance, Shot Inca ---- 39
3.19 Arrival time versus distance, Shot Inca ---- 42
3.20 Positive duration versus distance, Shot Inca ---- 42
3.21 Total impulse versus distance, Shot Inca ---- 42
4.1 A-scaled height of burst, pressure versus distance curves, average surface ---- 47
4.2 A-scaled pressure versus distance, Shot Cherokee ---- 47
4.3 Modified Sachs scaling versus distance, Shot Cherokee ---- 47
4.4 A-scaled pressure versus distance, Shot Yuma ---- 48
4.5 A-scaled corrected peak dynamic pressure versus distance, Shots Lacrosse and Zuni ---- 50
4.6 A-scaled corrected peak dynamic pressure versus distance, Shot Yuma ---- 50
4.7 A-scaled height of burst curves, arrival time versus distance ---- 50
4.8 A-scaled height of burst curves, positive duration versus distance ---- 51
4.9 A-scaled height of burst curves of impulse versus distance ---- 51
4.10 A-scaled height of burst, pressure versus distance curves, good surface ---- 51

4.11 A-scaled peak overpressure versus distance, Shot Inca ---------- 52
4.12 A-scaled peak overpressure versus distance, Shot Inca ---------- 52
5.1 Comparison of Operation Redwing and Operation Castle surface shots with 1.6 kt free-air curve ---------- 53
A.1 Pressure-sensing capsule, old style ---------- 57
A.2 Pressure-sensing capsule, new style ---------- 57
A.3 Haydon motor, showing governor ---------- 57
A.4 Haydon motor, phantom view ---------- 57
A.5 Turntable rotation versus time ---------- 59
A.6 $P_t$ gage, recording side ---------- 59
A.7 $P_t$ gage, incased ---------- 59
A.8 $P_t$ gage, motor drive side ---------- 60
A.9 Close-up of star gear and capsule ---------- 60
A.10 Exploded view of photo-cell assembly ---------- 60
A.11 Schematic diagram of pressure-time electronic circuit ---------- 61
A.12 Electronic components of the photo-initation circuit ---------- 62
A.13 Photo-initiation battery and relay ---------- 62
A.14 Assembled view of q gage ---------- 64
A.15 Exploded view of q gage ---------- 64
A.16 q-gage shock-tube record, underdamped ---------- 64
A.17 q-gage shock-tube record, overdamped ---------- 64
C.1 Structure and gage locations, Man-Made Island No. 1 ---------- 110
C.2 Structure and gage locations, Man-Made Island No. 2 ---------- 110
C.3 Structure and gage locations, Man-Made Island No. 3 ---------- 111

TABLES

2.1 Station Locations, Shot Cherokee ---------- 14
2.2 Station Locations, Shot Yuma ---------- 14
2.3 Station Locations, Shot Zuni ---------- 15
2.4 Station Locations, Shot Inca ---------- 15
2.5 Station Locations, Shot Lacrosse ---------- 16
3.1 Scaling Factors ---------- 22
3.2 Air-Blast Data, Shot Lacrosse ---------- 23
3.3 Air-Blast Data, Shot Cherokee ---------- 28
3.4 Average Plotted Values from Shot Cherokee ---------- 30
3.5 Air-Blast Data, Shot Zuni ---------- 33
3.6 Air-Blast Data, Shot Yuma ---------- 37
3.7 Air-Blast Data, Shot Inca ---------- 40
3.8 Dynamic Pressure Data, Shot Inca ---------- 41
4.1 A-Scaled Air-Blast Data, Shot Lacrosse ---------- 45
4.2 A-Scaled Air-Blast Data, Shot Zuni ---------- 45
4.3 A-Scaled Air-Blast Data, Shot Cherokee ---------- 45
4.4 Modified Sachs Scaling, Shot Cherokee ---------- 46
4.5 A-Scaled Air-Blast Data, Shot Yuma ---------- 46
4.6 A-Scaled Air-Blast Data, Shot Inca ---------- 46
A.1 Capsule Specifications ---------- 56
A.2 Gage Performance ---------- 63
C.1 Blast Diffraction Data ---------- 109

# Chapter 1
# INTRODUCTION

## 1.1 OBJECTIVES

General objectives of Project 1.1 were: (1) to instrument certain shots during Operation Redwing and obtain basic information of the propagation of blast waves over different surfaces from various yields and heights of burst; and (2) supply measurements of overpressure and dynamic pressure at certain locations in support of other projects.

The specific objective of Project 1.1 was to determine the pressure versus time and dynamic pressure versus time variations with distance from ground zero on five shots during Operation Redwing. These shots were: (1) Lacrosse, a medium kiloton-range surface burst; (2) Cherokee, a megaton-range air burst; (3) Zuni, a megaton-range surface burst; (4) Yuma, a fractional kiloton-range tower shot; and (5) Inca, a small kiloton-range tower shot.

Project 1.1 had the prime responsibility for basic air-blast instrumentation on Shots Cherokee, Zuni and Yuma. On Shots Lacrosse and Inca the project participated to provide back-up instrumentation for the electronic recording system used by Projects 1.2, 1.10, and 30.2 of Sandia Corporation (SC).

The secondary specific objectives of Project 1.1 were to (1) record the diffraction phenomenon over the man-made islands for Project 3.1; (2) furnish dynamic pressure measurements to Project 1.5 for evaluation of vehicle damage; and (3) furnish water pressure measurements to Project 1.9 for wave height studies from Shot Zuni.

## 1.2 BACKGROUND

Since the advent of devices having an equivalent blast yield in the megaton range, there has been a need for more data on the air-blast phenomenology generated by the detonation of these devices. The first complete air-blast instrumentation attempted for a multi-megaton device was on Operation Castle (Reference 1). While the objectives of the Operation Castle project were carried out successfully, the operation left much to be desired in the study of blast wave propagation from high-yield devices. One prime need was an air drop of a high-yield device in the megaton range. This was needed to check the partitioning of blast energy, scaling laws, and height of burst curves which have been established from multi-kiloton yields detonated primarily from tower shots and air drops. To supplement existing data, Project 1.1 instrumented Shot Cherokee, an air drop with a predicted yield of 4.5 Mt.

Surface bursts at NTS had been limited to one detonation of approximately 1 kt. The reason for such limitation was the danger of fallout and the residual contamination which restricts the use of that test area for future shots. At the EPG the greater majority of shots had been surface bursts over water as well as land. Although there have been more surface bursts at the EPG, air-blast instrumentation has been limited because of the adverse conditions under which measurements had to be made. Therefore, a need existed for more blast data from surface bursts in the megaton range as well as the medium kiloton range. There were some nonideal wave forms recorded at the close-in stations on Shot 6 of Operation Castle (Reference 2). To further investigate this, Project 1.1 instrumented a blast line on Shot Lacrosse, (a surface burst which had a

predicted yield of from 25 to 50 kt). On Shot Zuni, (a surface burst which had a predicted yield of 1 to 3 Mt), two blast lines were instrumented, one along the Tare Complex and the other on Site Uncle.

The weapons effects test shot on Operation Teapot had many objectives, one of which was a study of the propagation of a shock wave over different surfaces such as asphalt, water and desert. There was a need for data concerning the propagation of a precursor over a natural vegetated surface, for comparison with data obtained over such artificial surfaces. Project 1.1 participated in Shot Inca along two blast lines to supplement the data recorded by Project 1.10. One blast line was along a cleared area, while the other was along a vegetated area.

## 1.3 DYNAMIC PRESSURE CORRECTIONS

At a meeting of the nuclear blast-measurement agencies called early in 1958, various agencies considered the problem of dynamic-pressure corrections and agreed upon a common course of action.

A standardized nomenclature was also established as shown below.

$q_c = (P_p - P_s)$

$M = u/c$ = local free stream Mach number

$P_0$ = ambient preshock static overpressure

$\Delta p$ = free stream static overpressure

$\Delta p_p$ = total head pitot overpressure

Primes are used to denote uncorrected as-read gage values.

To correct the measured data as agreed upon at the meeting a code, or calculation procedure, was established for one of the BRL electronic computers (EDVAC) to apply the appropriate correction. These corrections are necessary to obtain the free stream value of dynamic pressure.

The first step in applying the gage correction, Mach flow correction, and compressibility correction is to calculate the primary Mach number (M) from the following equations.

For $M < 1$

$$\frac{\Delta p'_p + P_0}{\Delta p' + P_0} = \left(1 + \frac{\gamma - 1}{2} M^2\right)^{\frac{\gamma}{\gamma - 1}} \tag{1.1}$$

For $M < 1$

$$\frac{\Delta p'_p + P_0}{\Delta p' + P_0} = \left[\frac{\left(\frac{\gamma + 1}{2} M^2\right)^{\gamma}}{\left(\frac{2}{\gamma + 1} M^2 - \frac{\gamma - 1}{\gamma + 1}\right)}\right]^{\frac{1}{\gamma - 1}} \tag{1.2}$$

A gage similar to the BRL dynamic pressure gage has been calibrated in the Cornell Wind Tunnel at various Mach numbers (Reference 2). The primary Mach number is used to apply the wind tunnel calibration factors to the total head and side-on q-gage measurements. When these corrections are applied, new values of $(\Delta p_p + P_0)$ and $(\Delta p + P_0)$ are obtained and consequently a new value of M is calculated.

Since the dynamic pressure $q_c$ is related to the side-on overpressure and Mach number the new value of M is used in the following equation.

$$q_c = \frac{\gamma(\Delta p + P_0) M^2}{2} \tag{1.3}$$

The peak value of $q_c$ has been tabulated in Tables 3.2, 3.5, 3.6 and 3.8 and plotted in all curves showing peak dynamic pressure versus distance.

# Chapter 2
# PROCEDURE

## 2.1 OPERATIONS

The measurement of air blast from a large-yield device poses a serious problem because it necessitates the establishment of blast lines which are sometimes as much as 8 miles in length. It is impractical to attempt this with electronic instrumentation, which requires shelters, cables, and ditches. Self-initiating, self-recording gages, that can be installed from one to several days before a shot and operate successfully at shot time, solve this problem. The gages used by Project 1.1, which had been field tested on previous operations (References 1 and 3), met these requirements. All stations were project installed with the exception of the 113-type station (See Section 2.3.1). The overall project was flexible, since, in the event of cancellation or relocation of a shot, a new blast line could be reinstrumented in a few days by project personnel.

Project 1.1 participated in five shots during the operation. The spread in yield was from 0.188 kt to 3.8 Mt, and the spread in height of burst was from 9 feet to 4,320 feet.

Some shots were development devices with wide ranges of predicted yields. Therefore, it was difficult to design blast lines that would assure measurement of all desired information. Where there was a wide range in expected yield for a particular shot, predicted pressure distance curves were made for both extremes in yield; and a blast line was established based on an average of the two. Gage ranges were chosen so there would be no overstressing of the recording element in event the upper yield limit was realized.

TM 23-200, revised edition, 1 June 1955 (Reference 4), was used to predict pressures at various distances from ground zero on all shots. During the operational phase of the tests, better yield values were established on some shots, and it was necessary to change gage ranges, since ground distances had already been established.

## 2.2 INSTRUMENT STATIONS

A total of 55 Project 1.1 gage stations were instrumented during the operation. Forty-two were installed by project personnel. In addition to the 55 project stations, 9 were installed for Project 1.9 water wave studies, and 12 for Project 3.1 diffraction studies. The station types and locations for all shots are listed in Tables 2.1 through 2.5.

2.2.1 Gage Station Types. The three different number-series of stations used during the operation are described as follows:

1. Series 113, Contractor Stations, All blast line stations for Shot Cherokee, with the exception of the one on Site Charlie, were contractor installed. Stations 113.01 through 113.06 were installed on the reef between Sites Charlie and Dog, while Stations 113.07 through 113.11 were installed on man-made islands on Sites Dog and Able. The two types used are shown in Figures 2.1 and 2.2.

2. Series 114, Project-Installed Pressure-Time Stations. The stations installed by project personnel consisted of a base plate mounted on the end of a 3-inch pipe approximately 9 inches long. The gage case was mounted to the other end of the pipe, and the assembly buried with the top of the gage flush with the surface. The surface material removed, in order to place the gage, was packed in around the gage and smoothed flush with the gage.

3. Series 115, Project-Installed Pressure-Time and q Station. The only difference in the Series 114 and 115 stations was the addition of a q gage to measure dynamic pressure. The q



SECRET

gage mount was the same type used on Operation Teapot. A survey stake was furnished by the contractor, while installation and material were furnished by the project. The Project 1.1 q gages were installed with the center line of the gage 3 feet above the surface, with the exception of the reef stations.

4. Series 112, Project-Installed Pressure-Time Station. The pressure-time station located at intended ground zero on Site Charlie was given a 112.01 number, although there was no difference in this station and Series 114.

Gages furnished and installed for Projects 1.5 and 3.1 were of Series 114 or 115.

TABLE 2.1 STATION LOCATIONS, SHOT CHEROKEE

| Station Number | Site | Distance from GZ | | Coordinates | | Type and Number of Measurements | |
|---|---|---|---|---|---|---|---|
| | | Intended | Actual | North | East | | |
| | | ft | ft | | | $p_t$ | q |
| 112.01 | Charlie | 0 | 19,143 | 172,172 | 82,082 | 2 | — |
| 113.01 | Reef | 3,500 | 17,500 | 171,277 | 85,465 | 3 | 1 |
| 113.02 | between | 5,000 | 16,970 | 170,894 | 86,918 | 3 | 1 |
| 113.03 | Charlie | 9,000 | 16,162 | 169,872 | 90,783 | 3 | 1 |
| 113.04 | and | 13,000 | 16,323 | 168,851 | 94,650 | 3 | 1 |
| 113.05 | Dog | 16,000 | 17,068 | 168,084 | 97,551 | 3 | 1 |
| 113.06 | | 19,000 | 18,282 | 167,318 | 100,451 | 3 | 1 |
| 113.07 | man- | 20,455 | 19,349 | 166,564 | 101,753 | 3 | 1 |
| 113.08 | made | 23,955 | 20,482 | 166,514 | 105,359 | 3 | 1 |
| 113.09 | island | 28,955 | 23,512 | 166,401 | 110,456 | 3 | 1 |
| 113.10 | Dog | 35,580 | 26,453 | 166,496 | 117,561 | 3 | 1 |
| 113.11 | Able | 12,000 | 30,711 | 167,515 | 71,022 | 3 | 1 |

2.2.2 Station Locations. The station location, ground distances, coordinates, types, and number of gages are shown in Tables 2.1 and 2.5. The column headed $p_t$ indicates pressure-time measurements, and q indicates dynamic pressure-time measurements. The blast line layouts for the various shots are shown in Figures 2.3 through 2.7.

TABLE 2.2 STATION LOCATIONS, SHOT YUMA

| Station Number | Site | Distance from Ground Zero | Coordinates | | Type and Number of Measurements | |
|---|---|---|---|---|---|---|
| | | | North | East | | |
| | | ft | | | $p_t$ | q |
| 114.01 | Sally | 0 | 130,603 | 112,154 | 2 | — |
| 115.01 | Sally | 150 | 130,520 | 112,280 | 3 | 1 |
| 115.02 | Sally | 250 | 130,460 | 112,360 | 2 | 1 |
| 115.03 | Sally | 361 | 130,410 | 112,460 | 2 | 1 |
| 115.04 | Sally | 401 | 130,400 | 112,500 | 2 | 1 |
| 114.02 | Sally | 500 | 130,310 | 112,560 | 2 | — |
| 115.05 | Sally | 603 | 130,260 | 112,650 | 1 | 1 |
| 114.03 | Sally | 602 | 130,140 | 112,810 | 1 | — |
| 114.04 | Sally | 1,000 | 130,[illegible]0 | 112,980 | 2 | — |

## 2.3 INSTRUMENTATION

All gages used to accomplish the objectives were direct-recording type instruments. They were essentially the same gages as used on Operation Teapot (Reference 3), but with slight modifications. The modifications and details concerning the gages are presented in Appendix A.

2.3.1 The BRL Pressure-Time ($p_t$) Gage. The BRL gage was simple in principle and operation. It was battery powered and could be initiated by the light or heat from a fireball. The ini-

tiation circuit started the turntable and a coated record disk to rotate at a constant rpm establishing a time base. When the shock wave arrived, the pressure entered a sensitive capsule, causing it to expand. The distance it expanded was a function of pressure and was recorded on the record disk by means of a stylus scratching the coating from the disk. The width of the record trace scratched by the stylus was approximately 0.00025 inch.

TABLE 2.3 STATION LOCATIONS, SHOT ZUNI

| Station Number | Site | Distance from Ground Zero | Coordinates | | Type and Number of Measurements | |
|---|---|---|---|---|---|---|
| | | | North | East | | |
| | | ft | | | $P_t$ | q |
| 114.05 | Sugar | 3,141 | 100,370 | 113,443 | 2 | — |
| 114.06 | Sugar | 5,089 | 100,713 | 115,366 | 1 | — |
| 115.06 | Sugar | 5,685 | 100,693 | 115,970 | 2 | 1 |
| 114.07 | Roger | 7,004 | 100,942 | 117,269 | 1 | — |
| 115.07 | Roger | 8,292 | 100,978 | 118,569 | 2 | 1 |
| 115.08 | Peter | 10,392 | 101,160 | 120,659 | 1 | 1 |
| 114.08 | Peter | 11,693 | 101,596 | 121,913 | 2 | — |
| 115.09 | Oboe | 13,796 | 102,470 | 123,910 | 1 | 1 |
| 114.09 | Oboe | 16,511 | 103,600 | 126,457 | 2 | — |
| 114.10 | Uncle | 4,458 | 98,945 | 106,018 | 2 | — |
| 115.10 | Uncle | 5,078 | 98,756 | 105,427 | 1 | 1 |
| 114.11 | Uncle | 5,907 | 98,503 | 104,637 | 1 | — |
| 115.11 | Uncle | 6,849 | 98,216 | 103,744 | 2 | 1 |
| 115.12 | Uncle | 9,880 | 97,300 | 100,860 | 2 | 1 |
| 156.01 | Uncle | 10,018 | 99,650 | 100,304 | 1 | — |
| 156.02 | Uncle | 9,917 | 99,754 | 100,409 | 1 | 2 |
| 114.41 | Nan | — | — | — | 1 | — |

2.3.2 BRL Dynamic Pressure (q) Gage. The BRL q gage used the same principle of recording pressure versus time as the $p_t$ gage. The difference was the use of two pressure sensing elements and two pressure inlet holes. The gage was a pitot tube with the total or stagnation pressure inlet hole in the nose and the side-on pressure inlet hole in the top of the body approxi-

TABLE 2.4 STATION LOCATIONS, SHOT INCA

| Station Number | Site | Distance from Ground Zero | Coordinates | | Type and Number of Measurements | |
|---|---|---|---|---|---|---|
| | | | North | East | | |
| | | ft | | | $P_t$ | q |
| 115.13 | Pearl | 900* | 133,202 | 106,165 | 2 | 1 |
| 115.14 | Pearl | 900 | 133,060 | 106,060 | 2 | 1 |
| 115.15 | Pearl | 1,114* | 133,537 | 106,414 | 2 | 1 |
| 115.16 | Pearl | 1,114 | 132,850 | 106,175 | 2 | 1 |
| 115.17 | Pearl | 1,310* | 133,452 | 106,607 | 2 | 1 |
| 115.18 | Pearl | 1,310 | 132,797 | 106,379 | 2 | 1 |
| 115.19 | Pearl | 1,450* | 133,240 | 106,728 | 2 | 1 |
| 115.20 | Pearl | 1,450 | 132,763 | 106,524 | 2 | 1 |
| 115.21 | Pearl | 1,600* | 133,340 | 106,887 | 2 | 1 |
| 115.27 | Pearl | 1,600 | 132,692 | 106,656 | 2 | 1 |
| 115.28 | Pearl | 2,130 | 132,760 | 107,290 | 1 | — |

* Stations in uncleared vegetated area.

mately 4 diameters from the nose hole. To obtain dynamic pressure versus time, the record of side-on pressure versus time was subtracted from the record of total pressure versus time. These uncorrected records are presented in Appendix B. The correction factors as given in Section 1.3 were applied to the total and side-on records and the corrected peak dynamic pressures are listed in Tables 3.2, 3.5, 3.6 and 3.8.



SECRET

2.3.3 Blast Line Layouts. The Shot Lacrosse ground zero was on an artificial island at the end of a causeway about 450 feet off the north end of Site Yvonne. The location of the BRL instrument stations is shown in Figure 2.3. This shot was heavily instrumented for parameters other than air blast. The extensive pipe array for diagnostic measurements is shown in Figure 2.8. Some of the stations were in line of sight of the device cab at ground zero while others were partially shielded because of an earth berm (10 to 12 feet above grade). The berm was located in the middle of the island and extended from ground zero to approximately 2,600 feet. The tabulation of data concerning station numbers, locations and other pertinent information is presented in Table 2.1. It should be noted that all stations on this shot were located on one island.

Intended air zero for Shot Cherokee was Site Charlie. The blast line to the east consisted of six reef stations, one station each on the man-made islands and one on Site Dog. One station was established on Site Able, which was southwest of the target island. The blast-line layout is shown in Figure 2.4. All data concerning the station and gage layout are listed in Table 2.2. The expected range of pressures as predicted from TM 23-200 (Reference 4) was from 200 psi

TABLE 2.5 STATION LOCATIONS, SHOT LACROSSE

| Station Number | Site | Distance from Ground Zero | Coordinates | | Type and Number of Measurements | |
|---|---|---|---|---|---|---|
| | | | North | East | | |
| | | ft | | | $P_t$ | q |
| 114.15 | Yvonne | 1,180 | 105,705 | 124,500 | 2 | — |
| 115.22 | Yvonne | 1,590 | 105,290 | 124,640 | 1 | 1 |
| 115.23 | Yvonne | 1,950 | 104,980 | 124,990 | 1 | 1 |
| 115.24 | Yvonne | 2,500 | 104,566 | 125,499 | 2 | 1 |
| 114.16 | Yvonne | 2,770 | 104,356 | 125,646 | 2 | — |
| 115.25 | Yvonne | 3,350 | 104,060 | 126,330 | 2 | — |
| 115.31 | Yvonne | 3,900 | 103,570 | 126,600 | 1 | 1 |
| 114.18 | Yvonne | 4,387 | 103,060 | 126,900 | 1 | — |
| 115.26 | Yvonne | 5,200 | 102,431 | 127,199 | 2 | 1 |
| 114.19 | Yvonne | 7,050 | 100,750 | 128,000 | 1 | — |

to 1 psi and the stations were located to give the best coverage for this span of pressures. Each of the 113 series stations consisted of three $p_t$ gages and one q gage. Ground zero station on Site Charlie had two $p_t$ gages. At station 113.01, a distance of 3,500 feet, it was planned to measure surface overpressure versus time and dynamic pressure versus time in the regular reflection region. While at station 113.02, located 5,000 feet from ground zero, it was planned to measure surface overpressure versus time and dynamic pressure versus time in the early phase of the Mach reflection region.

The blast lines for Shot Zuni were established on the basis of a surface burst with a predicted yield of 3 to 5 Mt. One blast line extended to the east along the Tare Complex, a distance of 16,500 feet. Although the shock front had to travel over water part of the time to reach some of the stations, it was considered a ground-surface blast line. The second blast line, to the west, started at the eastern tip of Site Uncle, which meant the shock front would travel almost 4,500 feet across the deep water channel before reaching the first station. The blast line continued in a westward direction ending at a distance of 9,880 feet. With this unique blast line the shock front would travel the first 4,500 feet over water while the remaining portion or approximately 5,400 feet would be over a heavily vegetated surface. The blast-line layout is shown in Figure 2.5 and the station distances are listed in Table 2.3.

The blast-line layout for Shot Yuma was unusual in that it was only 1,000 feet long. The distances were established from a height of burst of 200 feet and a predicted yield of 0.2 kt. The line was on one island and the surface was soft sand with sparse tufts of grass. The stations and distances are listed in Table 2.4, while the layout is shown in Figure 2.6.

Two blast lines were established for Shot Inca. One line consisted of five stations along a vegetated surface and the other line consisted of five stations at similar distances along a cleared surface. The cleared surface was a soft sand surface, while the vegetation consisted of some vine (Ipomea) and grass cover, plus almost complete coverage with broadleaf shrubs (Scaevola)

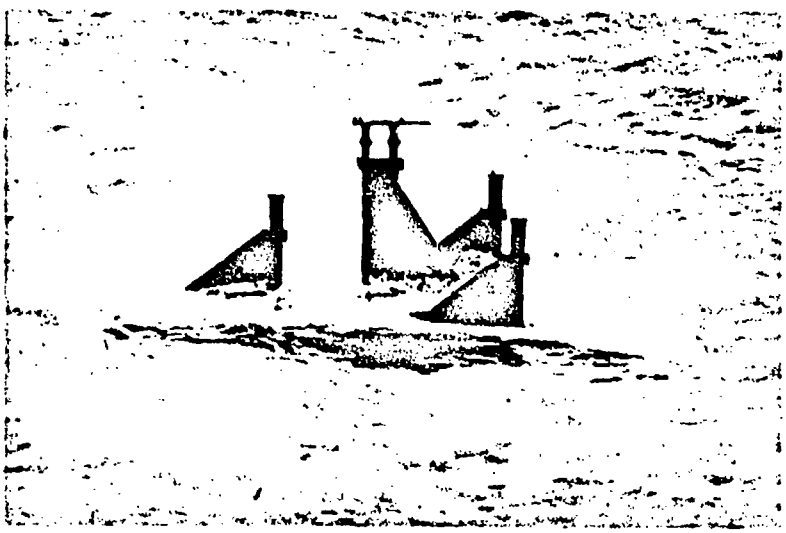

Figure 2.1 Type 113 reef station.

10 to 15 feet high. The experiment was designed for a 7 kt yield at a height of burst of 200 feet. The blast-line layout is shown in Figure 2.7. The pertinent details concerning the blast lines are listed in Table 2.5. A special station was installed on Site Olive to measure the effect of orientation on the BRL q gage. Four gages were installed at the same distance with the axis of

Figure 2.2 Type 113 man-made island station.

the center line of the gage at various angles from zero orientation. One gage, which was considered the standard, was oriented with the nose pointing at ground zero (0 degrees). A second q gage was oriented with the axis 32 degrees from ground zero, while a third gage was 41 degrees and the fourth gage was 50 degrees. This station was located at 2,640 feet, where a classical wave shape was expected.

2.3.4 Method of Calibration. All pressure sensing elements were calibrated at the factory and BRL was furnished with a tabulation of the 50, 100 and 200 percent values on those up to the 0 to 50 psi range. The 0 to 100 psi range was tabulated at 50, 85, 100 and 170 percent while the 0 to 150 psi range was tabulated at the 50, 80, 100 and 160 percent. The 0 to 200 psi range was

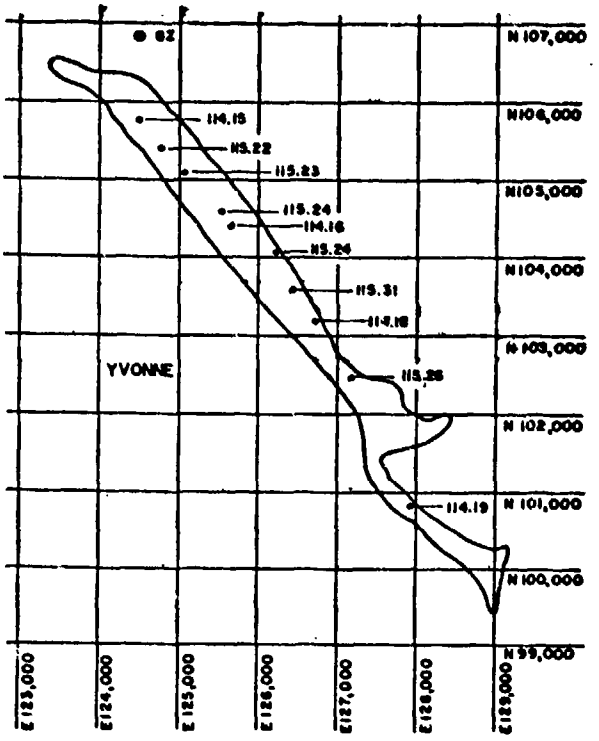


Figure 2.3 Shot Lacrosse blast-line layout.

tabulated at 50, 75, 100 and 150 percent and the 0 to 400 psi range at 50, 62.5, 100 and 125 percent. The company also supplied BRL with a plot of deflection versus pressure, on all pressure elements. Spot checks were made on the elements when they were delivered and the values were always in agreement with less than ± 0.2 percent variation. All elements used on the operation were recalibrated on return to the laboratory and the small variation was still in evidence.

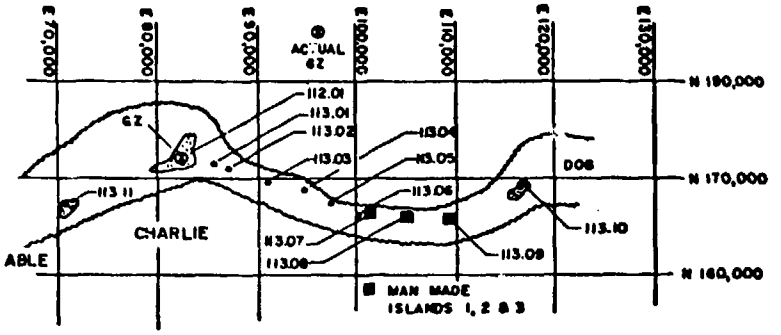


Figure 2.4 Shot Cherokee blast-line layout.

## 2.4 DATA REQUIREMENTS

The data required by Project 1.1 to accomplish its objectives were measurements of overpressure versus time along the ground surface at various distances and dynamic pressure versus time at various distances. To record this phenomena the BRL $p_t$ and q gages were used. Both

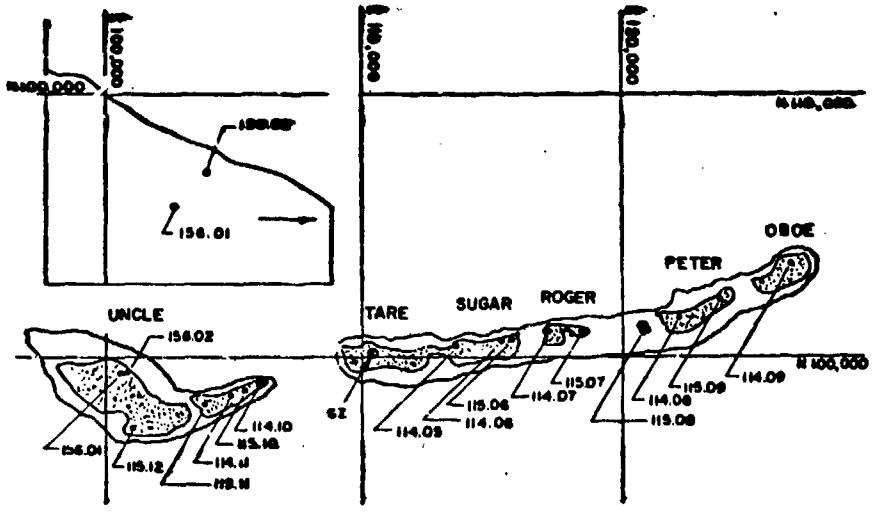


Figure 2.5 Shot Zuni blast-line layout.

gages use the same principle, that is, recording a deflection proportional to pressure on a revolving disk. The BRL q gage recorded the total overpressure and static or side-on overpressure and then one curve was subtracted from the other to obtain the dynamic pressure.

The pressure versus time curve which was scratched on a glass disk had a curved base line

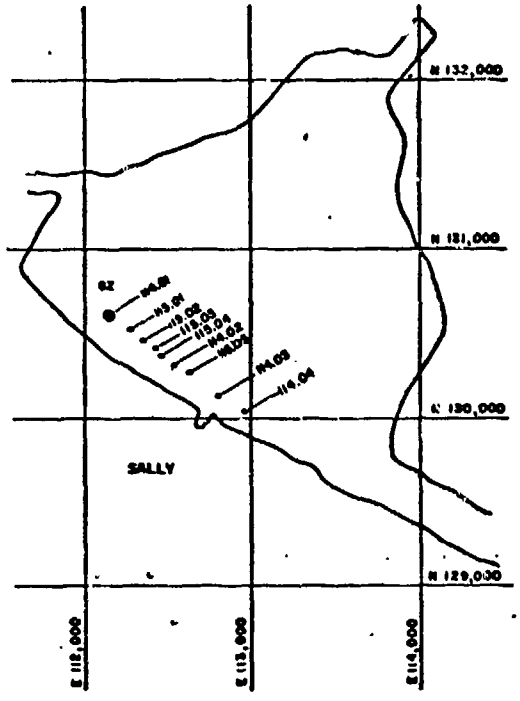


Figure 2.6 Shot Yuma blast-line layout.

and the deflection was not always a linear representation of pressure. Therefore, it was necessary to reduce the record to linear form. On previous operations this was accomplished by the use of a toolmakers microscope where the deflection was read in thousandths of an inch and rotation read in degrees, minutes and seconds. Calibrations were then applied to obtain pressure versus time.

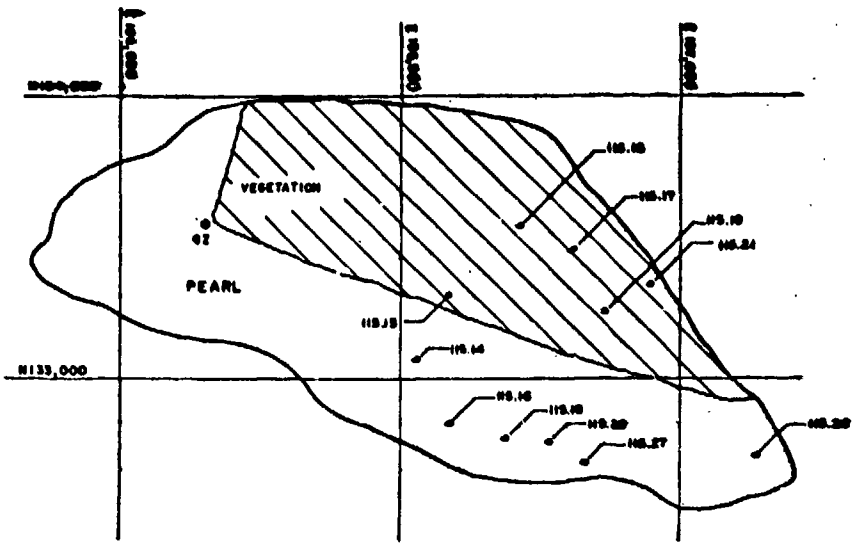


Figure 2.7 Shot Inca blast-line layout.

A new method was developed to read the records from Operation Redwing. Magnetic reading heads were mounted to the microscope and the output in digital units was recorded on IBM cards which were programmed through the Electronic Discrete Variable Computer (EDVAC). The output of the EDVAC for the pressure versus time records was in the form of IBM cards from which tabulations and plots were made. The input to the EDVAC was programmed for time versus pressure and time versus impulse.

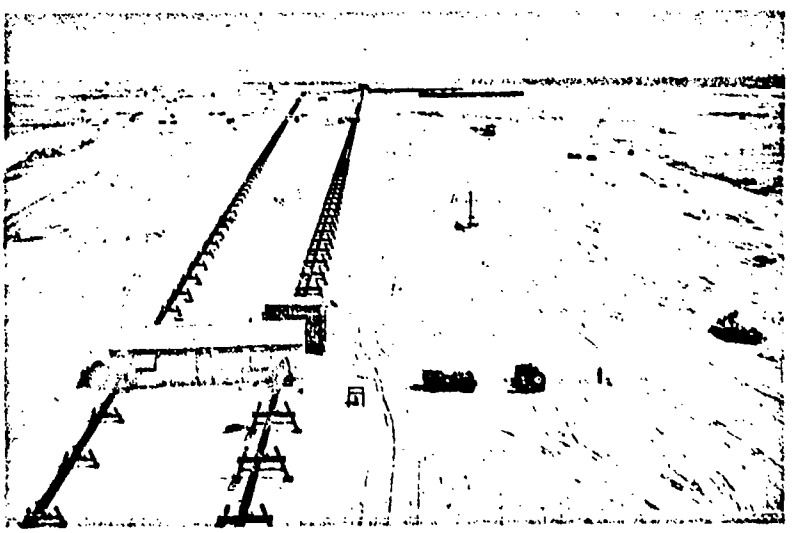

Figure 2.8 Shot Lacrosse blast-line obstructions.

For obtaining dynamic pressure, the total pressure versus time values and the side-on pressure versus time values were programmed through the EDVAC where one curve was subtracted from the other. When the time on the separate curves did not coincide, the computer interpolated between the pressure at a time just preceding and the pressure at a time beyond the time in question. The time-pressure-impulse values for the total, static and dynamic pressure records were all tabulated and plotted for final presentation.

# Chapter 3
# RESULTS

## 3.1 SCALING

To check the scaling laws for various yields and heights of burst it is necessary to normalize air-blast data to some standard so comparisons can be made. The standard which has been established is a 1 kt radiochemical yield at sea level ambient pressure and 20 degrees centigrade. (A new standard sea-level ambient temperature of 15C was established February 1958, but is not used in this report.) On Shots Lacrosse, Yuma and Inca the yield was established from the radiochemical method, but on the larger yields, such as Shots Cherokee and Zuni, the yield was determined by the hydrodynamic method.

The following scaling relations have been accepted as standard and were used in this report.

$$\text{Pressure:} \quad S_p = \frac{14.7}{P_0}$$

$$\text{Distance:} \quad S_d = \left(\frac{P_0}{14.7}\right)^{1/3} \left(\frac{1}{W}\right)^{1/3}$$

$$\text{Time:} \quad S_t = \left(\frac{T_0 + 273}{293}\right)^{1/2} \left(\frac{P_0}{14.7}\right)^{1/3} \left(\frac{1}{W}\right)^{1/3}$$

$$\text{Impulse:} \quad S_i = \left(\frac{T_0 + 273}{293}\right)^{1/2} \left(\frac{14.7}{P_0}\right)^{2/3} \left(\frac{1}{W}\right)^{1/3}$$

Where: $W$ = Yield of the device in kilotons

$P_0$ = Ambient pressure in psi at burst height or measurement height

$T_0$ = Ambient temperature in degrees Centigrade at burst height or measurement height

Scaling to ambient conditions at burst height is known as straight Sachs scaling or A-scaling and is used for the scaling factors presented in Table 3.1.

## 3.2 SHOT LACROSSE

This shot was a surface burst with a predicted yield of 40 kt and measured yield of 37.8 kt. Ground zero was on an artificial island at the end of a causeway about 450 feet off the north end of Site Yvonne.

3.2.1 Gage Performance. A total of 15 $p_t$ gages and 6 $q$ gages were installed for this shot. Records obtained from the $p_t$ gages at the last four stations were unsatisfactory, because the thermal radiation did not melt the carbon paper patch placed over the pressure inlet hole and the gage at the last station did not run. It was necessary to cover the pressure inlet hole because fine blown sand tended to clog the hole when it was uncovered. Since this was a surface shot and there were many structures and earth mounds obscuring the line of sight, the gages at the greater distances were shielded from the thermal pulse. The station at 7,050 feet did not start from the photo initiator and the thermal link was still in position.

3.2.2 Air-Blast Pressure Versus Time. Peak overpressure measured along the blast line by BRL ranged from 136 psi to 4.6 psi. These were surface pressure measurements since the gage face was installed flush with the surface of the ground. The measurements at the stations along the blast line are listed in Table 3.2. The records of pressure versus time for Shot Lacrosse are presented in Appendix B.

Although this was a surface burst, a precursor type wave form was recorded at Station 114.15, which was located 1,180 feet from ground zero. The precursor was short lived and the cyclic change noted on the Operation Teapot precursors was not recorded (Reference 3). The wave form was classical at Station 115.23, located at 1,950 feet. Values of recorded peak overpressure are plotted in Figure 3.1.

TABLE 3.1 SCALING FACTORS, AMBIENT CONDITIONS AT BURST HEIGHT

| Shot | Lacrosse | Cherokee | Zuni | Yuma | Inca |
|---|---|---|---|---|---|
| Yield | 37.8 kt | 3.8 Mt | 3.53 Mt | 0.188 kt | 14.8 kt |
| Method | Radiochemical | Hydrodynamic | Hydrodynamic | Radiochemical | Radiochemical |
| Height of Burst, feet | 14.8 | 4,320 | 9.25 | 200 | 200 |
| $P_o$, psi | 14.62 | 12.60 | 14.64 | 14.53 | 14.53 |
| $T_o$, C | 20.6 | 16.3 | 28.6 | 25.2 | 24.3 |
| $S_p$ | 1.005 | 1.167 | 1.004 | 1.012 | 1.012 |
| $S_d$ | 0.2970 | 0.0609 | 0.0655 | 1.7371 | 0.4057 |
| $S_t$ | 0.2972 | 0.0605 | 0.0656 | 1.7541 | 0.4087 |
| $S_i$ | 0.2987 | 0.0706 | 0.0658 | 1.7761 | 0.4134 |
| Height of Burst Scaled to 1 kt at Sea Level | 4.4 | 263.1 | 6.66 | 347.4 | 81.1 |

3.2.3 Dynamic Pressure. Dynamic pressure values measured on Shot Lacrosse are presented in Table 3.2. The uncorrected values were obtained by subtracting the static or side-on overpressure from the total or stagnation overpressure. That is $q'_c = \Delta p'_p - \Delta p'$. This does not mean that the peak $\Delta p'_p$ value minus the peak $\Delta p'$ value, as listed in the table, will always give the peak $q_c$ value because the peak values may occur at different times. To present a realistic value of $q'_c$, the curves have been smoothed where excessive oscillations occur at the initial portion of the record. The dynamic pressures were corrected for compressibility and flow as mentioned in Section 1.3, and the corrected peak pressures are listed in Table 3.2. A curve of corrected dynamic pressure versus distance is plotted in Figure 3.2. Records of total, side-on and dynamic pressure (uncorrected) are presented in Appendix B.

3.2.4 Arrival Time, Duration and Impulse. The blast wave arrival time measured on all records has been corrected for the motor start-up time and listed in Table 3.2 along with position duration and impulse. The procedure for applying this correction is presented in Appendix A. Corrected values of blast arrival time are plotted in Figure 3.3. In the same figure the duration of the positive pressure versus distance has also been plotted. At stations where the arrival time of the blast wave was less than 400 msec it was also necessary to apply a correction factor to the positive pressure duration (see Section A of Appendix A).

The positive impulse for all $p_t$ records and $\Delta' p$ records on which a complete history of pressure versus time was measured are plotted in Figure 3.4. Impulse values of dynamic pressure have not been plotted because they should be larger than shown in Table 3.2. On some of the

TABLE 3.2 AIR-BLAST DATA, SHOT LACROSSE

Gage designations: $p_t$ = side-on pressure versus time, $p_t$ gage; $\Delta p'_p$ = total pressure versus time, q gage; $\Delta p'$ = side-on pressure versus time, q gage; $q'_c$ = dynamic pressure versus time.

| Location | Site | Ground Range | Gage Type and Number | Peak Overpressure | Arrival Time | Positive Duration | Total Impulse | Corrected Dynamic Pressure, $q_c$ | Remarks |
|---|---|---|---|---|---|---|---|---|---|
| | | ft | | psi | sec | sec | psi-sec | psi | |
| 114.15 | Yvonne | 1,100 | $p_t$-106 | 135.0 | 0.105 | 0.371 | 5.235 | — | |
| | | | $p_t$- 75 | 136.0 | 0.100 | 0.345 | 4.961 | — | |
| 115.22 | Yvonne | 1,500 | $p_t$-201 | 56.3 | — | — | — | — | * |
| | | | $\Delta p'_p$- 26 | 160.0 | 0.23[illegible] | 0.16[illegible] | 2.823 | — | |
| | | | $\Delta p'$- 26 | 50.0 | 0.235 | 0.617 | 11.895 | — | |
| | | | $q'_c$- 26 | 110.0 | 0.235 | — | — | 73.5 | † |
| 115.23 | Yvonne | 1,950 | $p_t$-137 | 35.9 | 0.371 | 0.547 | 4.104 | — | |
| | | | $\Delta p'_p$- 15 | 49.7 | 0.445 | 0.617 | 6.654 | — | |
| | | | $\Delta p'$- 15 | 34.7 | 0.445 | 0.483 | 4.141 | — | |
| | | | $q'_c$- 15 | 18.0 | 0.445 | 2.196 | 4.000 | 15.9 | |
| 115.24 | Yvonne | 2,500 | $p_t$- 49 | 17.9 | 0.747 | 0.661 | 3.457 | — | |
| | | | $p_t$- 83 | 21.1 | 0.679 | 0.662 | 3.756 | — | |
| | | | $\Delta p'_p$- 17 | 32.9 | 0.710 | 0.636 | 4.867 | — | |
| | | | $\Delta p'$- 17 | — | — | — | — | — | † |
| | | | $q'_c$- 17 | — | — | — | — | — | † |
| 114.16 | Yvonne | 2,770 | $p_t$- 76 | 15.7 | 0.914 | 0.731 | 3.304 | — | |
| | | | $p_t$-202 | 15.8 | 0.970 | 0.730 | 3.456 | — | |
| 115.25 | Yvonne | 3,350 | $p_t$- 53 | 10.0 | 1.369 | 0.867 | 2.816 | — | |
| | | | $p_t$-125 | 7.3 | 1.252 | 0.915 | 2.877 | — | ‡ |
| | | | $\Delta p'_p$- 18 | 13.1 | 1.460 | 0.556 | 2.401 | — | |
| | | | $\Delta p'$- 18 | 10.6 | 1.460 | 0.556 | 2.067 | — | |
| | | | $q'_c$- 18 | 2.5 | 1.460 | 0.443 | 0.336 | 2.3 | |
| 115.31 | Yvonne | 3,900 | $p_t$- 65 | 3.7 | 1.568 | 0.723 | 1.455 | — | ‡ |
| | | | $\Delta p'_p$- 16 | 8.9 | 1.915 | 0.694 | 2.220 | — | |
| | | | $\Delta p'$- 16 | 7.8 | 1.915 | 0.692 | 1.965 | — | |
| | | | $q'_c$- 16 | 1.1 | 1.915 | 0.694 | 0.256 | 1.04 | |
| 114.18 | Yvonne | 4,375 | $p_t$-109 | 3.8 | 2.080 | 0.963 | 1.694 | — | ‡ |
| 115.26 | Yvonne | 5,200 | $p_t$-169 | 3.0 | 2.642 | 1.052 | 1.452 | — | ‡ |
| | | | $p_t$-148 | 4.5 | — | — | — | — | * |
| | | | $\Delta p'_p$- 19 | 5.0 | 2.623 | 0.943 | 1.815 | — | |
| | | | $\Delta p'$- 19 | 4.5 | 2.623 | 0.928 | 1.651 | — | |
| | | | $q'_c$- 19 | 0.5 | 2.623 | 0.859 | 0.164 | 0.46 | |
| 114.19 | Yvonne | 7,650 | $p_t$-138 | No Readable Record | | | | | |

* Peak pressure only obtained.
† Values could not be obtained.
‡ Pressure value not considered valid.



SECRET

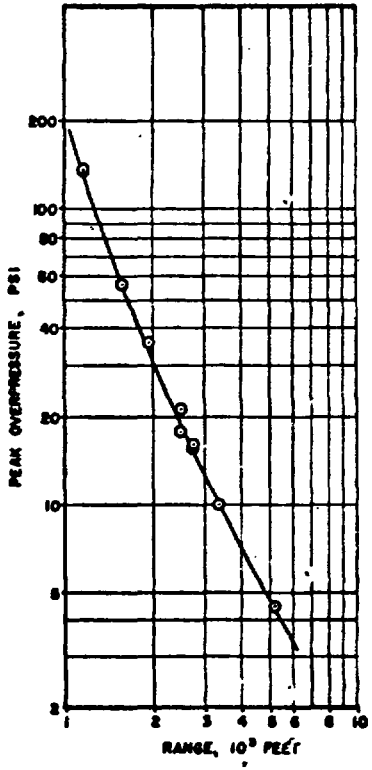


Figure 3.1 Pressure versus distance, Shot Lacrosse.

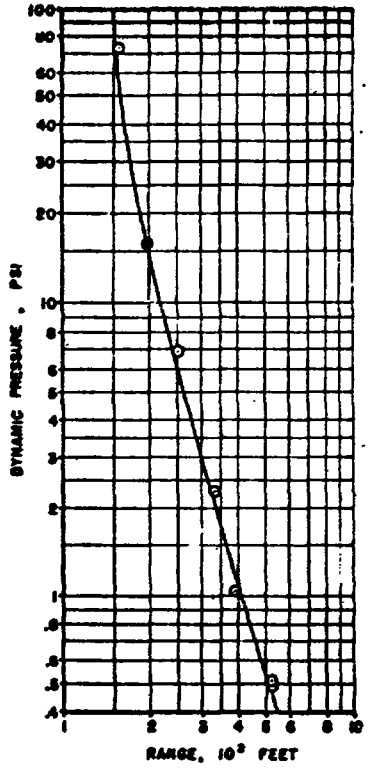


Figure 3.2 Dynamic pressure versus distance, Shot Lacrosse.

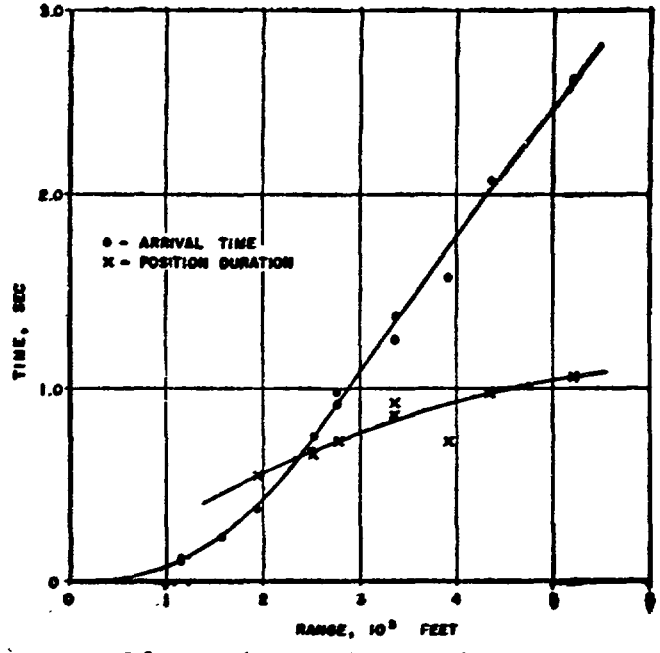


Figure 3.3 Arrival time and positive duration versus distance, Shot Lacrosse.

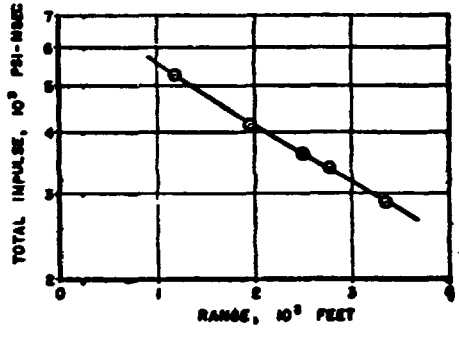


Figure 3.4 Impulse versus distance, Shot Lacrosse.

records the rise time of the side-on pressure record is faster than the total pressure record. This then implies a negative dynamic pressure during the initial portion of the record and therefore a negative impulse during that portion. This inconsistency can be seen on the records presented in Appendix B, and must be reckoned with when correlating other blast parameters with dynamic impulse.

### 3.3 SHOT CHEROKEE

Shot Cherokee was the first air drop of a megaton-yield device. It was planned to detonate at an altitude greater than 1 times the fireball radius so that basic blast phenomenology could be measured on a true free-air burst. The successful accomplishment of the projects' objectives on this shot was seriously hampered by an error in the placement of the device at the intended air zero. The length of the blast line was changed from one starting at ground zero and ending at 35,580 feet to a blast line starting at 17,500 feet and extending to 30,711 feet (Figure 2.4).

3.3.1 Gage Performance. Project 1.1 had a larger participation on this shot than any of the other shots. A total of 35 $p_t$ gages and 11 q gages were installed for the blast line instrumentation. Twelve $p_t$ gages and three q gages were installed for the blast diffraction studies over the man-made islands.

Considerable instrumentation difficulty was encountered during the preshot phase. Malfunction of both initiation methods was the primary difficulty encountered. The photo initiation circuit was preinitiating and the cause could not be immediately determined. Details on the circuit and the malfunction are explained in Appendix B. There was considerable delay in the shot day. The thermal links, which were used as a back-up initiation system, began to preinitiate. The links were under a stress and the low melting point alloy had a tendency to creep when exposed over an extended period. The metal creep allowed the switch to close starting the gage before shot time. Therefore, it was necessary to make frequent inspection trips and reset gages that had run.

Nine of the 47 $p_t$ gages and 3 of the 14 q gages recorded peak overpressure only, because of the preinitiation of the gages.

3.3.2 Air-Blast Pressure Versus Time. The nearest station to the actual ground zero was approximately 17,000 feet; therefore all high pressure phenomena were lost, as were measurements in the regular reflection region. The accuracy of many of the records was diminished because the ranges of the pressure-sensing capsules was 10 to 40 times greater than the actual pressure arriving at the stations. On Site Charlie, the intended ground zero, a capsule range of 0 to 400 psi was used, but the actual pressure measured was less than 12 psi.

Of the 38 pressure-time records obtained, six were considered unreliable for plotting a curve of pressure versus distance because of the small amplitude of the record or the extreme oscillation believed to be caused by the orientation of the detonation with regard to the gage mounts (Figure 2.1).

There appears to be a deviation in the pressure-distance curve where the reef stations end and the land stations begin. As shown in Table 3.5 and Figure 3.5, Reef Stations 113.05 and 113.06 are nearer ground zero, but show a lower pressure than Station 113.07 which is at a greater distance, but located on a man-made island where the gages were installed flush with the surface. In Figure 3.6, a record from Station 113.07 and one from 113.06 are plotted on the same time and pressure scale. This figure shows quite well the effect of the gage mount in lowering the initial portion of the recorded pressure versus time. In Figure 3.7, records of pressure versus time from a series of shock tube tests are presented. Records were made using a $\frac{1}{4}$ scaled model of the mount and, under similar conditions, records were made using a large baffle on the end of the mount. Results of these tests indicate that a reduction of as much as 25 percent may be expected when using the type gage mount used along the reef for Shot Cherokee. Pressure values have been plotted in Figure 3.5 assuming a 25 percent attenuation in pressure due to gage mount.

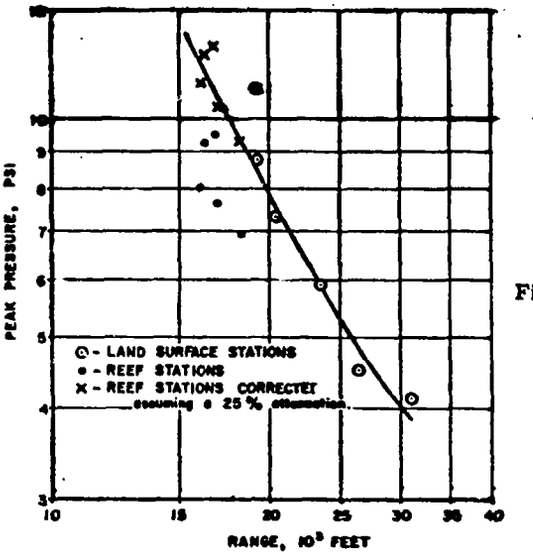


Figure 3.5 Pressure versus distance, Shot Cherokee.

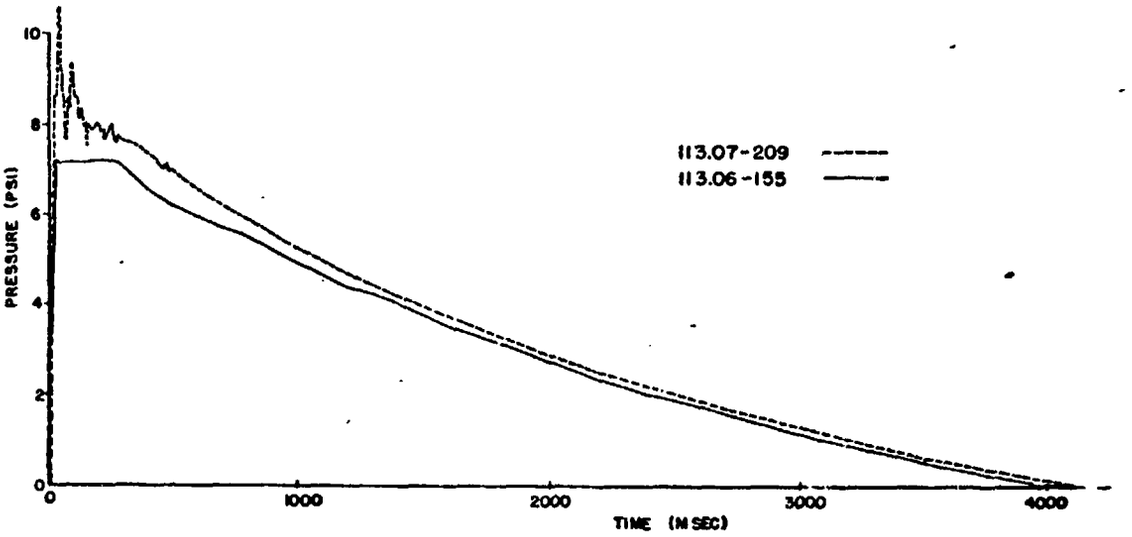


Figure 3.6 Plot of Stations 113.06 and 113.07.

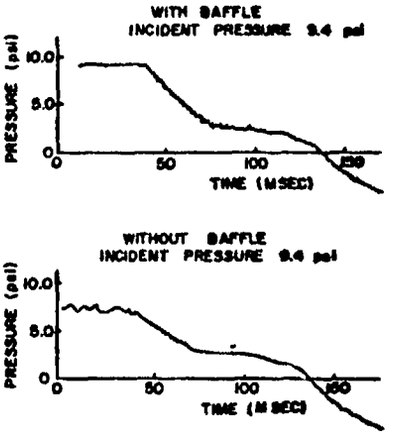


Figure 3.7 Plot of shock tube record with and without baffle.



SECRET

The gages at any one reef station check well when compared with each other, but the wave shape is not consistent at the various reef stations (see Appendix B). Three records from Station 113.09 are plotted in Figure 3.8 to show the comparison of three gages in similar positions on a man-made island. The difference in the initial portion of the record is caused by the reflected wave from the structure arriving at the gages at different times because of the separation of the gages. Average values of peak pressures, arrival times, durations and impulse are listed in Table 3.4.

3.3.3 Dynamic Pressure. Records obtained from the q gages were essentially a complete loss for obtaining usable dynamic pressure. The gage being unidirectional was oriented toward the intended ground zero, but the air-zero error caused the shock front to strike the gages at angles other than normal to the axis. The shock front struck some of the gages from the rear, some broad side and some from the front at large angles. The angles between the axis of the q gage and the actual ground zero are listed in Table 3.3. An angle of 90 degrees would mean the shock front struck broadside, while at greater than 90 degrees it would be from the rear. From the q gage records presented in Appendix B, it can be seen that when the shock front strikes the gage at any angle other than normal to the axis a lowering of recorded pressure of both the total and static records occurs. The values from Stations 113.01, 113.02, 113.03 and 113.04 have not been listed in Table 3.3 due to extremely small deflections causing unreliability and inconsistency of the data.

3.3.4 Arrival Time, Duration and Impulse. Arrival times of the shock front at the gage positions are listed in Table 3.3 and plotted in Figure 3.9. When compared with the arrival times measured by electronic instrumentation on Man-Made Islands 1, 2 and 3, and Sites Dog and Able, the self-recording gage times are consistently low. It is believed that the majority of the gages did not initiate from the photo circuit, but rather from the thermal link. On this shot the photo-circuit pickup was directional and faced intended ground zero. A three density filter was used so the gage would not initiate in bright sunlight. Therefore, it is felt that the light from the detonation entering the photo pickup from the side or rear did not initiate many of the gages. In many instances, because of the difficulty with the creep in the thermal links, two were sometimes used on a gage. Since the flat side was not facing actual ground zero, there was an increased lag in the parting time of the link. This lag was not consistent and might vary from a few milliseconds to more than one second. All arrival times have been adjusted for the lag due to the start up time of the motors.

The durations of the positive pressure pulse, along with arrival times, are listed in Table 3.3 and plotted in Figure 3.9. Durations from the q gages are not plotted because of the difficulty in determining the time at which the cross over takes place. This difficulty was caused by the extremely small deflections and excessive pressure fluctuations due to vortex shedding from the q gage body.

The impulse of the positive pressure pulse is listed in Table 3.3 and plotted in Figure 3.9. There is some scatter from the reef station gages but this would be expected since there was also scatter in the pressure measurements. The values plotted in Figure 3.9 were taken from the average values listed in Table 3.4.

## 3.4 SHOT ZUNI

Shot Zuni was a 3.5 megaton-yield device detonated approximately 9 feet above ground surface. Project 1.1 instrumented two blast lines for this shot. The blast-line layout was similar to the one established on Shot 3 of Operation Castle (Reference 1). The blast line area on Site Uncle which had been cleared for Operation Castle had grown over with heavy vegetation for Operation Redwing. Project 1.1 also instrumented two Stations, 156.01 and 156.02, for Project 1.5. These stations were located near the concrete cubicle structure and will be described in this report. Certain stations were instrumented to measure pressure caused by the passage of water over

TABLE 3.3 AIR-BLAST DATA, SHOT CHEROKEE

Gage designations: $p_t$ = side-on pressure versus time, $p_t$ gage; $\Delta p'_p$ = total pressure versus time, q gage; $\Delta p^s$ = side-on pressure versus time, q gage; $q'_c$ = dynamic pressure versus time.

| Station | Site | Ground Range | Angle of Orientation | Gage Type and Number | Peak Overpressure | Arrival Time | Positive Duration | Total Impulse |
|---|---|---|---|---|---|---|---|---|
| | | ft | deg | | psi | sec | sec | psi-sec |
| 112.01 | Charlie | 19,142 | — | $p_t$- 14 | 10.9* | 8.236* | † | † |
| | | | | $p_t$- 94 | † | † | † | † |
| 113.01 | Reef East of Charlie | 17,500 | 112 | $p_t$-107 | † | 6.894* | † | † |
| | | | | $p_t$-222 | † | † | † | † |
| | | | | $p_t$- 49 | † | † | † | † |
| 113.02 | Reef East of Charlie | 16,970 | 108 | $p_t$- 2 | 9.1 | 6.962 | ‡ | ‡ |
| | | | | $p_t$-217 | 8.0 | 6.440 | 3.413 | 14.215 |
| | | | | $p_t$-167 | 11.4‡ | † | 4.638 | 21.418 |
| 113.03 | Reef East of Charlie | 16,162 | 94 | $p_t$- 54 | 8.0 | 6.396 | 3.166 | 12.442 |
| | | | | $p_t$-213 | 12.9‡ | † | † | † |
| | | | | $p_t$- 13 | 8.0 | 6.413 | 3.178 | 12.600 |
| 113.04 | Reef East of Charlie | 16,323 | 80 | $p_t$- 66 | 9.3 | 6.733 | 3.451 | 13.382 |
| | | | | $p_t$-153 | 9.1 | 7.191 | 3.608 | 12.269 |
| | | | | $p_t$- 64 | 9.2 | 6.575 | 3.802 | 14.340 |
| 113.05 | Reef East of Charlie | 17,068 | 70 | $p_t$- 70 | 7.5 | 7.415 | 3.612 | 12.402 |
| | | | | $p_t$-122 | 10.4‡ | † | † | † |
| | | | | $p_t$-219 | 7.7 | † | 3.735 | 12.533 |
| | | | | $\Delta p'_p$- 5 | 6.8* | † | † | † |
| | | | | $\Delta p^s$- 5 | 5.0* | † | † | † |
| | | | | $q'_c$- 5 | 1.8* | † | † | † |
| 113.06 | Reef East of Charlie | 18,282 | 61 | $p_t$- 93 | 6.7 | 8.185 | 3.986 | 11.955 |
| | | | | $p_t$-206 | 6.9 | 8.692 | 3.948 | 12.519 |
| | | | | $p_t$-155 | 7.2 | 8.342 | 3.964 | 12.471 |
| | | | | $\Delta p'_p$- 6 | 3.4* | † | † | † |
| | | | | $\Delta p^s$- 6 | 2.2* | † | † | † |
| | | | | $q'_c$- 6 | 1.2* | † | † | † |
| 113.07 | Man-Made Island No. 1 | 19,349 | 57 | $p_t$-218 | 8.7 | 8.956 | 3.938 | 12.208 |
| | | | | $p_t$-209 | 8.8 | 8.865 | 4.108 | 13.658 |
| | | | | $p_t$- 97 | 8.5 | 8.695 | 4.057 | 13.068 |
| | | | | $\Delta p'_p$- 7 | 8.5 | 9.496 | 2.930 | 9.125 |
| | | | | $\Delta p^s$- 7 | 7.4 | 9.496 | 2.886 | 8.153 |
| | | | | $q'_c$- 7 | 2.0 | 9.496 | 5.000 | 0.696 |
| 113.08 | Man-Made Island No. 2 | 20,462 | 50 | $p_t$-203 | 9.5‡ | † | † | † |
| | | | | $p_t$-164 | 7.2 | 9.845 | 4.347 | 12.588 |
| | | | | $p_t$-204 | 10.3‡ | † | † | † |
| | | | | $\Delta p'_p$- 8 | † | † | † | † |
| | | | | $\Delta p^s$- 8 | 5.0 | 9.546 | ‡ | ‡ |
| | | | | $q'_c$- 8 | † | † | † | † |



SECRET

TABLE 2.3 CONTINUED

| Station | Site | Ground Range | Angle of Orientation | Gage Type and Number | Peak Overpressure | Arrival Time | Positive Duration | Total Impulse |
|---|---|---|---|---|---|---|---|---|
| | | ft | deg | | psi | sec | sec | psi-sec |
| 112.09 | Man-Made Island No. 2 | 23,512 | 41 | $p_t$- 80 | 6.0 | 12.138 | 4.788 | 11.334 |
| | | | | $p_t$-221 | 5.9 | 12.163 | 4.732 | 11.192 |
| | | | | $p_t$-210 | 5.8 | 12.362 | 4.608 | 11.085 |
| | | | | $\Delta p^i_p$- 9 | 6.1 | 12.799 | 4.452 | 10.707 |
| | | | | $\Delta p^i$- 9 | 4.2 | 12.799 | 4.332 | 7.992 |
| | | | | $q^i_c$- 9 | 1.9 | 12.799 | 9.534 | 3.548 |
| 113.10 | Dog | 26,453 | 32 | $p_t$- 23 | 4.5 | 14.735 | 4.883 | 9.017 |
| | | | | $p_t$- 1 | 5.3‡ | † | † | † |
| | | | | $p_t$- 61 | 5.3‡ | † | † | † |
| | | | | $\Delta p^i_p$- 10 | 4.7* | † | † | † |
| | | | | $\Delta p^i$- 10 | 4.1* | 13.804 | † | † |
| | | | | $q^i_c$- 10 | 0.6* | † | † | † |
| 113.11 | Able | 30,711 | 12 | $p_t$-206 | 4.7‡ | † | † | † |
| | | | | $p_t$- 81 | 4.4‡ | † | † | † |
| | | | | $p_t$- 21 | 4.1 | 17.153 | 6.128 | 10.447 |
| | | | | $\Delta p^i_p$- 11 | 4.5* | † | † | † |
| | | | | $\Delta p^i$- 11 | 4.0* | † | † | † |
| | | | | $q^i_c$- 11 | 0.5* | † | † | † |
| 115.28 | Man-Made Island No. 1 | 19,349 | 57 | $\Delta p^i_p$- 12 | 8.2* | † | † | † |
| | | | | $\Delta p^i$- 12 | 5.6* | † | † | † |
| | | | | $q^i_c$- 12 | 2.6* | † | † | † |
| 115.29 | Man-Made Island No. 2 | 20,482 | 50 | $\Delta p^i_p$- 13 | 7.0 | 10.630 | 4.303 | 10.531 |
| | | | | $\Delta p^i$- 13 | 5.5 | 10.630 | 4.054 | 9.490 |
| | | | | $q^i_c$- 13 | 1.5 | 10.630 | 11.500 | 3.162 |
| 115.30 | Man-Made Island No. 3 | 23,512 | 41 | $\Delta p^i_p$- 14 | † | † | † | † |
| | | | | $\Delta p^i$- 14 | 5.0 | 12.700 | 2.124 | 4.759 |
| | | | | $q^i_c$- 14 | † | † | † | † |
| 114.22 | Man-Made Island No. 1 | 19,349 | 57 | $p_t$- 99 | 8.8 | † | 3.779 | 12.289 |
| 114.23 | | | | $p_t$- 32 | 12.4‡ | † | † | † |
| 114.24 | | | | $p_t$-135 | 9.0 | 9.885 | 4.433 | 12.946 |
| 114.30 | | | | $p_t$- 78 | 9.8 | † | 4.027 | 12.785 |
| 114.25 | Man-Made Island No. 2 | 20,482 | 50 | $p_t$- 58 | 7.4 | 9.885 | 4.246 | 11.965 |
| 114.26 | | | | $p_t$- 28 | 7.4 | † | 4.186 | 12.390 |
| 114.27 | | | | $p_t$- 31 | 7.3 | 9.765 | 4.261 | 11.939 |
| 114.28 | | | | $p_t$-106 | 7.1 | 8.793 | 4.199 | 11.162 |
| 114.29 | | | | $p_t$-220 | 7.3 | 10.027 | 4.200 | 11.992 |
| 114.30 | | | | $p_t$- 41 | 7.0 | † | 4.669 | 12.332 |
| 114.31 | | | | $p_t$- 29 | 7.7 | 10.328 | 4.095 | 11.101 |
| 114.40 | | | | $p_t$-171 | 7.5 | 9.574 | 4.294 | 12.237 |

*Questionable record, not presented in Appendix B.
† Value could not be obtained.
‡ Value not considered valid.
‖ Peak pressure only.



SECRET

TABLE 3.4 AVERAGE PLOTTED VALUES, SHOT CHEROKEE

| Station | Site | Range | Peak Overpressure | Arrival Time | Positive Duration | Total Impulse |
|---|---|---|---|---|---|---|
| | | ft | psi | sec | sec | psi-sec |
| 112.01 | Charlie | 19,143 | 10.9 | 8.236 | — | — |
| 113.01 | Reef | 17,500 | — | 6.894 | — | — |
| 113.02 | Reef | 16,970 | 9.5 | 6.711 | 3.413 | 14.215 |
| 113.03 | Reef | 16,162 | 8.0 | 6.404 | 3.172 | 12.521 |
| 113.04 | Reef | 16,323 | 8.2 | 6.533 | 3.620 | 13.330 |
| 113.05 | Reef | 17,068 | 7.8 | 7.415 | 3.674 | 12.468 |
| 113.06 | Reef | 18,282 | 6.9 | 8.406 | 3.966 | 12.315 |
| 113.07 | Man-Made Island No. 1 | 19,349 | 8.9 | 9.105 | 4.057 | 12.826 |
| 113.08 | Man-Made Island No. 2 | 20,482 | 7.3 | 9.731 | 4.280 | 11.970 |
| 113.09 | Man-Made Island No. 3 | 23,512 | 5.9 | 12.362 | 4.709 | 11.270 |
| 113.10 | Dog | 26,453 | 4.5 | 14.736 | 4.883 | 9.017 |
| 113.11 | Able | 30,711 | 4.1 | 17.153 | 6.128 | 10.447 |

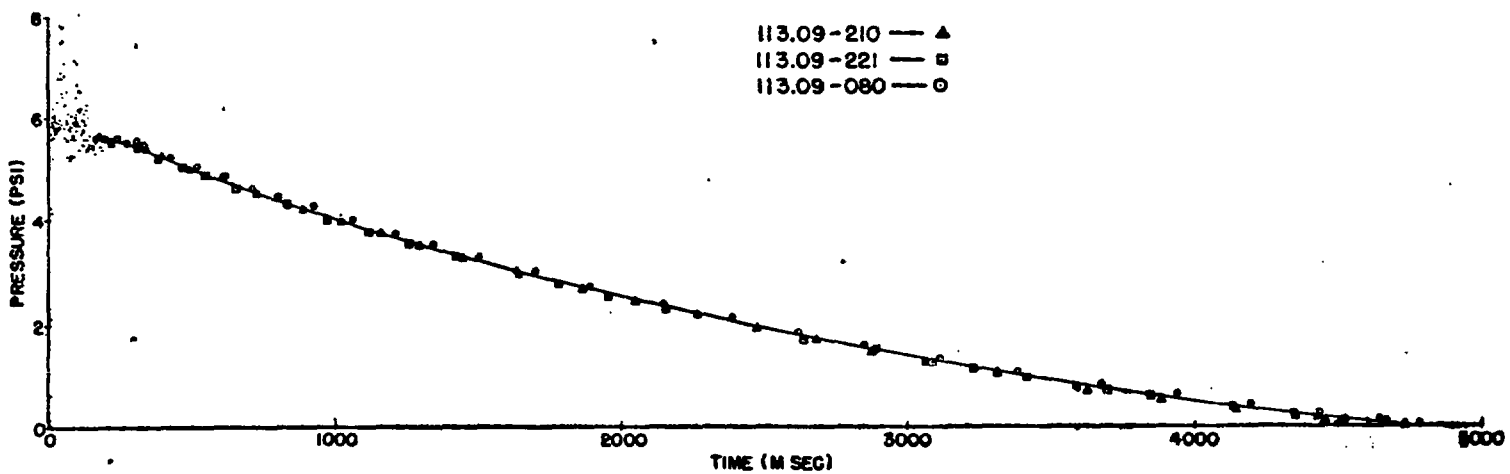


Figure 3.8 Comparison of records of pressure versus time from three gages at Station 113.09.

SECRET

gages. From the water pressure measured, the height of the water wave could be determined. No deflections that could be attributed to water pressure were observed on the records.

3.4.1 Gage Performance. There were 15 $p_t$ gages installed for blast line measurements. Eight $p_t$ gages were installed for measuring water pressure and two for measuring air blast at the Project 1.5 structure. Three of the close-in $p_t$ gages were blown or washed from their

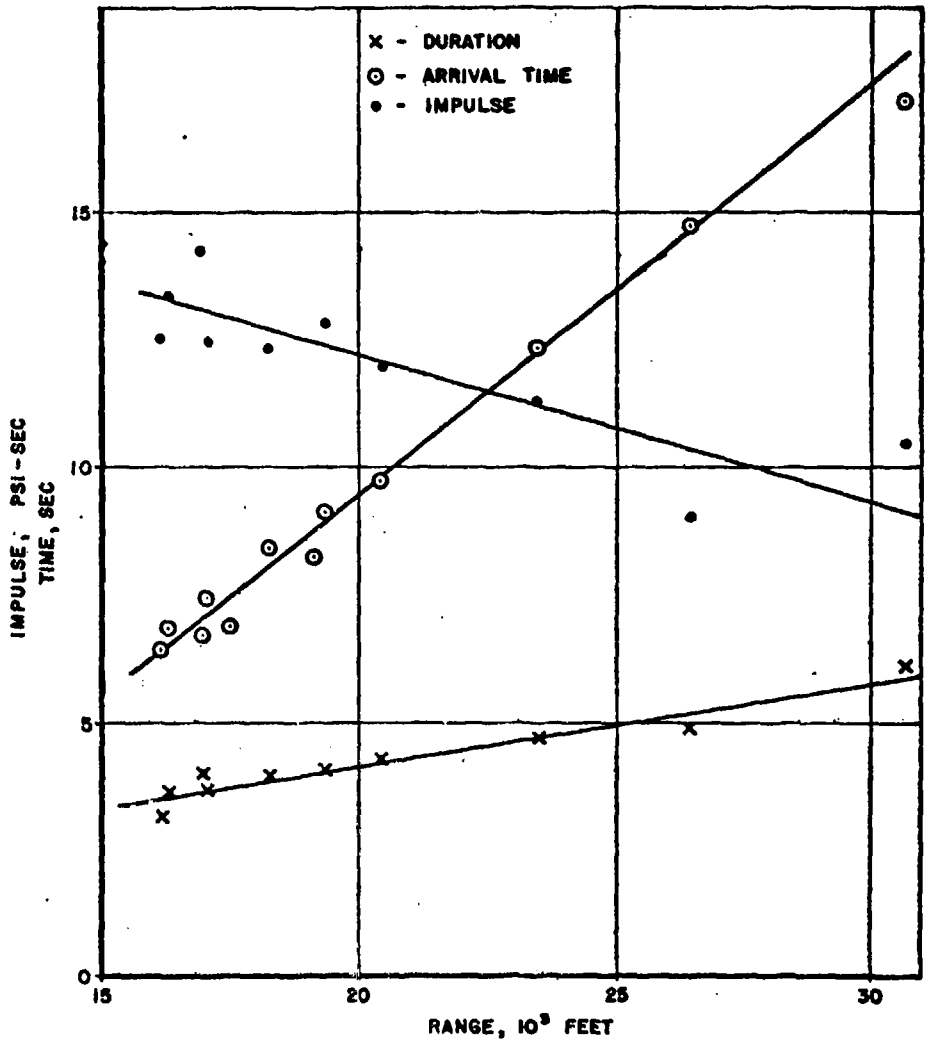


Figure 3.9 Impulse, arrival time, duration versus distance, Shot Cherokee.

mounts and were not recovered. One $p_t$ gage record disk was broken and the pieces were so small the record could not be salvaged. Four of the 21 disks recovered from the $p_t$ gages recorded peak pressure only. The same preinitiation difficulties experienced on Shot Cherokee were still evident on Shot Zuni.

Of the nine q gages installed, seven were recovered on the first entry day. The other two

were not recovered until the following day, because Station 115.06 was blown or washed 450 feet to the rear and was found covered with about a foot of water. The q gage at Station 115.07 was also blown or washed 40 feet to the northeast and partially covered with sand. At Station 115.10, the mount was in place, but was bent so the gage pointed upward. The nose of the gage was found 150 feet to the rear with no disk on the turntable. The mount at Station 115.11 was in place with the complete gage, but bent back at an angle of approximately 45 degrees. The q gage facing ground zero at Station 156.02 was bent 30 degrees and both forward guy wires were broken. The gage mounted at an orientation of 45 degrees from ground zero was bent over, horizontal to the ground, with all guy wires broken.

3.4.2 Air-Blast Pressure Versus Time. There is definite evidence that a precursor-type wave was generated by the Shot Zuni detonation. In Appendix B the records of pressure versus time are presented. The wave shapes at Stations 115.06, 114.07 and 115.07 on the Tare Complex indicated a precursor was formed and extended to a distance greater than 8,300 feet. The next station along the Tare Complex was located at 10,400 feet and appeared to be classical in shape although there was a slight disturbance at the initial peak. It is felt that the disturbance recorded at this station and at the stations at greater distances along the Tare Complex was a function of the location of the gage and the roughness of the terrain, rather than the precursor.

The blast line on Site Uncle had considerable washing over the first stations. The mounts used on Station 114.10 were used on Operation Castle and were essentially flush with the surface of the ground before the shot. One gage at this station had a split capsule and the disk in the other gage was broken into small pieces and could not be read. The disk from the gage at Station 115.10 was also broken and only a peak overpressure is presented. The gage at Station 114.11 recorded a pressure versus time record, but the initial portion of the record was not considered reliable for any wave shape consideration. It is felt that some of the irregularities in the decaying portion of the positive pressure phase were due to the glass disk slipping on the turntable because of extreme acceleration. The records from both gages at Station 115.11 show the expected precursor wave shape. Again on Gage 214, it appeared that the disk slipped and caused an apparent change in pressure. The initial portion of the two records showed a favorable comparison. The two gages at Station 115.12 agreed in wave shape and both showed a rounded front as though the precursor had not completely cleaned up. Again it appeared that the disk slipped on Gage 068 at approximately 600 msec (see Appendix B).

Stations 156.01 and 156.02 were installed for Project 1.5, but are reported in this section. Station 156.02 located at 9,600 feet, was nearer ground zero and much closer to the water surface. This station recorded a wave shape similar to Station 115.08, located at 10,400 feet on the Tare Complex. Station 156.01, located at 9,700 feet, was only 100 feet farther from ground zero, but because of the shape of the shore line the shock front had to travel over several hundred more feet of land to reach the station. The wave shape was similar to that recorded at Station 115.12, although the peak was a little more rounded.

The curve of pressure versus distance is plotted in Figure 3.10 and the peak values are listed in Table 3.5. There appears to be some difference in the two blast lines at the higher pressures, but the 23 psi pressure level occurs at the same distance on both blast lines. It appears from the pressure-time records in Appendix B and the pressure-distance curve in Figure 3.10 that the record from Station 114.11 could be classified as a Type B precursor wave shape, and the pressure would be expected to be lower than Station 115.11 which may be classified as a Type C wave shape. See Reference 5 for precursor wave-shape classification.

3.4.3 Dynamic Pressure. The dynamic pressure versus time is questionable on many of the records because some of the mounts were blown out of position and others were bent so the latter portion of the positive pressure pulse was striking the gages at extreme angles of pitch. This would tend to lower both the total measured pressure and side-on measured pressure, but not by the same amount. It is believed that the peak values are reasonably valid, but as can be seen in Table 3.5 the positive durations are inconsistent. The peak dynamic pressure values have been corrected for Mach flow and compressibility and plotted in Figure 3.11. The correction applied

**TABLE 3.5 AIR-BLAST DATA, SHOT ZUCC**

Gage designations: $p_t$ = side-on pressure versus time, $p_t$ gage; $\Delta p'_p$ = total pressure versus time, q gage; $\Delta p'$ = side-on pressure versus time, q gage; $q'_c$ = dynamic pressure versus time.

| Station | Site | Ground Range | Gage Type and Number | Peak Overpressure | Arrival Time | Positive Duration | Total Impulse | Corrected Dynamic Pressure, $q_c$ | Remarks |
|---|---|---|---|---|---|---|---|---|---|
| | | ft | | psi | sec | sec | psi-sec | psi | |
| 114.05 | Sugar | 3,160 | $p_t$-141 | — | — | — | — | — | Not Recovered |
| | | | $p_t$-126 | — | — | — | — | — | Not Recovered |
| 114.06 | Sugar | 5,096 | $p_t$- 86 | 67.0 | — | — | — | — | • |
| 115.06 | Sugar | 5,800 | $p_t$- 56 | 67.0 | † | 2.299 | 27.306 | † | |
| | | | $p_t$-165 | — | — | — | — | — | Not Recovered |
| | | | $\Delta p'_p$- 20 | 163.0 | 1.566 | 0.344 | 21.444 | † | |
| | | | $\Delta p'$- 20 | 110.0 | 1.566 | 0.344 | 14.961 | † | |
| | | | $q'_c$ - 20 | 56.0 | 1.566 | 0.344 | 6.189 | 48.2 | |
| 114.07 | Roger | 6,900 | $p_t$- 36 | 45.3 | † | 1.116 | 12.028 | † | |
| 115.07 | Roger | 8,300 | $p_t$-211 | 34.6 | † | ‡ | ‡ | † | |
| | | | $p_t$-114 | 35.0 | 2.148 | 2.166 | 19.813 | † | |
| | | | $\Delta p'_p$- 21 | 54.0 | 1.556 | 2.656 | 25.142 | † | |
| | | | $\Delta p'$- 21 | 35.0 | 1.556 | 3.166 | 24.275 | † | |
| | | | $q'_c$ - 21 | 20.0 | 1.556 | 0.455 | 5.350 | 17.5 | |
| 115.08 | Peter | 10,400 | $p_t$- 90 | 20.0 | 2.739 | 2.947 | 17.640 | † | |
| | | | $\Delta p'_p$- 22 | 29.4 | 3.265 | 0.917 | 12.681 | † | |
| | | | $\Delta p'$- 22 | 20.9 | 3.265 | 0.917 | 10.047 | † | |
| | | | $q'_c$ - 22 | 8.5 | 3.265 | 0.849 | 2.657 | 8.2 | |
| 114.08 | Peter | 11,700 | $p_t$-126 | 17.2 | 3.376 | 2.344 | 12.229 | † | |
| | | | $p_t$-163 | 17.0 | 3.353 | 3.601 | 16.704 | † | |
| 115.09 | Peter | 13,800 | $p_t$- 26 | 11.6 | — | — | — | — | • |
| | | | $\Delta p'_p$- 23 | 15.0 | 5.480 | 1.581 | 9.426 | † | |
| | | | $\Delta p'$- 23 | 11.5 | 5.480 | 1.476 | 6.884 | † | |
| | | | $q'_c$ - 23 | 3.7 | 5.480 | 3.662 | 3.660 | 3.2 | |
| 114.09 | Oboe | 16,500 | $p_t$- 9 | 8.0 | 5.639 | 3.817 | 11.208 | † | |
| | | | $p_t$- 24 | 8.6 | 6.249 | 3.732 | 11.420 | † | |
| 114.10 | Uncle | 4,470 | $p_t$- 11 | 200.0 | — | — | — | — | • |
| | | | $p_t$-204 | — | — | — | — | — | Not Recovered |
| 115.10 | Uncle | 5,090 | $p_t$-101 | 124.0 | — | — | — | — | • |
| | | | $\Delta p'_p$- 24 | — | — | — | — | — | Not Recovered |
| | | | $\Delta p'$- 24 | — | — | — | — | — | † |
| | | | $q'_c$ - 24 | — | — | — | — | — | † |
| 114.11 | Uncle | 5,920 | $p_t$-216 | 57.5 | 0.936 | 1.948 | 29.441 | † | |
| 115.11 | Uncle | 7,020 | $p_t$-214 | 67.7 | 1.270 | 1.578‡ | 25.590‡ | † | |
| | | | $p_t$-182 | 65.3 | 1.046 | 1.642 | 21.925 | † | |
| | | | $\Delta p'_p$- 25 | — | — | — | — | — | Not Recovered |
| | | | $\Delta p'$- 25 | — | — | — | — | — | † |
| | | | $q'_c$ - 25 | — | | — | — | — | † |



SECRET

TABLE 3.8 CONTINUED

| Station | Site | Ground Range | Gage Type and Number | Peak Overpressure | Arrival Time | Positive Duration | Total Impulse | Corrected Dynamic Pressure, $q_n$ | Remarks |
|---|---|---|---|---|---|---|---|---|---|
| | | ft | | psi | sec | sec | psi-sec | psi | |
| 115.12 | Uncle | 9,880 | $p_t$-104 | 23.5 | 2.362 | 2.570 | 17,180 | † | |
| | | | $p_t$- 66 | 23.5 | 2.154‡ | 2.038‡ | 18.720‡ | † | |
| | | | $\Delta p'_p$- 26 | 44.0 | — | — | — | — | * |
| | | | $\Delta p'$- 26 | 22.0 | — | — | — | — | |
| | | | $q'_c$- 26 | 21.2 | — | — | — | 17.8 | |
| 156.01 | Uncle | 9,700 | $p_t$- 82 | 21.3 | 4.660 | 2.722 | 17.796 | † | |
| 156.02 | Uncle | 9,600 | $p_t$-132 | 23.0 | 2.515 | 2.358 | 16.216 | † | |
| | | | $\Delta p'_p$- 27 | 27.0 | 2.930 | † | † | † | |
| | | | $\Delta p'$- 27 | 23.0 | 2.930 | † | † | † | |
| | | | $q'_c$- 27 | 13.5 | 2.930 | † | † | 11.1 | |
| 114.41 | Nan | — | $p_t$-136 | — | — | — | — | — | † |
| | | | $\Delta p'$ | 24.5 | † | 2.364 | 21.370 | † | |
| 156.01 | Uncle | 9,700 | $q'_c$ (electronic) | 20.0 | † | 2.772 | 3.551 | 17.0 | |

* Peak pressure only obtained. † Value could not be obtained. ‡ Value not considered valid.

was for clean air, and any sand, dust, or water loading was not considered. The blast wave had to travel over a considerable land area to reach Station 115.12. It should be noted that the dynamic pressure measured at Station 115.12, located at 9,880 feet in the vegetated area, was much greater than the value recorded at Station 156.02, which was 280 feet nearer ground zero but near

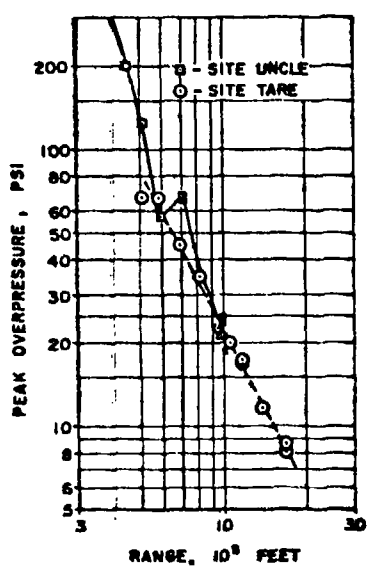


Figure 3.10 Peak overpressure versus distance, Shot Zuni.

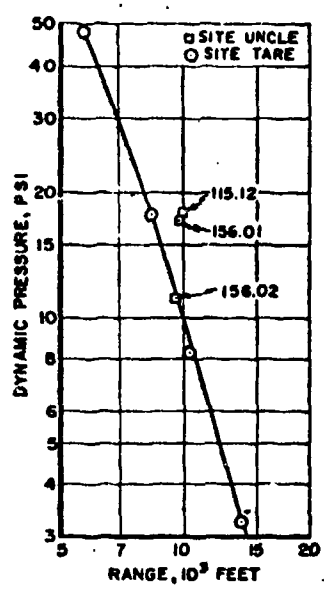


Figure 3.11 Corrected peak dynamic pressure versus distance, Shot Zuni.

the water surface. The electronic q gage at Station 156.01, located at 9,700 feet, recorded approximately the same dynamic pressure as Station 115.12. As mentioned in Section 3.4.2, the shock front had to travel over some land area to reach Station 156.01.

3.4.4 Arrival Time, Duration and Impulse. The corrected values of arrival time are listed in Table 3.5, and plotted in Figure 3.12. There is some scatter of arrival times, although Station 115.07, at 8,300 feet, is the only value which falls outside the expected spread for this shot. The values of positive duration are also plotted in the same figure. There is considerable scat-

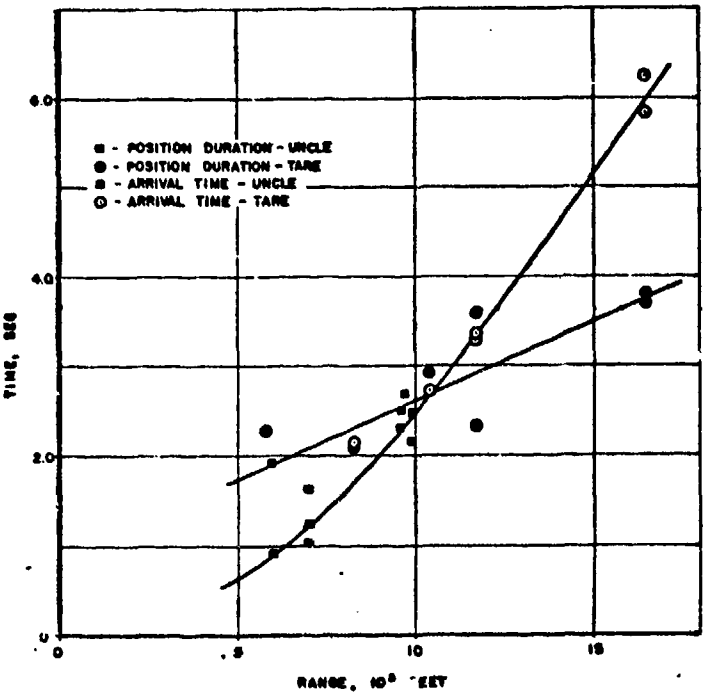


Figure 3.12 Arrival time and positive duration versus distance, Shot Zuni.

ter in the data points but this was expected since it appears from some of the records that the glass disk slipped on the turntable causing a shift in base line which changed the positive duration of those records.

The total positive impulse is listed in Table 3.5 and plotted in Figure 3.13. There is much

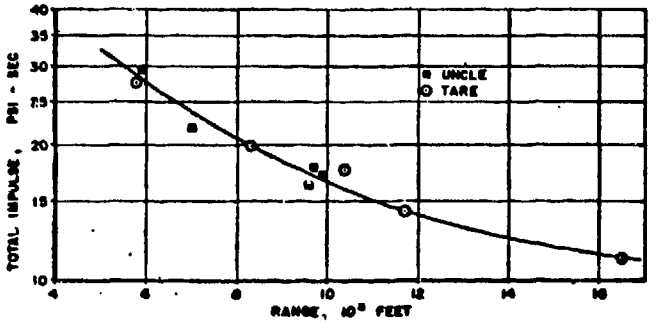


Figure 3.13 Total impulse versus distance, Shot Zuni.

less scatter of the impulse values than the duration values. The dynamic pressure impulse values have not been plotted because it is felt they would be misleading. Some of the q gages were displaced great distances and many of the mounts were bent, which changed the angle of orientation of the gage axis and the shock front and caused the measured pressure to decay at a rate other than normal.



SECRET

## 3.5 SHOT YUMA

Shot Yuma was detonated at a 200-foot height of burst. The predicted yield was approximately 0.3 kt with an upper limit of 2 kt. The actual measured radiochemical yield was 0.188 kt. Shot Yuma was the first fractional-kiloton device to be detonated at the EPG. Therefore, it afforded an opportunity to expand the knowledge of blast phenomena resulting from small nuclear detonations.

3.5.1 Gage Performance. Because of the small yield, the expected duration of the positive pressure pulse was extremely short. Therefore, a higher speed was used to drive the turntable. A 3-rpm motor is normally used for medium and high yield devices, but to gain better time resolution a 10-rpm motor was used for this shot. The 10-rpm motor appeared to be more sensitive to acceleration than did the 3-rpm. The measurement of pressure versus time was not recorded by some of the gages because the motor apparently stopped just after the shock front the gage and then started again during the decay of the positive pressure pulse. When this happens the positive duration and impulse values are lost.

3.5.2 Surface Air-Blast Pressures. The blast line for this shot was only 1,000 feet long. Therefore, the arrival times were short. Because of the start-up time of the motors it was necessary to correct the arrival time and also the positive duration. At the close-in stations the motor was still accelerating to attain a constant rpm during the arrival time and the positive duration. The peak overpressure values listed in Table 3.6 are plotted in Figure 3.14. Four extra $p_t$ gages were installed for Shot Yuma to test new initiation circuits. The circuits were dependent upon nuclear radiation for initiation rather than thermal or light. One gage out of the three worked and the fourth gage was not recovered. Refinements will be made and the new circuits will be tested on future operations.

There was considerable scatter between some measurements made at the same distance. At present no explanation can be found for the difference in the two $p_t$ records from Stations 115.01 and 115.02. These records do not fall within the normal scatter expected from two gages at the same distance. Average values of peak overpressure are plotted in Figure 3.14.

3.5.3 Dynamic Pressure Measurements. The q gages showed evidence of extreme acceleration and all records with the exception of the last station were reliable for peak pressures only and not for duration or impulse. Most of the gages started but when the shock front arrived the turntable slowed down and then started again or stopped completely. The peak recorded dynamic pressure values, with the corrected values, are listed in Table 3.6. The corrected values are plotted in Figure 3.14.

3.5.4 Arrival Time, Duration and Impulse. The recorded values of arrival time, duration and impulse are listed in Table 3.6. The arrival times and durations are plotted in Figure 3.15. Corrections for the lag in motor start-up time have been applied to the arrival time, duration, and impulse measurements where applicable. Only one value for dynamic impulse was recorded, and it is listed in the table but is not plotted. Although there appeared to be some scatter of values plotted in Figure 3.15, it must be noted that these were extremely small units of time and distance.

Values of impulse are plotted and presented in Figure 3.16. All points with the exception of two values show a good trend.

## 3.6 SHOT INCA

Project 1.1 instrumented Shot Inca to back up the electronic measurements being made by Project 1.10. The gage pressure transducers were selected based on a predicted yield of 7 kt. The actual radiochemical yield was measured as 14.8 kt. Whenever the actual yield of a device becomes approximately 100 percent greater than predicted, it poses many problems for the proj-

TABLE 3.6 AIR-BLAST DATA, SHOT YUMA

Gage designations: $p_t$ = side-on pressure versus time, $p_t$ gage; $\Delta p^t_p$ = total pressure versus time, q gage; $\Delta p^t$ = side-on pressure versus time, q gage; $q^t_c$ = dynamic pressure versus time.

| Station | Site | Distance | Gage Type and Number | Peak Pressure | Arrival Time | Positive Duration | Impulse | Corrected Dynamic Pressure, $q_c$ | Remarks |
|---|---|---|---|---|---|---|---|---|---|
| | | ft | | psi | sec | sec | psi-sec | psi | |
| 114.01 | Sally | 0 | $p_t$-202 | — | — | — | — | — | Not Recovered |
| | | | $p_t$- 75 | — | — | — | — | — | Not Recovered |
| 115.01 | Sally | 151 | $p_t$- 49 | 107.0 | — | — | — | — | * |
| | | | $p_t$- 76 | 58.0 | — | — | — | — | * |
| | | | $\Delta p^t_p$- 16 | 63.0 | — | — | — | — | † |
| | | | $\Delta p^t$- 16 | 82.0 | — | — | — | — | † |
| 115.02 | Sally | 251 | $p_t$-201 | 33.6 | — | 0.038 | 0.227 | — | |
| | | | $p_t$-106 | 42.4 | 0.065 | 0.047 | 0.609 | — | |
| | | | $\Delta p^t_p$- 19 | 67.9 | 0.064 | 0.051 | 0.964 | — | |
| | | | $\Delta p^t$- 19 | 38.4 | 0.064 | 0.050 | 0.637 | — | |
| | | | $q^t_c$- 19 | 29.5 | 0.064 | 0.051 | 0.328 | 24.6 | |
| 115.03 | Sally | 363 | $p_t$- 53 | 24.0 | — | — | — | — | * |
| | | | $p_t$- 83 | 26.0 | 0.110 | 0.077 | 0.540 | — | |
| | | | $\Delta p^t_p$- 15 | 35.2 | † | † | † | — | |
| | | | $\Delta p^t$- 15 | 24.9 | † | † | † | — | |
| | | | $q^t_c$- 15 | 11.0 | † | † | † | 10.0 | |
| 115.04 | Sally | 401 | $p_t$-137 | 21.0 | 0.150 | 0.092 | 0.499 | — | |
| | | | $\Delta p^t_p$- 17 | 35.0 | 0.143 | — | — | — | ‡ |
| | | | $\Delta p^t$- 17 | 18.7 | 0.143 | — | — | — | ‡ |
| | | | $q^t_c$- 17 | 30.4 | 0.143 | — | — | — | † |
| 114.02 | Sally | 501 | $p_t$-138 | 14.1 | 0.184 | 0.083 | 0.337 | — | |
| 115.05 | Sally | 604 | $p_t$- 89 | 11.5 | 0.290 | 0.156 | 0.512 | — | |
| | | | $\Delta p^t_p$- 18 | 13.1 | 0.256 | 0.135 | 0.487 | — | |
| | | | $\Delta p^t$- 18 | 10.6 | 0.256 | 0.131 | 0.419 | — | |
| | | | $q^t_c$- 18 | 2.5 | 0.256 | 0.115 | 0.068 | 2.2 | |
| 114.03 | Sally | 803 | $p_t$- 67 | 6.4 | 0.437 | 0.164 | 0.356 | — | |
| 114.04 | Sally | 1,000 | $p_t$- 98 | 4.8 | 0.547 | 0.159 | 0.270 | — | |
| 115.01 | Sally | 151 | $p_t$-167 | — | — | — | — | — | |
| 115.04 | Sally | 401 | $p_t$- 40 | 25.5 | — | — | — | — | * |
| 114.02 | Sally | 501 | $p_t$- 27 | 15.2 | — | 0.082 | 0.325 | — | * |
| 114.04 | Sally | 1,000 | $p_t$- 73 | 4.7 | — | — | — | — | * |

* Peak pressure only obtained.
† Value not considered valid.
‡ Questionable record, not presented in Appendix B.



SECRET

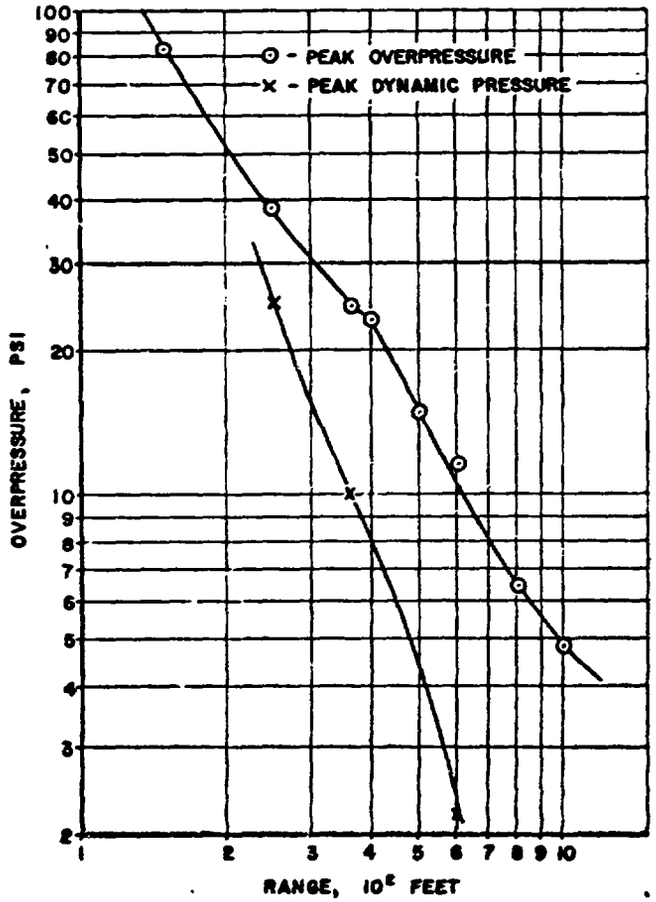


Figure 3.14 Peak overpressure and corrected dynamic pressure, Shot Yuma.

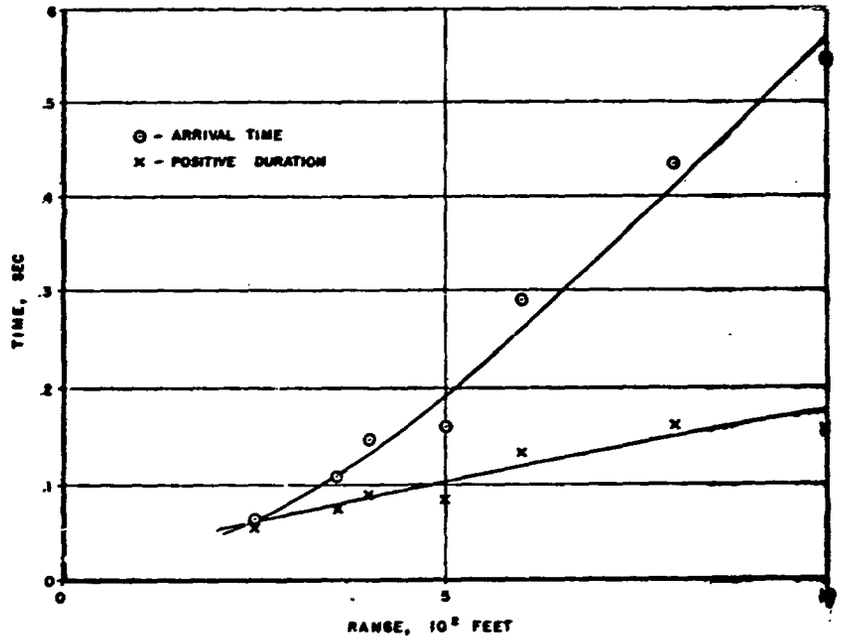


Figure 3.15 Arrival time and positive duration versus distance, Shot Yuma.

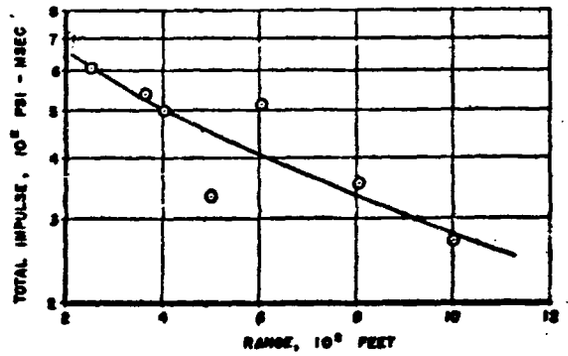


Figure 3.16 Impulse versus distance, Shot Yuma.

ect personnel assigned the task of data reduction and analysis. Some of these problems will be pointed out in the following sections.

3.6.1 Gage Performance. The gage performance for this shot was good as far as the initiation of the gage was concerned. Of the 20 blast-line gages installed, 2 gave peak pressure only. The same percentage of failure was noted for the q gages where one out of ten failed to start. Ten gages with experimental initiation circuits were installed and one out of the ten initiated. These were dependent on nuclear radiation for initiation and the one that started was at 1,160 feet. On Shot Inca, a failure of q gage mounts similar to that noted on Shot Zuni was experienced. The stations at which the mounts failed and the approximate angles they were bent from the vertical are also noted in Table 3.8.

3.6.2 Surface Air-Blast Pressures. Two blast lines were instrumented for Shot Inca. One line consisted of five stations along a vegetated line and the other line consisted of five stations at similar distances along a cleared line. There were two regular $p_t$ gages at each station and one q gage at each station. Many of the pressure sensitive capsules were permanently deformed

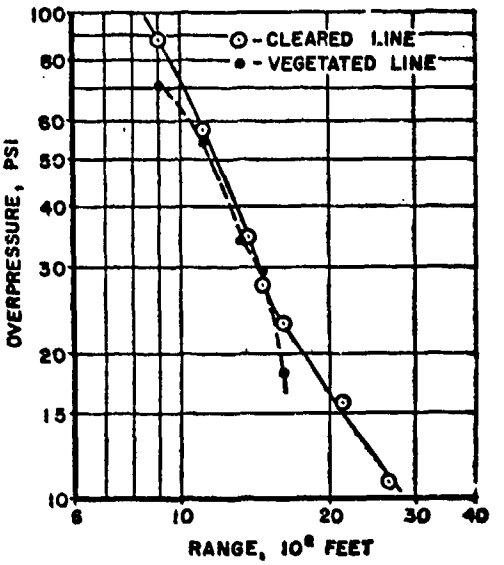


Figure 3.17 Peak overpressure versus distance, Shot Inca.

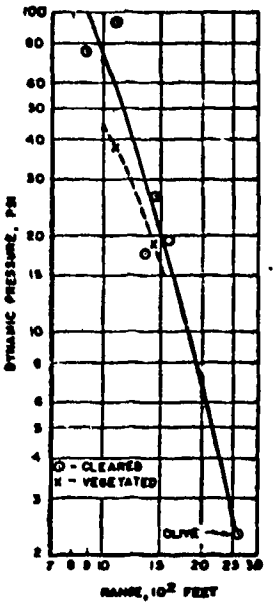


Figure 3.18 Corrected peak dynamic pressure versus distance, Shot Inca.

because of the excessive pressure experienced. Attempts were made to calibrate similar capsules and determine the pressure required to record a similar deflection. This procedure was felt to be fairly accurate for peak values but capsules overstressed beyond certain limits would not return to zero deflection at zero overpressure and similar capsules would not decay at the same rate. Therefore, only the curves of pressure versus time which are felt to be reasonably accurate are presented in Appendix B, although the peak values are used in plotting. The values of peak overpressure are listed in Table 3.7 and the mean average of these values is plotted in Figure 3.17.

There appears to be a definite separation in the two curves of pressure versus distance presented in Figure 3.17. The values of peak overpressure along the cleared line are higher than the values along the vegetated line with the exception of Station 115.19 at 1,450 feet from ground zero. Some values of pressure plotted along the cleared line represent as many as four measurements, since certain stations had four $p_t$ gages installed. A mean average was plotted for these stations.

TABLE 2.7 AIR-BLAST DATA, SHOT INCA

Gage designations: $p_i$ - side-on pressure versus time, $p_i$ gage; $\Delta p'_p$ - total pressure versus time, q gage; $\Delta p^s$ - side-on pressure versus time, q gage, $q^s_c$ - dynamic pressure versus time.

| Station | Site | Ground Range | Gage Type and Number | Peak Overpressure | Arrival Time | Positive Duration | Total Impulse | Corrected Dynamic Pressure, $q_c$ | Remarks |
|---|---|---|---|---|---|---|---|---|---|
| | | ft | | psi | sec | sec | psi-sec | psi | |
| 115.14 | Pearl, Cleared | 900 | $p_i$-269 | 86.6 | 0.105 | 0.344 | 2.766 | — | |
| | | | $p_i$- 76 | — | — | — | — | — | * |
| 115.16 | Pearl, Cleared | 1,100 | $p_i$- 7 | 62.6 | 0.170 | 0.381 | 4.456 | — | |
| | | | $p_i$-286 | 52.0 | — | — | — | — | † |
| 115.18 | Pearl, Cleared | 1,360 | $p_i$- 70 | 38.0 | 0.262 | 0.320 | 3.306 | — | † |
| | | | $p_i$-138 | 38.0 | — | — | — | — | † |
| | | | $p_i$-182 | 36.0 | 0.280 | 0.403 | 4.227 | — | † |
| | | | $p_i$-296 | 35.9 | — | — | — | — | ‡ |
| 115.20 | Pearl, Cleared | 1,450 | $p_i$- 67 | 27.9 | 0.305 | 0.406 | 3.329 | — | |
| | | | $p_i$-137 | 26.2 | 0.335 | 0.391 | * | — | |
| | | | $p_i$- 39 | 30.1 | — | — | — | — | ‡ |
| | | | $p_i$-166 | 26.6 | — | — | — | — | ‡ |
| 115.27 | Pearl, Cleared | 1,600 | $p_i$- 49 | 23.6 | — | — | — | — | ‡ |
| | | | $p_i$- 66 | 22.6 | 0.423 | 0.439 | 3.170 | — | |
| | | | $p_i$- 64 | 22.5 | — | — | — | — | ‡ |
| | | | $p_i$- 65 | 23.9 | — | — | — | — | ‡ |
| 115.28 | Pearl, Cleared | 2,130 | $p_i$- 76 | 15.4 | — | — | — | — | ‡ |
| | | | $p_i$-161 | 16.2 | — | — | — | — | ‡ |
| 115.29 | Olive | 2,640 | $p_i$- 6 | 10.7 | — | — | — | — | ‡ |
| | | | $p_i$- 71 | 11.0 | — | — | — | — | ‡ |
| 115.29 | Olive, 0 degrees | 2,640 | $\Delta p^s_p$ - 9 | 12.7 | 1.063 | 0.566 | 2.367 | — | |
| | | | $\Delta p^s$- 9 | 14.2 | 1.063 | 0.581 | 2.046 | — | |
| | | | $q^s_c$- 9 | 2.3 | 1.063 | 0.450 | 0.329 | 2.3 | |
| | 32 degrees | 2,640 | $\Delta p^s_p$- 16 | 10.8 | 1.195 | 0.569 | 1.889 | — | |
| | | | $\Delta p^s$- 16 | 9.1 | 1.195 | 0.466 | 1.614 | — | |
| | | | $q^s_c$- 16 | 1.7 | 1.195 | 1.457 | 0.431 | — | |
| | 41 degrees | 2,640 | $\Delta p^s_p$- 12 | 9.6 | 1.260 | 0.559 | 1.942 | — | |
| | | | $\Delta p^s$- 12 | 7.6 | 1.260 | 0.551 | 1.613 | — | |
| | | | $q^s_c$- 12 | 1.8 | 1.260 | 1.555 | 0.306 | — | |
| | 50 degrees | 2,640 | $\Delta p^s_p$- 10 | 9.3 | 1.275 | 0.586 | 1.766 | — | |
| | | | $\Delta p^s$- 10 | 9.2 | 1.275 | 0.577 | 1.697 | — | |
| | | | $q^s_c$- 10 | 3.2 | 1.275 | 0.601 | 0.066 | — | |
| 115.13 | Pearl, Vegetated | 900 | $p_i$-149 | 90.6 | 0.100 | 0.256 | 2.337 | — | |
| | | | $p_i$-291 | — | — | — | — | — | * |
| 115.15 | Pearl, Vegetated | 1,100 | $p_i$- 65 | 54.0 | 0.180 | 0.493 | 5.771 | — | |
| | | | $p_i$- 73 | 48.0 | — | — | — | — | † |
| 115.17 | Pearl, Vegetated | 1,310 | $p_i$- 57 | 36.0 | — | — | — | — | |
| | | | $p_i$- 83 | 32.5 | 0.288 | 0.328 | 2.497 | — | ‡ |
| 115.19 | Pearl, Vegetated | 1,450 | $p_i$- 5 | 23.0 | 0.318 | 0.463 | 3.764 | — | |
| | | | $p_i$- 27 | — | — | — | — | — | * |
| 115.21 | Pearl, Vegetated | 1,600 | $p_i$- 49 | 17.0 | 0.360 | 0.466 | 2.945 | — | |
| | | | $p_i$-215 | 16.9 | 0.350 | 0.410 | 3.179 | — | |

* Capsule split or hit stop; values not considered valid.
† Questionable record; not presented in Appendix B.
‡ Peak pressure only obtained.



SECRET

TABLE 3.8 DYNAMIC PRESSURE DATA, SHOT INCA

Gage designations: $p_t$ = side-on pressure versus time, $p_t$ gage; $\Delta p^t_p$ = total pressure versus time, q gage; $\Delta p^s$ = side-on pressure versus time, q gage; $q^t_c$ = dynamic pressure versus time.

| Station | Site | Ground Range | Gage Type and Number | Peak Pressure | Corrected Dynamic Pressure, $q_c$ | Mount Displacement from Vertical |
|---|---|---|---|---|---|---|
| | | ft | | psi | psi | deg |
| 115.14 | Pearl, Cleared | 900 | $\Delta p^s_p$-19 | 181.0 | — | — |
| | | | $\Delta p^t$-19 | 90.0 | — | — |
| | | | $q^t_c$-19 | 96.0 | 74.3 | 90 |
| 115.16 | Pearl, Cleared | 1,100 | $\Delta p^s_p$- 6 | 198.0 * | — | — |
| | | | $\Delta p^s$- 6 | 61.7 | — | — |
| | | | $q^t_c$- 6 | 136.3 | 92.8 | 30 |
| 115.18 | Pearl, Cleared | 1,360 | $\Delta p^t_p$-15 | 54.0 | — | — |
| | | | $\Delta p^t$-15 | 46.0 | — | — |
| | | | $q^t_c$-15 | 20.0 | 17.5 | 0 |
| 115.29 | Pearl, Cleared | 1,450 | $\Delta p^s_p$-14 | 47.6 | — | — |
| | | | $\Delta p^t$-14 | 31.0 | — | — |
| | | | $q^t_c$-14 | 37.0 | — | 0 |
| 115.27 | Pearl, Cleared | 1,600 | $\Delta p^s_p$- 8 | 49.0 | — | — |
| | | | $\Delta p^t$- 8 | 26.0 | — | — |
| | | | $q^t_c$- 8 | 23.0 | 19.4 | 0 |
| 115.13 | Pearl, Vegetated | 900 | $\Delta p^t_p$- 3 | 142.0 | — | — |
| | | | $\Delta p^t$- 3 | — | — | — |
| | | | $q^t_c$- 3 | — | — | 90 |
| 115.15 | Pearl, Vegetated | 1,100 | $\Delta p^t_p$- 5 | 115.0 | — | — |
| | | | $\Delta p^t$- 5 | 71.0 | — | — |
| | | | $q^t_c$- 5 | 44.0 | 37.6 | 30 |
| 115.17 | Pearl, Vegetated | 1,310 | $\Delta p^t_p$-17 | 52.8 | — | — |
| | | | $\Delta p^t$-17 | — | — | — |
| | | | $q^t_c$-17 | — | — | 15 |
| 115.19 | Pearl, Vegetated | 1,450 | $\Delta p^t_p$-18 | 51.0 | — | — |
| | | | $\Delta p^t$-18 | 29.0 | — | — |
| | | | $q^t_c$-18 | 22.0 | 18.8 | 0 |
| 115.21 | Pearl, Vegetated | 1,600 | $\Delta p^t_p$-12 | — | — | — |
| | | | $\Delta p^t$-12 | 27.2 | — | — |
| | | | $q^t_c$-12 | — | — | 0 |

* Peak pressure only obtained.



SECRET

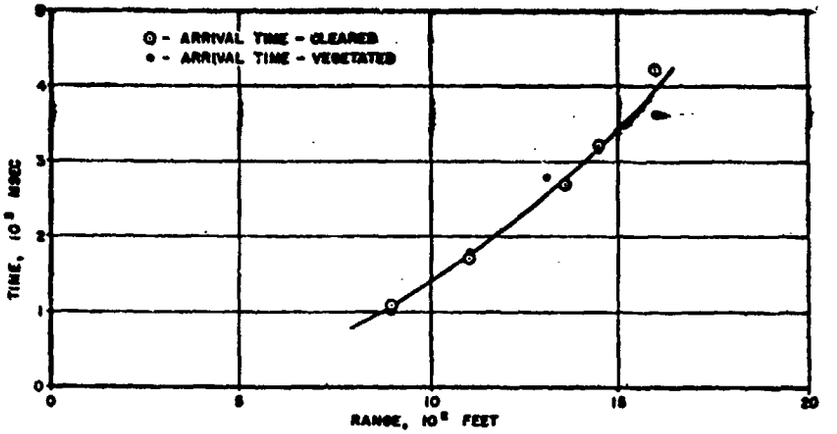


Figure 3.19 Arrival time versus distance, Shot Inca.

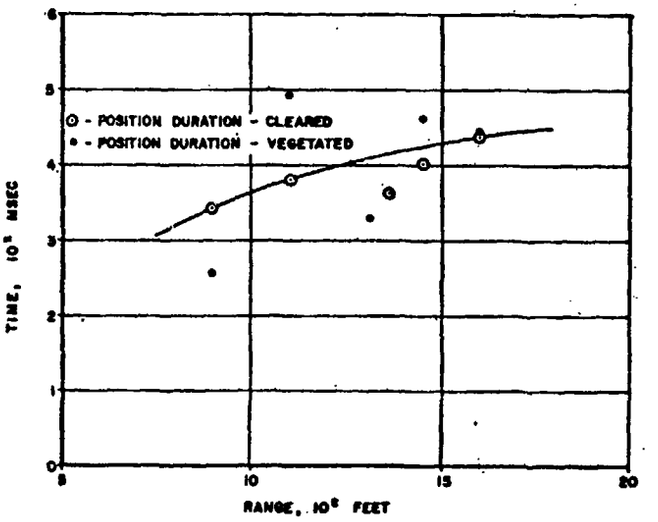


Figure 3.20 Positive duration versus distance, Shot Inca.

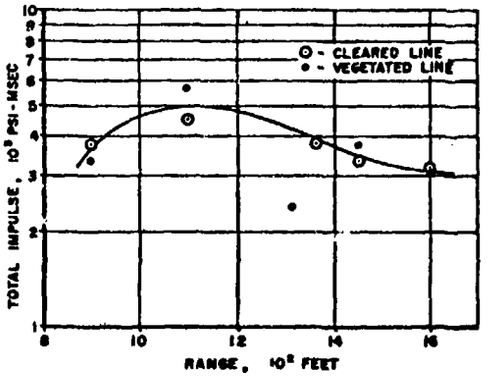


Figure 3.21 Total impulse versus distance, Shot Inca.



SECRET

3.6.3 Dynamic Pressure Measurements. Dynamic pressure measurements made along both blast lines are questionable for pressure versus time values and in many cases the peak dynamic pressure values are also questionable. The higher-than-expected yield and strong precursor were the factors contributing to the poor records. The q gage mounts at Stations 115.13, 115.14, 115.15, 115.16 and 115.17 were all bent back at various angles, which pointed the nose of the q gage upward. The response of the q gage mount is not known experimentally but calculations based on dynamic pressure and the mount configuration show that at dynamic pressures of from 300 to 400 psi the gage mount may tilt back 15 degrees within 20 msec, while at dynamic pressures of from 20 to 30 psi it would take 80 msec to bend 15 degrees. It is felt that a change in orientation of 15 degrees would appreciably change the dynamic pressure recorded by the BRL q gage.

Peak dynamic pressure values are questionable at many stations because of the overstressing of the pressure sensing capsules. Some capsules were permanently deformed, which made it impossible to determine the pressure from the over-calibration of a similar capsule. The peak overpressure values of the total and side-on elements are listed in Table 3.8. The maximum corrected difference between the two records has been plotted in Figure 3.18.

3.6.4 Arrival Time, Positive Duration and Total Impulse. Corrected values of arrival time, duration, and impulse are listed in Table 3.7. The curve of arrival time versus ground distance is plotted in Figure 3.19. It must be assumed from the curve that there was no appreciable difference in the arrival time along the two blast lines.

The values of positive duration are plotted in Figure 3.20. There is a considerable scatter of points and it is difficult to see any trend or difference between the two blast lines with the exception that there is more scatter along the vegetated line.

With a difference in pressure along the two lines and the scatter in positive duration along the two blast lines, a great scatter was expected in the impulse values. Only one value appears out of line in the plot of impulse values in Figure 3.21. The impulse values do not follow the usual trend of decreasing with distance, since the values at 900 feet on both lines are lower than those at 1,100 feet.

3.6.5 Orientation Effect on the BRL q Gage. All q gages installed on Shot Cherokee were subjected to flow in direction other than along the axis of the gage. It was thought that some of the records could be interpreted if the effect of the angle of orientation could be determined. Four q gages were installed for Shot Inca at a distance of 2,640 feet on Site Olive. The angles of orientation were 0, 32, 41, and 50 degrees. These angles were chosen to match the gages at Man-Made Islands Nos. 2 and 3 and Site Dog. The measured values for the gages are listed in Table 3.7 and the curves of pressure versus time are presented in Appendix B. From these curves the difficulty in applying any correction factor to the measured pressure at a given angle to obtain the 0 degree conditions is quite obvious. It is felt by the authors that computing dynamic pressure versus time from the records measured at ground baffle gages would better represent the input conditions than attempting to correct the measured dynamic pressure by any angle of orientation factor.

# Chapter 4
# DISCUSSION

## SURFACE AIR-BLAST DATA

A. Air-blast measurements recorded by the $p_t$ gages were surface measurements, with the exception of the reef stations where the gage face varied from 2 feet to 6 feet above the water surface, depending on the tide. The measured values of overpressure, duration, arrival time and impulse have been scaled to 1 kt at sea level, using ambient conditions at burst height. These scaled values have been tabulated for the various shots and presented in Tables 4.1 through 4.6. Shot Cherokee values were also scaled using the modified Sachs scaling where the ambient conditions at the surface are considered. Because of the yield and height of burst the shock front traveled most of the distance along surface and it is felt that using the ambient conditions along the surface may be a more logical approach.

4.1.1 Surface Bursts, Shots Lacrosse and Zuni. Both Shots Lacrosse and Zuni were considered surface bursts and on both shots a precursor was documented in the higher pressure region. The precursors formed at the NTS appeared to be stronger and a clean or classical wave shape was not realized until the 6 to 10 psi region was reached. The precursors formed at the EPG died out sooner and a classical wave shape was realized at a higher pressure level, 35 psi on Shot Lacrosse and 20 psi on Shot Zuni. It should be noted that a precursor has not been documented from a surface burst at the NTS, and therefore no direct comparison could be made.

The extent of the precursor cycle is a function of both the yield and height of burst. As the height of burst is lowered the angle of incidence of the thermal radiation is increased and there is less heating of the surface at the greater distances. Therefore, for surface and near surface bursts the precursor will complete its cycle sooner and a classical wave shape will appear at shorter ground distances and higher pressures than would be expected for the same yield at higher heights of burst.

Comparisons of values taken from the curves of pressure versus distance for Shots Lacrosse and Zuni are presented in Figure 4.1 where they are plotted with the height of burst curves for an average surface taken from TM 23-200 (Reference 4). Only the Site Tare blast line was considered for this comparison and, as can be seen, the two shots showed little scatter. The A-scaled values for average overpressure, dynamic pressure, arrival time, duration, and impulse for Shot Lacrosse are listed in Table 4.1. Similar values for Shot Zuni are listed in Table 4.2.

4.1.2 Air Bursts, Shots Cherokee, Yuma and Inca. The first air burst of the series instrumented by Project 1.1 was Shot Cherokee. Unfortunately, the upper range of pressure measured was below 11 psi and the lower range was greater than 4 psi. Therefore, the range of pressure was small but the number of records and the documentation was extensive. Peak overpressure values were A-scaled using the Sachs scaling method and plotted in Figure 4.2. Points from the curve in Figure 4.2 are plotted in Figures 4.1 and 4.10, where the comparison with the average surface and good surface height of burst curves can be seen. The indication here is that a particular pressure level extends to a greater distance than would be predicted from the average or good surface height of burst curves. The scaling is based on a yield of 3.8 Mt, although there is a ± 0.3 spread. If a yield of 4.1 Mt were used in obtaining the scaling factors, it would move the values much closer to the average and good surface curves, but the trend would still be in the same direction. The average values from Table 3.4 have been scaled using the straight Sachs scaling and listed in Table 4.3 and plotted in Figure 4.2. The same values from Table 3.4 were

TABLE 4.1 A-SCALED AIR-BLAST DATA, SHOT LACROSSE

| Station | Site | Ground Range | Peak Pressure | Arrival Time | Positive Duration | Total Impulse | Corrected Dynamic Pressure, $q_c$ |
|---|---|---|---|---|---|---|---|
| | | ft | psi | sec | sec | psi-sec | psi |
| 114.15 | Yvonne | 350 | 136.0 | 0.038 | 0.110 | 1.564 | — |
| 115.22 | Yvonne | 472 | 56.6 | — | — | — | 73.7 |
| 115.23 | Yvonne | 579 | 36.1 | 0.130 | 0.162 | 1.226 | 15.9 |
| 115.24 | Yvonne | 742 | 19.6 | 0.212 | 0.197 | 1.077 | — |
| 114.16 | Yvonne | 823 | 15.6 | 0.280 | 0.217 | 1.010 | — |
| 115.25 | Yvonne | 995 | 10.9 | 0.389 | 0.265 | 0.850 | 2.3 |
| 115.31 | Yvonne | 1,156 | — | 0.486 | 0.215 | — | 1.04 |
| 114.18 | Yvonne | 1,300 | — | 0.618 | 0.286 | — | — |
| 115.26 | Yvonne | 1,544 | 4.5 | 0.765 | 0.313 | — | 0.46 |
| 114.19 | Yvonne | 2,094 | — | — | — | — | — |

TABLE 4.2 A-SCALED AIR-BLAST DATA, SHOT ZUNI

| Station | Site | Ground Range | Peak Overpressure | Arrival Time | Positive Duration | Total Impulse | Corrected Dynamic Pressure, $q_c$ |
|---|---|---|---|---|---|---|---|
| | | ft | psi | sec | sec | psi-sec | psi |
| 114.05 | Sugar | 207 | — | — | — | — | — |
| 114.06 | Sugar | 334 | 67.3 | — | — | — | — |
| 115.06 | Sugar | 380 | 67.3 | — | 0.151 | 1.797 | 48.3 |
| 114.07 | Roger | 452 | 45.5 | — | — | — | — |
| 115.07 | Roger | 544 | 24.2 | 0.161 | 0.143 | 1.304 | 17.6 |
| 115.08 | Peter | 661 | 20.1 | 0.189 | 0.193 | 1.161 | 8.2 |
| 114.08 | Peter | 766 | 17.2 | 0.249 | 0.195 | 0.952 | — |
| 115.09 | Peter | 904 | 11.6 | — | — | — | 3.2 |
| 114.09 | Oboe | 1,061 | 6.2 | 0.386 | 0.248 | 0.744 | — |
| 114.10 | Uncle | 293 | 200* | — | — | — | — |
| 115.10 | Uncle | 333 | 124.8 | — | — | — | — |
| 114.11 | Uncle | 386 | 57.7 | 0.061 | 0.128 | 1.937 | — |
| 115.11 | Uncle | 469 | 66.8 | 0.076 | 0.106 | 1.443 | — |
| 115.12 | Uncle | 647 | 23.6 | 0.182 | 0.164 | 1.128 | 17.9 |
| 156.01 | Uncle | 633 | 21.4 | — | 0.179 | 1.171 | 17.0 |
| 156.02 | Uncle | 629 | 23.1 | 0.165 | 0.155 | 1.067 | 11.1 |

* Capsule overstressed.

TABLE 4.3 A-SCALED AIR-BLAST DATA, SHOT CHEROKEE

| Station | Site | Range | Peak Overpressure | Arrival Time | Positive Duration | Total Impulse |
|---|---|---|---|---|---|---|
| | | ft | psi | sec | sec | psi-sec |
| 112.01 | Charlie | 1,106 | 12.7 | 0.498 | — | — |
| 113.01 | Reef East of Charlie | 1,008 | — | 0.417 | — | — |
| 113.02 | Reef East of Charlie | 1,032 | 11.1 | 0.406 | 0.206 | 1.003 |
| 113.03 | Reef East of Charlie | 934 | 9.3 | 0.387 | 0.192 | 0.884 |
| 113.04 | Reef East of Charlie | 994 | 10.7 | 0.413 | 0.219 | 0.941 |
| 113.05 | Reef East of Charlie | 1,039 | 8.5 | 0.449 | 0.222 | 0.880 |
| 113.06 | Reef East of Charlie | 1,113 | 8.0 | 0.509 | 0.240 | 0.849 |
| 113.07 | Man-Made Island No. 1 | 1,178 | 10.4 | 0.551 | 0.245 | 0.906 |
| 113.08 | Man-Made Island No. 2 | 1,247 | 8.5 | 0.589 | 0.259 | 0.848 |
| 113.09 | Man-Made Island No. 3 | 1,432 | 6.9 | 0.748 | 0.285 | 0.796 |
| 113.10 | Dog | 1,611 | 5.3 | 0.891 | 0.295 | 0.637 |
| 113.11 | Able | 1,870 | 4.6 | 1.038 | 0.371 | 0.738 |



SECRET

TABLE 4.4 MODIFIED SACHS SCALING, SHOT CHEROKEE

| Station | Site | Range | Peak Overpressure | Arrival Time | Positive Duration | Total Impulse |
|---|---|---|---|---|---|---|
| | | ft | psi | sec | sec | psi-sec |
| 112.01 | Charlie | 1,225 | 10.9 | 0.528 | — | — |
| 113.01 | Reef East of Charlie | 1,120 | — | 0.442 | — | — |
| 113.02 | Reef East of Charlie | 1,086 | 9.5 | 0.430 | 0.219 | 0.915 |
| 113.03 | Reef East of Charlie | 1,034 | 8.0 | 0.410 | 0.203 | 0.806 |
| 113.04 | Reef East of Charlie | 1,045 | 9.2 | 0.438 | 0.232 | 0.858 |
| 113.05 | Reef East of Charlie | 1,092 | 7.6 | 0.475 | 0.236 | 0.803 |
| 113.06 | Reef East of Charlie | 1,170 | 6.9 | 0.539 | 0.254 | 0.793 |
| 113.07 | Man-Made Island No. 1 | 1,228 | 8.9 | 0.584 | 0.260 | 0.826 |
| 113.08 | Man-Made Island No. 2 | 1,341 | 7.3 | 0.624 | 0.274 | 0.771 |
| 113.09 | Man-Made Island No. 3 | 1,505 | 5.9 | 0.792 | 0.302 | 0.726 |
| 113.10 | Dog | 1,693 | 4.5 | 0.944 | 0.313 | 0.581 |
| 113.11 | Able | 1,966 | 4.1 | 1.100 | 0.393 | 0.673 |

TABLE 4.5 A-SCALED AIR-BLAST DATA, SHOT YUMA

| Station | Site | Distance | Peak Pressure | Arrival Time | Positive Duration | Total Impulse | Dynamic Pressure, $q_c$ |
|---|---|---|---|---|---|---|---|
| | | ft | psi | sec | sec | psi-sec | psi |
| 114.01 | Sally | 0 | — | — | — | — | — |
| 115.01 | Sally | 262 | 83.5 | — | — | — | — |
| 115.02 | Sally | 436 | 38.9 | 0.114 | 0.082 | 1.082 | 25.1 |
| 115.03 | Sally | 631 | 24.8 | 0.193 | 0.135 | 0.959 | 10.1 |
| 115.04 | Sally | 696 | 23.6 | 0.263 | 0.161 | 0.886 | — |
| 114.02 | Sally | 870 | 14.9 | 0.284 | 0.146 | 0.588 | — |
| 115.05 | Sally | 1,049 | 11.6 | 0.509 | 0.275 | 0.909 | 2.2 |
| 114.03 | Sally | 1,395 | 6.5 | 0.766 | 0.288 | 0.632 | — |
| 114.04 | Sally | 1,737 | 4.9 | 0.959 | 0.279 | 0.480 | — |

TABLE 4.6 A-SCALED AIR-BLAST DATA, SHOT INCA

| Station | Site | Ground Range | Peak Overpressure | Arrival Time | Positive Duration | Total Impulse |
|---|---|---|---|---|---|---|
| | | ft | psi | sec | sec | psi-sec |
| 115.14 | Pearl, Cleared | 365 | 89.0 | 0.043 | 0.141 | 1.556 |
| 115.16 | Pearl, Cleared | 446 | 57.7 | 0.069 | 0.156 | 1.843 |
| 115.18 | Pearl, Cleared | 552 | 34.9 | 0.111 | — | 1.570 |
| 115.20 | Pearl, Cleared | 588 | 28.0 | 0.131 | 0.163 | 1.376 |
| 115.27 | Pearl, Cleared | 649 | 23.5 | 0.173 | 0.179 | 1.310 |
| 115.28 | Pearl, Cleared | 864 | 15.6 | — | — | — |
| 115.29 | Pearl, Cleared | 1,071 | 11.0 | — | — | — |
| 115.13 | Pearl, Vegetated | 365 | 81.0 | 0.041 | 0.105 | 1.380 |
| 115.15 | Pearl, Vegetated | 446 | 47.6 | 0.074 | 0.201 | 2.388 |
| 115.17 | Pearl, Vegetated | 552 | 34.6 | 0.116 | 0.134 | 1.032 |
| 115.19 | Pearl, Vegetated | 588 | 29.3 | 0.129 | 0.189 | 1.584 |
| 115.21 | Pearl, Vegetated | 649 | 18.2 | 0.149 | 0.181 | 1.240 |

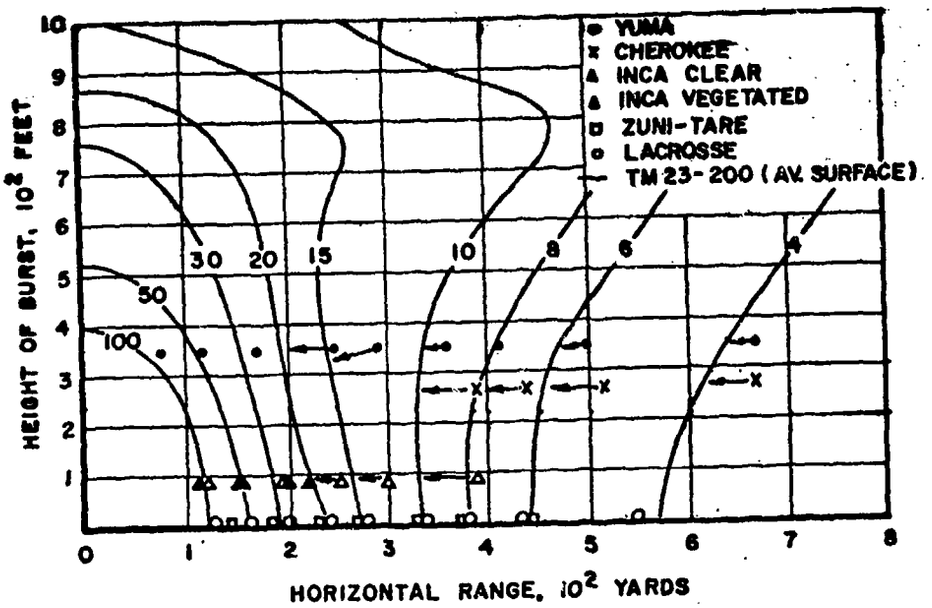


Figure 4.1 A-scaled height of burst, pressure versus distance curves, average surface.

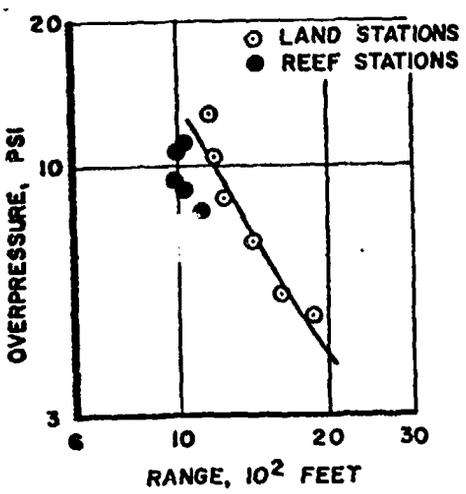


Figure 4.2 A-scaled pressure versus distance, Shot Cherokee

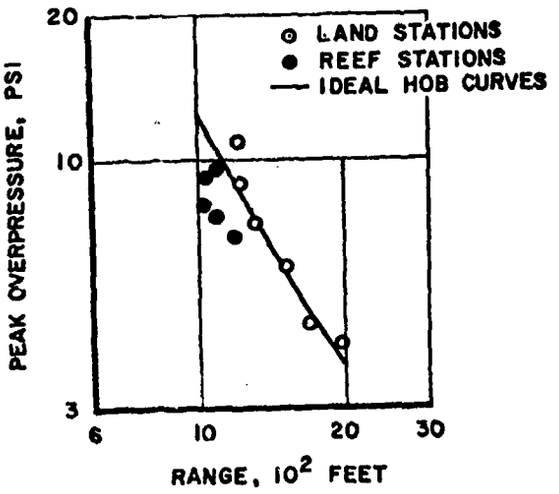


Figure 4.3 Modified Sachs scaling versus distance, Shot Cherokee.

also scaled using Sachs modified scaling and these values are listed in Table 4.4 and plotted in Figure 4.3. The curve drawn in Figure 4.3 was taken from ideal height of burst curves as defined and discussed in WT-782 (Reference 6). There is excellent correlation between the ideal height of burst case and the modified Sachs scaling.

Shot Yuma was the fourth shot instrumented by Project 1.1. The measured values have been scaled to 1 kt at sea level and listed in Table 4.5. The scaled pressures are plotted in Figure 4.4, along with a curve from the ideal height of burst curves and the average surface height of burst curves. The measured pressures fall between these two curves, and it would appear that the validity of scaling fractional kiloton devices is verified. The scaled pressures have also been plotted in Figures 4.1 and 4.10, where the comparison with other Operation Redwing shots can be seen.

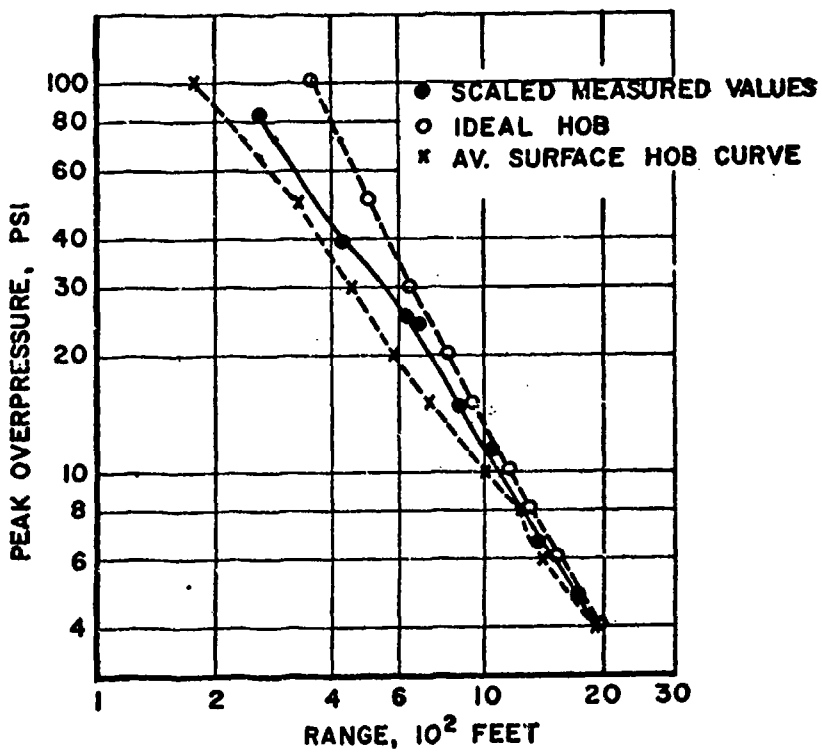


Figure 4.4 A-scaled pressure versus distance, Shot Yuma.

The ground surface pressure measurements recorded on Shot Inca have been scaled to 1 kt, using the Sachs straight scaling or A-scaling. The values from both surfaces have been plotted on the average surface and good surface height of burst curves in Figures 4.1 and 4.10 to show the comparison with the other shots. The comparison of the cleared line with the height of burst curves for a good surface is better than the comparison with the average surface. The vegetated line compares well with the average surface height of burst curves, although a vegetated line should be considered a poor surface.

The pressures have also been scaled and plotted in Figure 4.11 and 4.12, along with good and average surface curves of pressure versus distance.

## 4.2 DYNAMIC PRESSURE MEASUREMENTS

BRL q gages were installed on all shots in which Project 1.1 participated. The gages appeared to give reliable peak readings from the total and side-on pressure elements. The difference be-

tween the two measured pressures is defined as the uncorrected dynamic pressure. The dynamic pressures have been corrected for Mach flow, compressibility and gage configuration and compared with the theoretical value of $\frac{1}{2} \rho u^2$, which is expressed in terms of side-on pressure in the equation:

$$q_c = \frac{2.5 (P_s)^2}{P_s + 7P_0} \tag{4.1}$$

Where: $P_s$ = Peak side-on overpressure

$P_0$ = Atmosphere pressure

4.2.1 Dynamic Pressure from Surface Bursts, Shots Lacrosse and Zuni. The free-air pressure-distance curve from TM 23-200 was used as a basis for calculating an A-scaled dynamic pressure curve. Using the free air for a 1 kt yield, a free-air dynamic pressure curve for a yield of 1 kt was calculated from equation 4.1. The 1 kt free-air dynamic pressure curve was then scaled to an equivalent yield of 1.6 kt and plotted in Figure 4.5. The scaled values of dynamic pressure measured on Shots Lacrosse and Zuni are plotted in the same figure. Since Shot Zuni was almost 1,000 times greater in yield than Shot Lacrosse and the yield values were arrived at by different methods it would appear that the scaling laws have been verified and the 1.6 W theory fits the measured data better than the 2 W theory.

4.2.2 Dynamic Pressure Measurements from Air Bursts, Shots Yuma, Cherokee and Inca. The dynamic pressures measured on Shot Yuma have been scaled to 1 kt and plotted in Figure 4.6. The side-on pressure from the ground surface $p_t$ gages did not fit the average surface or ideal height of burst curves and therefore the dynamic pressures were not expected to fit any height of burst curve. Values of dynamic pressure were calculated from the measured curve in Figure 4.4 using equation 4.1. This curve, along with the measured values scaled to 1 kt, is presented in Figure 4.6. The correlation is excellent.

The dynamic pressure measurements made on Shot Cherokee were considered a total loss. The decision was based on records from Shot Inca where three gages were placed at angles similar to those on Shot Cherokee and results showed that any attempt to establish a correction factor was impractical.

Dynamic pressure measurements made along the blast lines on Shot Inca were all questionable on two counts. First, the pressure capsules were overstressed to such an extent that any method of recalibration or establishing a similar calibration curve from another capsule was questionable. Secondly, the gage mounts failed at the close-in stations and therefore any values of pressure versus time were also of doubtful value. The peak dynamic pressure value from Shot Inca has not been scaled and compared with other shots.

## 4.3 TIME OF ARRIVAL MEASUREMENTS

The time of arrival of the shock front at the various horizontal ranges for the five shots have been A-scaled and plotted in the form of height of burst curves in Figure 4.7. The time of arrival curves from Reference 4 are also presented in Figure 4.7 for comparison. Most of the points plotted show arrival times less than indicated from Reference 4 which, if true, means that there is still some lag in the timing mechanism that has not been accounted for.

## 4.4 DURATION MEASUREMENTS

The durations of the positive pressure phase of the shock waves produced by the detonations of the various shots have all been A-scaled and plotted in Figure 4.8 with the height of burst curves from Reference 4. There is considerable deviation from the established curves but there was also a wide range of yields and ground surfaces which would contribute to the scatter.

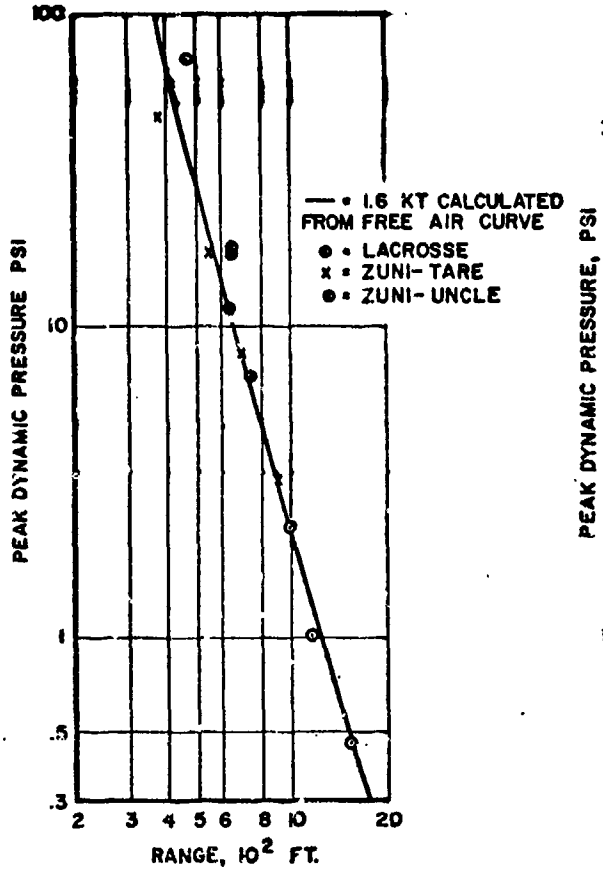


Figure 4.5 A-scaled corrected peak dynamic pressure versus distance, Shots Lacrosse and Zuni.

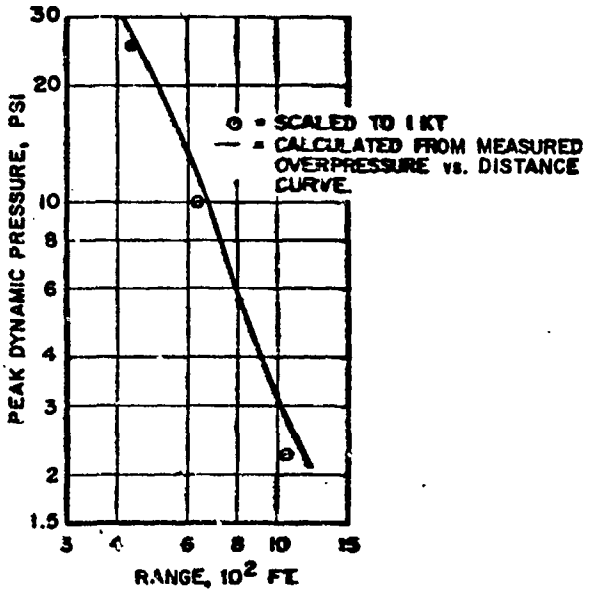


Figure 4.6 A-scaled corrected peak dynamic pressure versus distance, Shot Yuma.

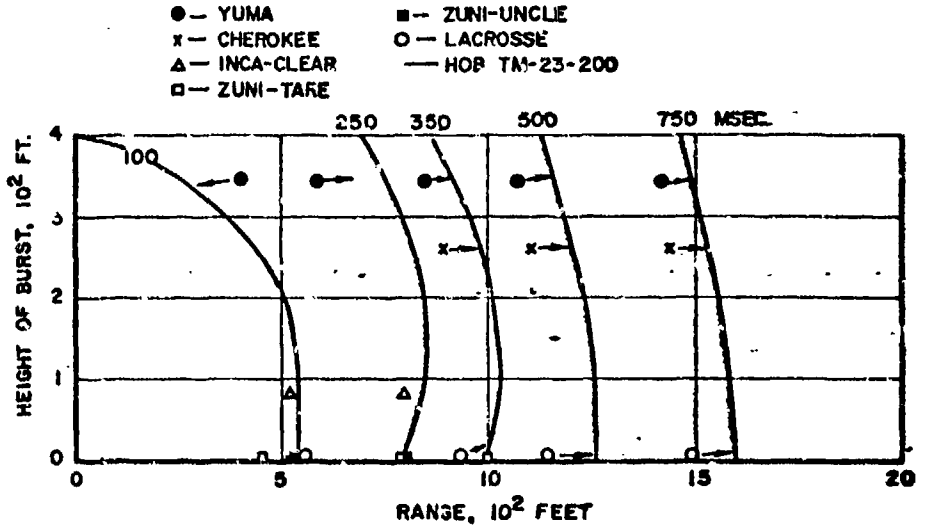


Figure 4.7 A-scaled height of burst curves, arrival time versus distance.



SECRET

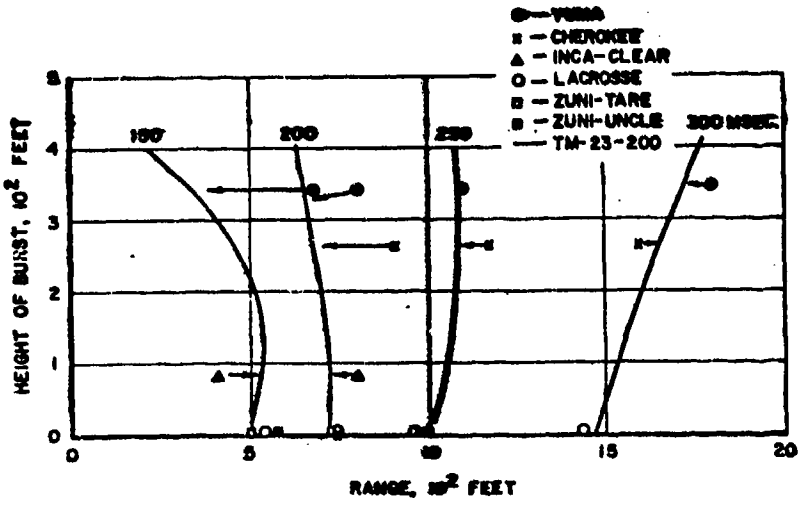


Figure 4.8 A-scaled height of burst curves, positive duration versus distance.

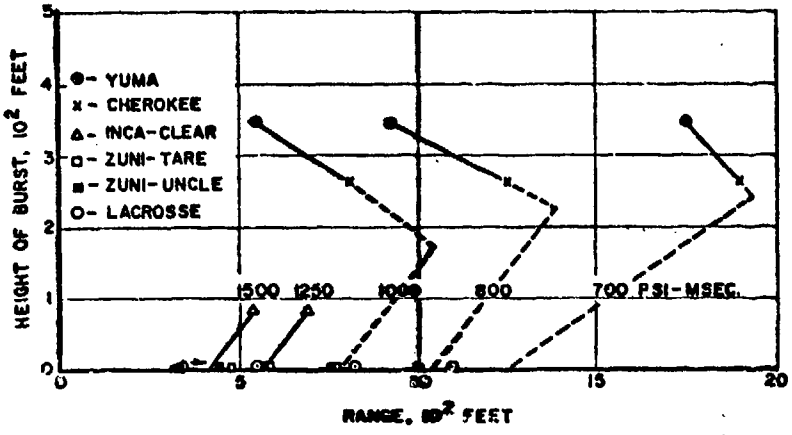


Figure 4.9 A-scaled height of burst curves of impulse versus distance.

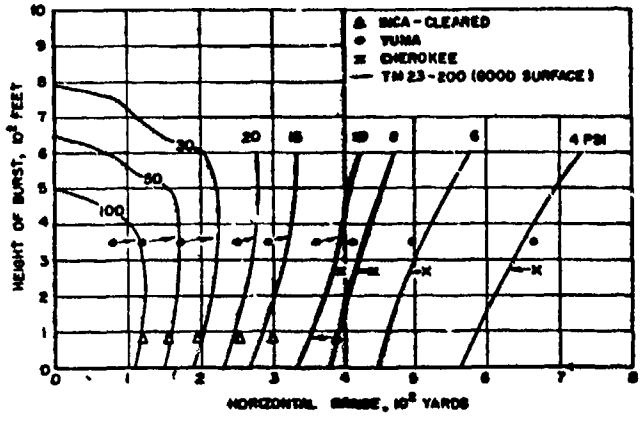


Figure 4.10 A-scaled height of burst, pressure versus distance curves, good surface

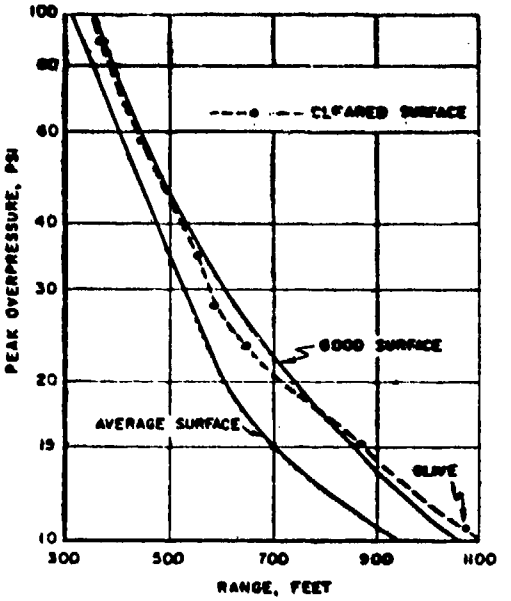


Figure 4.11 A-scaled peak overpressure versus distance, Shot Inca.

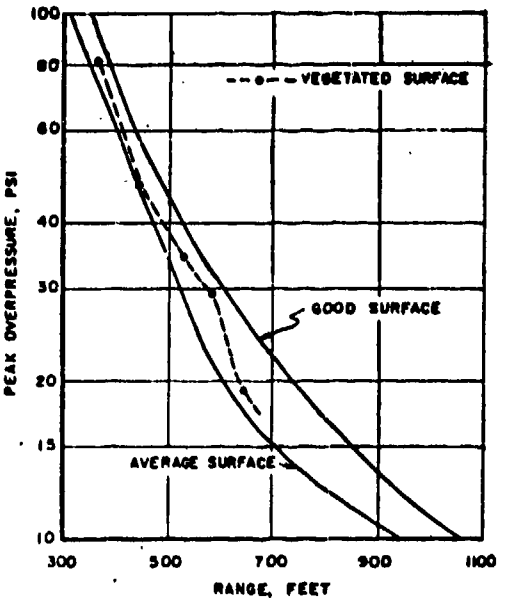


Figure 4.12 A-scaled peak overpressure versus distance, Shot Inca.

## 4.5 POSITIVE IMPULSE MEASUREMENTS

The total impulse of the pressure time curves have been A-scaled and plotted in Figure 4.9. Since there are no impulse-height of burst curves in Reference 4, the points have been connected where possible and where the curves are in doubt, dashed lines have been used.

# Chapter 5
# CONCLUSIONS and RECOMMENDATIONS

## 5.1 INSTRUMENTATION

The instrumentation of the five shots during Operation Redwing with the BRL self-recording gages achieved a high degree of success. Failure to obtain measurements at some stations was usually not a fault of the gage alone but a combination of other factors such as bad yield predictions, error in positioning the device, and environmental extremes.

Self-recording instrumentation has proved to be extremely valuable for making a large number of measurements over long ranges under extreme environmental conditions.

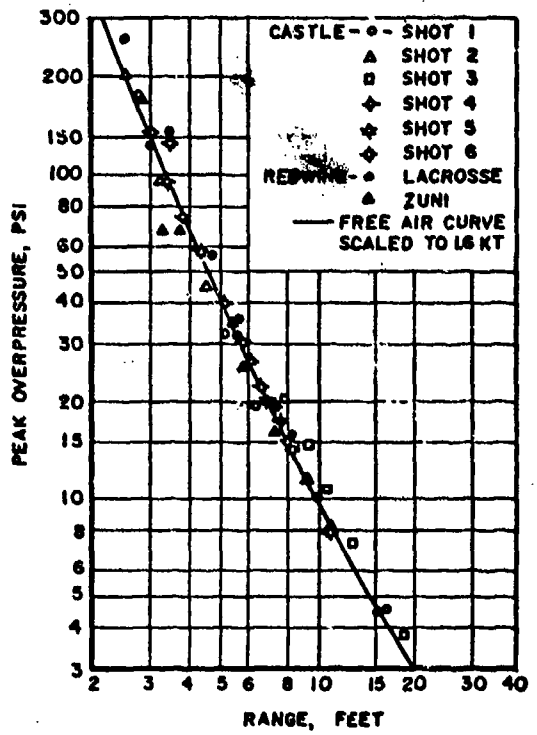


Figure 5.1 Comparison of Operation Redwing and Operation Castle surface shots with 1.6 kt free-air curve.

The design of the gage was satisfactory although a more reliable electronic initiation circuit and thermal link is desirable.

## 5.2 AIR-BLAST PARAMETERS

There was a wide range of yields and heights of burst during the operation and the following conclusions were drawn from the data presented in this report.

5.2.1 Precursors. Two surface bursts were instrumented by Project 1.1 and a precursor was documented on both. Shot Lacrosse (37.8 kt) and Shot Zuni (3.53 Mt) were both scaled to 1 kt and it was found that on the smaller yield shot the precursor cleared up much sooner indicating that the formation and extent of a precursor is a function of yield. On Shot Lacrosse a classical wave was recorded at a scaled distance of 579 feet, and on Shot Zuni a classical wave was recorded at 681 feet on Site Tare. The strength of the precursor was also a function of the height of burst at the lower scaled heights, that is from 0 feet to 100 feet.

5.2.2 Yield Determination. The radiochemical method of determining yield was used on the surface burst Lacrosse, while the hydrodynamic method was used on the surface burst Zuni. The values of peak overpressure and dynamic pressure from both shots were scaled to 1 kt and the correlation of pressures at similar scaled distances was excellent at distances beyond the effect of the precursor. This correlation helped to further establish the validity of the two methods of determining the yield.

5.2.3 1.6 W Concept. The peak overpressure from the two surface bursts was scaled to 1 kt and compared with values from surface bursts on previous operations (Reference 1). The agreement between the two operations is good as shown in Figure 5.1. As pointed out in Reference 1, the empirical value of 1.6 W is a more realistic value than the ideal 2 W concept when using a free-air curve of pressure versus distance for predicting the peak overpressure to be expected from a surface burst.

## 5.3 RECOMMENDATIONS

It is recommended that a statistical number of gages be employed whenever precursor phenomena is measured on future tests, since the formation of different phases of the precursor cycle occurs over a relatively short range. A greater emphasis should be placed on the measurement of dynamic pressure within the precursor region because of the increased damage caused to structures and equipment exposed in the zone of precursor action.

# Appendix A
# INSTRUMENTATION DESIGN

## A.1 INTRODUCTION

Self-contained, direct-recording gages for the measurement of air-blast pressures were first tested on a developmental basis of BRL during Operation Upshot-Knothole. Full-scale projects for measurement of air-blast phenomena using this type of gage were undertaken for Operation Castle (Reference 1) and Operation Teapot (Reference 3). Operation Castle led to the production of a pressure-time gage, a dynamic-pressure gage, a peak-pressure gage, and a very-low-pressure gage. All these were used successfully on Operation Castle. Difficulties encountered and experience gained on this operation led to many modifications of these gages for use on Operation Teapot. The modified equipment was successful, producing pressure-time records on better than 82 percent of the gage installations. A continuing development program has been pursued with particular stress on timing, resolution of the pressure record, and initiation devices.

## A.2 PRESSURE-SENSING ELEMENTS

The basic component common to the pressure-time gage and the q gage is a pressure-sensing capsule. In 1955, a contract placed with the U. S. Gage Division, American Machine and Metals Inc., resulted in improved manufacturing techniques and design changes. These produced capsules with approximately 0.050-inch displacement at rated pressure and capable of withstanding 100 percent overload in the lower range of elements without serious hysteresis. Particular attention was paid to linearity of the trace as the capsule expands. Deviations of trace of not more than 1 degree from a normal to the mounting base were achieved. At the recording speeds commonly used in these gages, deviations of this order result in a less than 2-ms error in time. The new capsules are slightly larger in diameter, with deeper corrugations, welded seams, O ring seals, and osmium-tipped styli, instead of the sapphire tips previously used. These tips are less subject to shattering and provide electrical contact for the electronic pulse.

Operationally, these capsules were similar to those used on Operations Castle and Teapot by Ballistics Research Laboratory (BRL). Comparative photographs of the old and new capsules are shown in Figures A.1 and A.2. They consist of two nested diaphragms, welded together and silver-soldered to a mounting base. An increase in outside air pressure, entering through a small inlet, caused expansion of the diaphragms. A light osmium-tipped spring stylus soldered to the center of the free diaphragm recorded this motion as a ½-mil-wide scratch on a coated glass recording blank. The amplitude of this scratch was proportional to the movement of the diaphragm, which in turn was proportional to the applied air pressure. Ten ranges of capsules, from 0 to 1 psi up to 0 to 400 psi, were in general use in these self-recording gages. Basic specifications are given in Table A.1.

A.2.1 Calibration. Calibration of the new capsules was accomplished on a Leeds and Northrup X-Y recorder. The output of a Statham strain-gage-type pressure transducer was fed through amplifiers to the pen (X-axis) of the recorder. Capsule deflection was measured by a micrometer head equipped with a null detector and servo system operating a slide-wire potentiometer which, in turn, controlled the chart drive (or y axis). The resulting calibration record was a plot of capsule deflection as a function of applied pressure. The error of this calibration was less than 0.5 percent.

Unfortunately, the q gages would not accept the new capsules because of space limitations. Capsules used on Operations Castle and Teapot were rehabilitated and recalibrated for use in these gages.

A.2.2 Recording Blanks. The recording medium of the scratch-type self-recording gage was an aluminized glass disc similar to those used on previous projects (see Reference 3). Difficulty had been experienced with the coating, necessitating excessive stylus pressure to produce a readable record. In pre-Redwing applications, it was felt that low temperature was the cause of the malfunction. Laboratory tests, however, did not bear this out, since perfectly readable scratches were obtained at ¼-ounce stylus pressure at temperatures as low as -40 C. Field experiences indicated that the quartz protective coating was preventing the stylus from scratching through the aluminized coating. For Operation Redwing, quartz coating was omitted. Tests in the laboratory did not indicate any great increase in scratching from handling due to this omission.



SECRET

A.2.3 Drive Motor. The heart of the time base in the pressure-versus-time and dynamic-pressure gages was the A. W. Haydon, Series 5600, chronometrically governed motor (Figures A.3 and A.4). This motor had a permanent-magnet-field construction and required 7 to 9 volts for operation. In the gages, the motors were powered by six Mallory RM-1R mercury cells delivering 8 volts, with enough capacity to operate the motor for over 6 hours. The chronometric governor regulated the motor velocity by comparing the motor velocity to that of a watch-type balance wheel and adjusting the motor current until both were identical. Specifications state that this governor would regulate the speed to better than 1 percent under 10 g acceleration, from 10 to 300 cps.

A study was undertaken in BRL to determine the reliability of the motor under field conditions. Tests were performed to obtain turntable relation, as a function of time, from the instant power was applied until it was removed, and to study the effect of shock as great as 80 g.

The first tests determined the consistency of the time required for the motor to reach constant velocity. Oscillograph traces were made showing motor current, turntable rotation, and reference time for both free motors and motors loaded in the manner in which they were to be used. This data was then plotted as turntable rotation versus time (Figure A.5). The data showed that the motors attained full velocity in approximately 100 msec, exceeded their rated velocity, and then settled down to constant speed. Overshoot and oscillation were decreased by loading, but in no case lasted longer than 400 msec. The error between the actual displacement and a linear extrapolation to zero rotation of constant velocity never exceeded 20 msec after + 50 msec. The time difference between the extrapolated line and zero (i.e., start-up time for computing purposes) was 65 msec, with a standard deviation of 11 msec.

The second set of tests was made to determine the effect of shock on turntable velocity. Again oscillograph traces were made of turntable rotation, motor current, and reference time while the gage was subjected to shock in a Barry Corporation, Type 150 VD, medium-impact-shock machine. The motors were tested under impacts as high as 80 g, with a duration of 12 msec. Shock-acceleration tests were run in preference to vibration-acceleration tests, since the former more closely duplicated field conditions. The gages withstood impact shock of at least 50-g magnitude without appreciably affecting record accuracy. Deviations from the linear line did not exceed 5 msec at 50 g. At higher accelerations, the velocity oscillated after the instant of shock in some cases, and occasionally the glass recording disc broke. Acceleration shock of 50 g or less, however, did not materially affect motor and turntable velocity.

TABLE A.1 CAPSULE SPECIFICATIONS

| | |
|---|---|
| Diaphragm material | Ni Span-C, Phosphor bronze, 0-1 psi. |
| Deflection, at rated pressure | 0-1 to 0-150 psi approx. 0.050 inch.<br>0-200 and 0-400 psi approx. 0.040 inch. |
| Linearity | ± 0.5 percent. |
| Hysteresis | ± 0.5 percent. |
| Natural frequency, undamped | 1,200 to 2,000 cps, depending on pressure range |
| Rise time | 3 ms or less. |
| Operating range | 0-1 to 0-150 psi, 200 percent of rated pressure<br>0-200 to 0-400 psi, 150 percent of rated pressure. |
| Pressure inlet opening | 0.152 inch diameter. |
| Diameter | 0.75 inch to 2.00 inches, depending on pressure range. |

## A.3 PRESSURE-TIME GAGE

The pressure-time ($p_t$) gages used on Operation Redwing were a modification of the ones used on Operation Teapot, which in turn were modified Operation Castle gages. As noted under Section A.2, the capsules and recording blanks were improved to produce a more accurate and more readable record. A transistorized photocell circuit was added to replace the old vacuum-tube-operated circuit. An improved thermal link and mounting were devised. A delayed-time-pulse generator replaced the time-base oscillator used previously. A cam and switch were added to give up to four revolutions of the turntable. An arming switch was added to permit the gage to be installed several days before the shot and actuated in a short time, just before the area was cleared. These changes made the $p_t$ gage an even more reliable and accurate instrument while maintaining its portability, ease of installation, and recovery. It was entirely self-



SECRET

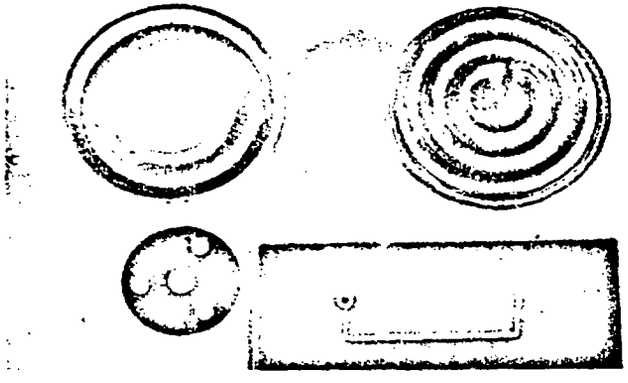

Figure A.1 Pressure-sensing capsule, old style.

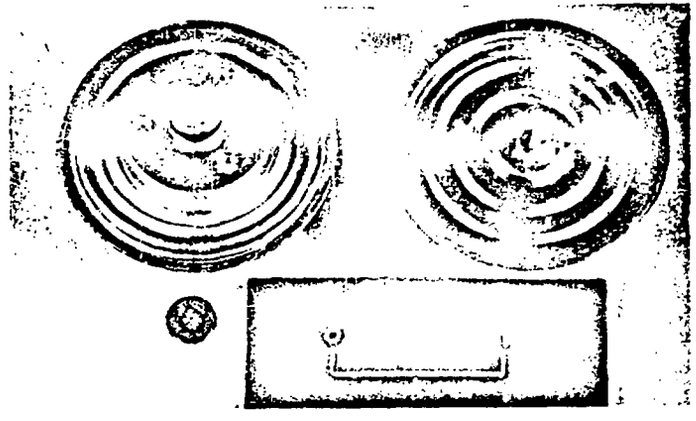

Figure A.2 Pressure-sensing capsule, new style.



SECRET

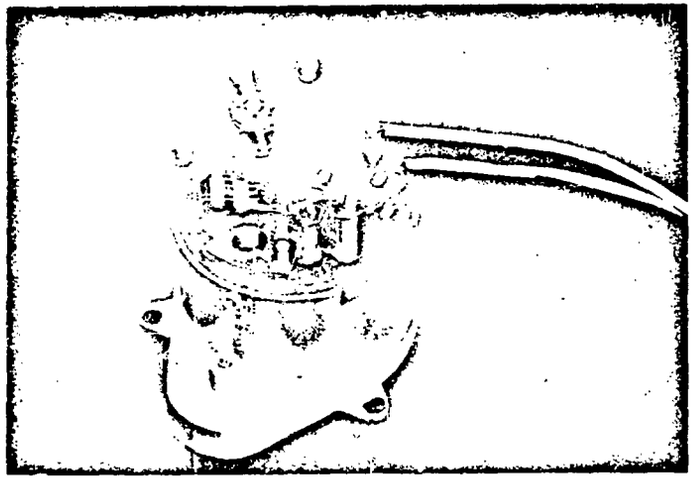

Figure A.3 Haydon motor, showing governor.

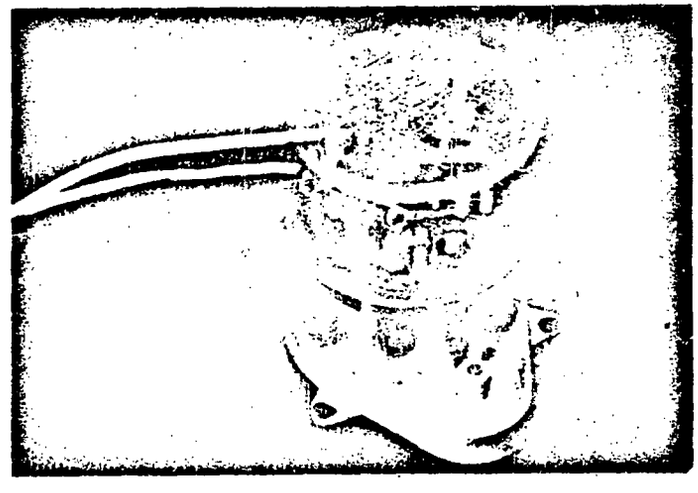

Figure A.4 Haydon motor, phantom view.

contained, small in size, and relatively inexpensive. It did not require the long lengths of cable, complex recording equipment and expensive shelters associated with electronic systems for obtaining pressure data. It has proven itself to be an efficient gage for obtaining pressure-time data over a wide range of pressures and distances and has lent itself admirably to installation in structures and shelters. Figure A.7 shows the gage encased and ready for installation. Figure A.6 shows the recording side of the gage, while Figure A.8 shows the motor-drive side.

A.3.1 Mechanical Construction. The outside gage case was the same as used for Operations Castle and Teapot. For project-installed stations, the base-plate type of mounting was the same as used on Operation Teapot. Contractor installed stations used 6-inch, threaded pipe imbedded in concrete. Gages were screwed in place by project personnel.

The gage frame was modified by shortening the channel to 5-$\frac{1}{2}$ inches to allow the use of a larger unit holding the complete electronic system and power supply. The old mounting holdes for the capsule were plugged and remachined to accept the new capsule mounting. The hole for the old photocell entrance bushing was plugged and a relocated hole put in for the new photo-initiator bushing. A $\frac{1}{4}$-20 screw hole was added to permit final activation of the gage without the necessity of removing the gage from the case.

The turntable bearing housing remained the same. Turntable diameter was reduced to 2-$\frac{1}{2}$ inches, with a notch and pin added to operate a star gear and cam to permit up to four complete revolutions of the turntable before the cam operated a microswitch completely cutting off the gage, giving operation times of 20, 40, 60, and 80 seconds. Figure A.9 shows a closeup of the star gear and cam and the new capsule mount.

A double-pole, single-th row microswitch was bolted to one side of the gage frame directly under the screw hole in the face plate mentioned above. Prior to activation, a short screw was fitted in this hole. This screw was not long enough to operate the microswitch. To activate the gage, a longer button-head screw was used to close the microswitch, which completed two circuits: one, the battery circuit for the motor and the other the battery supply for the electronic photo cell and timing pulse.

The six batteries which furnished power for the drive motor were held in an Austincraft holder mounted on the side of the channel frame.

The capsule was mounted slightly to the rear of its old location and turned 180 degrees, permitting the recording disk to be turned around. This obviated the necessity of springing the stylus to insert the disk. It also speeded up the placing of the disk on the gage, which previously was quite a tedious task.

Other details of construction are similar to those used on gages employed during Operation Teapot and full information can be obtained from Reference 3.

A.3.2 Thermal Initiation. The thermal initiator used on Operation Redwing was an improved version of the ones used previously. Laboratory experimentation showed that a 300-percent improvement in breaking time of the thermal link was achieved by using wider strips of shim brass 0.003 inch thick, soldered together with a low-melting alloy (150 F) rather than the $\frac{1}{4}$-by-$\frac{1}{2}$-inch strips used on other operations. To strengthen the mounting holes at each end, $\frac{3}{16}$-inch-inside-diameter eyelets were staked in the holes. These strips were tested to a minimum breaking strength of 25 pounds.

Unfortunately, the links did not fully meet the design specifications, and some difficulty was experienced on early Operation Redwing shots. After the gage had been activated for a period of time, the link would part, initiating the gage. This occurred to a small degree on Shot Lacrosse and to a large extent on Shot Cherokee, especially on the reef stations. The number of failures on Shot Lacrosse was minimized by a check and replacement of defective links late on D-1. On Shot Cherokee, the number of pre-shot initiations due to thermal link failure was kept to a minimum by the use of double links on stations showing a tendency to part links. It is felt that the large number of failures on the reef stations was due to a constant salt-water bath, setting up electrolysis between the dissimilar metals of the link.

Too late to obtain a replacement, it was discovered that the alloy used to solder the halves of the link together was not the one specified but one containing mercury. The shim brass supplied was a soft-brass and not a hard-brass shim stock as specified.

A field correction was made on the existing links by removing the old solder and resoldering the links with the correct alloy. Shots Zuni and Yuma showed that this corrected the trouble as no link failures were experienced. The thermal links were supported by a $\frac{3}{4}$-inch wide U bracket with a tension-adjusting screw on one end. In operation these links held up a spring-loaded plunger. When the incident thermal radiation heated the link to about 150 F, the alloy melted, allowing the link to part and permitting the plunger to drop and close the microswitch. This method proved quite effective as a backup initiator in case of failure of the electronic system.

A.3.3 Photoelectric Initiation. The photoelectric-initiation device, activated by the incident light from the detonation, was redesigned to insure greater reliability and sensitivity. The new circuit employed a photo-conductive cadmium sulphide cell, a transistor amplifier, and a sensitive relay. In addition, a circuit to provide a time-reference pulse on the pressure-time record is described in A.3.4.

Figure A.10 is an exploded view of the assembly, showing the miniature photocell, insulated bushing, pressure tight housing, and a cylindrical lucite lens to focus incident light on the photo-sensitive

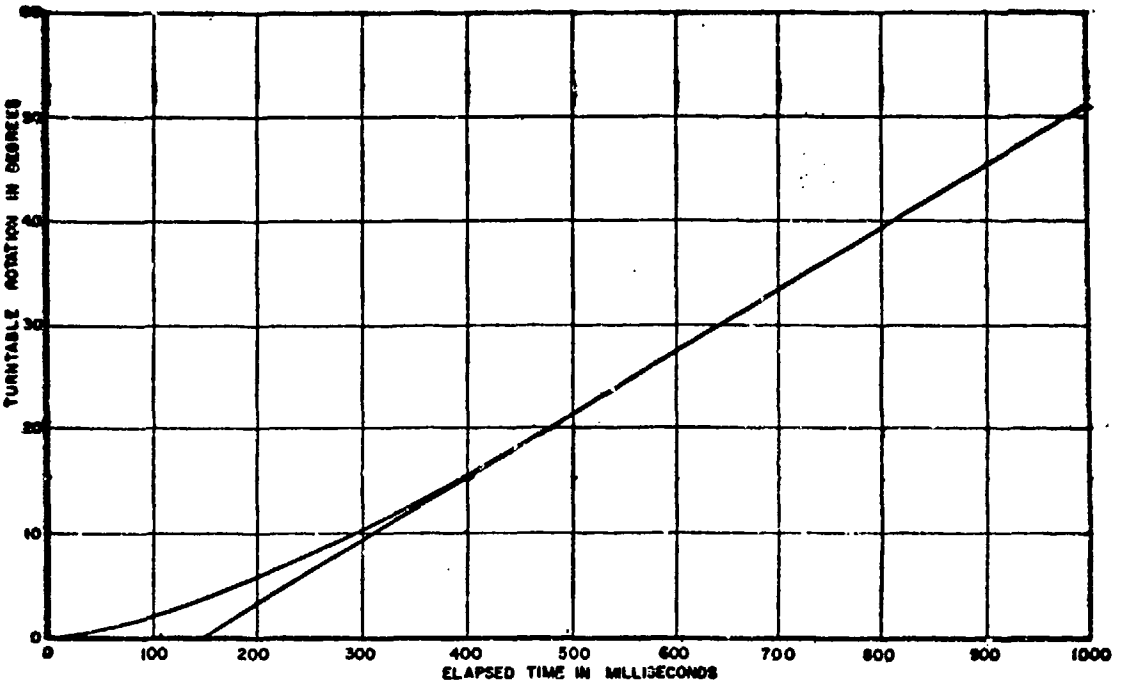


Figure A.5 Turntable rotation versus time.

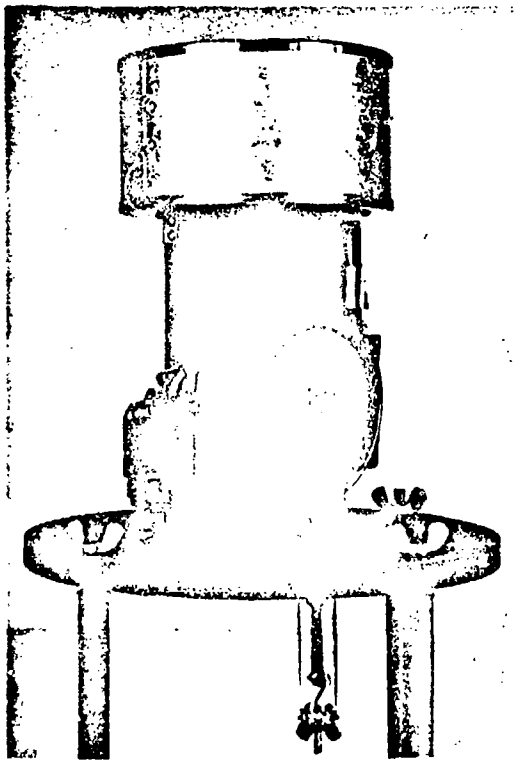

Figure A.6 $p_t$ gage, recording side.

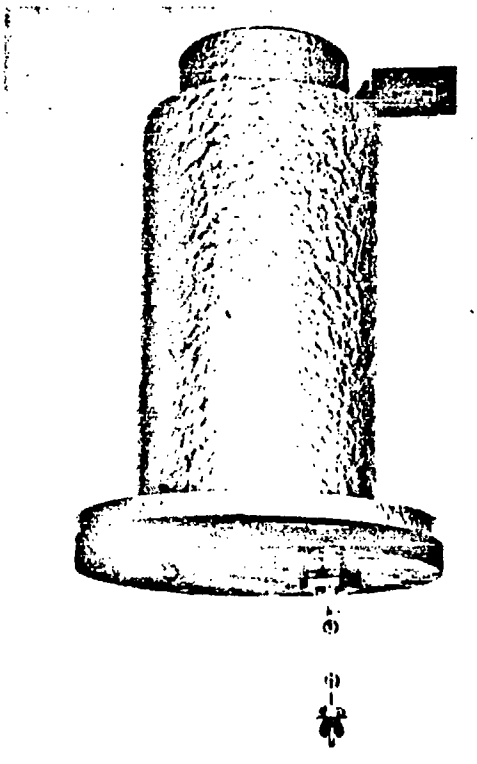

Figure A.7 $p_t$ gage, incased.



SECRET

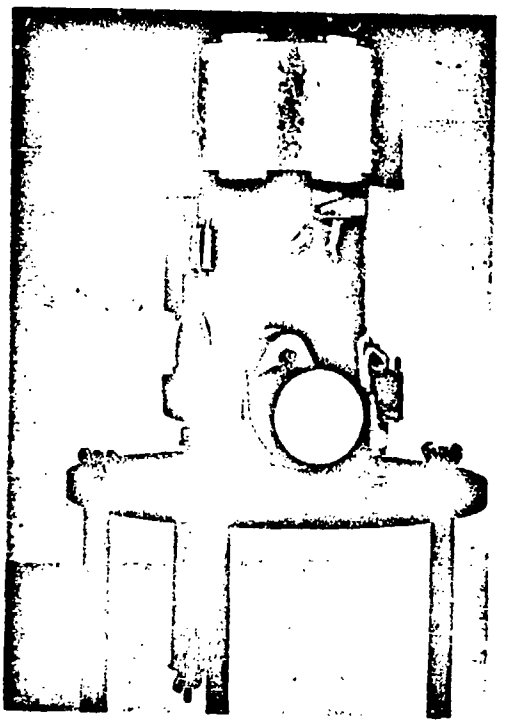

Figure A.8 $p_t$ gage, motor drive side.

Figure A.9 Close-up of star gear and capsule.

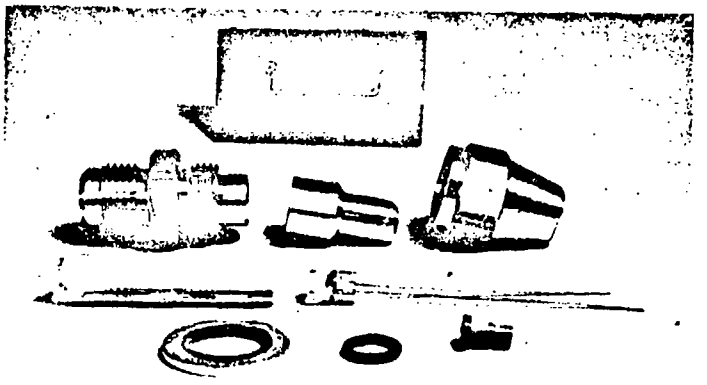

Figure A.10 Exploded view of photo-cell assembly.



SECRET

element. In operation, a density-of-3 neutral filter was placed directly over the photocell to reduce the quiescent current and to eliminate preinitiation by random impulses of light.

Figure A.11 is a schematic diagram of the complete circuit of the pressure-time gage. To prepare the gage for recording, SW1, the activating switch, a normally open microswitch, was closed, completing the ground return lead. Prior to initiation, the CK 722 transistor was biased nearly to cutoff by R1, which was returned to the positive side of the 45-volt

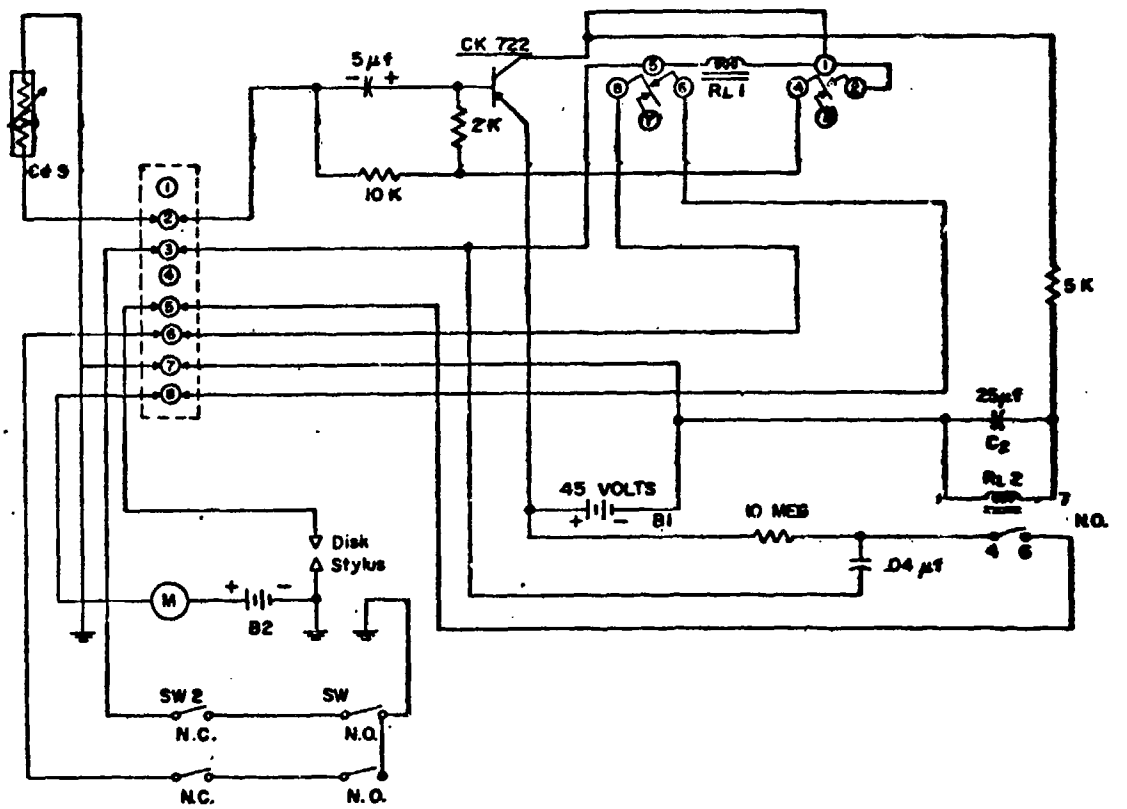


Figure A.11 Schematic diagram of pressure-time electronic circuit.

battery (B1). At zero time, light impinging upon the photocell reduced its resistance by a factor of approximately $10^6$, causing a large negative pulse to appear at Point A. This negative pulse, coupled to the base of the transistor through capacitor (C1), made the transistor conduct heavily, closing the sensitive relay (RL1), which was in series with the transistor collector and the negative side of the 45-volt battery.

A pair of normally open contacts on RL1 were used to latch the relay electrically in the closed position by placement of the relay coil directly across the 45-volt battery. This resulted in an increased current of 5.6 ma through the relay to insure continuous contact closure against the effects of ground shock and blast. The second pair of normally open contacts on RL2 were used to apply voltage from the 9-volt mercury-cell source, B2, to the recording motor (M). This started the recording cycle, and the turntable continued to rotate a predetermined number of revolutions until the star cam opened the normally closed microswitch (SW2), disconnecting the motor and transistor from their respective voltage supplies.

Difficulties were also experienced with the photo-initiation circuit. These were probably twofold, one being due to moisture and the other to an insufficient light filter. The difficulties were alleviated to some extent by the use of a desiccant in the gages and by replacement of the original 2.2 density filter with a 3.0 density filter. It is planned to further test these circuits in a climatic test chamber at the laboratory. Future circuits will probably be completely potted to guard against moisture damage to them.

The construction of the photo initiation and timing unit is shown in Figure A.12 and A.13. Figure A.12 shows the electronic components mounted on a terminal board. The entire assembly was connected to the



SECRET

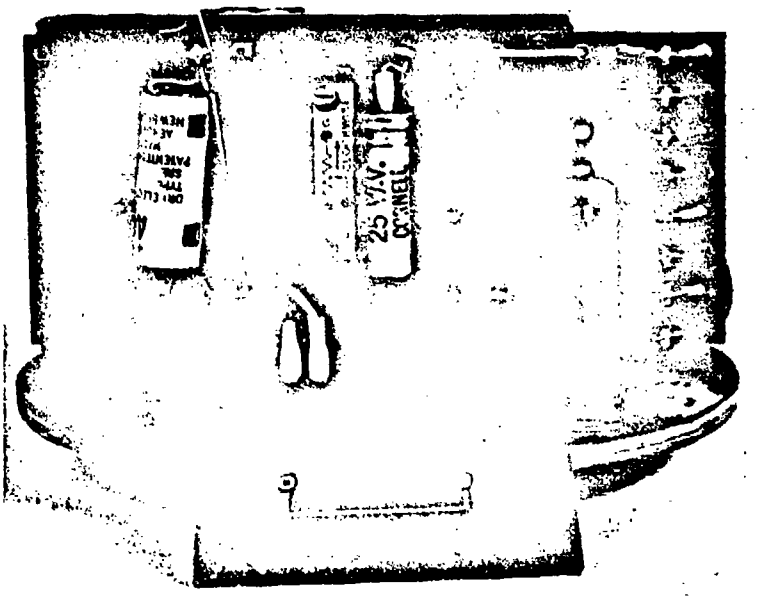

Figure A.12 Electronic components of the photo-initiation circuit.

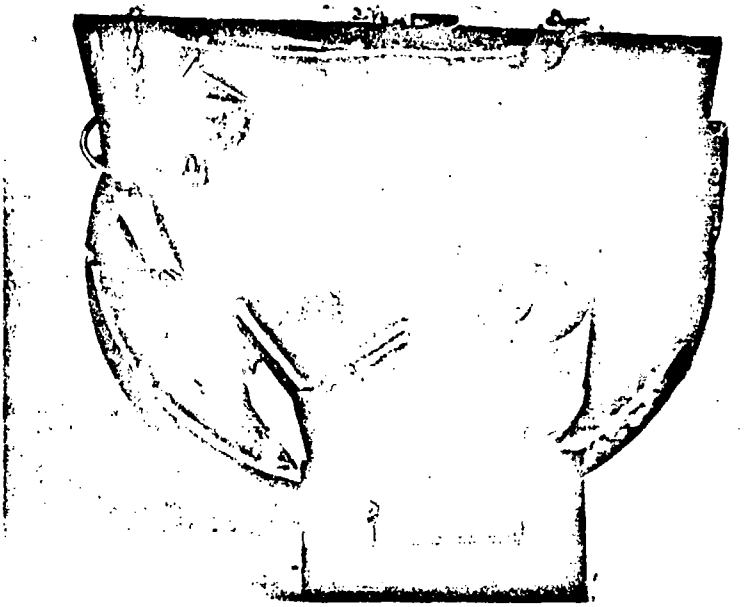

Figure A.13 Photo-initiation battery and relay.

gage by the blue-ribbon plug shown at the bottom center of Figure A.12. The plug facilitated replacement of defective units.

A.3.4 Timing. In order to establish a time reference, a pulse was placed on the pressure-time record at approximately 130 msec after zero time by the time-delay circuit shown in Figure A.11. At zero time, a positive pulse was developed at the collector of the transistor and fed to an RC circuit made up of R2 and C2, which closed RL2 at a time determined by the values of R2 and C2. A pair of normally open contacts on RL2 discharged Capacitor C3 through the aluminized coating of the recording disk, producing a small dot on the pressure-time trace at the desired time. Capacitor C3 was connected to the disk by the recording stylus and the brush assembly shown in the Center of Figure A.9.

A.3.5 Calibration. To test and calibrate the photoinitiation and timing unit, the photocell was exposed to light from a 100-watt projector at a distance of 2 feet through a shutter set at 0.01 sec. Time was measured by a Hewlett Packard Model 524B electronic counter. The voltage pulse generated by the photocell was used to start the counter, which was then stopped when the delayed time pulse was applied to the recording disk. In this manner, all the delays inherent in the system were included in the measurement of the time interval. The accuracy of the delayed time pulse was 1.0 msec. Each gage was calibrated individually and the delay time marked on the gage.

TABLE A.2 GAGE PERFORMANCE

| Shot | $p_t$ Pressure-Time Gages | | | | | q Dynamic-Pressure Gages | | | | |
|---|---|---|---|---|---|---|---|---|---|---|
| | Total $p_t$ Gages | $p_t$ Record | Peak Only | No Record | Gage not Recovered | Total q Gages | $p_t$ Record | Peak Only | No Record | Gage not Recovered |
| Lacrosse | 15 | 12 | 2 | 1 | 6 | 6 | 5 | 0 | 1 | 0 |
| Cherokee | 47 | 34 | 9 | 4 | 0 | 14 | 6 | 4 | 4 | 0 |
| Zuni | 25 | 17 | 3 | 1 | 4 | 9 | 6 | 0 | 3 | 0 |
| Yuma | 14 | 10 | 2 | 0 | 2 | 5 | 5 | 0 | 0 | 0 |
| Inca | 20 | 16 | 2 | – | 2 | 10 | 8 | 0 | 3 | 0 |

## A.4 DYNAMIC-PRESSURE GAGE

The dynamic-pressure q gage was modified little from the one used on Operation Teapot. The old gages recovered from the last operation were rebuilt and thoroughly checked. Battery power supplies were replaced, old relays cleaned and tested, and replacements installed where necessary. Motors were calibrated and adjusted to within 0.1 percent of rated speed. A light cut was taken off the nose section to remove a majority of the dents and scratches received during previous tests. The main body of the gage was cleaned and painted with a baked-enamel finish which was found to be excellent for rust and abrasion resistance. A timing motor, similar to one used in the gages on Operation Castle, was put in to permit the gage to operate for nearly 60 seconds. The thermal link assembly was changed to allow the use of the new quick-acting link. Figures A.14 and A.15 show assembled and exploded views of the gage.

Considerable research and a shock-tube-testing program was carried on to determine an adequate method of damping the total pressure-sensing element to prevent overshoot and oscillation at certain critical pressures. The best solution proved to be a sieve-like restriction placed directly over the capsule inlet.

Figure A.16 shows a record of a shock-tube shot with an undamped total pressure element. Overshoot, in this instance, amounts to approximately 25 percent with severe oscillations following. The initial rise-time was of the order of 1.5 msec, and the duration of the flat-top portion approximately 45 msec.

Figure A.17 shows an overdamped capsule. Here the overshoot and oscillations have been successfully squelched, but the rise time has increased to approximately 9.0 msec. The undamped capsule has an inlet area of approximately 0.009 inch$^2$, the overdamped one an area of 0.0023 inch$^2$. The sieve is a piece of shim brass with 16 No. 80 drilled holes directly over the capsule inlet. The sieve used on Operation Redwing q gages had an area of 0.005 inch$^2$, (16 No. 76 drilled holes). This gave a damping approaching 0.7 critical and a rise time of approximately 2 msec. These made the gage more reliable and increased the accuracy of reading the record by reducing the amount of interpolation during the overshoot-and-oscillation phase.

## A.5 GAGE PERFORMANCE

The total number of gages installed, and a summary of performance on the five shots are listed in Table A.2. The column entitled peak only means that there was a malfunction in the initiation system or the drive motor. In all cases it is felt that the malfunction was preinitiation, whereby at least a peak pressure was recorded.

A listing of no record on a $p_t$ gage does not necessarily mean a malfunction of the gage but could be



SECRET

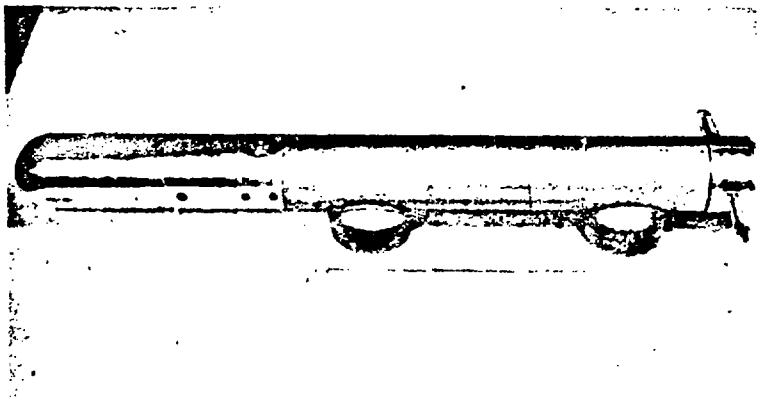

Figure A.14 Assembled view of q gage.

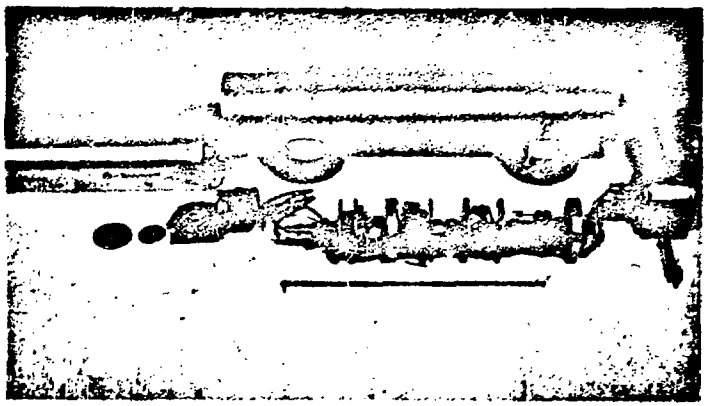

Figure A.15 Exploded view of q gage.

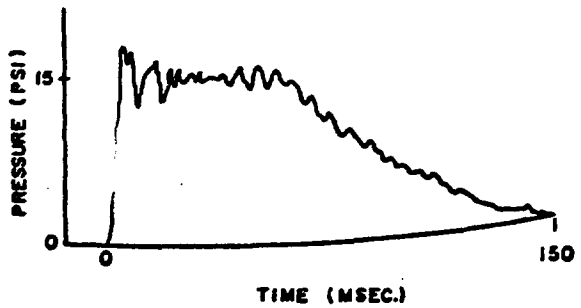


Figure A.16 q-gage shock-tube record, underdamped.

Figure A.17 q-gage shock-tube record, overdamped.

one of two reasons: (1) the deflection was too small to read, or (2) the glass disk was broken.

Gages which were not recovered are listed in a separate column since it is not known whether the gage obtained a record or not.

The loss of records on the q gage was caused by broken recording disks or insufficient stylus pressure on the recording disk. In the present q gage there is no way to adjust the stylus pressure after the recording disc has been installed.

## A.6 POST OPERATION GAGE EXAMINATION

In order to better understand the results obtained on Operation Redwing and explain some of the apparent discrepancies in the records, a program of gage examination and component tests was undertaken upon the return of the recovered gages to the laboratory.

A.6.1 Record Check. All gages that were returned with the pressure sensing capsule still installed were carefully checked for capsule number versus gage number and these records compared with the field records. No discrepancies were noted.

A.6.2 Capsule Examination. The pressuring sensing capsules were removed from the gages and examined for obvious damage such as overstressing due to overpressures above the design limit and stylus damage due to high accelerations. All recovered capsules were recalibrated and the results compared with preshot calibration curves. The agreement between the two sets of curves was excellent except in the case of overstressed capsules. Approximate calibration of overstressed capsules was achieved by selecting another capsule of similar pressure-deflections characteristics and subjecting it to a pressure sufficient to cause a deflection equal to the deflection recorded at shot time. This pressure was approximately equal to the pressure to which the gage was subjected.

A.6.3 Protective Screen. Protective screens which were placed over the capsules were carefully examined. A method of determining the amount of stoppage of the air passage due to clogging of the screens was devised. Most of the material clogging the screens was opaque so that an optical method of inspection appeared satisfactory. A simple photoelectric cell and amplifier with an indicating meter was built. A clean unused screen was placed between the light source and the photo cell. This was then considered as a screen of 100 percent air passage and the scale on the indicating meter marked as 100 percent. Neutral density filters of known density were then added between the screen and the photo cell and the meter completely calibrated from 0 to 100 percent transmission. The recovered screens were in turn placed in the gap and calibrated as to percent open. Approximately 100 screens were calibrated and the results tabulated as follows:

| Percent of Screens | Percent Open |
|---|---|
| 15 | 0 to 15 |
| 30 | 15 to 50 |
| 25 | 50 to 90 |
| 30 | 90 to 100 |

Shock tube tests on the gages indicated that a 25 percent opening increased the rise time of the capsules by about 50 percent; in other words, from approximately 2 msec to approximately 3 msec. It would appear that in a majority of cases the stoppage was not serious enough to greatly affect the records. The material causing the stoppage was analyzed and divided into three general classes, i. e., salt water corrosion, coral deposit, and carbon paper deposit. Of these, corrosion was the most prevelant but accounted for the smallest part of the stoppage. Corrosion could occur before and after the shot. The deposit of small coral particles was the most serious but it is felt that this did not occur until after the passage of the shock wave. The carbon paper deposit was the residue from a protective cover placed over the pressure inlet to keep out salt water and small particles before shot time. Ordinarily this carbon paper burns away from thermal radiation before the arrival of the shock wave. In some cases where the thermal energy was insufficient or attenuated, the carbon paper was not completely burned away but small particles were forced into the pressure inlet by the shock wave.

A.6.4 Thermal Initiation Tests. Thermal initiator tests were divided into two groups, tests of the plunger and switch and tests of the thermal links. There was no evidence of failure of the plunger and switch assembly; however, a check of the time required for the switch to close after the parting of the link was conducted. To record this time of actuation, a Potter counter was used in a circuit which detected the instant of break of a link and the instant of make of a microswitch. A series of tests were performed to determine differences in actuating time of assemblies in an as-is condition, i. e., as returned from the field, cleaned and oiled condition, and with one O ring removed to avoid a compression condition. The results of these tests were:

| Condition | Number of Samples | Average Time Measured |
|---|---|---|
| As is | 20 | 2.65 |
| Cleaned and oiled | 23 | 2.99 |
| W/one O ring | 16 | 1.91 |

From these results, it was obvious that compression of the air trapped between the two diameters of the plunger slowed down the operation by approximately 1 msec. At the lower range of pressures, it was felt that one O ring would provide a sufficient pressure seal. A miniature plunger assembly has been built

and subjected to similar tests. While this assembly utilized two O rings, they were both of the same diameter. The results of these tests indicated that it operated slightly faster than the old unit with one O ring, with the new unit having an actuating time of the order of 1.8 msec.

The chief cause of failure of the thermal initiator was with the thermal link itself. During a period of from 1 to 3 days after installation, the thermal link either parted, or creep in the soldered joint permitted the switch to actuate. Laboratory tests under simulated conditions bore this out.

To check the breaking temperature of the links, a series of 12 links were set up in a frame under spring tension equal to that of the initiator assembly (8 to 10 pounds). An indicator light was wired to each link to show when a link had failed. The entire frame was put in a controlled temperature oven, which was brought slowly up to temperature. The links began parting at a temperature as low as 114 F and all had parted when the temperature reached 120 F. Links held under tension at room temperature for several days showed varying degrees of creep. It was determined that the manufacturer of the links added mercury to a standard alloy to make an alloy having the required melting point. Unfortunately, this addition changed the cold flow characteristics of the original standard alloy.

New links have been made and tested in the laboratory. They have the desired characteristics, i.e., breaking point of 150 to 165 F, minimum tensile strength of 25 pounds, and the ability to sustain an 8 pound load at elevated temperatures (115 to 120 F) for several weeks. These characteristics were achieved by the following means:

1. Use of Cerro de Pasco alloy No. 5000-7, a eutectic alloy having a narrow melting range. (nominal 158 F).

2. Use of hard brass shim stock for increased tensile strength.

3. Use of two pimple-like depressions to present a compression area to prevent creep experienced in a pure shear joint.

No data is available as to the length of time required for the links to part under actual field conditions. A program is being initiated for Operation Plumbbob to determine parting time of the link for varying yield-distance conditions. With this information, arrival time data will be possible from gages thermally initiated.

A.6.5 Electronic Circuit Tests. One hundred electronic photo-initiation and time pulse circuits were examined and checked upon their return to the laboratory. Seven checked satisfactorily, that is, both the photo-initiation circuit and the time delay pulse functioned. Seventy four circuits did not operate with both the initiation circuit and the time delay pulse connected but did check out when the pulse circuit was disconnected. It is felt that an interaction through the common plate supply caused this failure. Nineteen of the circuits completely failed to operate. Of these nineteen, nine had faulty relays and the other ten suffered from transistor failure. The inoperative relays were taken apart to determine the causes of failure and it appeared that they were damaged by excessive accelerations. The least sensitive position for these relays was determined and they were reoriented for future use. A relay failure at the time of the passage of the shock wave does not necessarily mean a gage failure, however, for by this time the thermal initiator back-up switch has functioned and independently keeps the circuit to the gage motor closed. Another possible cause of failure in field operation which did not show up in laboratory tests was the effect of moisture on the circuits. This effect will be minimized in future use by potting the entire circuit in plastic.

A.6.6 Drive Motor Tests. The turntable drive motors were carefully checked for obvious damage and were calibrated for rotational velocity. Approximately 50 motors were calibrated. Of these, three were definitely bad; they either did not run or ran erratically. One motor ran consistently 15 percent slow. The balance checked out well, having an error of less than 0.3 percent in rotational velocity.

A.6.7 Motor Start-Up Time. In establishing a pressure-time record, the calibration of time is as important as the pressure calibration. Just as pressure steps are not placed on the self-recording records at shot time, neither are there time marks on the record. The time scale is accurately determined by the rate of rotation of the recording disk. The angular rotation is converted to time in milliseconds at the same time that the deflection is changed to pressure.

The turntable which supports the record disk is driven by a Haydon chronometrically governed motor which is described in Section A.2.3. This motor is set and checked by the manufacturer for a certain number of rotations per minute. In all cases the variation from the rated rpm is small after the motor has had time to reach its rated speed. The average time required to establish the rated rpm for the three ranges of motors utilized in the BRL self-recording gages is 400 msec. These recording drive motors were calibrated at BRL and a sample curve is shown in Figure A.5. The slowest speed, a 3 rpm, has a slightly different calibration curve than the 10 and 40 rpm motors. The time calibration curves were obtained by attaching a small gear to a shaft in the governor, which was geared to the drive shaft of the motor. This added gear opened and closed a switch which provided a series of pulses with each pulse

representing 0.2 of a degree rotation of the turntable. These pulses, along with a 100-cycle time base from a Hewlett Packard frequency standard and the input current to the motor, were recorded on a Consolidated Electrodynamic Corporation recorder. The record of the current gave an accurate time at which the motor was turned on. The 100-cycle timing provided the time base for reading the angular rotation. The calibrations were made with the motor in the gage under load just as it is used in the field.

As was stated before, after 400 msec all calibration time curves are linear and a constant can be applied to convert angular rotation to time in milliseconds. In this case, the correction factor for arrival time can be obtained from the calibration curve by extending the linear portion of the curve back to zero rotation. This factor must be added to the calculated arrival time in order to correct for the delay in the motor start-up time. From the curve in Figure A.5, it is apparent that a constant value cannot be used to find the time in the positive duration when the corrected arrival time is less than 400 msec. On Operation Redwing, there were many records from Shot Yuma and Inca which fall into this category. In order to correct for the motor not being up to speed, each motor was calibrated by the method described above. Just as a nonlinear pressure curve was applied to the deflection, so a nonlinear time curve was used to convert the angular rotation to time. In using the nonlinear part of the calibration time curve, it is important to have a well marked zero time on the record since this zero time must be matched with the zero on the calibration time curve. On Shot Inca, both 3 and 10 rpm motors were used at the same station. This furnished a good check on the method used to correct for the nonlinearity in the time during the positive duration. The only loss in accuracy occurred when the arrival time was so short that the first part of the positive duration was compressed, making it difficult to read the record.

# *Appendix B*
# *PRESSURE-TIME RECORDS*

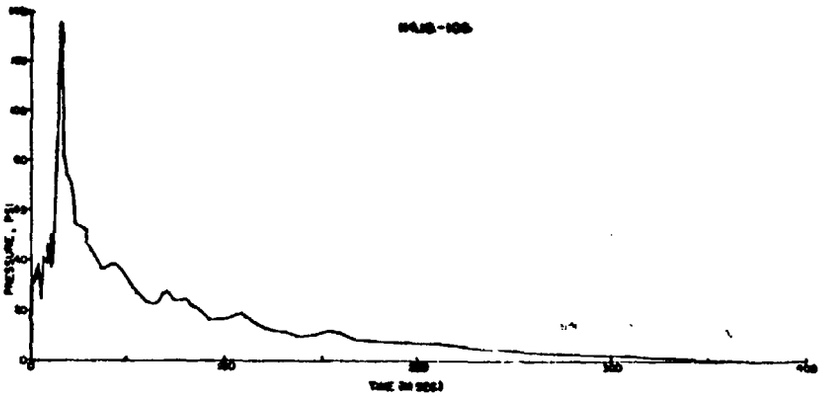

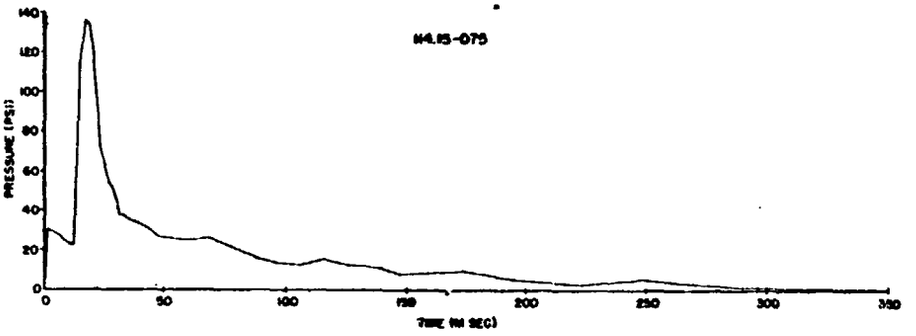
PRESSURE (PSI)
TIME (M SEC)

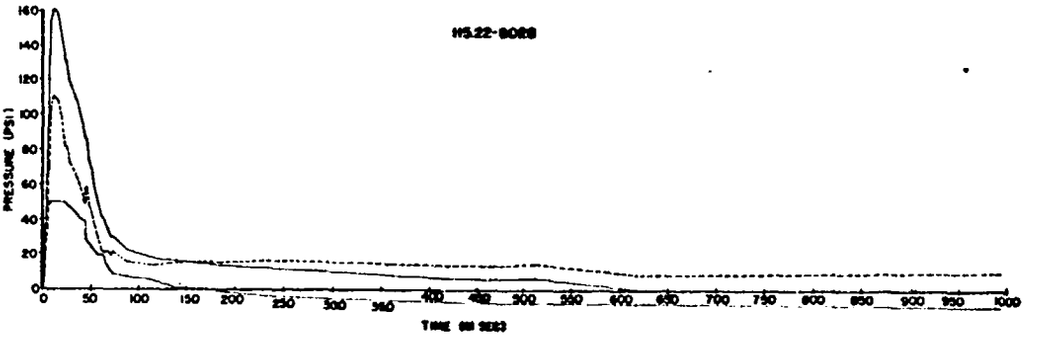
PRESSURE (PSI)
TIME (M SEC)

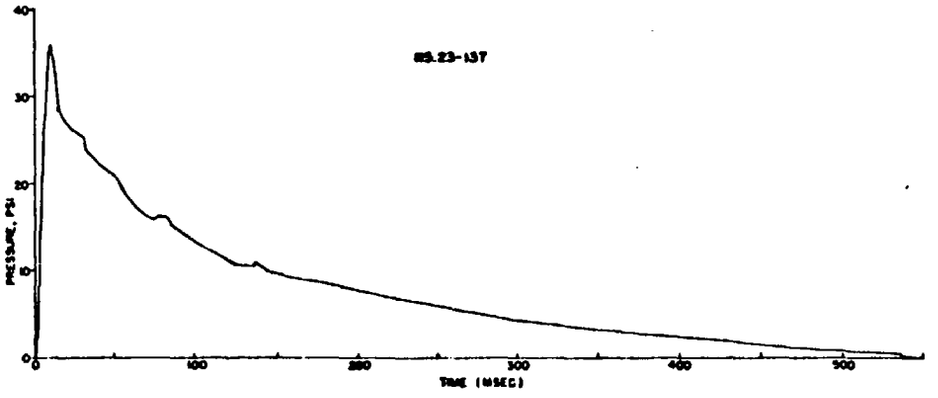
PRESSURE, PSI
TIME (MSEC)



SECRET

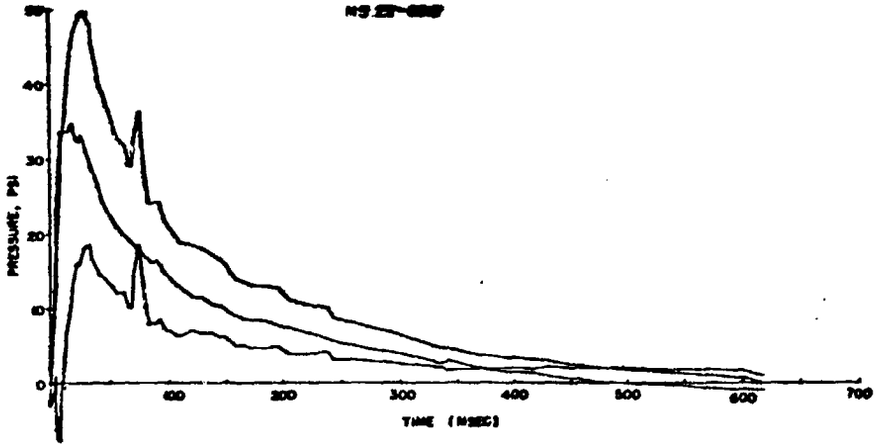
PRESSURE, PSI
TIME (MSEC)

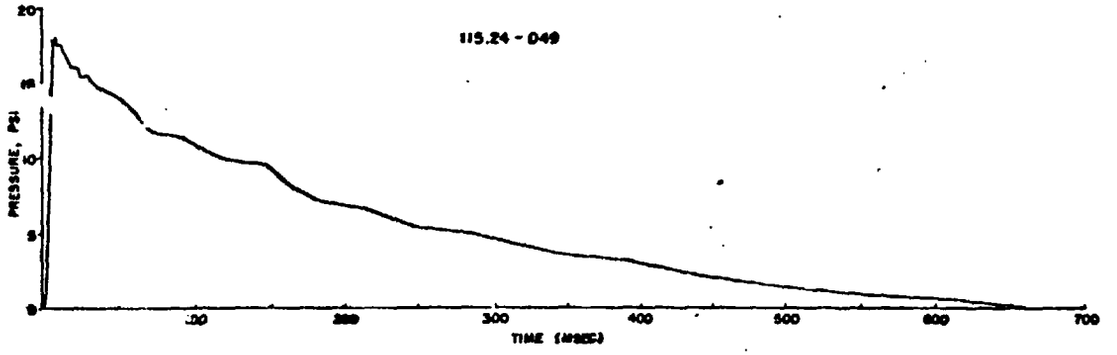
115.24 - 049
PRESSURE, PSI
TIME (MSEC)

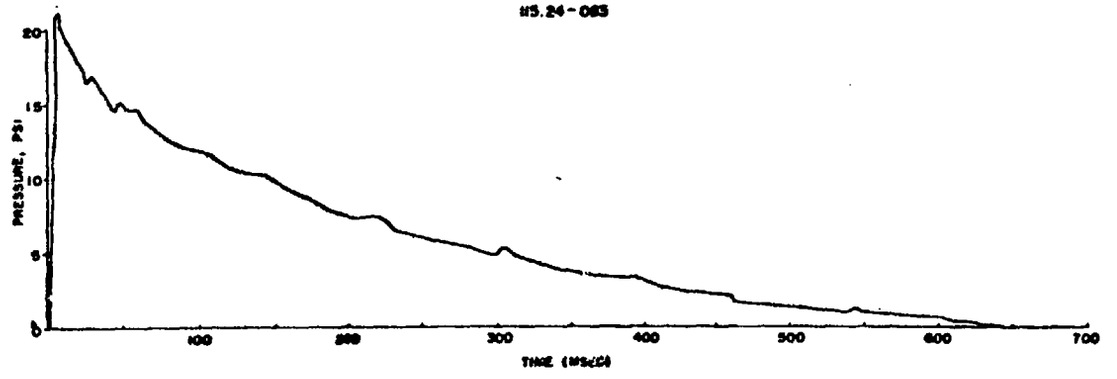
115.24 - 063
PRESSURE, PSI
TIME (MSEC)

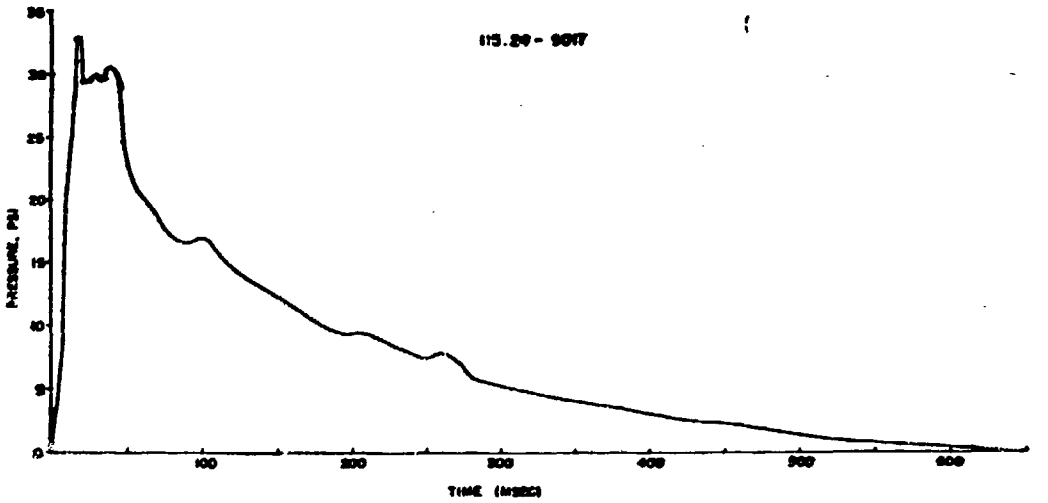
115.29 - 9017
PRESSURE, PSI
TIME (MSEC)

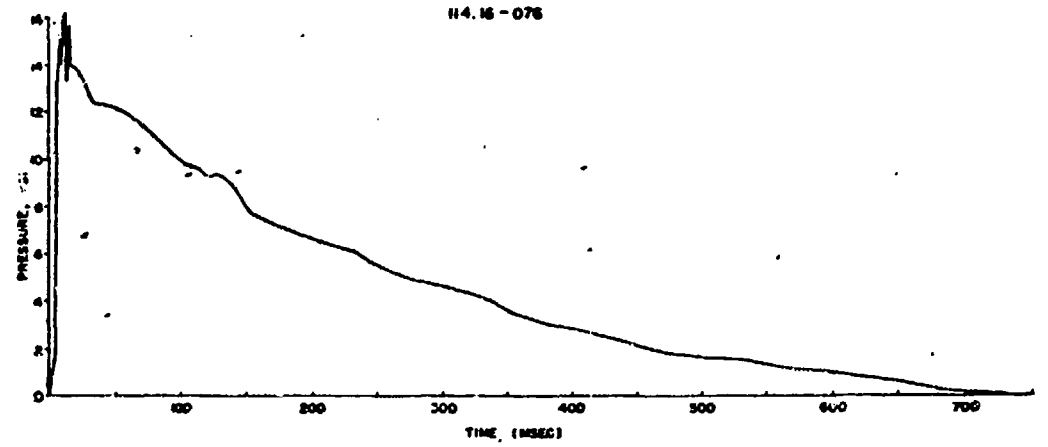
114.16 - 076
PRESSURE, PSI
TIME, (MSEC)

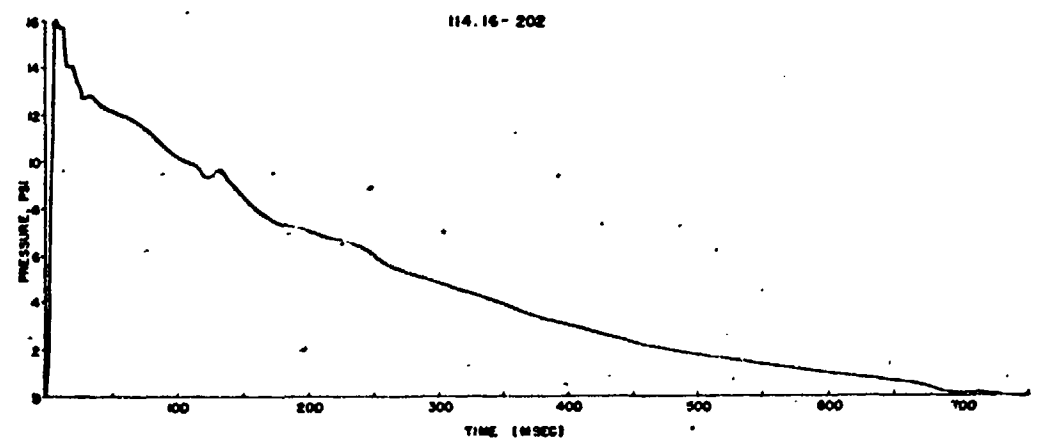
114.16 - 202
PRESSURE, PSI
TIME (MSEC)



SECRET

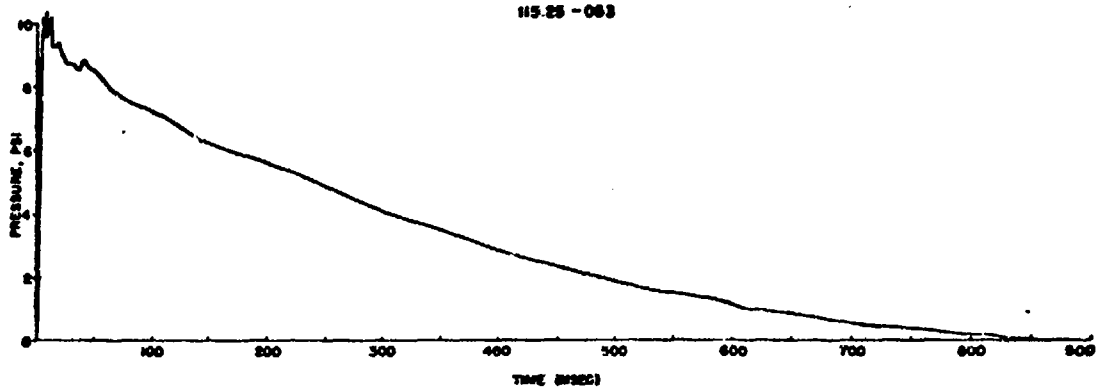
115.25 - 083
PRESSURE, PSI
TIME (MSEC)

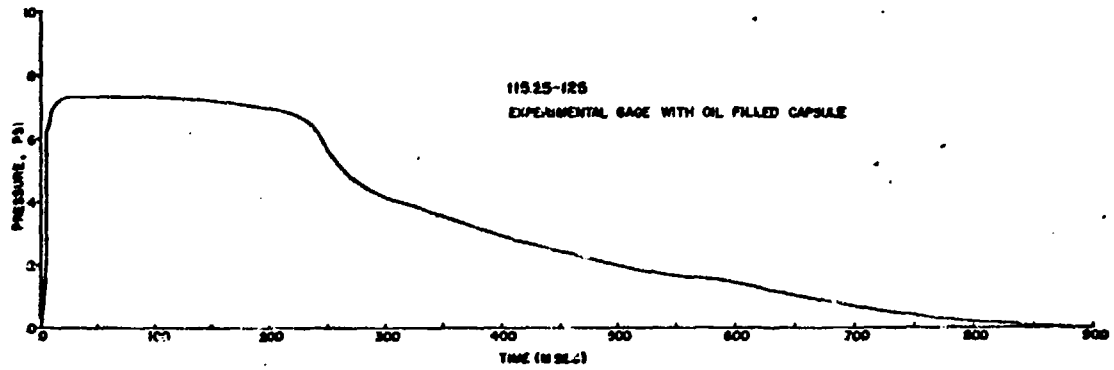
115.25-125
EXPERIMENTAL GAGE WITH OIL FILLED CAPSULE
PRESSURE, PSI
TIME (M SEC)

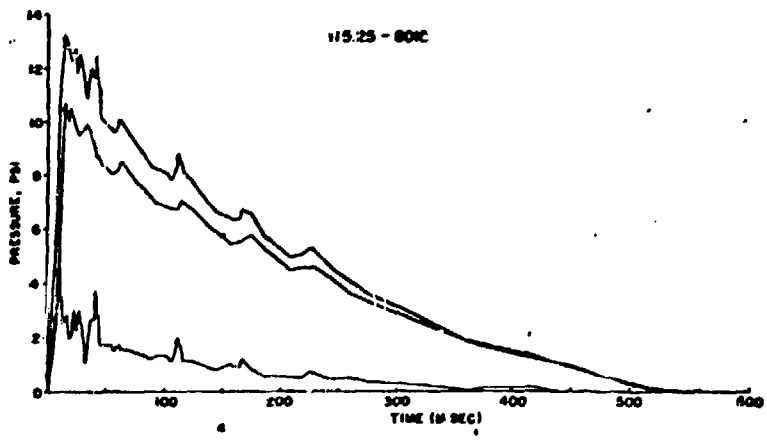
115.25 - 80XC
PRESSURE, PSI
TIME (M SEC)



SECRET

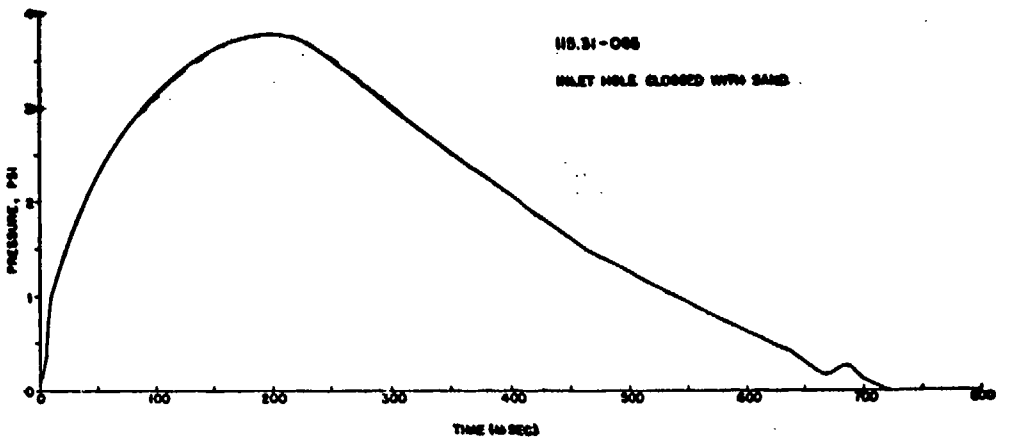
115.31-066
INLET HOLE CLOGGED WITH SAND
PRESSURE, PSI
TIME (MSEC)

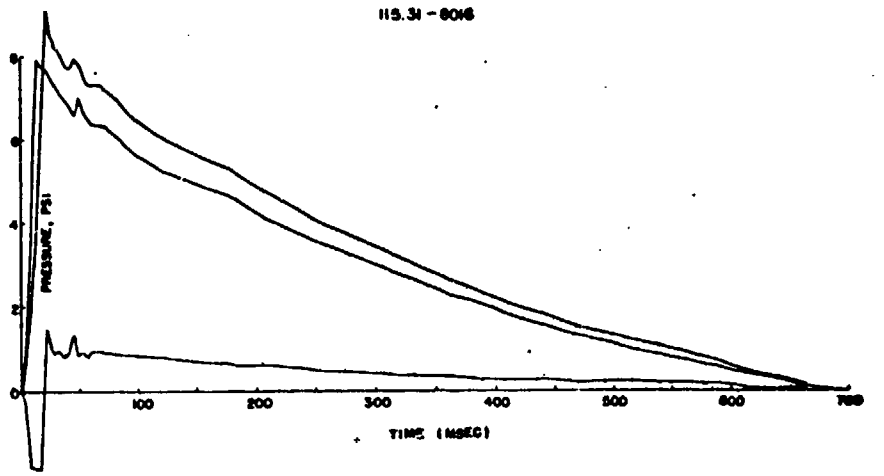
115.31-8016
PRESSURE, PSI
TIME (MSEC)

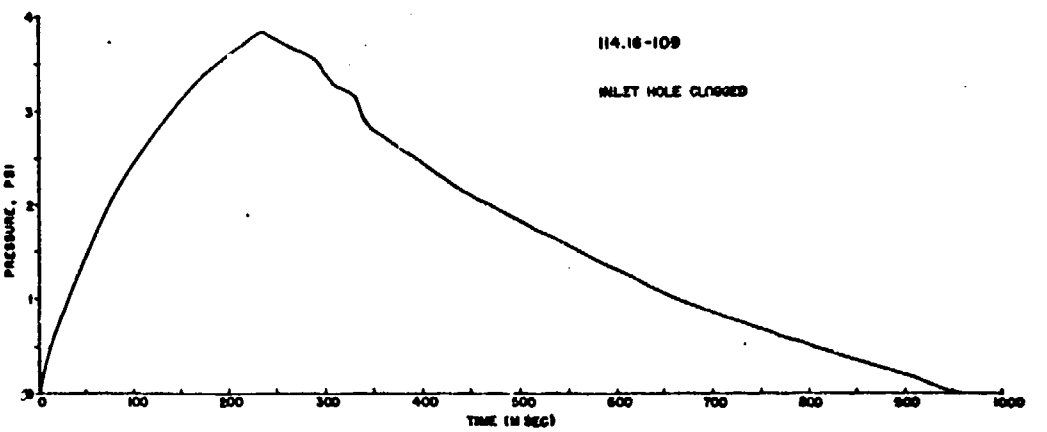
114.16-109
INLET HOLE CLOGGED
PRESSURE, PSI
TIME (M SEC)



SECRET

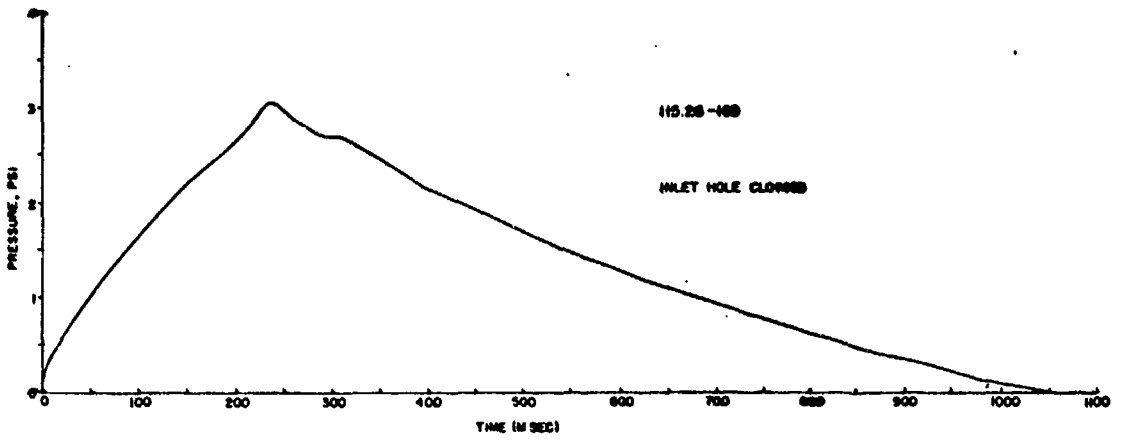
PRESSURE, PSI
INLET HOLE CLOSED
0
100
200
300
400
500
600
700
800
900
1000
1100
TIME (M SEC)

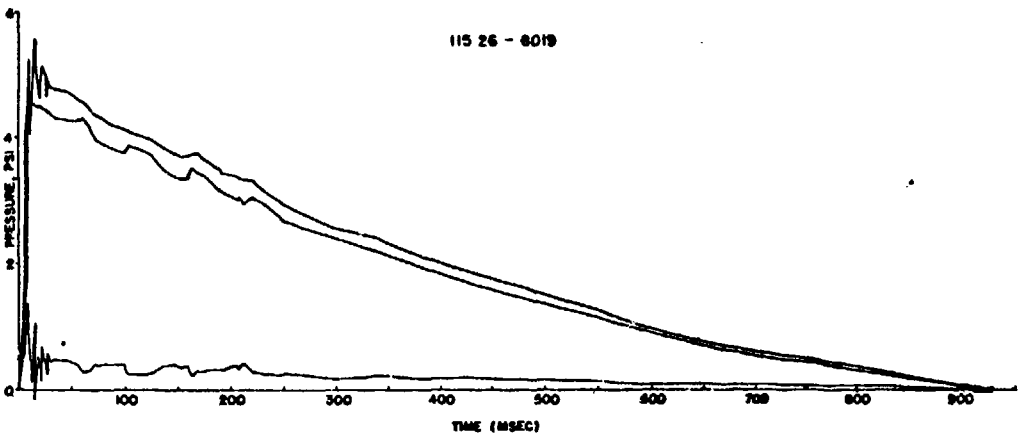
115 26 - 6019
PRESSURE, PSI
0
100
200
300
400
500
600
700
800
900
TIME (MSEC)

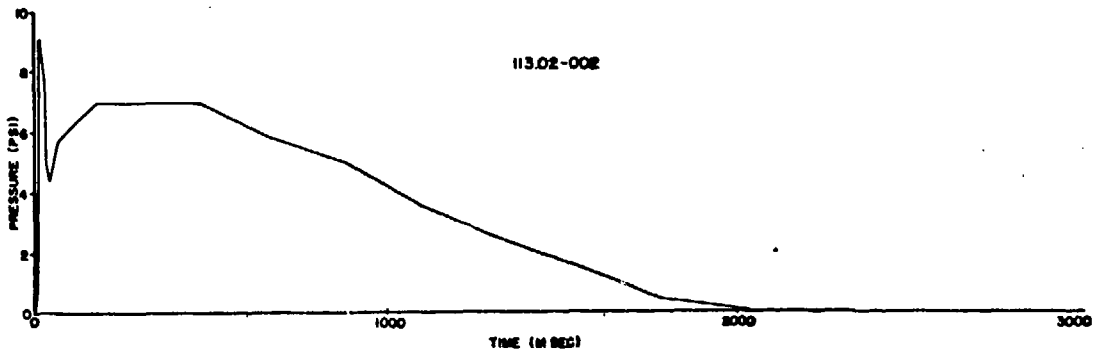
113.02-002
PRESSURE (PSI)
0
1000
2000
3000
TIME (M SEC)



SECRET

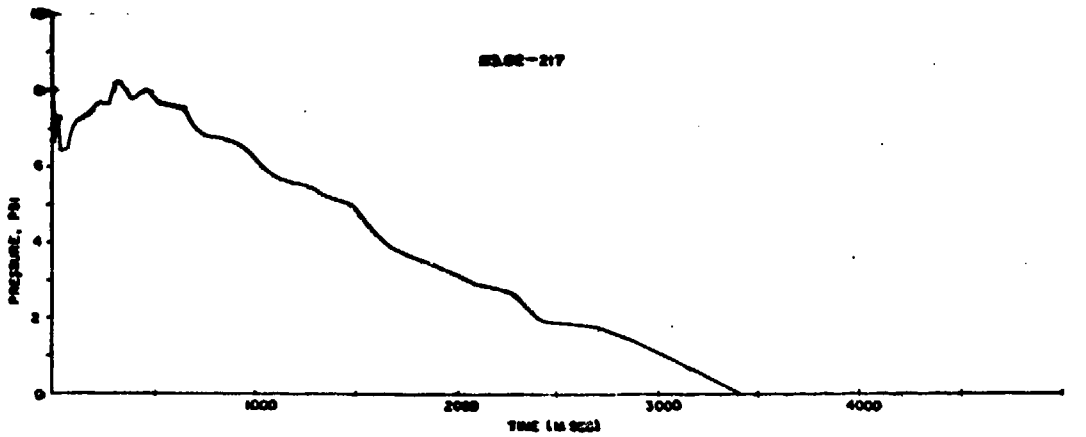
PRESSURE, PSI
0
2
4
6
8
1000
2000
3000
4000
TIME (M SEC)

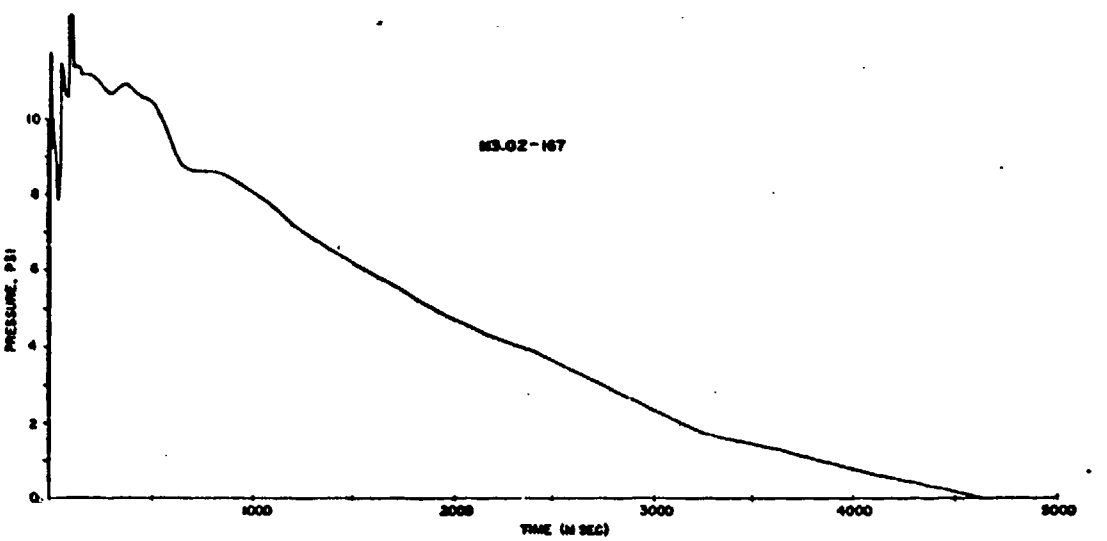
113.02-167
PRESSURE, PSI
0
2
4
6
8
10
1000
2000
3000
4000
5000
TIME (M SEC)

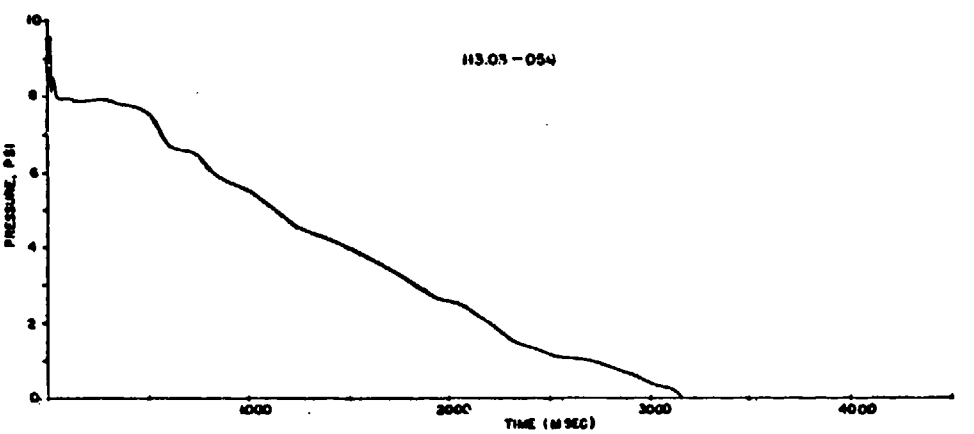
113.05-054
PRESSURE, PSI
0
2
4
6
8
10
4000
3000
4000
TIME (M SEC)



SECRET

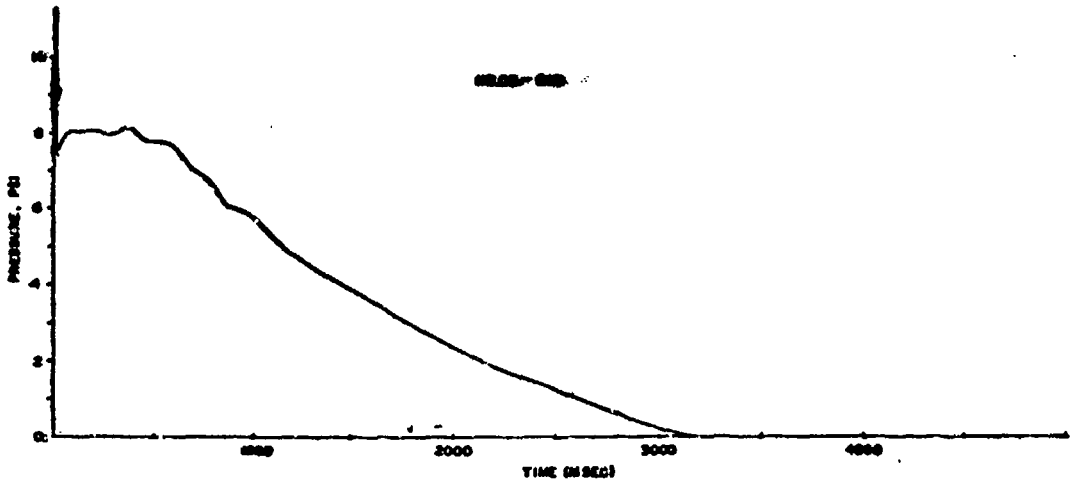
PRESSURE, PSI
2000
3000
4000
TIME (M SEC)

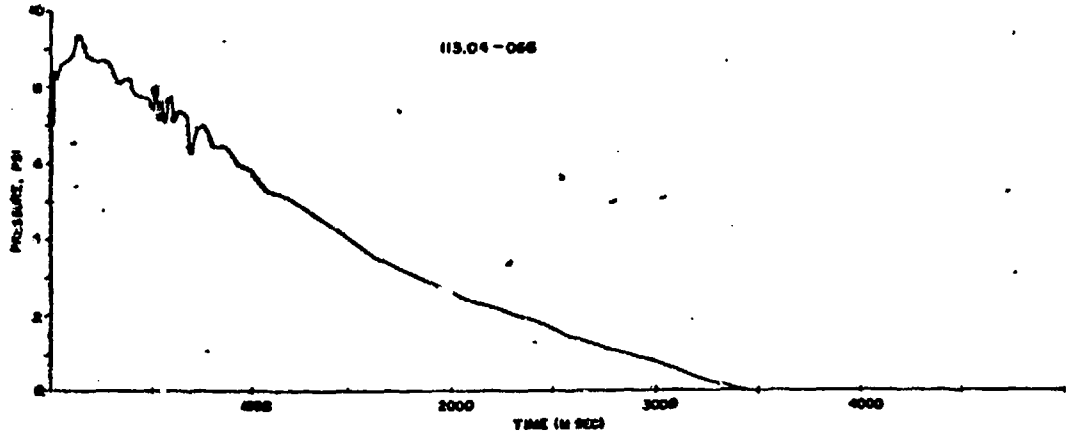
113.04 - 066
PRESSURE, PSI
2000
3000
4000
TIME (M SEC)

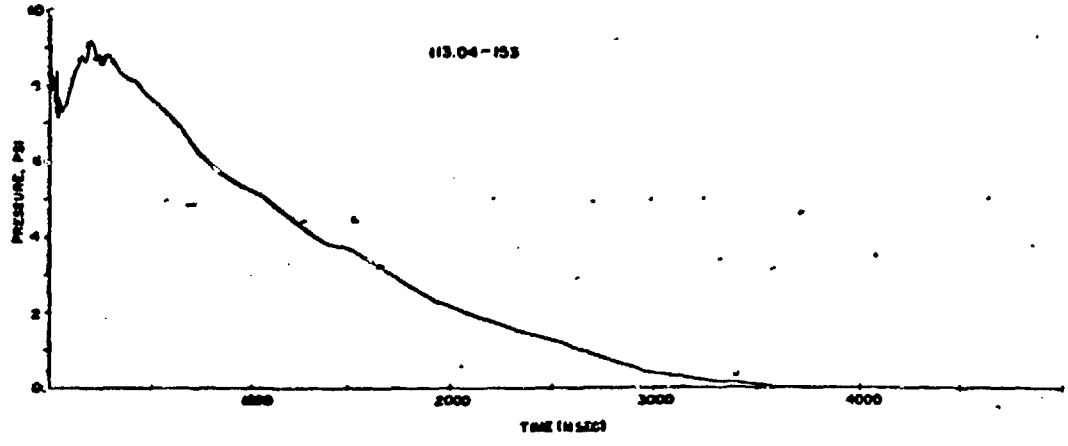
113.04 - 153
PRESSURE, PSI
2000
3000
4000
TIME (M SEC)



SECRET

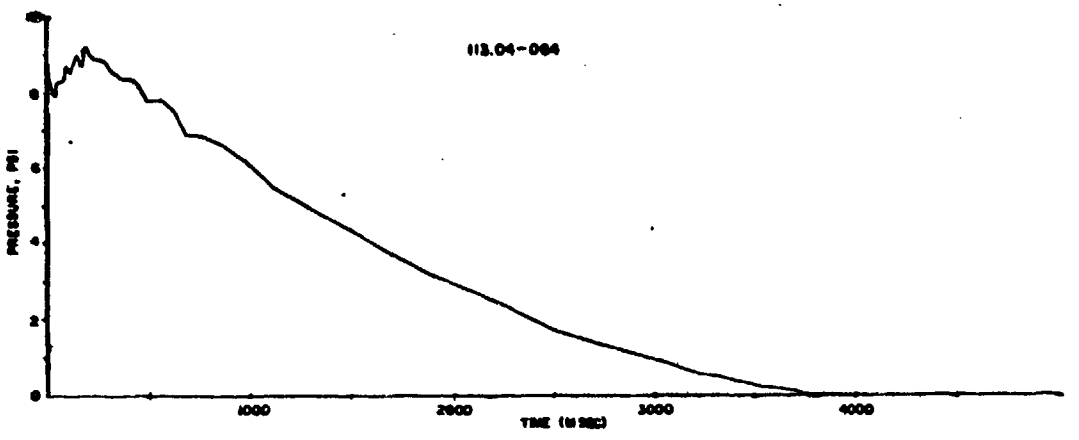
113.04-064
PRESSURE, PSI
0
2
4
6
8
1000
2000
3000
4000
TIME (M SEC)

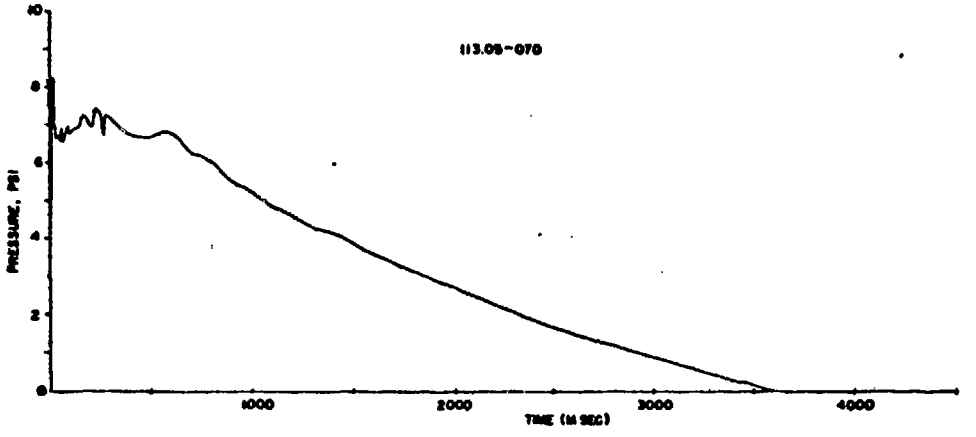
113.05-070
PRESSURE, PSI
0
2
4
6
8
10
1000
2000
3000
4000
TIME (M SEC)

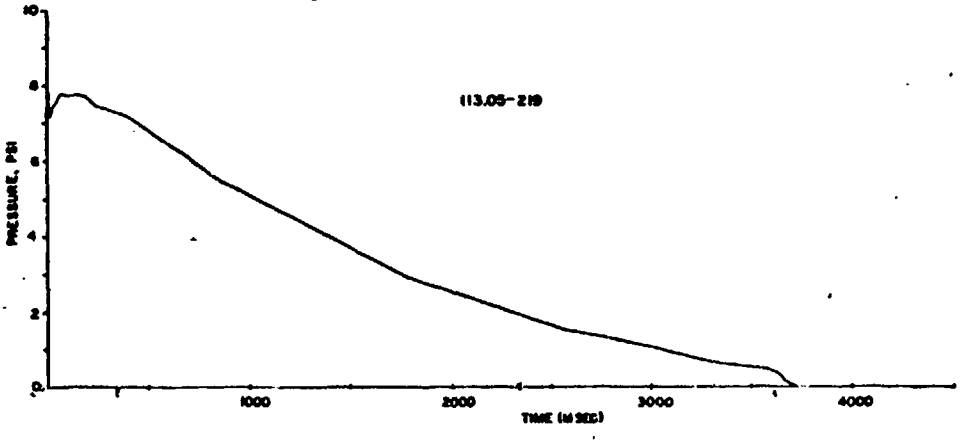
113.05-219
PRESSURE, PSI
0
2
4
6
8
10
1000
2000
3000
4000
TIME (M SEC)



SECRET

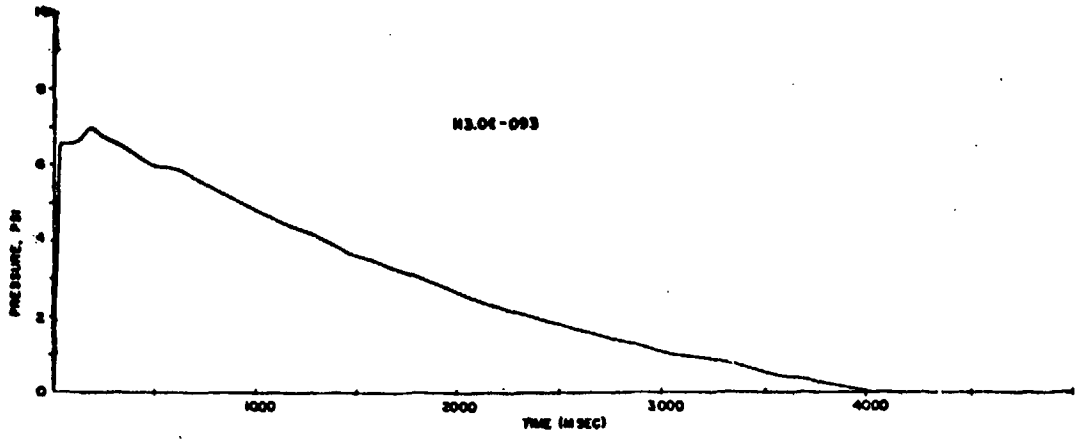
113.06-093
PRESSURE, PSI
0
2
4
6
8
10
1000
2000
3000
4000
TIME (M SEC)

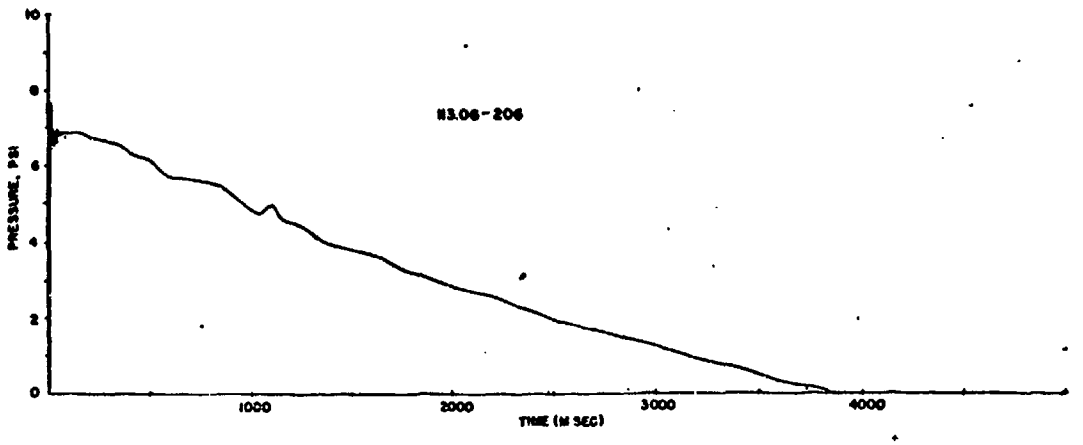
113.06-206
PRESSURE, PSI
0
2
4
6
8
10
1000
2000
3000
4000
TIME (M SEC)

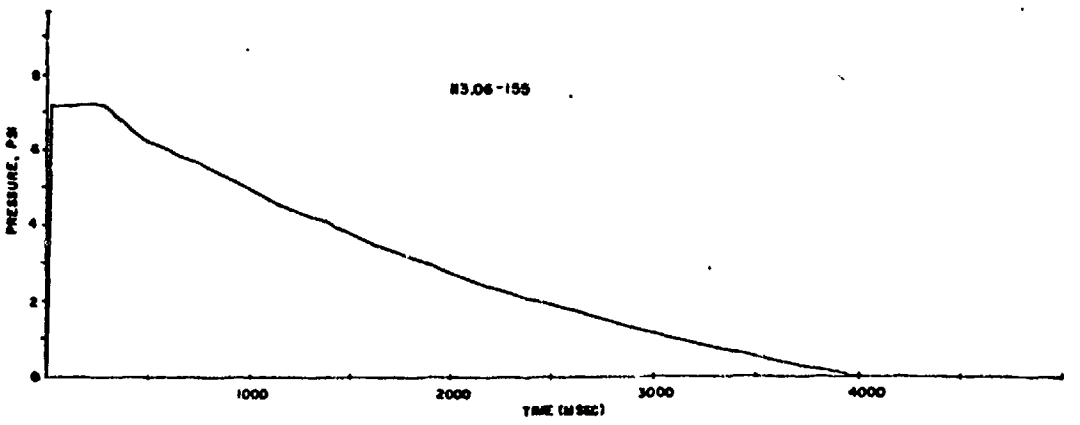
113.06-156
PRESSURE, PSI
0
2
4
6
8
1000
2000
3000
4000
TIME (M SEC)

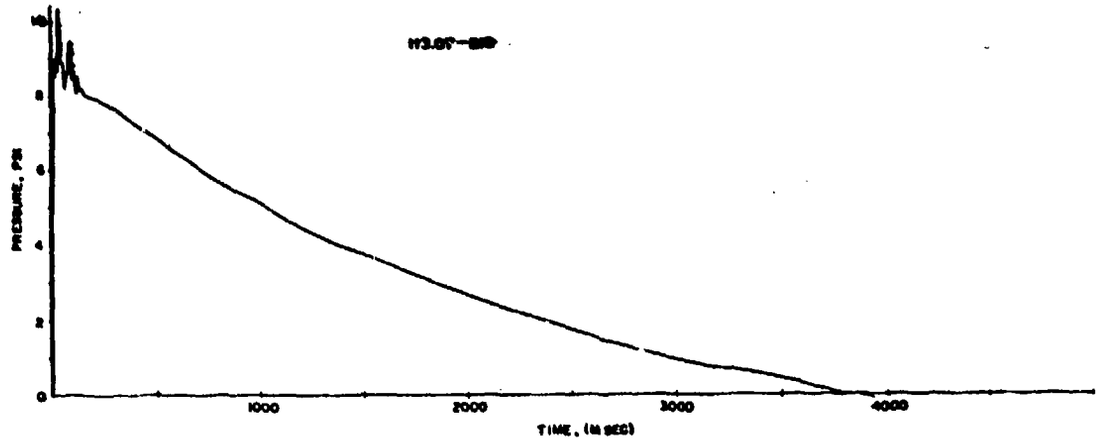
PRESSURE, PSI
0
2
4
6
8
10
1000
2000
3000
4000
TIME, (M SEC)

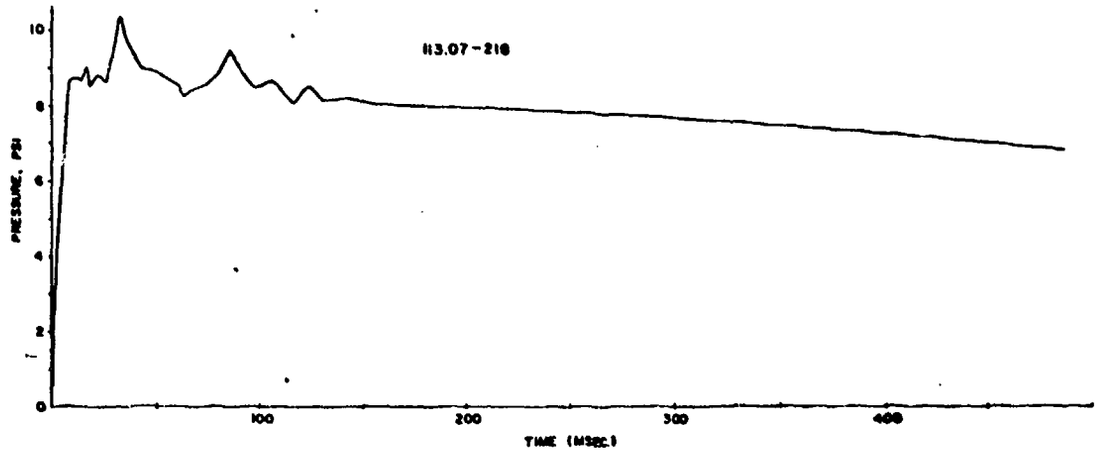
113.07-218
PRESSURE, PSI
0
2
4
6
8
10
100
200
300
400
TIME (MSEC)

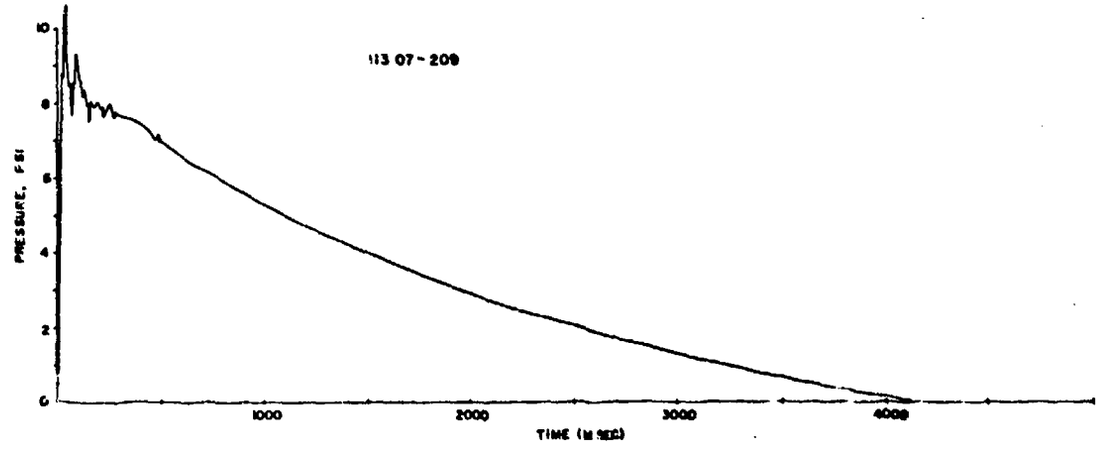
113 07-209
PRESSURE, PSI
0
2
4
6
8
10
1000
2000
3000
4000
TIME (M SEC)



SECRET

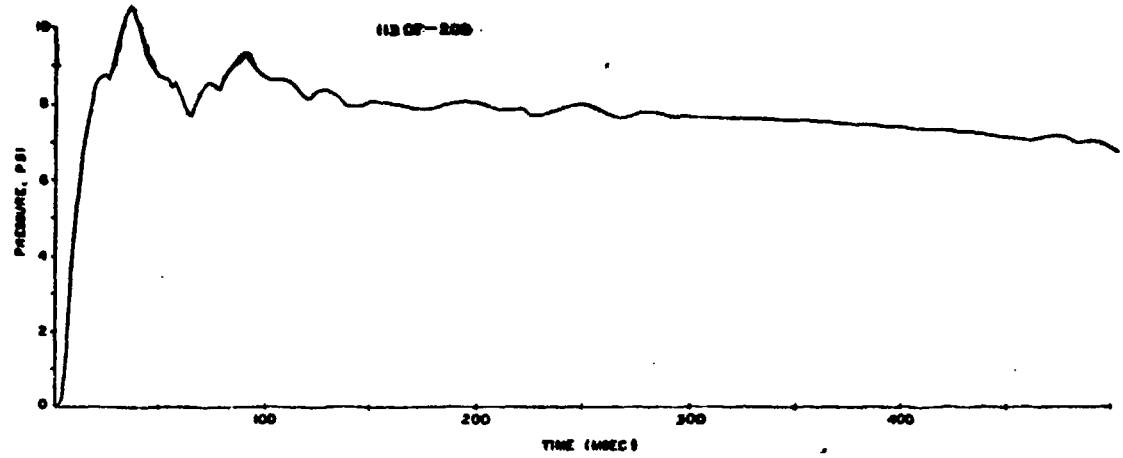
PRESSURE, PSI
0
2
4
6
8
10
100
200
300
400
TIME (MSEC)

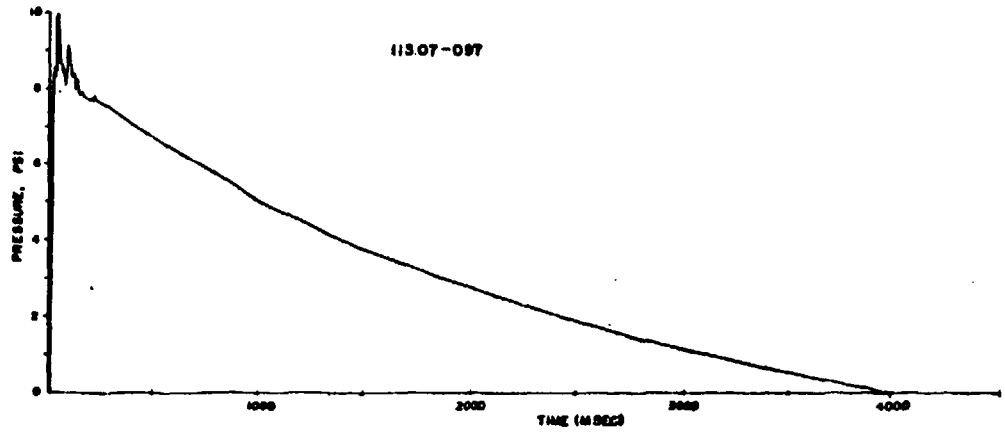
113.07-097
PRESSURE, PSI
0
2
4
6
8
10
1000
2000
3000
4000
TIME (MSEC)

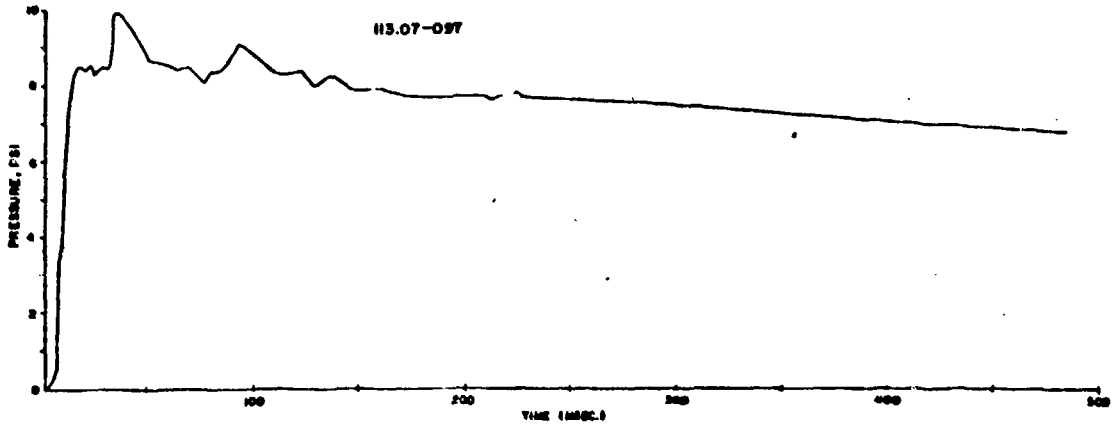
113.07-097
PRESSURE, PSI
0
2
4
6
8
10
100
200
300
400
500
TIME (MSEC.)



SECRET

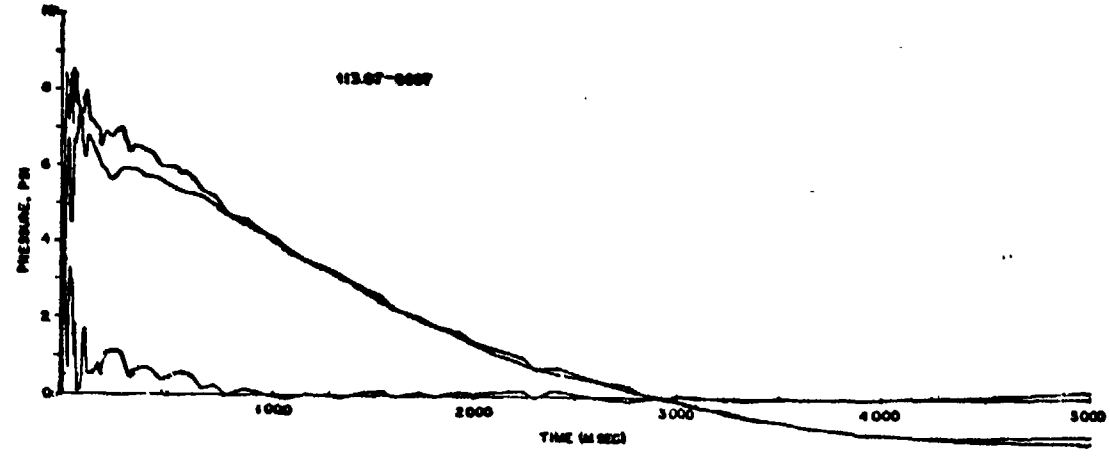
PRESSURE, PSI
0
2
4
6
8
1000
2000
3000
4000
5000
TIME (M SEC)

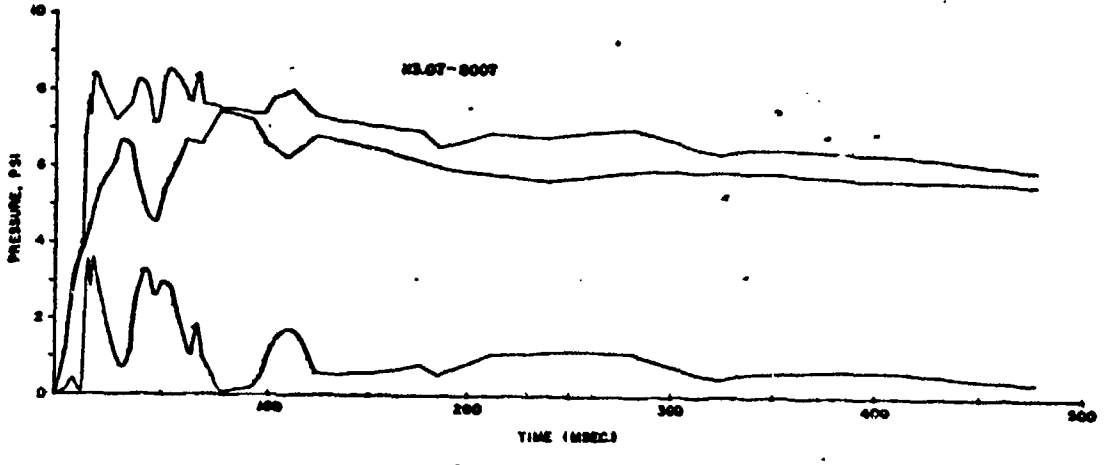
PRESSURE, PSI
0
2
4
6
8
10
200
300
400
500
TIME (MSEC.)

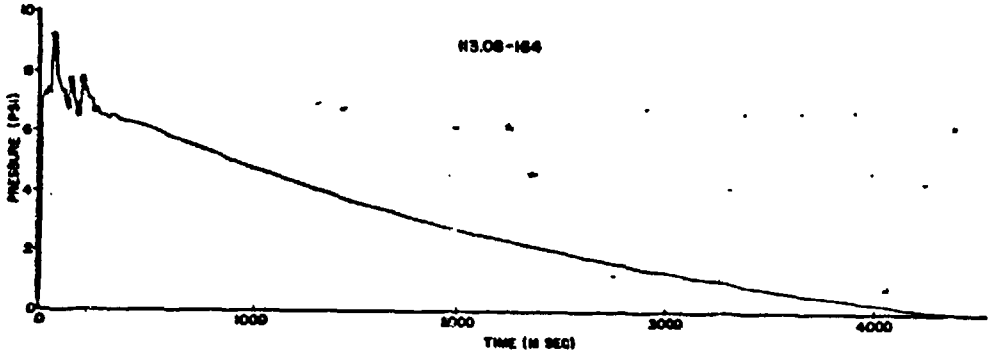
PRESSURE (PSI)
0
2
4
6
8
10
1000
2000
3000
4000
TIME (M SEC)



SECRET

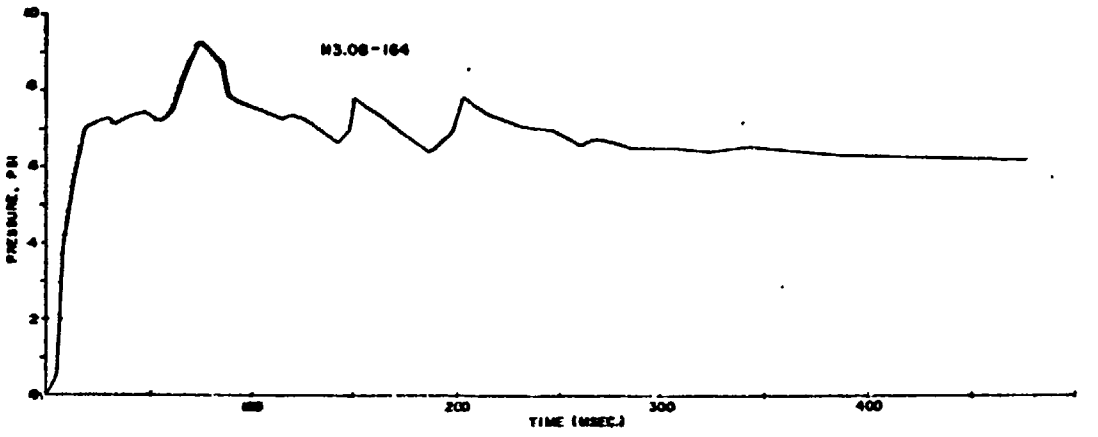
M3.08-164
PRESSURE, PSI
TIME (MSEC.)

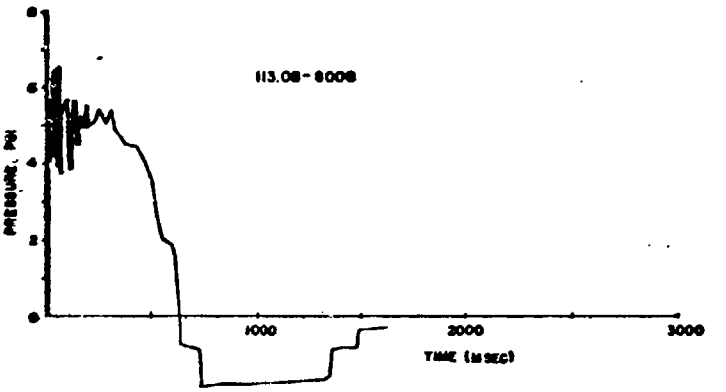
M3.08-8008
PRESSURE, PSI
TIME (MSEC)

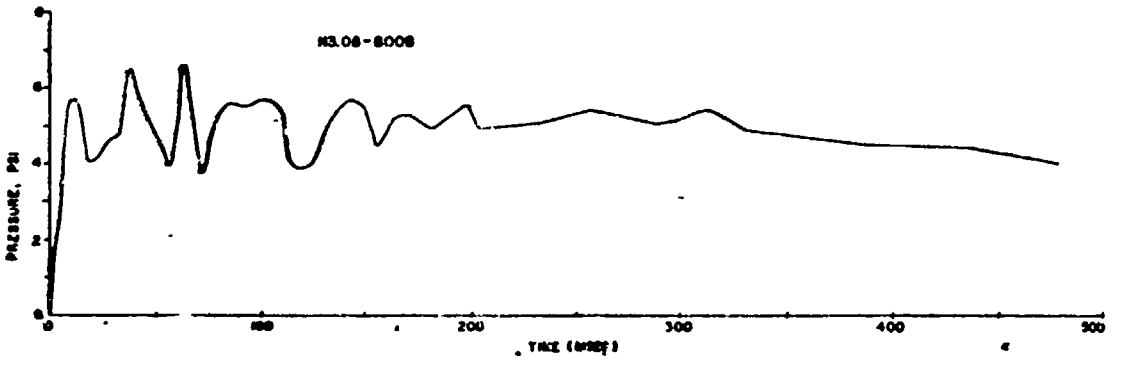
M3.08-8008
PRESSURE, PSI

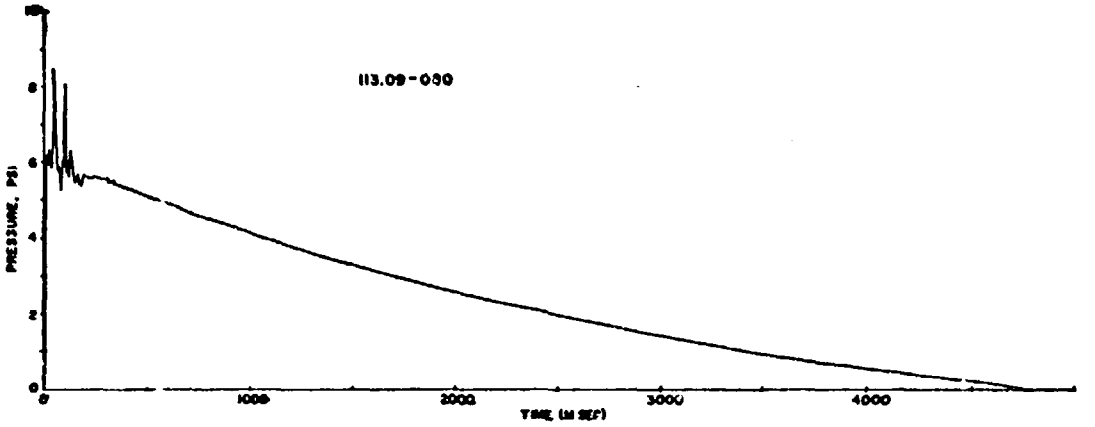
113.09-030
PRESSURE, PSI
0
2
4
6
8
1000
2000
3000
4000
TIME (M SEC)

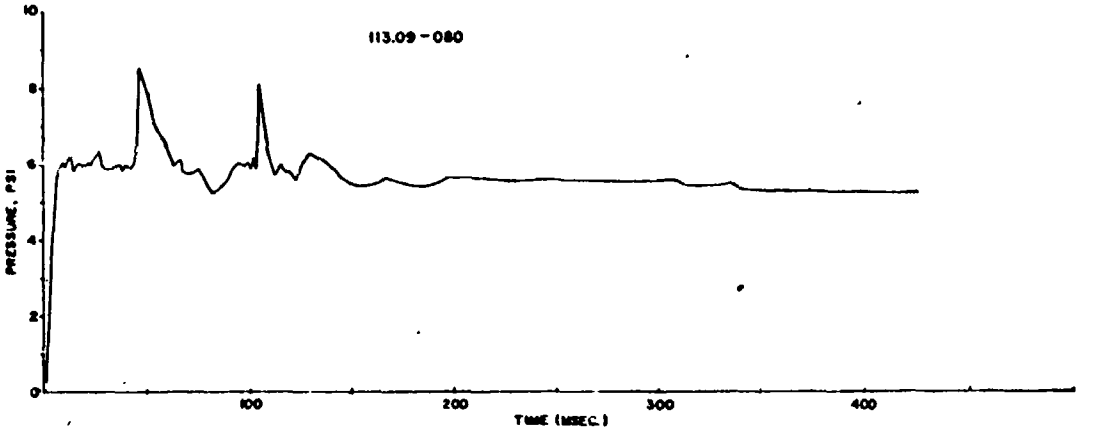
113.09-080
PRESSURE, PSI
0
2
4
6
8
10
100
200
300
400
TIME (MSEC.)

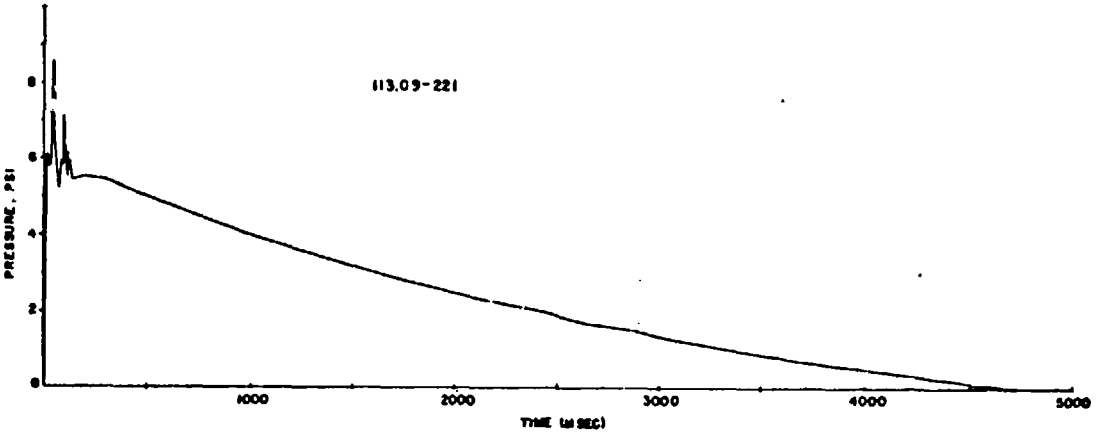
113.09-221
PRESSURE, PSI
0
2
4
6
8
1000
2000
3000
4000
5000
TIME (M SEC)

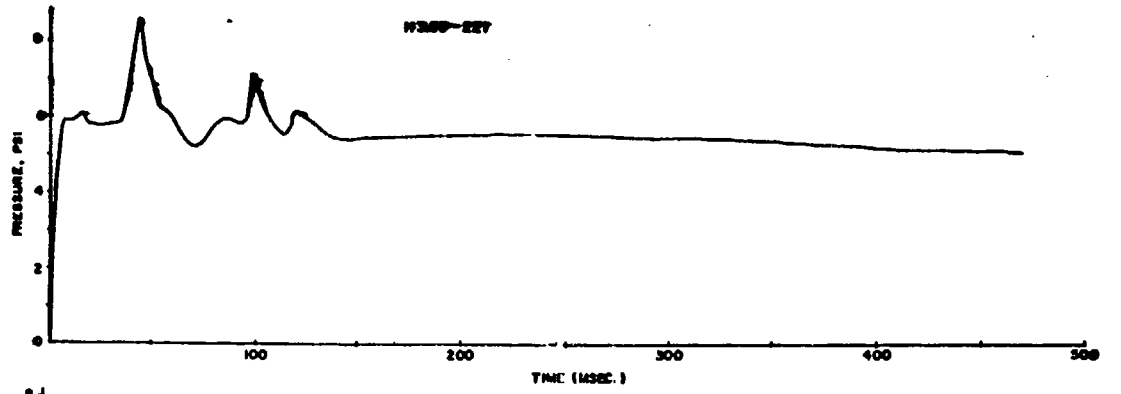
PRESSURE, PSI
TIME (MSEC.)

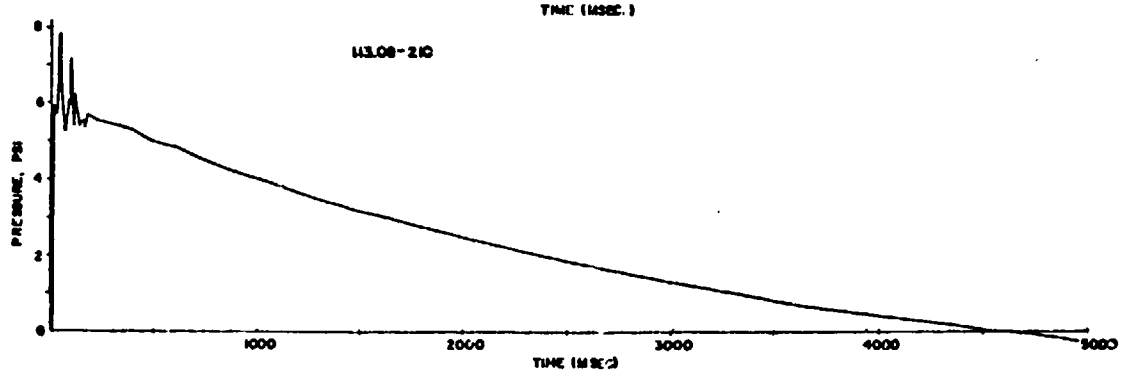
113.08-210
PRESSURE, PSI
TIME (MSEC.)

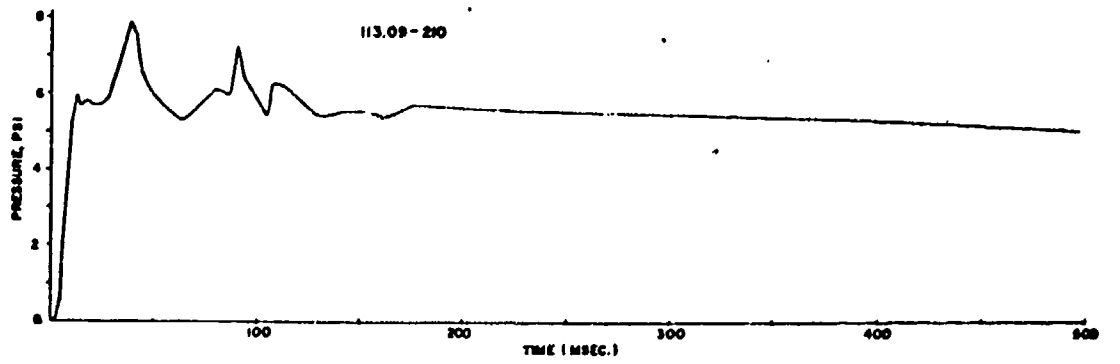
113.09-210
PRESSURE, PSI
TIME (MSEC.)

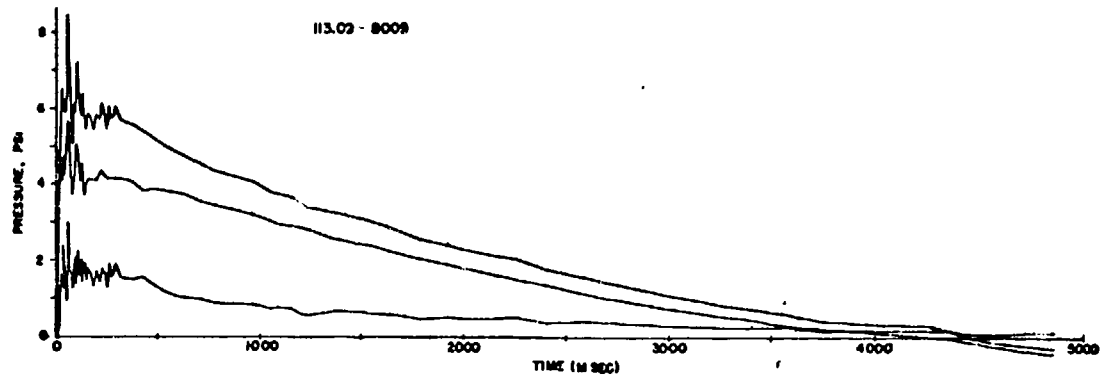
113.02-8009
PRESSURE, PSI
TIME (MSEC)

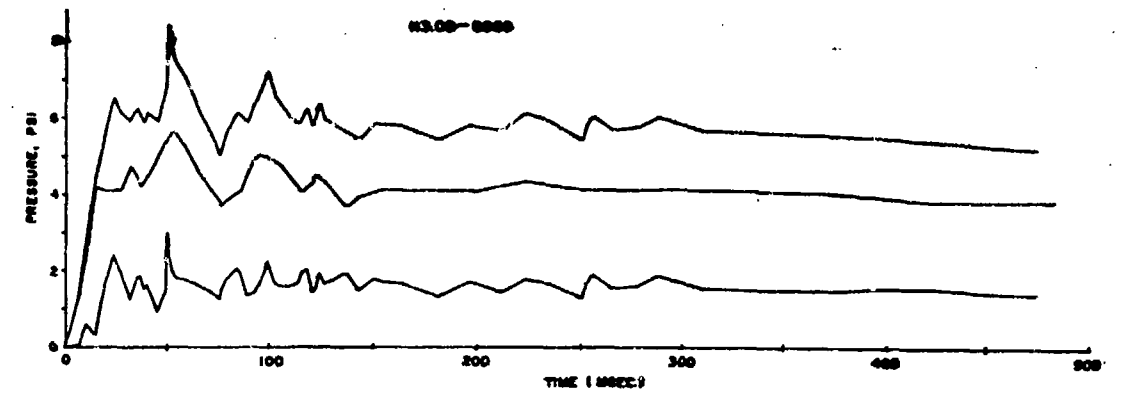
PRESSURE, PSI
0
2
4
6
8
0
100
200
300
400
500
TIME (MSEC.)

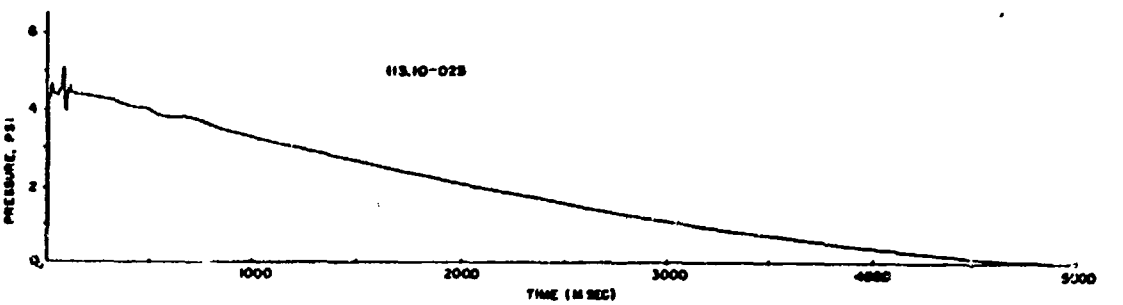
PRESSURE, PSI
0
2
4
6
1000
2000
3000
5000
TIME (MSEC)

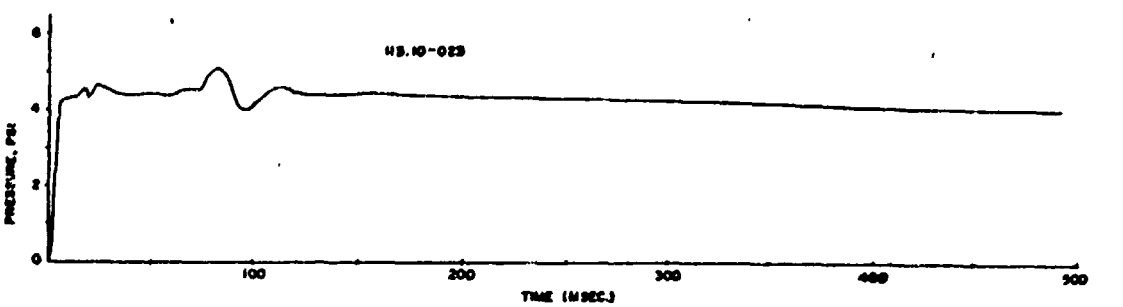
PRESSURE, PSI
0
2
4
6
100
200
300
400
500
TIME (MSEC.)

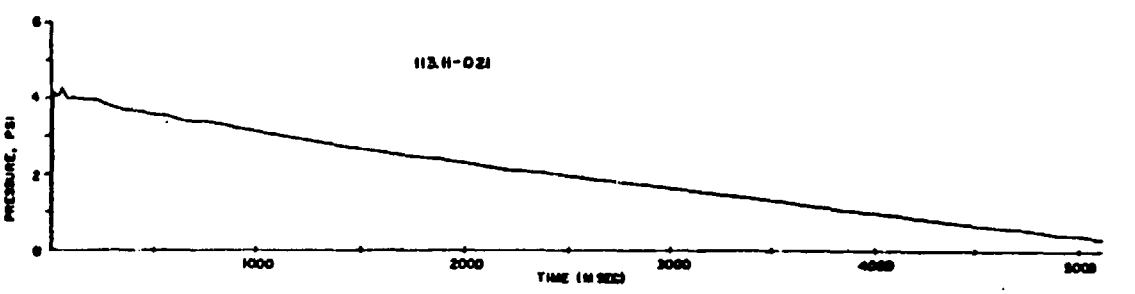
PRESSURE, PSI
0
2
4
6
1000
2000
3000
TIME (MSEC)

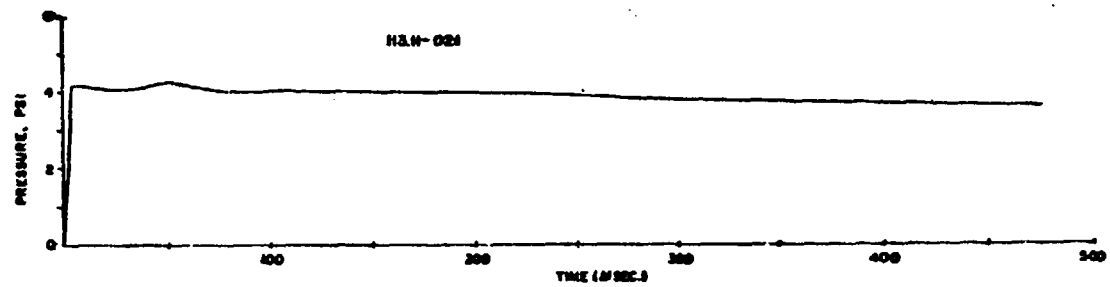


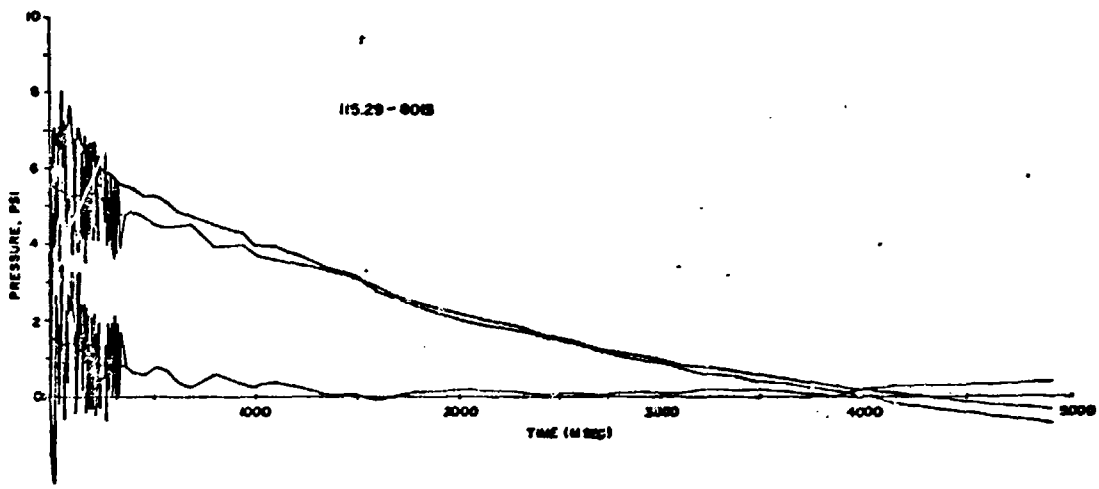


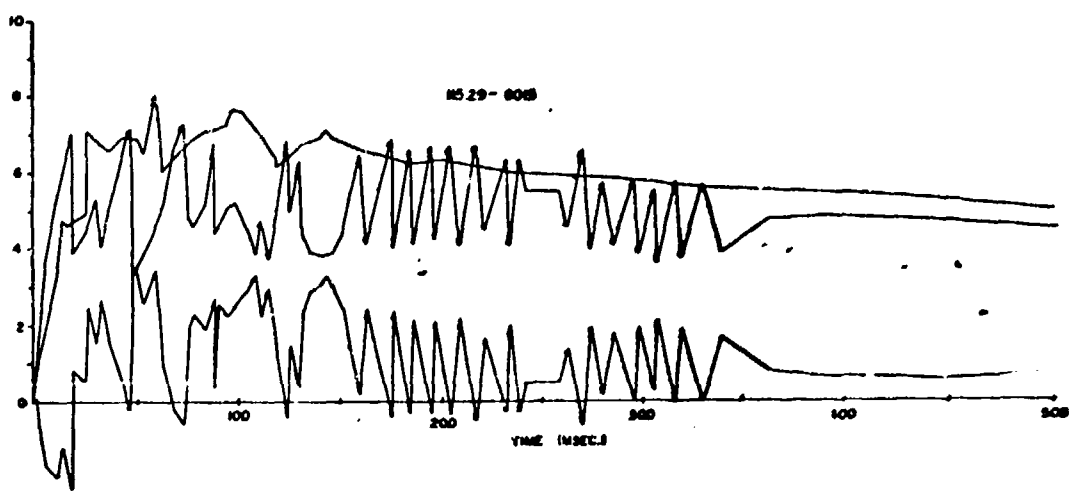




SECRET

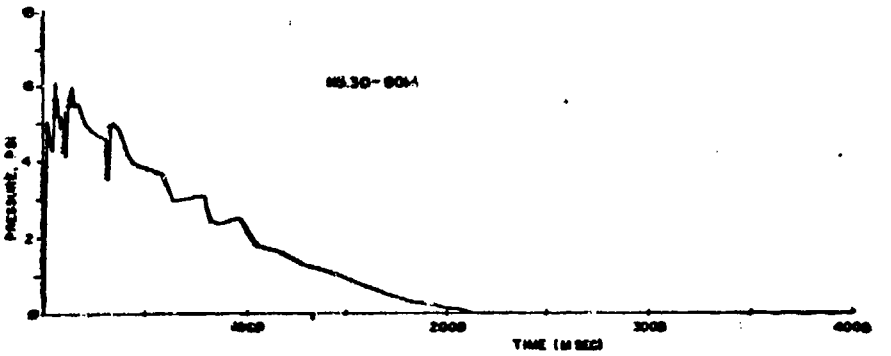
PRESSURE, PSI
TIME (M SEC)

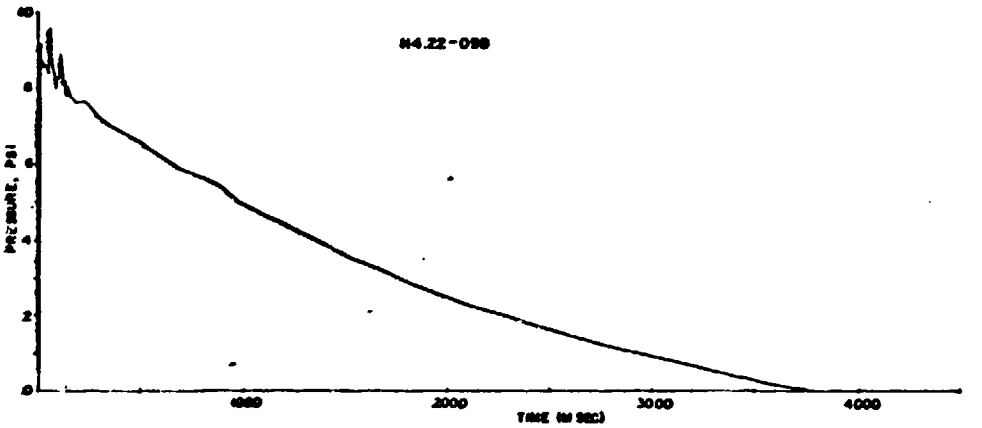
M4.22-098
PRESSURE, PSI
2000
3000
4000
TIME (M SEC)

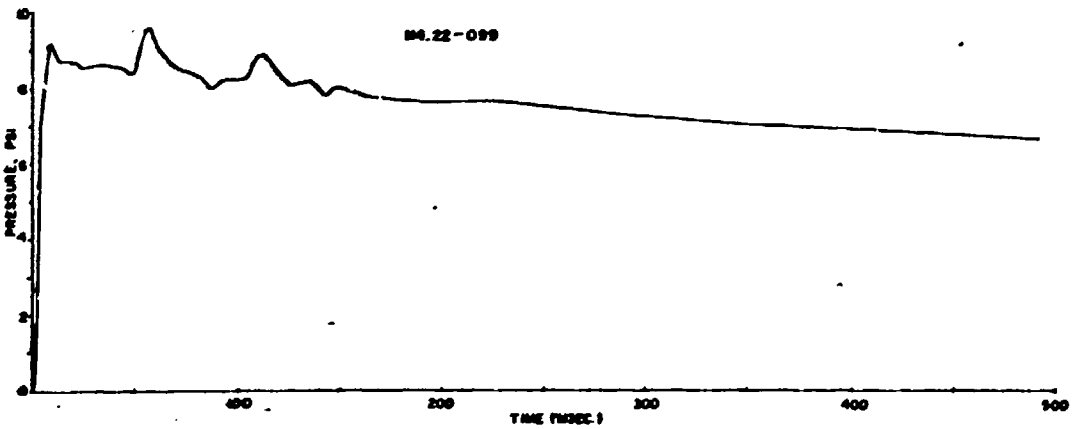
M4.22-099
PRESSURE, PSI
200
300
400
500



SECRET

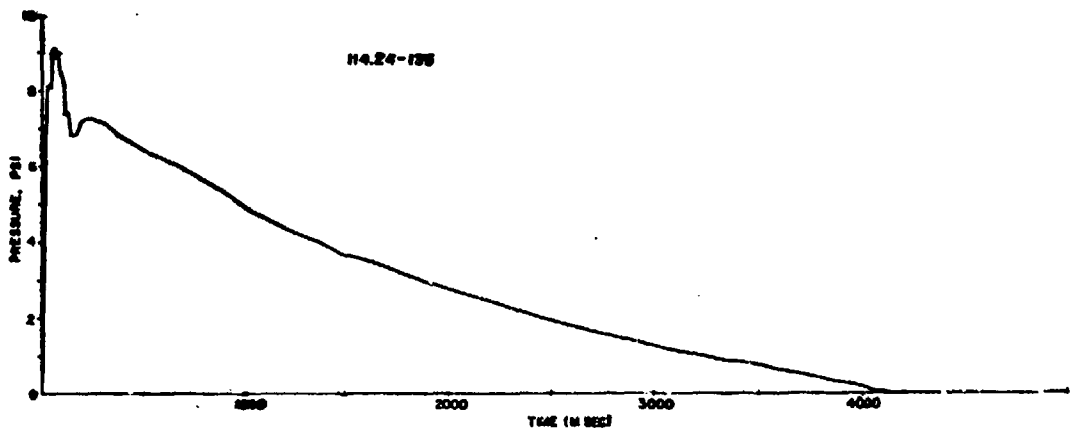
114.24-136
PRESSURE, PSI
0
2
4
6
8
2000
3000
4000
TIME (M SEC)

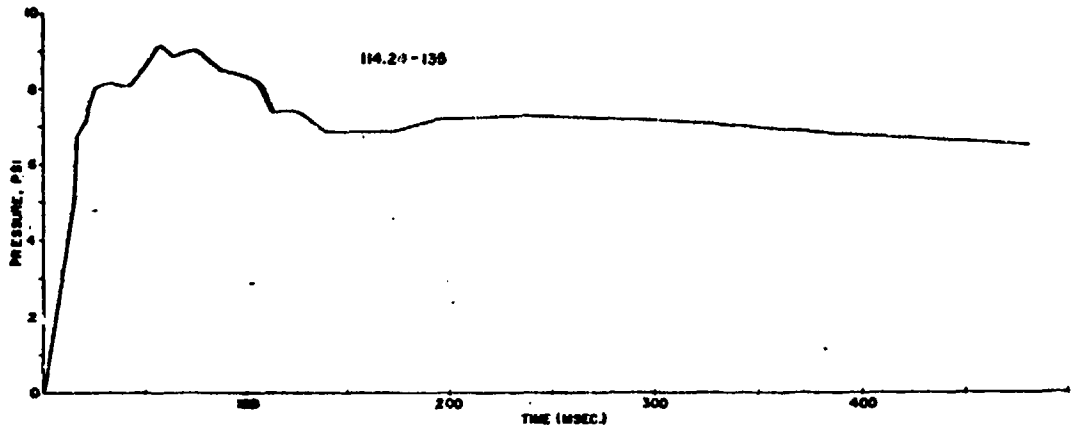
114.24-136
PRESSURE, PSI
0
2
4
6
8
200
300
400
TIME (MSEC.)

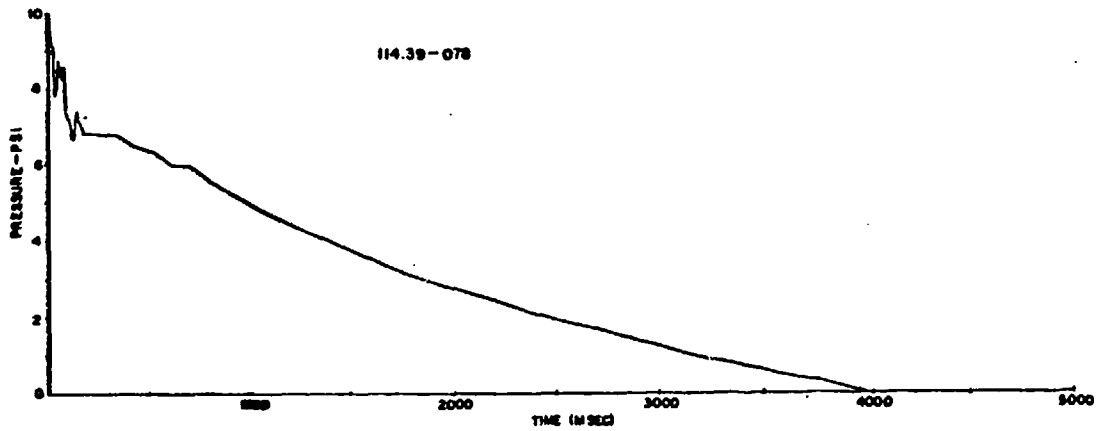
114.39-078
PRESSURE-PSI
0
2
4
6
8
10
2000
3000
4000
5000
TIME (M SEC)



SECRET

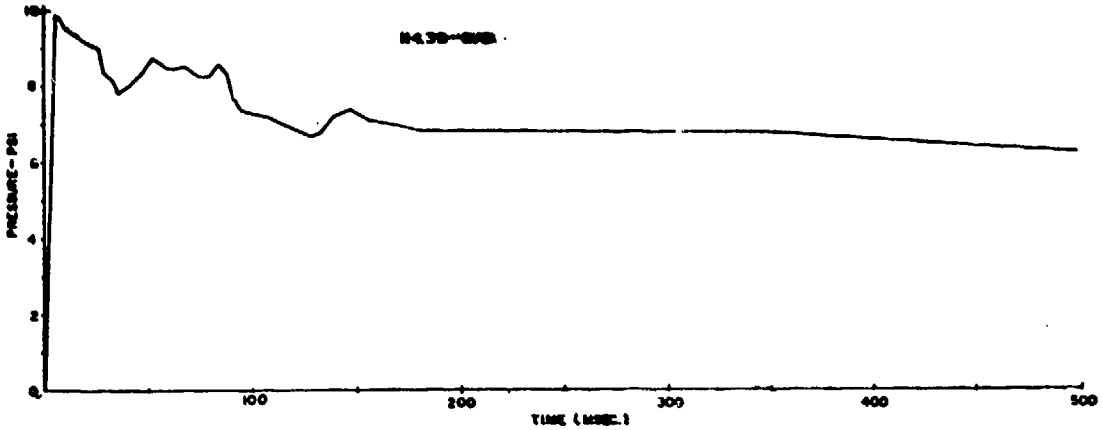
PRESSURE - PSI
0
2
4
6
8
100
100
200
300
400
500
TIME (MSEC.)

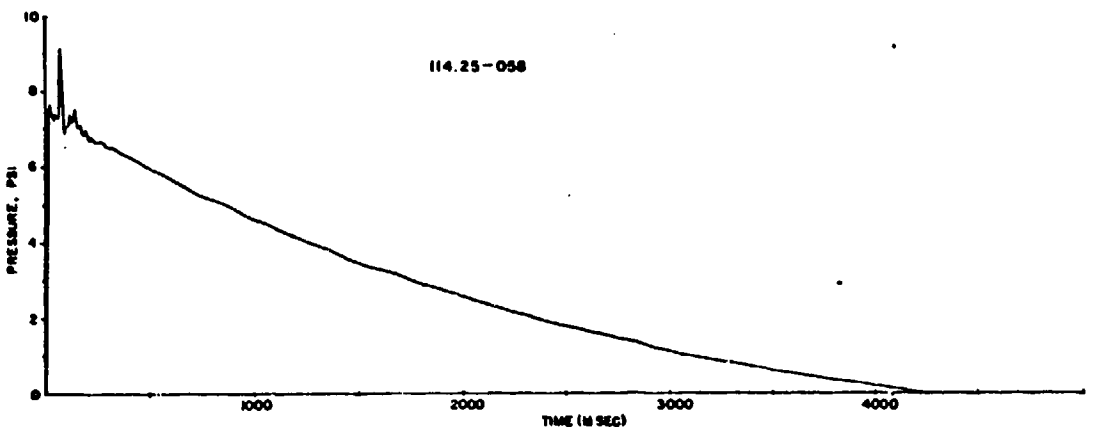
114.25-058
PRESSURE, PSI
0
2
4
6
8
10
1000
2000
3000
4000
TIME (M SEC)

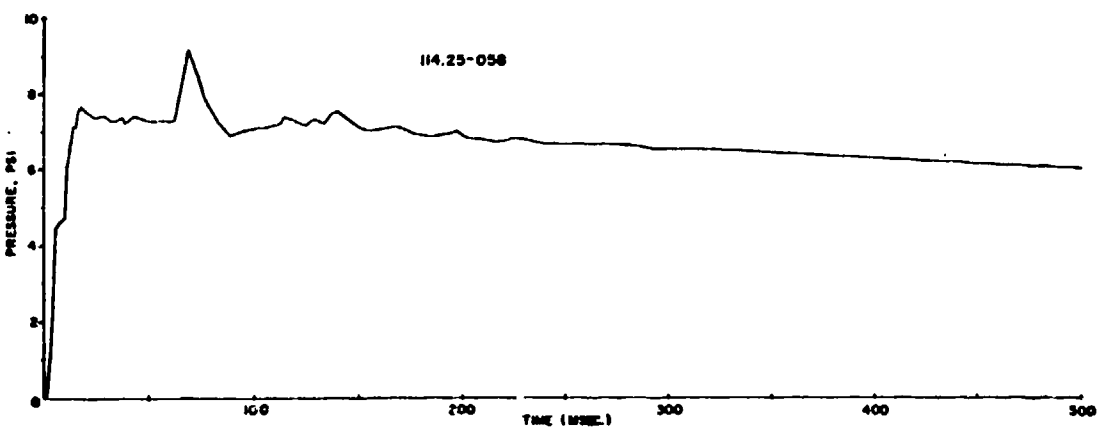
114.25-058
PRESSURE, PSI
0
2
4
6
8
10
100
200
300
400
500
TIME (MSEC.)



SECRET

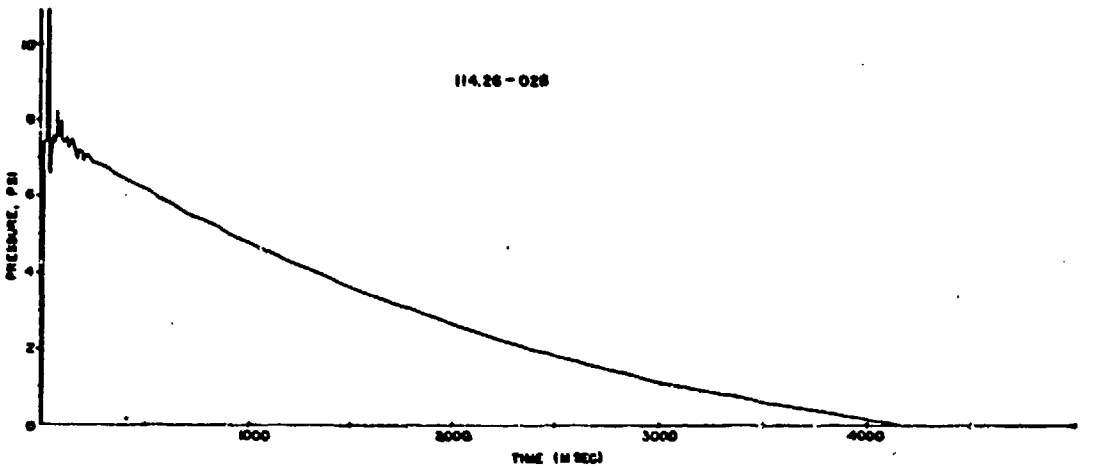
114.26-028
PRESSURE, PSI
0
2
4
6
8
10
1000
2000
3000
4000
TIME (MSEC)

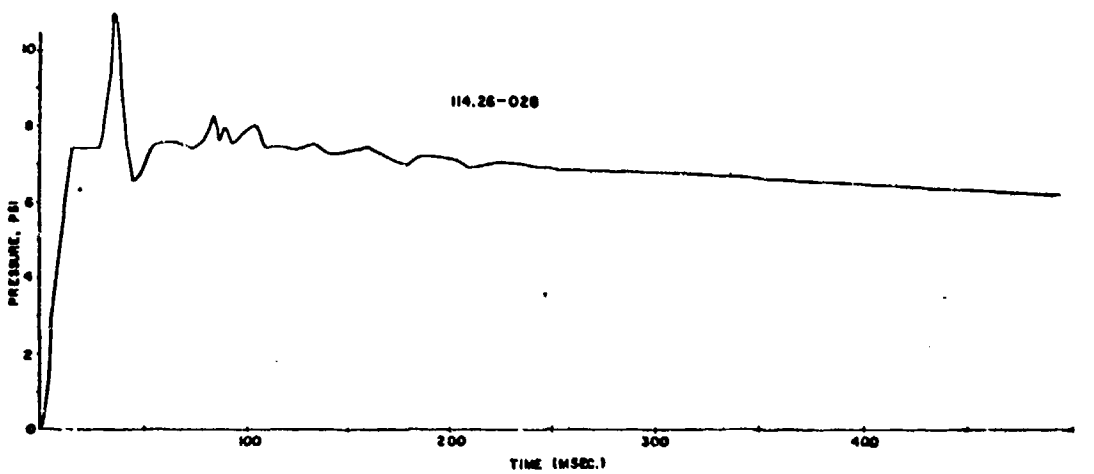
114.26-028
PRESSURE, PSI
0
2
4
6
8
10
100
200
300
400
TIME (MSEC.)

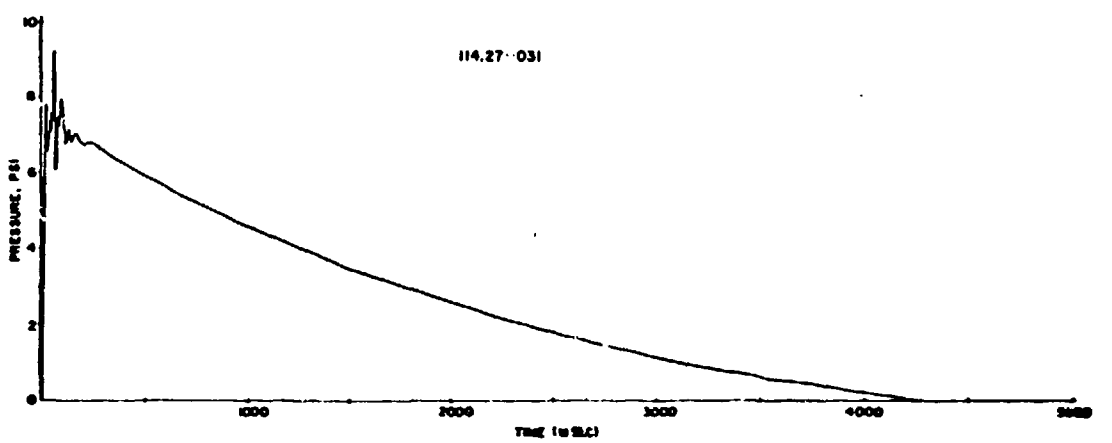
114.27-031
PRESSURE, PSI
0
2
4
6
8
10
1000
2000
3000
4000



SECRET

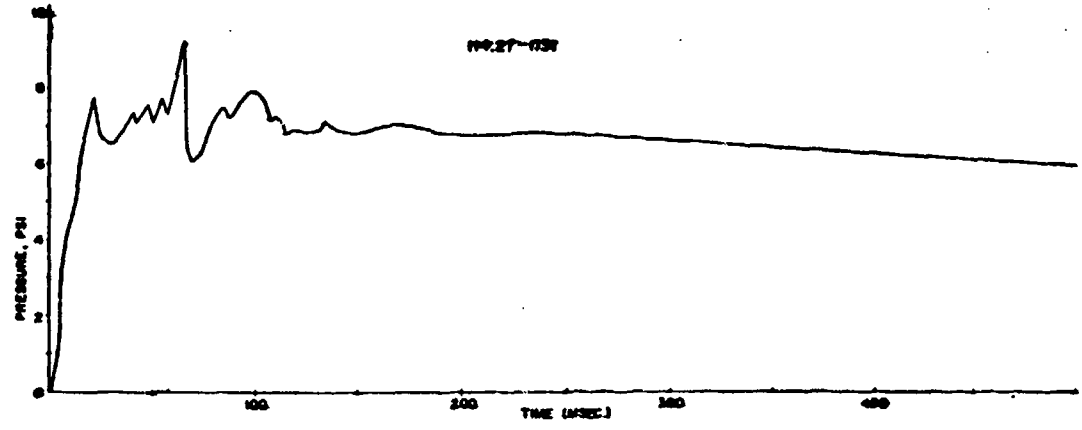
PRESSURE, PSI
TIME (MSEC)

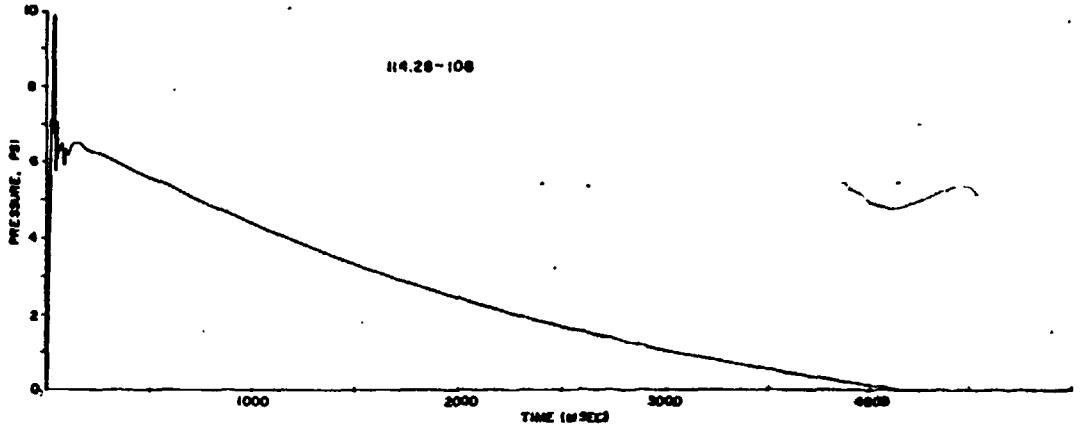
114.28-108
PRESSURE, PSI
TIME (MSEC)

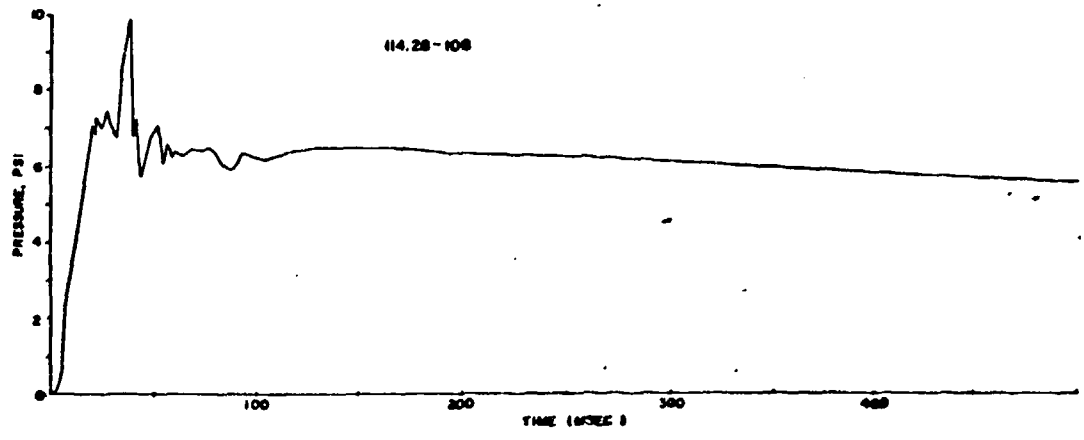
114.28-108
PRESSURE, PSI
TIME (MSEC)



SECRET

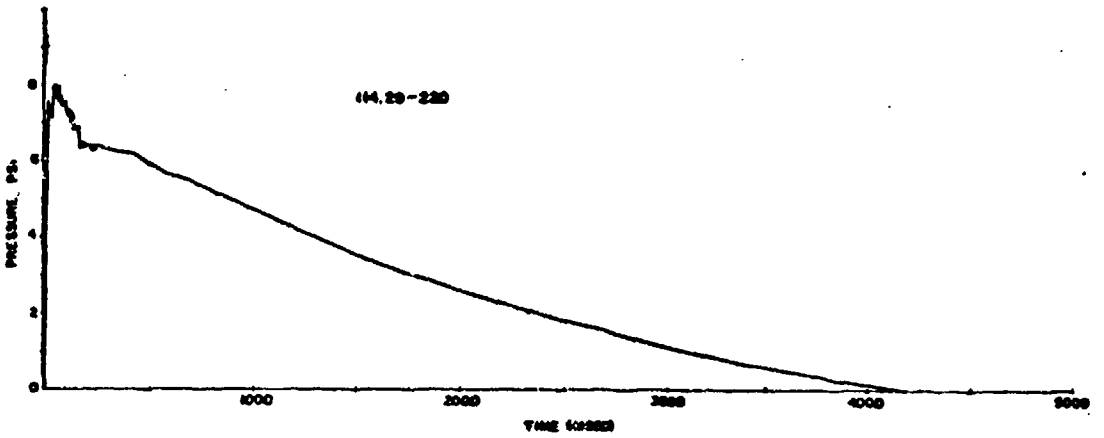
114.29-228
PRESSURE, PSI
0
2
4
6
8
1000
2000
3000
4000
5000

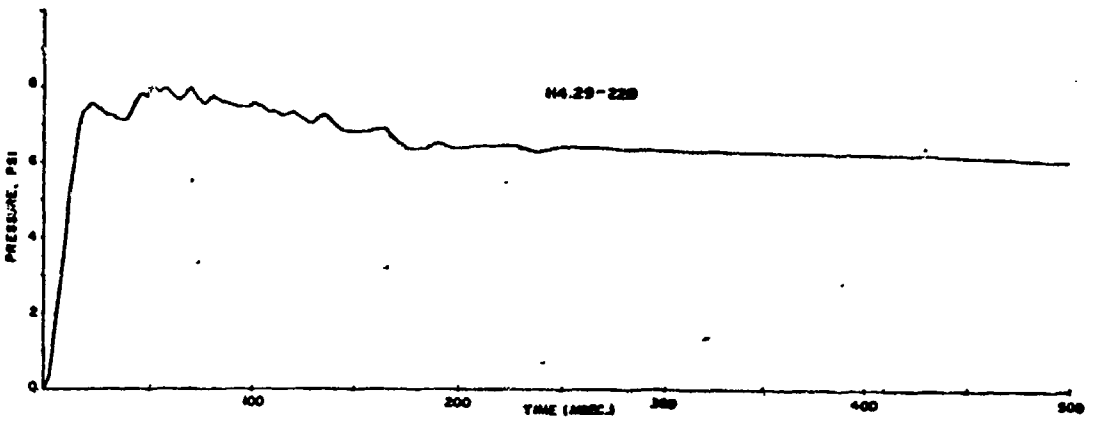
114.29-228
PRESSURE, PSI
0
2
4
6
8
400
200
TIME (MSEC.)
300
400
500

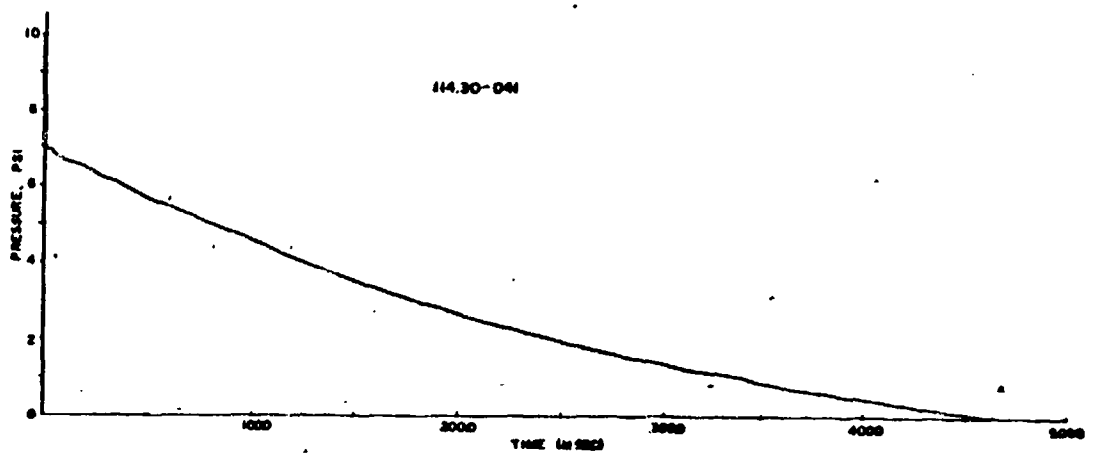
114.30-041
PRESSURE, PSI
0
2
4
6
8
10
1000
2000
3000
4000
5000



SECRET

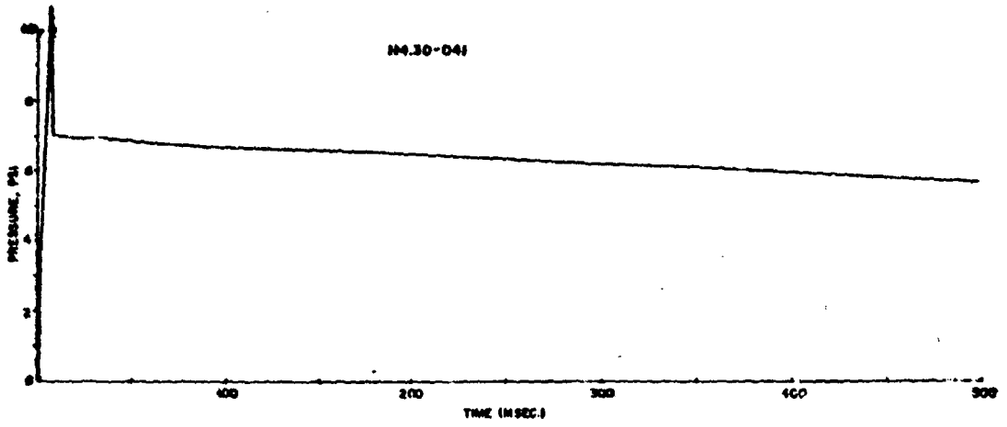
IN4.30-041
PRESSURE, PSI
TIME (M SEC.)

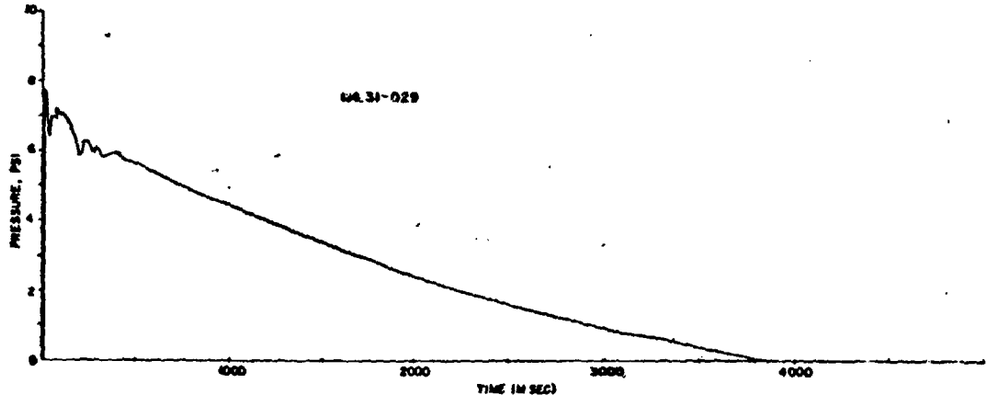
IN4.31-029
PRESSURE, PSI
TIME IN SEC)

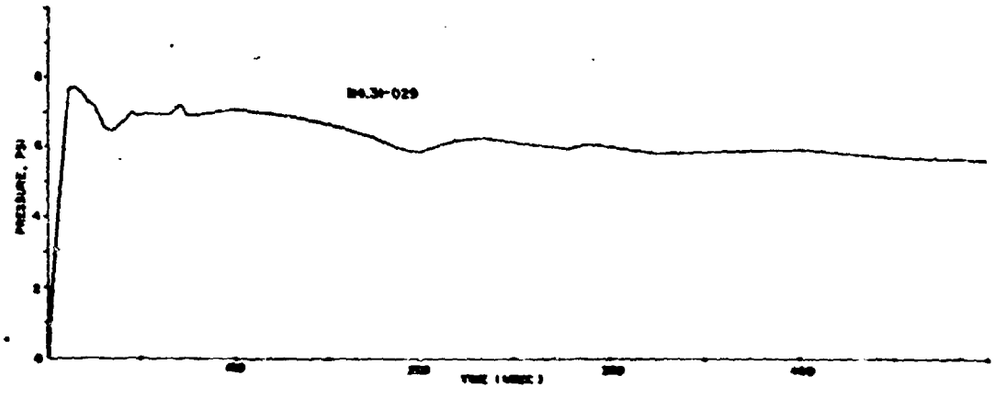
IN4.31-029
PRESSURE, PSI

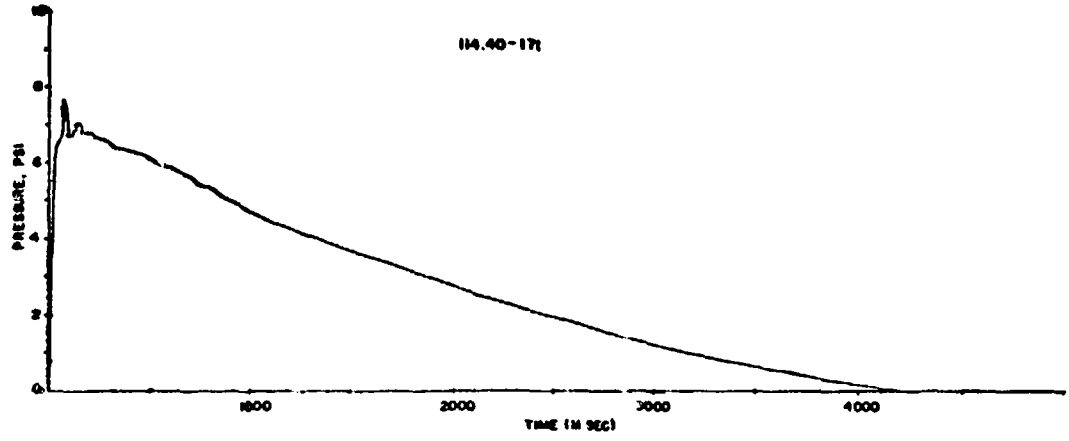
114.40-171
PRESSURE, PSI
0
2
4
6
8
2000
3000
4000
TIME (M SEC)

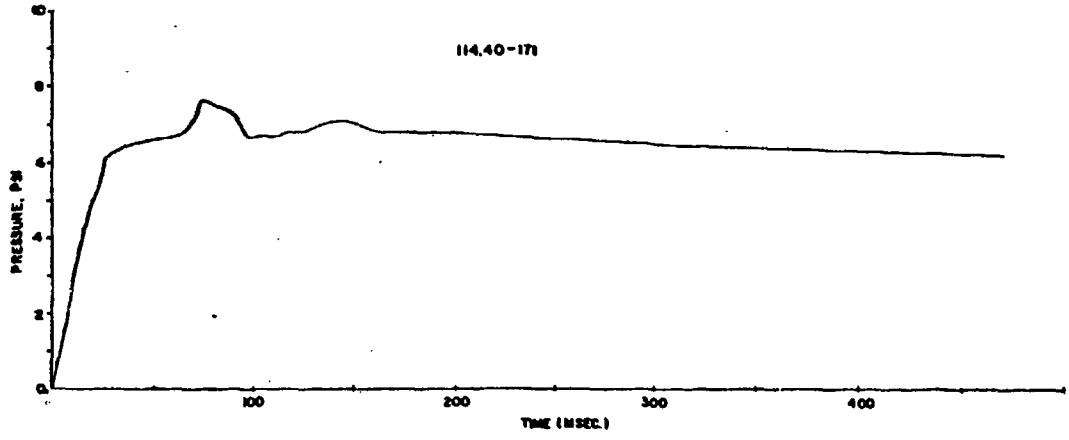
114.40-171
PRESSURE, PSI
0
2
4
6
8
10
100
200
300
400
TIME (MSEC.)

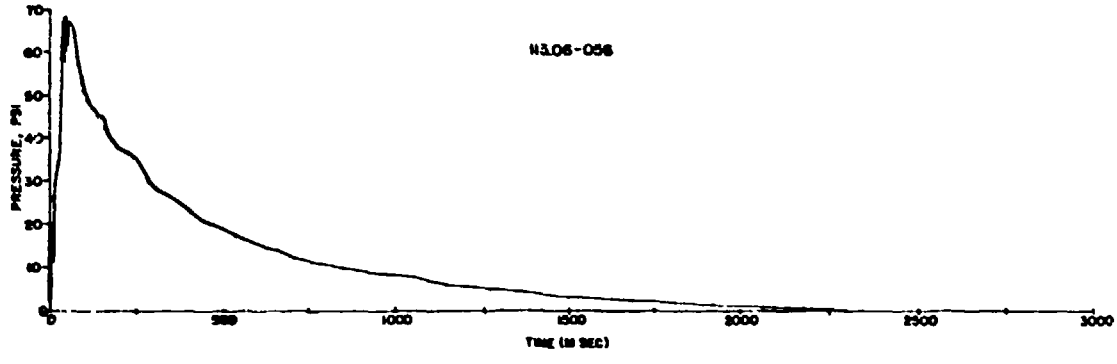
113.06-056
PRESSURE, PSI
0
10
20
30
40
50
60
70
1000
1500
2000
2500
3000
TIME (M SEC)



SECRET

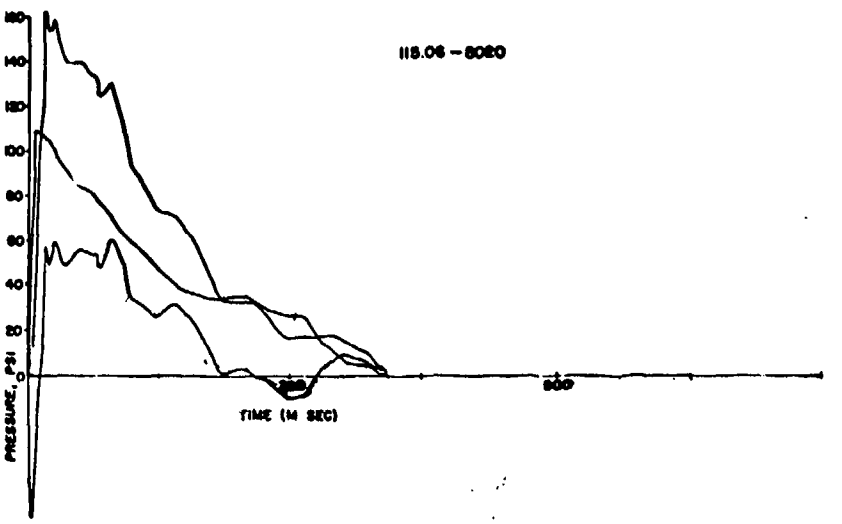
115.06 – 8080
PRESSURE, PSI
TIME (M SEC)

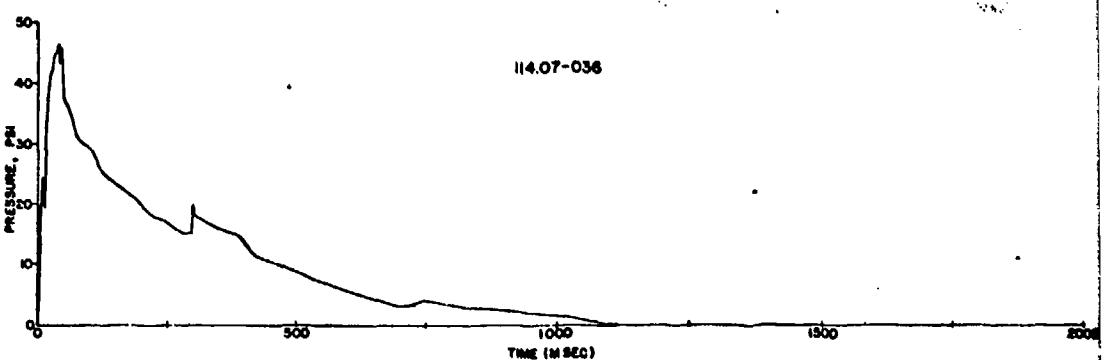
114.07-036
PRESSURE, PSI
TIME (M SEC)

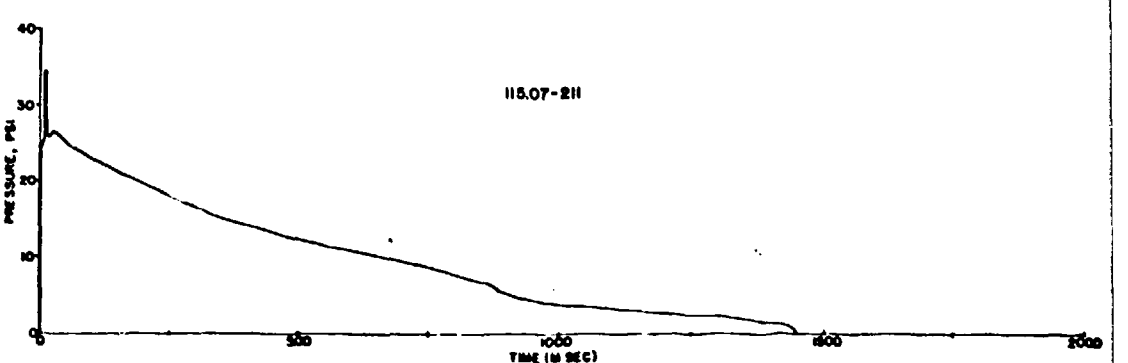
115.07-211
PRESSURE, PSI
TIME (M SEC)



SECRET

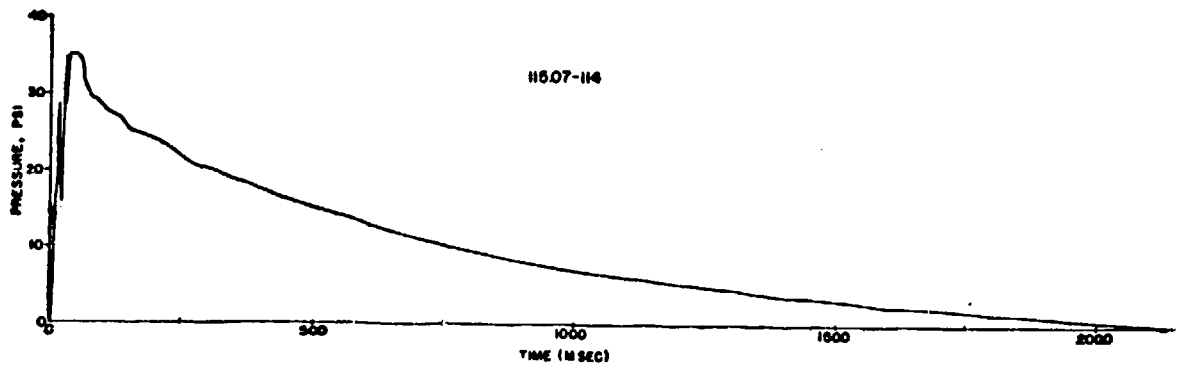
115.07-114
PRESSURE, PSI
0
10
20
30
40
500
1000
1500
2000
TIME (M SEC)

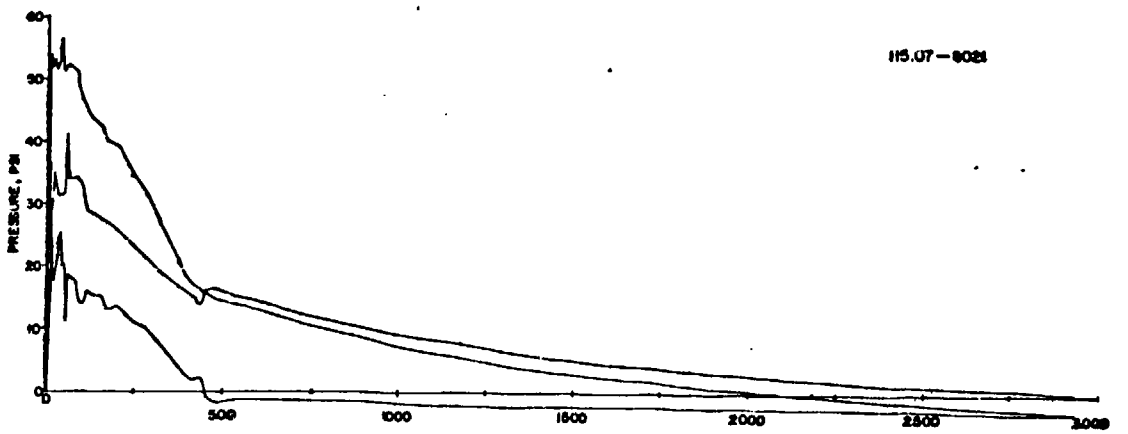
115.07—8021
PRESSURE, PSI
0
10
20
30
40
500
1000
1500
2000
2500
3000

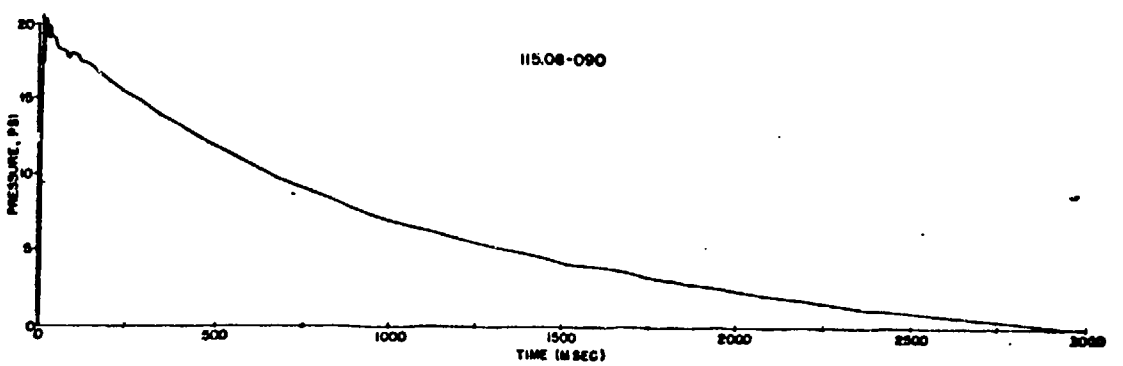
115.08-090
PRESSURE, PSI
0
5
10
15
20
500
1000
1500
2000
2500
3000
TIME (M SEC)



SECRET

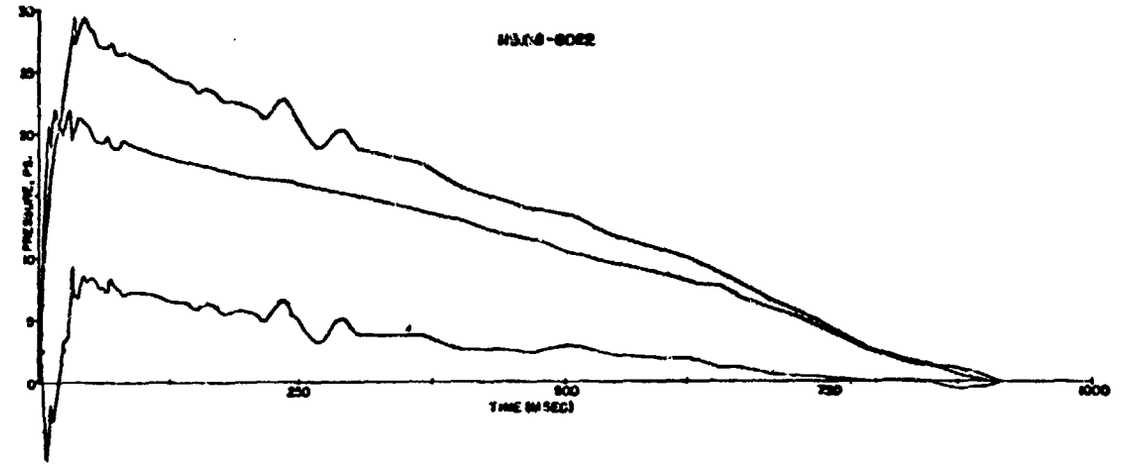
PRESSURE, PSI
TIME (M SEC)

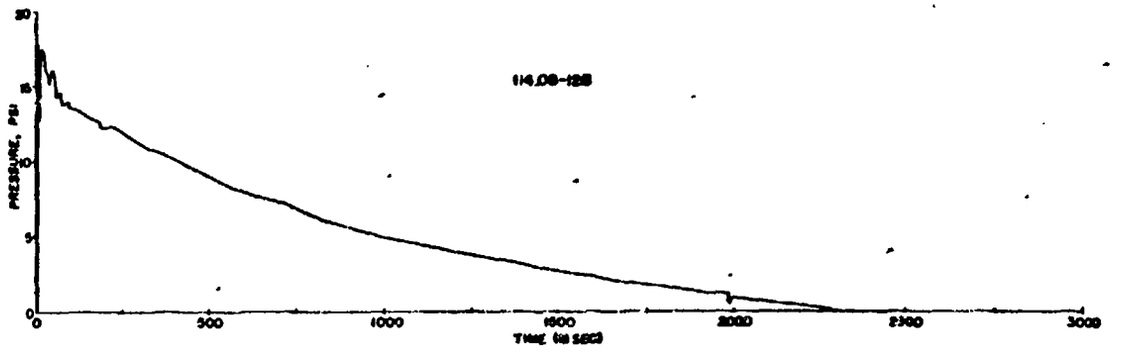
PRESSURE, PSI
TIME (M SEC)

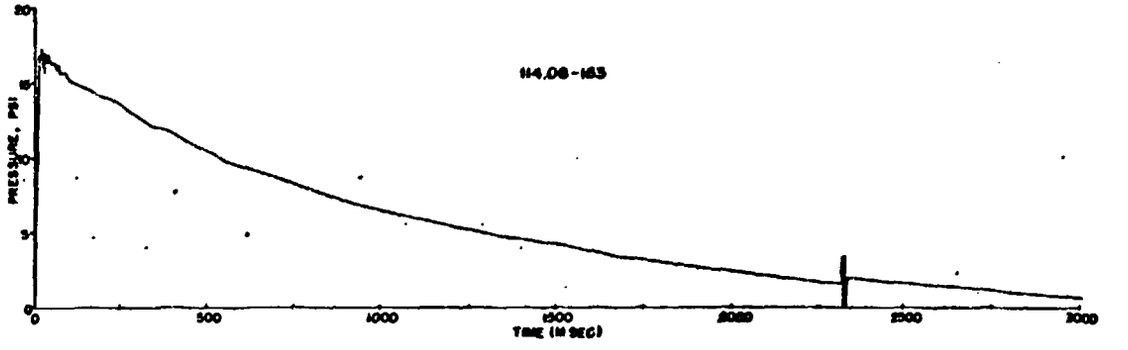
PRESSURE, PSI
TIME (M SEC)



SECRET

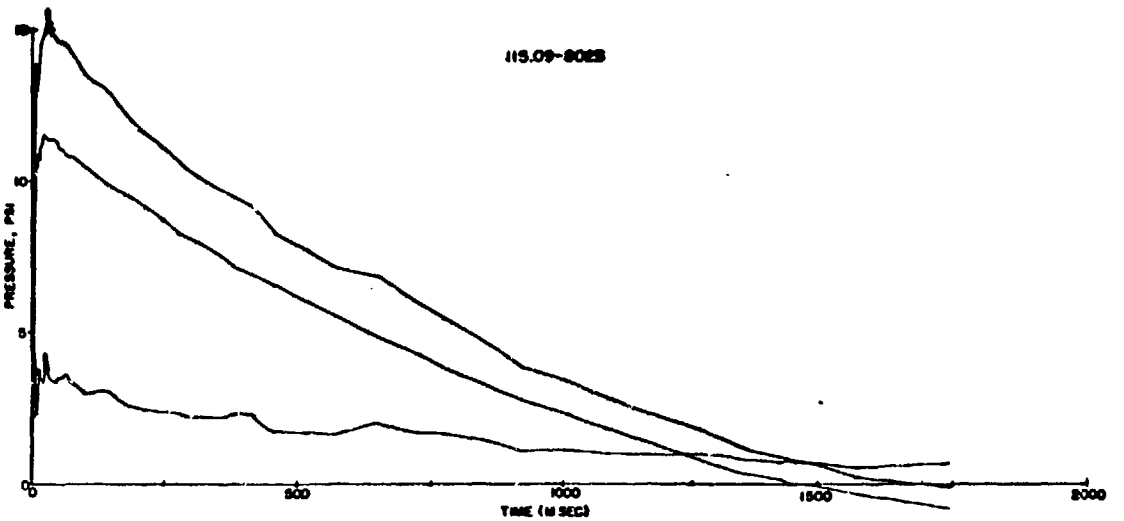
115.09-8028
PRESSURE, PSI
TIME (M SEC)

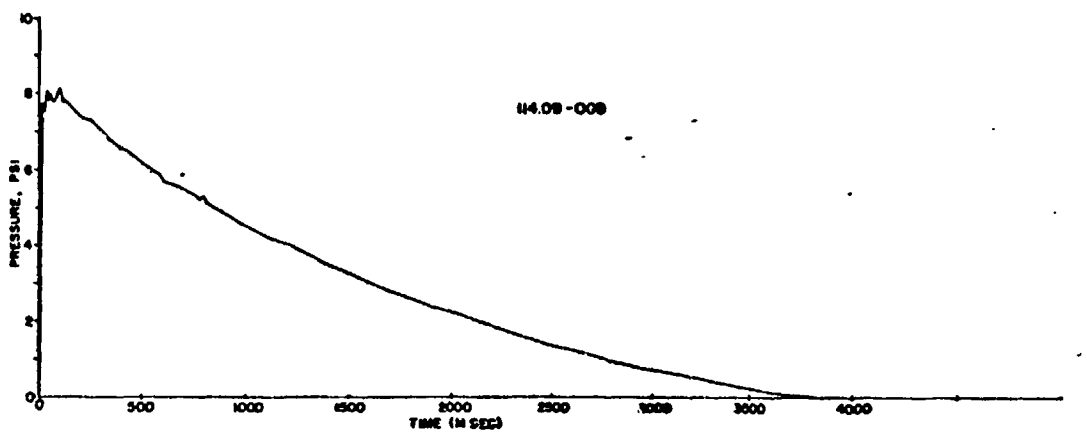
114.09-008
PRESSURE, PSI
TIME (M SEC)

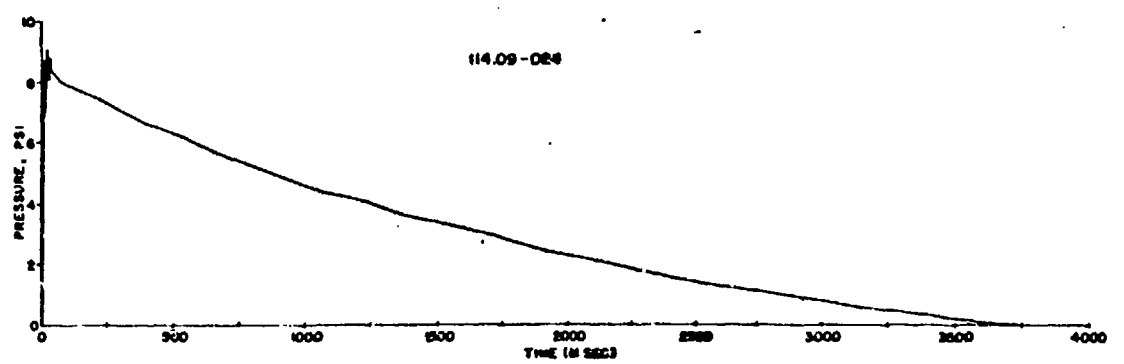
114.09-024
PRESSURE, PSI
TIME (M SEC)

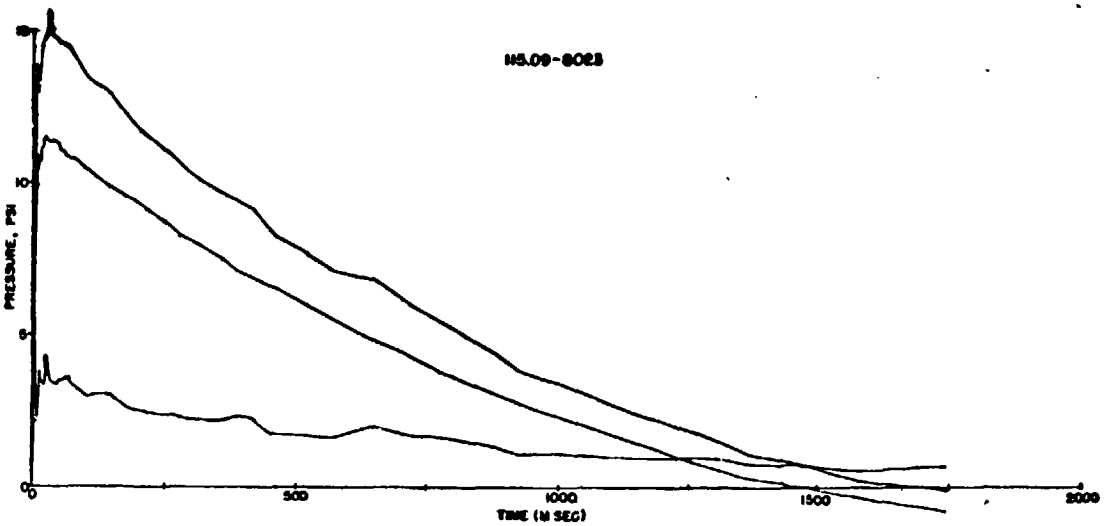
115.09-8023
PRESSURE, PSI
0
500
1000
1500
2000
TIME (M SEC)

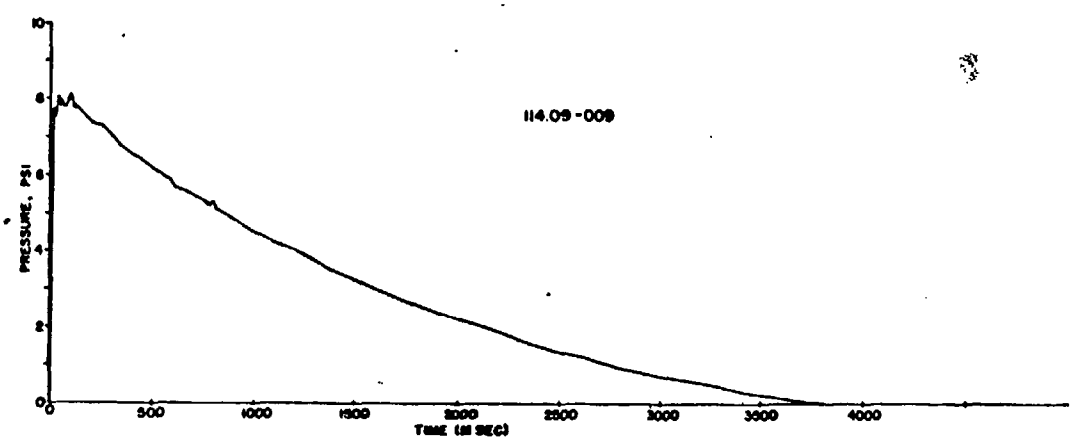
114.09-009
PRESSURE, PSI
0
2
4
6
8
10
500
1000
1500
2000
2500
3000
3500
4000
TIME (M SEC)

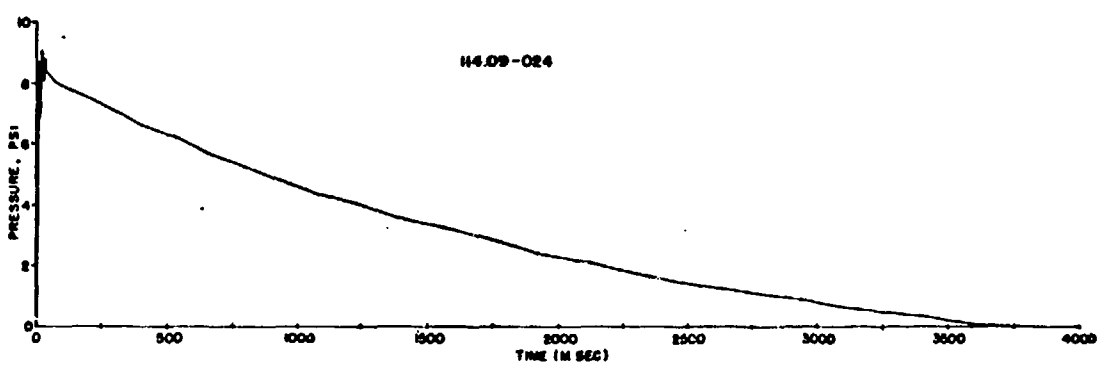
114.09-024
PRESSURE, PSI
0
2
4
6
8
10
500
1000
1500
2000
2500
3000
3500
4000
TIME (M SEC)



SECRET

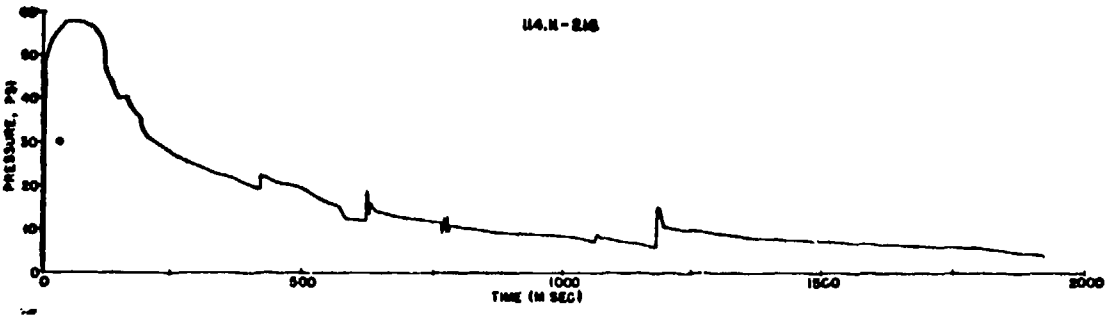
114.11-246
PRESSURE, PSI
0
500
1000
1500
2000
TIME (M SEC)

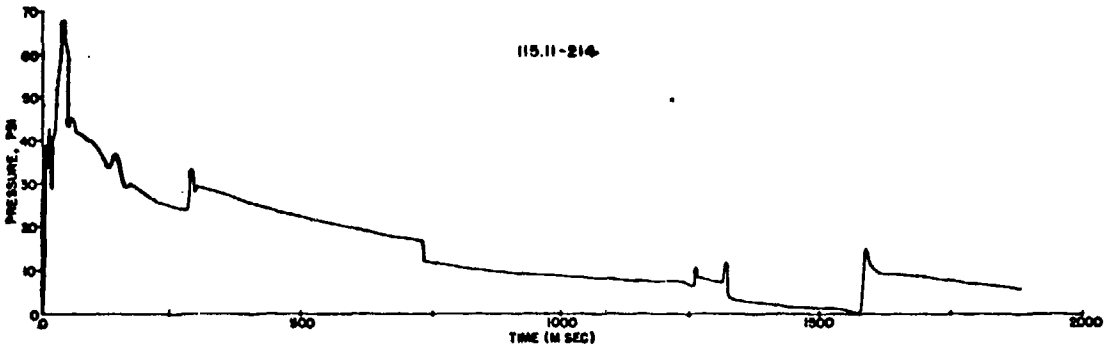
115.11-214
PRESSURE, PSI
0
500
1000
1500
2000
TIME (M SEC)

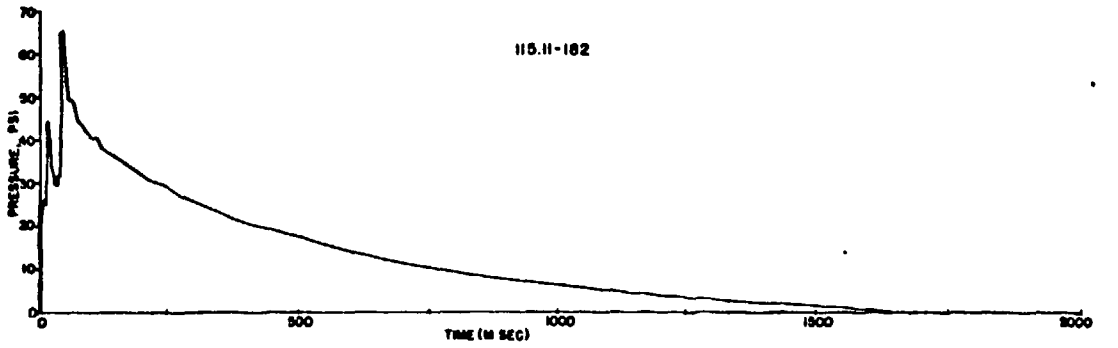
115.11-182
PRESSURE, PSI
0
500
1000
1500
2000
TIME (M SEC)

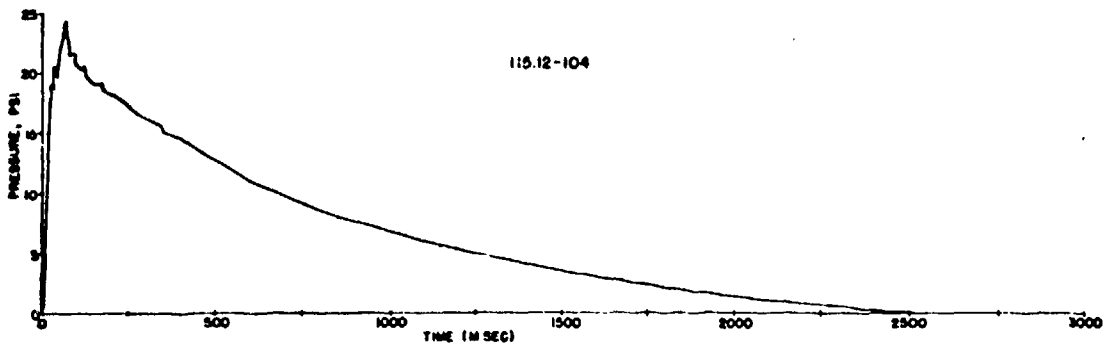
115.12-104
PRESSURE, PSI
0
500
1000
1500
2000
2500
3000
TIME (M SEC)



SECRET

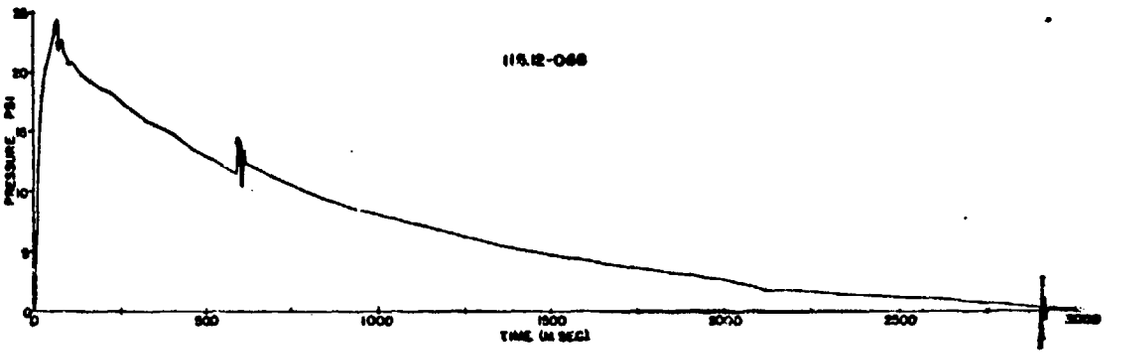
116.12-068
PRESSURE, PSI
TIME (M SEC)

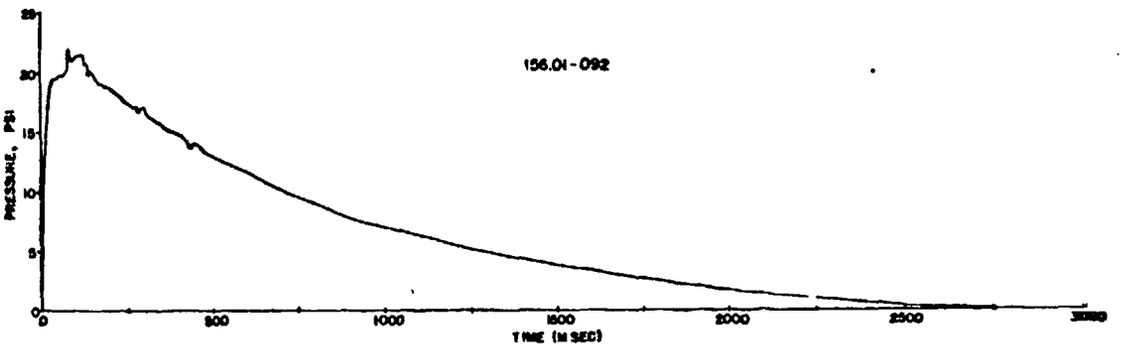
156.01-092
PRESSURE, PSI
TIME (M SEC)

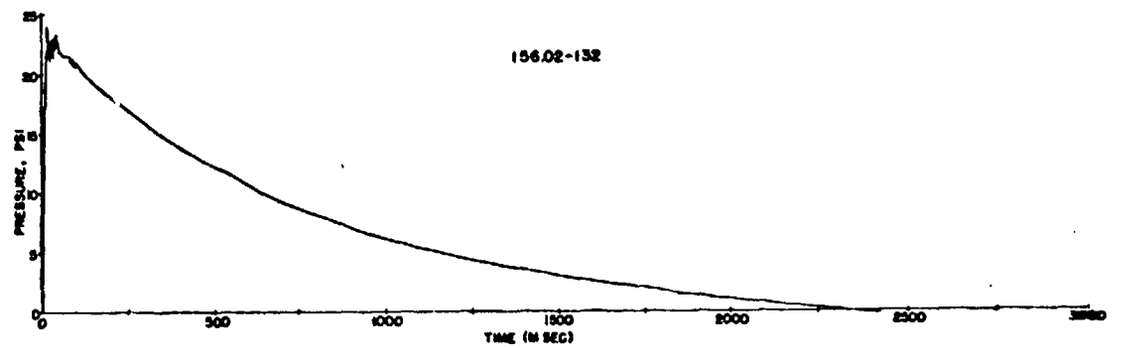
156.02-132
PRESSURE, PSI
TIME (M SEC)

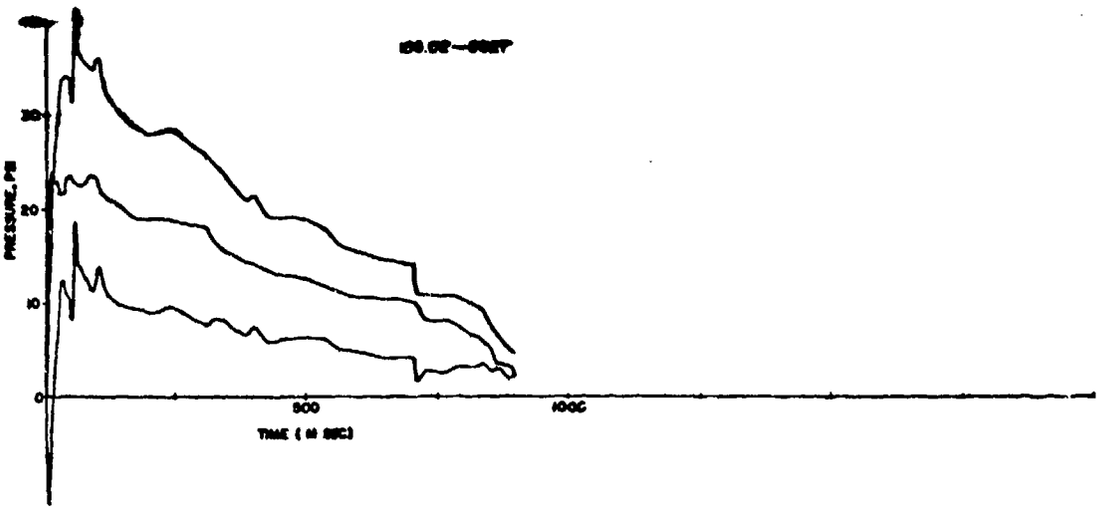
PRESSURE, PSI
20
10
0
500
1000
TIME ( IN SEC)

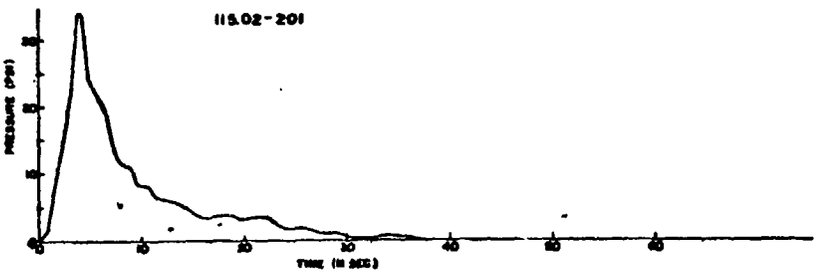
115.02-201
PRESSURE (PSI)
TIME (IN SEC)

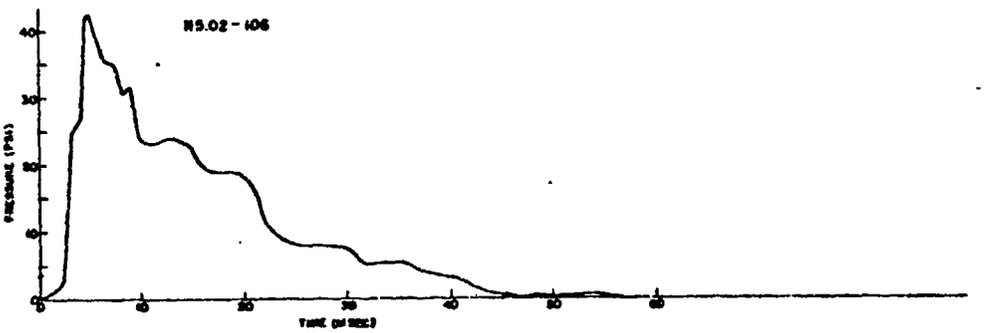
115.02-106
PRESSURE (PSI)

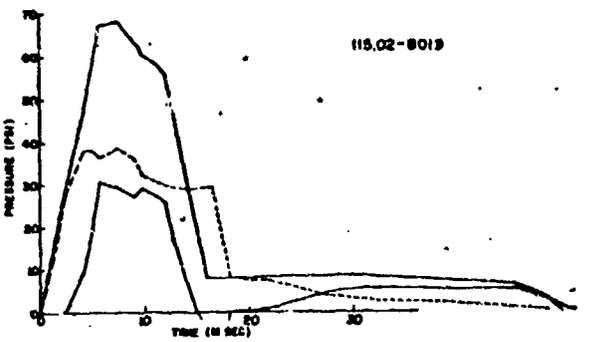
115.02-8019
PRESSURE (PSI)
TIME (IN SEC)



SECRET

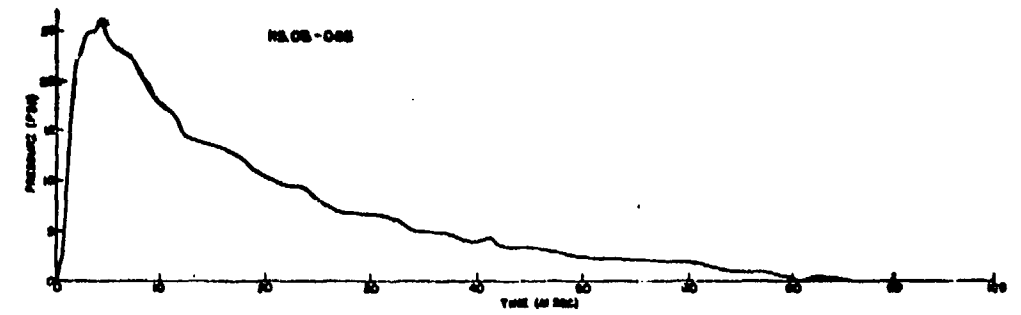

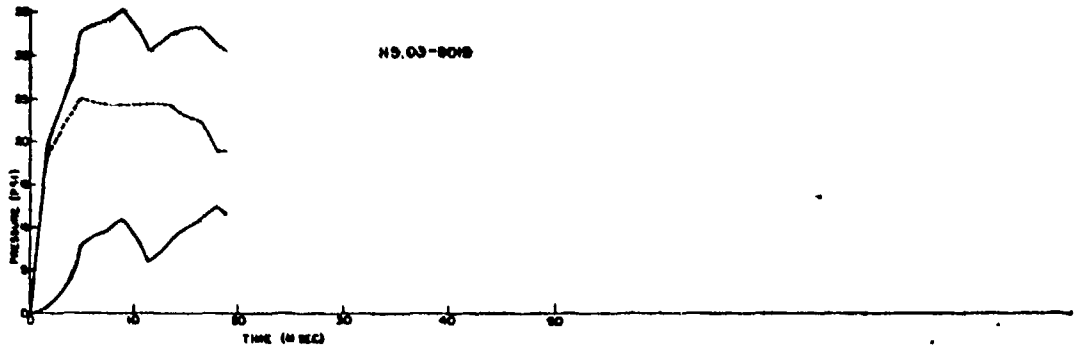

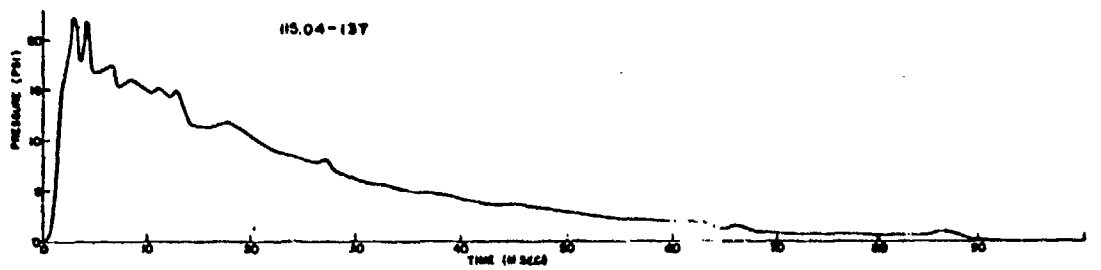

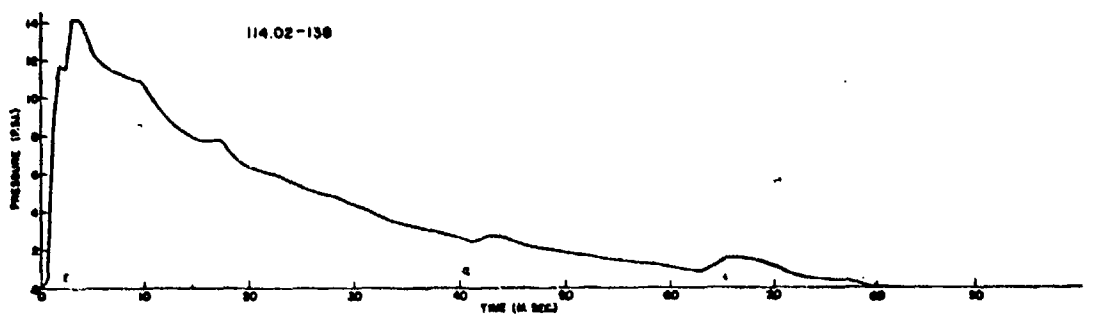

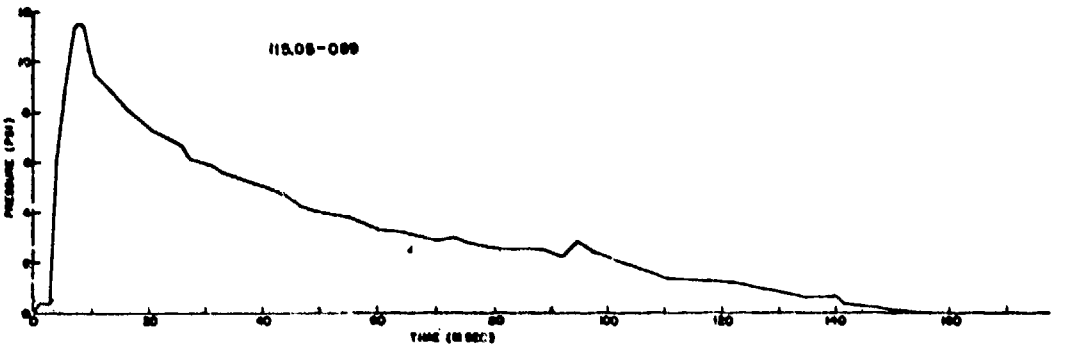
115.05-089
PRESSURE (PSI)
TIME (MSEC)

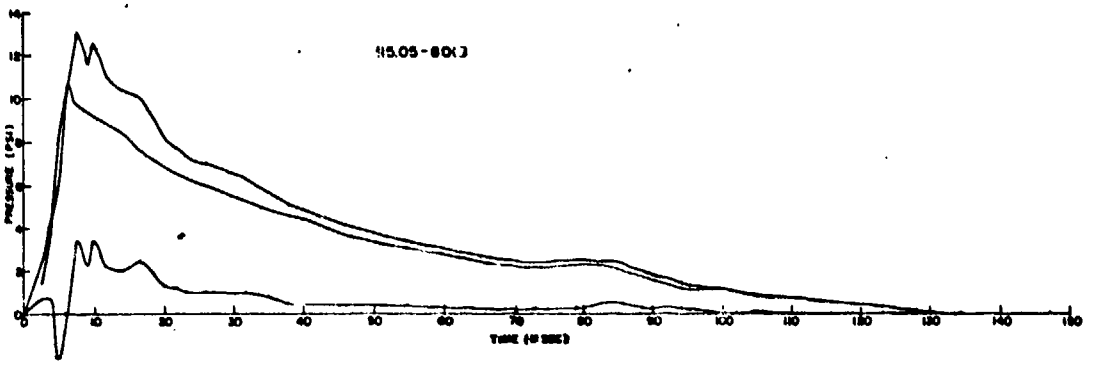
115.05-803
PRESSURE (PSI)
TIME (MSEC)

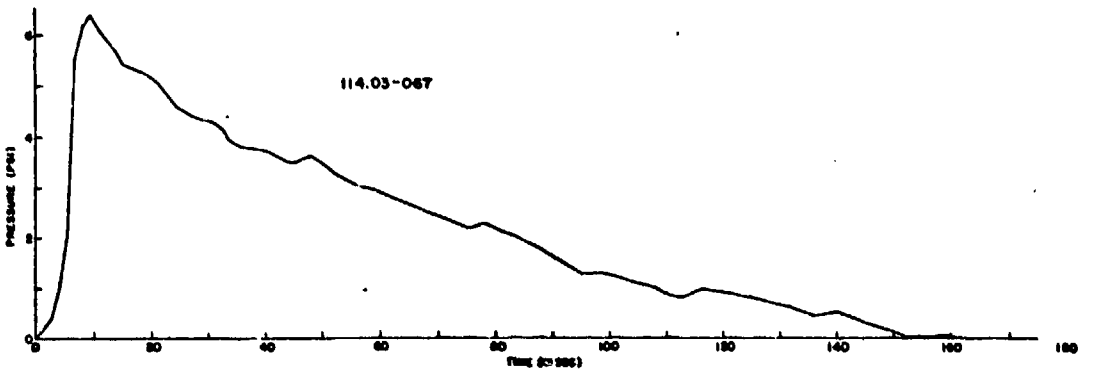
114.03-067
PRESSURE (PSI)
TIME (MSEC)

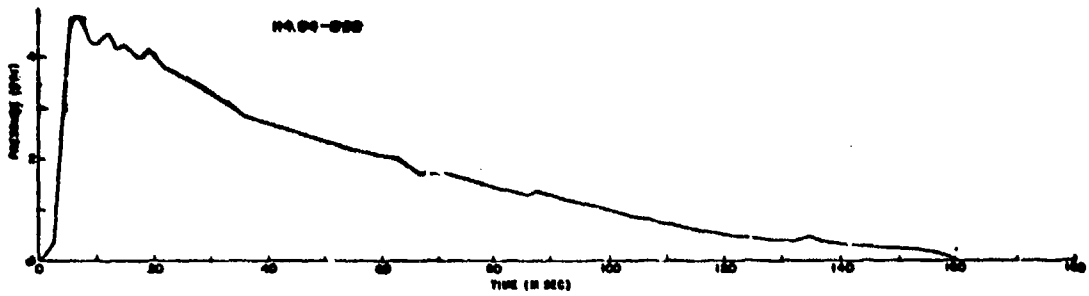

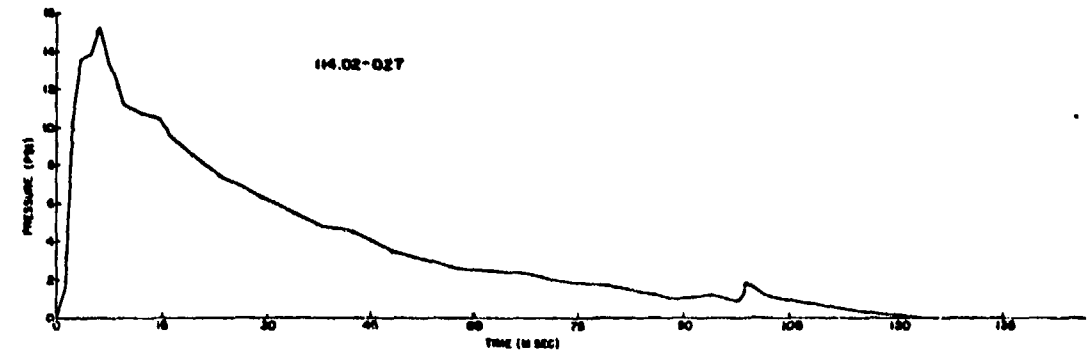
114.02-027
PRESSURE (PSI)
TIME (M SEC)

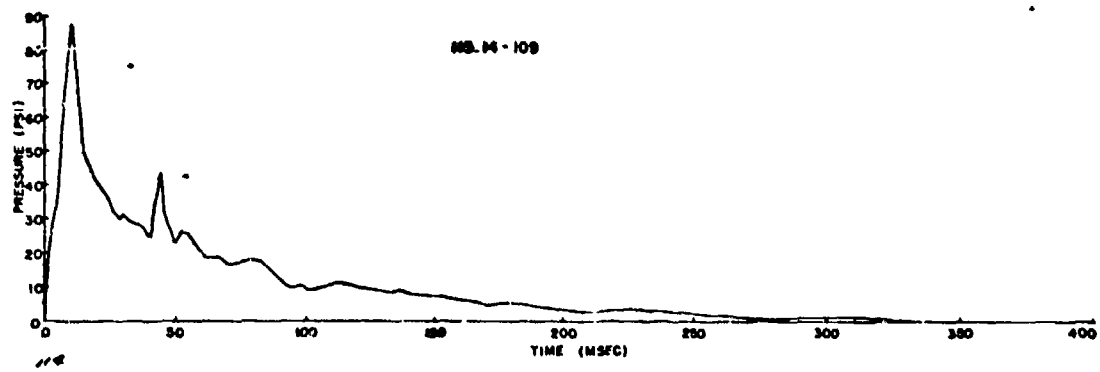
PRESSURE (PSI)
TIME (MSFC)

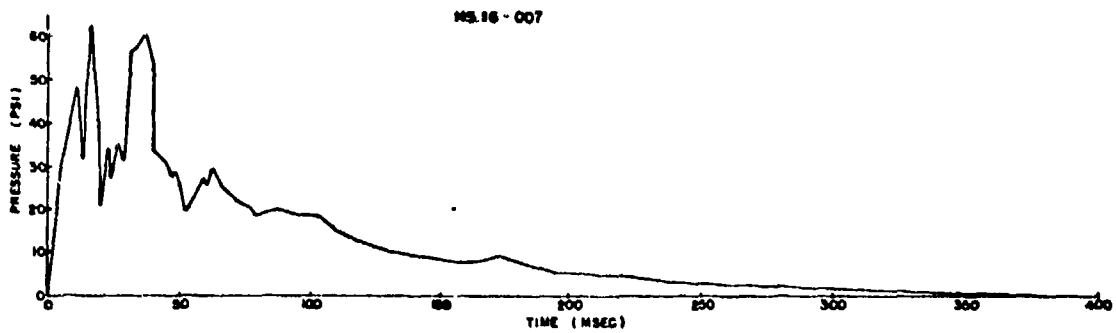
PRESSURE (PSI)
TIME (MSEC)



SECRET

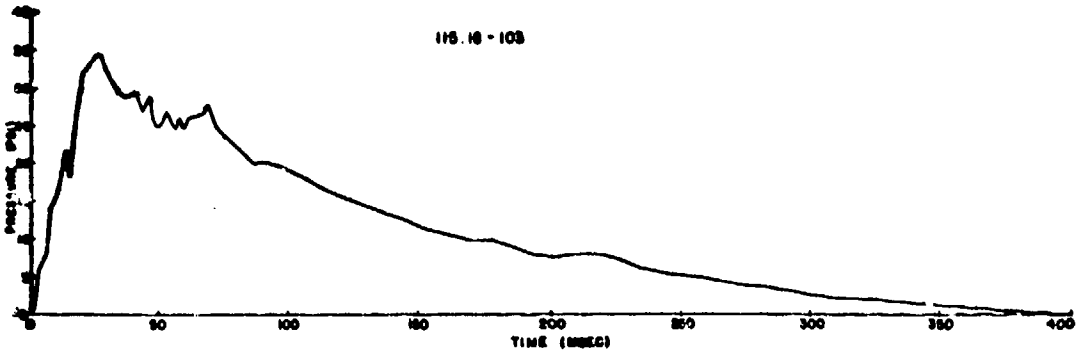
115.18 - 103
TIME (MSEC)

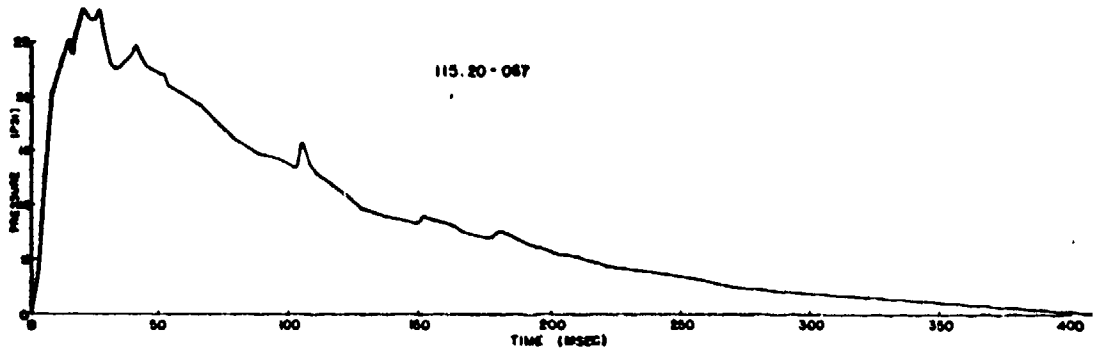
115.20 - 067
TIME (MSEC)

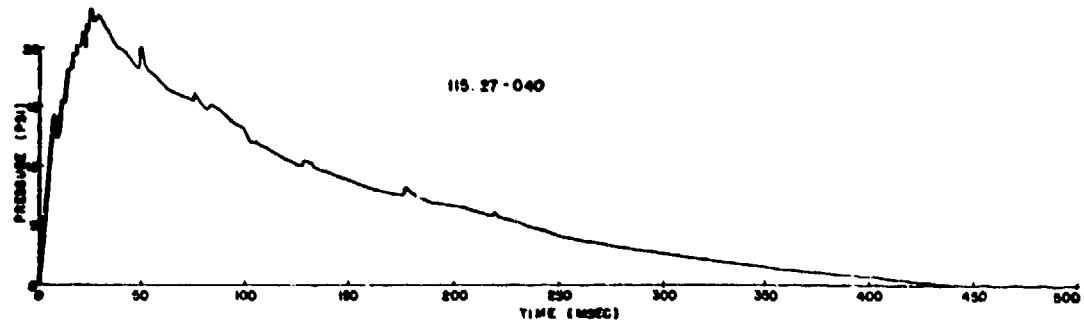
115.27 - 040
TIME (MSEC)

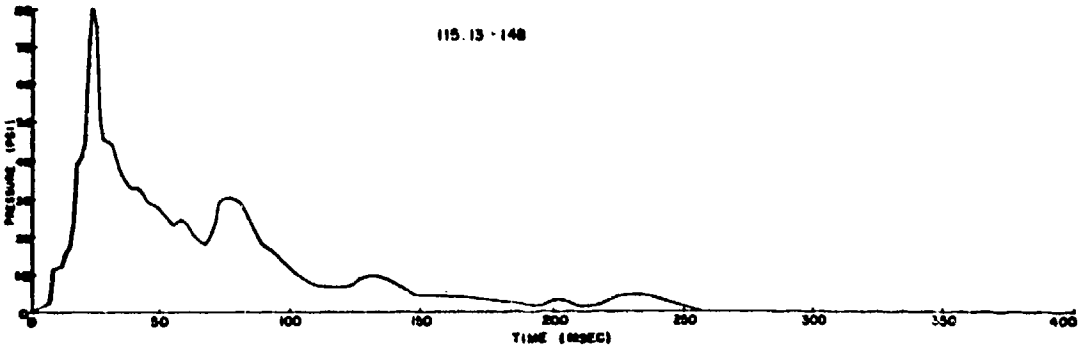
115.13 - 148
TIME (MSEC)

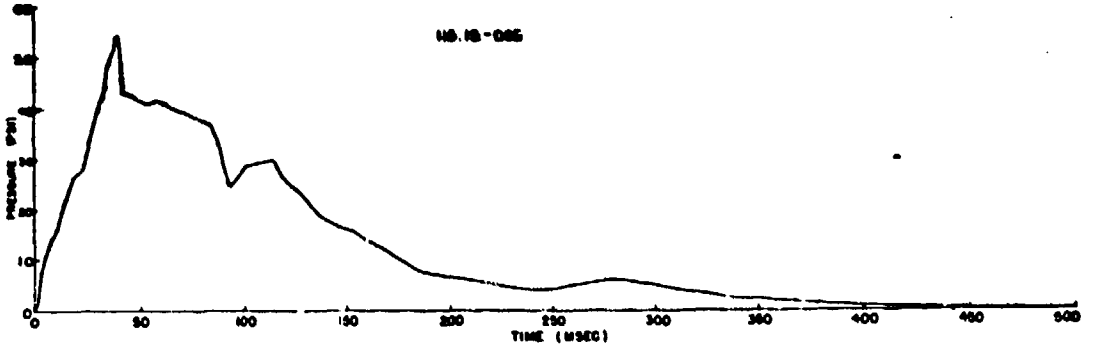
PRESSURE (PSI)
TIME (MSEC)

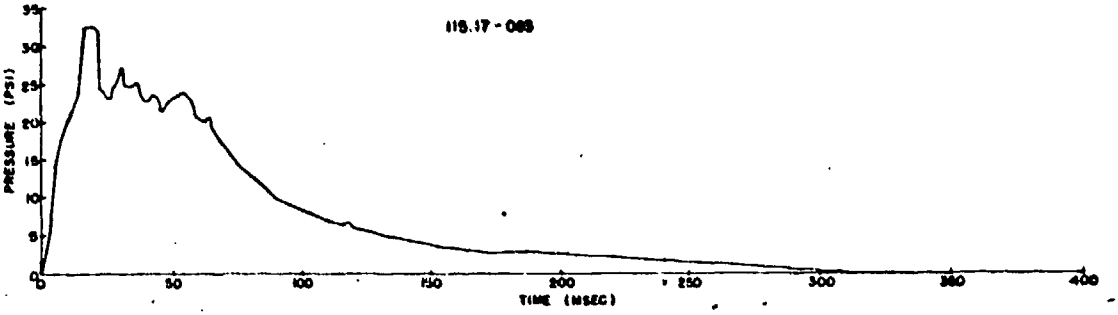
PRESSURE (PSI)
TIME (MSEC)

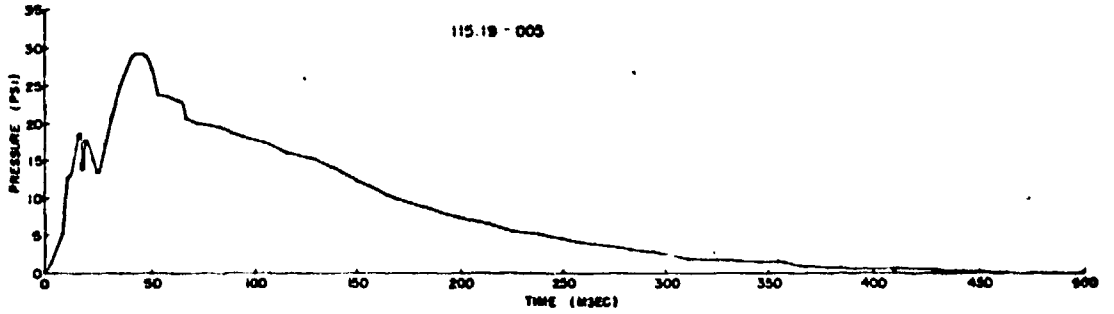
PRESSURE (PSI)
TIME (MSEC)

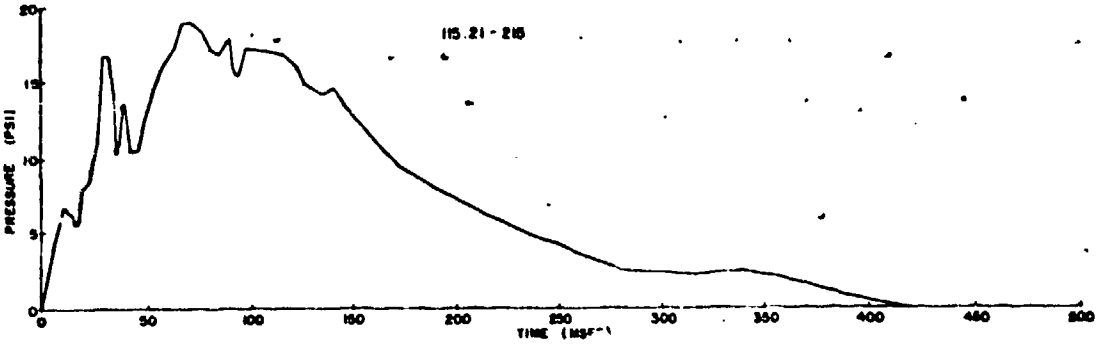
PRESSURE (PSI)



SECRET

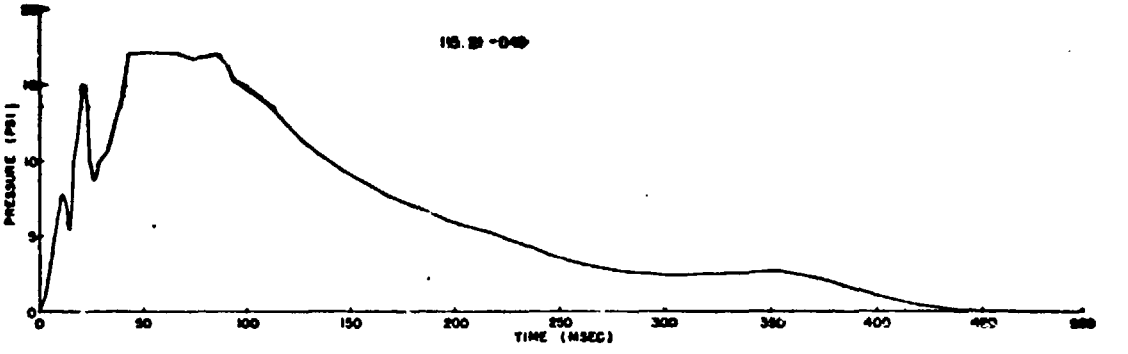
PRESSURE (PSI)
TIME (MSEC)

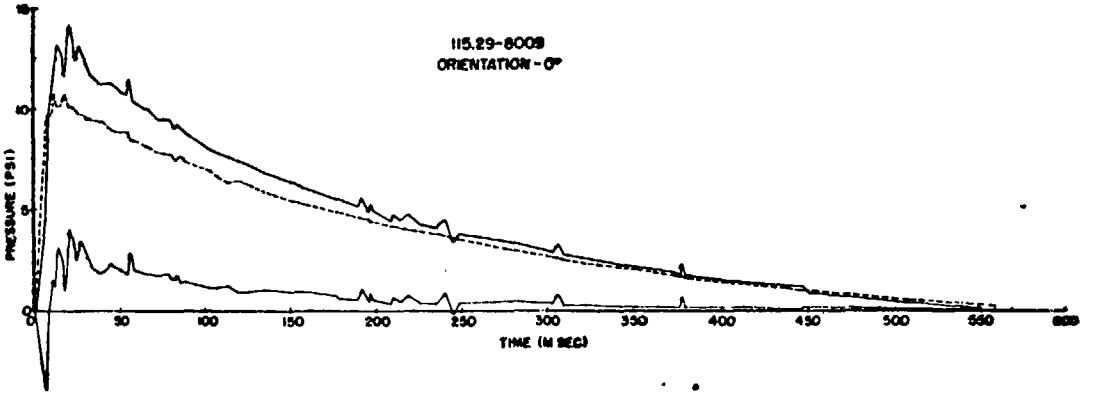
115.29-8009
ORIENTATION - 0°
PRESSURE (PSI)
TIME (M SEC)

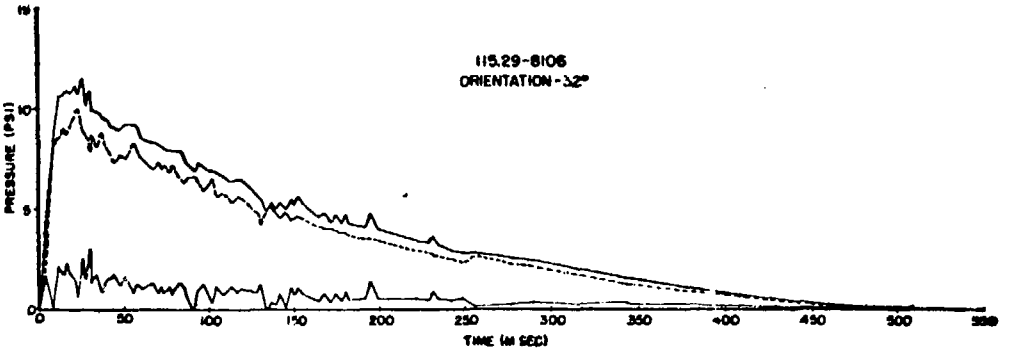
115.29-8106
ORIENTATION - 32°
PRESSURE (PSI)
TIME (M SEC)

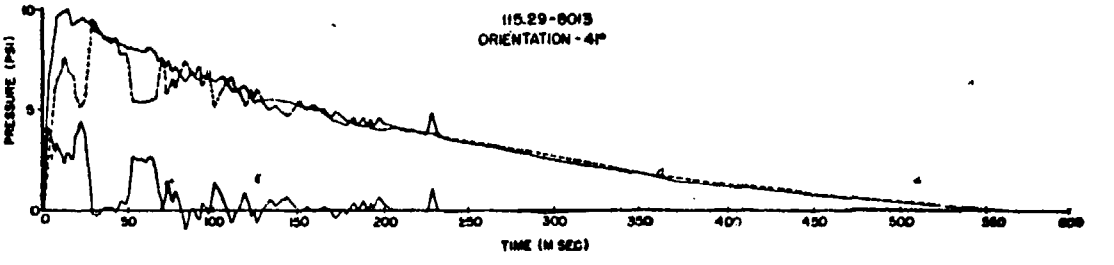
115.29-8013
ORIENTATION - 41°
PRESSURE (PSI)
TIME (M SEC)



SECRET

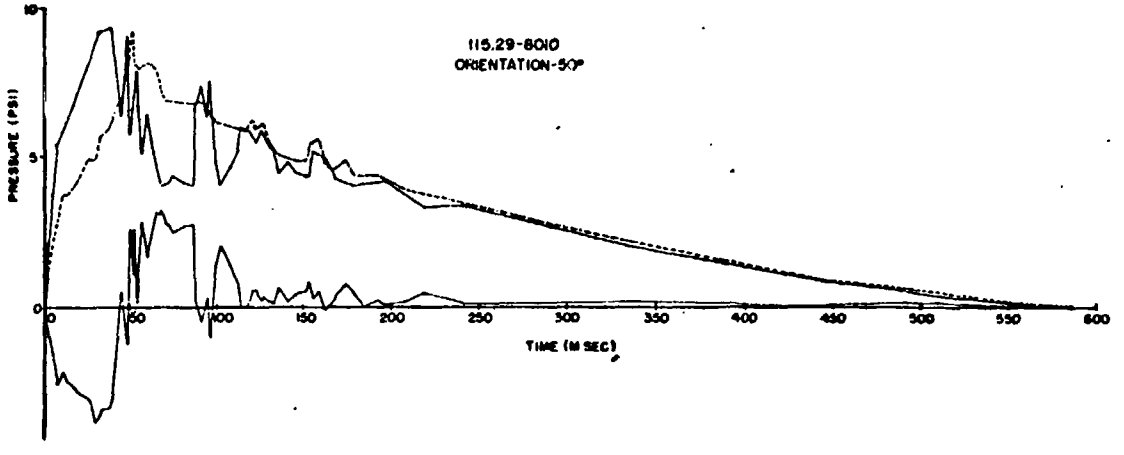
115.29-8010
ORIENTATION-50°
PRESSURE (PSI)
10
5
0
0
50
100
150
200
250
300
350
400
450
500
550
600
TIME (M SEC)



SECRET

# Appendix C
# ISLAND DIFFRACTION RECORDS

## C.1 INTRODUCTION

On Shot Cherokee, land space was not available at the desired distances for Project 3.1 structures instrumentation. Therefore, it was proposed that man-made islands be constructed along the Site Charlie-Dog Reef. This was an expensive proposition; therefore, it was desired to keep the island size to a minimum but still keep the structure free from turbulence that might be created by the diffraction of the blast wave over the island.

## C.2 SCALED MODEL STUDIES

Scaled models of island shapes and sizes were instrumented in the BRL shock tube. Gages were installed and pressure versus time was recorded along the surface of the model and at certain heights above the surface for several distances back from the leading edge. This was done to establish the minimum distance from the leading edge at which a structure might be placed and still be free from any effects of turbulence. On recommendations from BRL, the island size and configuration were established.

## C.3 ISLAND CONFIGURATION

The recommendation accepted was for an island 6 feet in height with the leading edge vertical for the first 4 feet and the top 2 feet rounded with a radius of curvature of 2 feet. The structure was to be placed 60 feet from the leading edge. The island size, structure location, and gage location are shown in Figures C.1, C.2 and C.3.

## C.4 DATA PRESENTATION

The data are presented in the form of records of pressure versus time, along with Table C.1, which lists measured values of other parameters. Values listed as peak pressure are those measured just after the initial pressure rise and not the peak caused by the reflected wave from the structures. These data have been transmitted to Project 3.1 for detail analysis and reporting. The records are identified by station and gage number.

TABLE C.1 BLAST DIFFRACTION DATA

| Station | Site | Distance | Gage Type and Number | Peak Overpressure | Arrival Time | Duration | Impulse |
|---|---|---|---|---|---|---|---|
| | | ft | | psi | sec | sec | psi-sec |
| 114.22 | Man-Made Island No. 1 | 19,338 | $p_t$- 99 | 8.8 | — | 3.779 | 12.289 |
| 114.23 | Man-Made Island No. 1 | 19,385 | $p_t$- 82 | 12.4 * | — | — | — |
| 114.24 | Man-Made Island No. 1 | 19,350 | $p_t$-135 | 9.0 | 9.885 | 4.433 | 12.946 |
| 114.39 | Man-Made Island No. 1 | 19,372 | $p_t$- 78 | 9.8 | — | 4.027 | 12.785 |
| 114.25 | Man-Made Island No. 2 | 20,656 | $p_t$- 58 | 7.4 | 9.885 | 4.246 | 11.965 |
| 114.26 | Man-Made Island No. 2 | 20,672 | $p_t$- 28 | 7.4 | — | 4.186 | 12.390 |
| 114.27 | Man-Made Island No. 2 | 20,703 | $p_t$- 31 | 7.3 | 9.765 | 4.281 | 11.935 |
| 114.28 | Man-Made Island No. 2 | 20,774 | $p_t$-108 | 7.1 | 8.793 | 4.199 | 11.182 |
| 114.29 | Man-Made Island No. 2 | 20,628 | $p_t$-220 | 7.3 | 10.027 | 4.200 | 11.992 |
| 114.30 | Man-Made Island No. 2 | 20,730 | $p_t$- 41 | 7.0 | — | 4.699 | 12.332 |
| 114.31 | Man-Made Island No. 2 | 20,663 | $p_t$- 29 | 7.7 | 10.228 | 4.095 | 11.101 |
| 114.40 | Man-Made Island No. 2 | 20,651 | $p_t$-171 | 7.2 | 9.574 | 4.294 | 12.237 |

* Peak reflected value.



SECRET

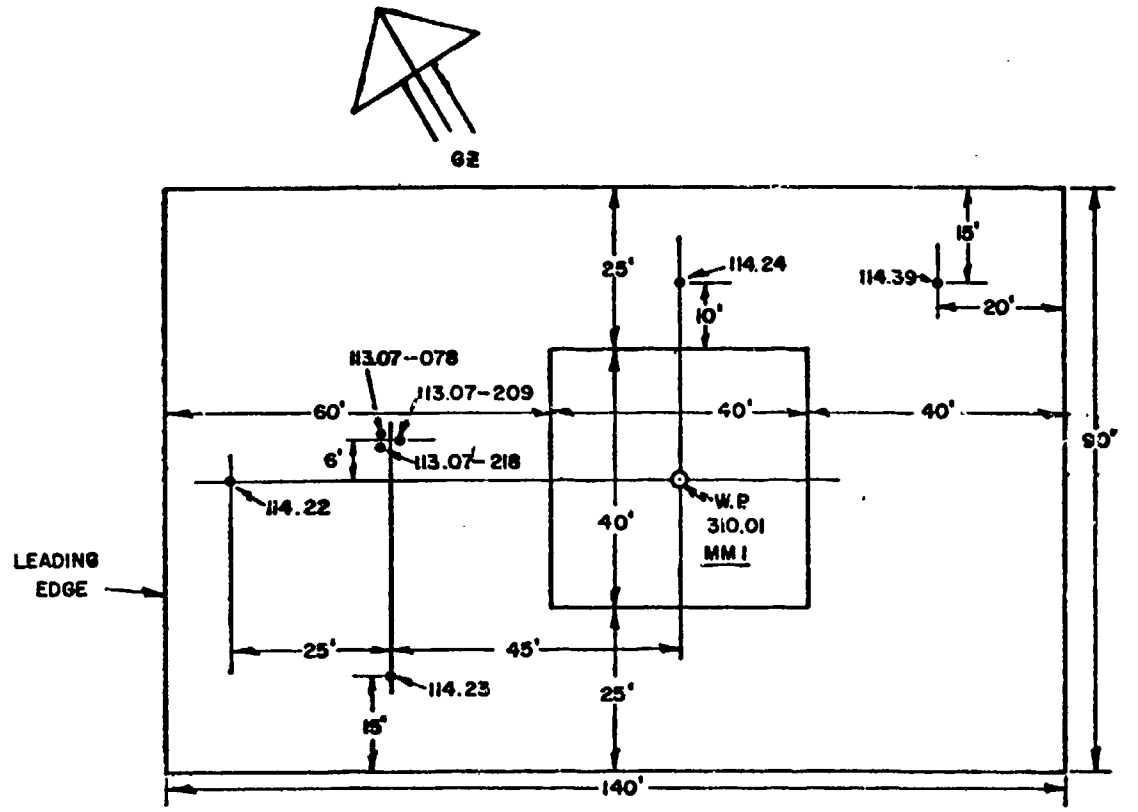


Figure C.1 Structure and gage locations Man-Made Island No. 1.

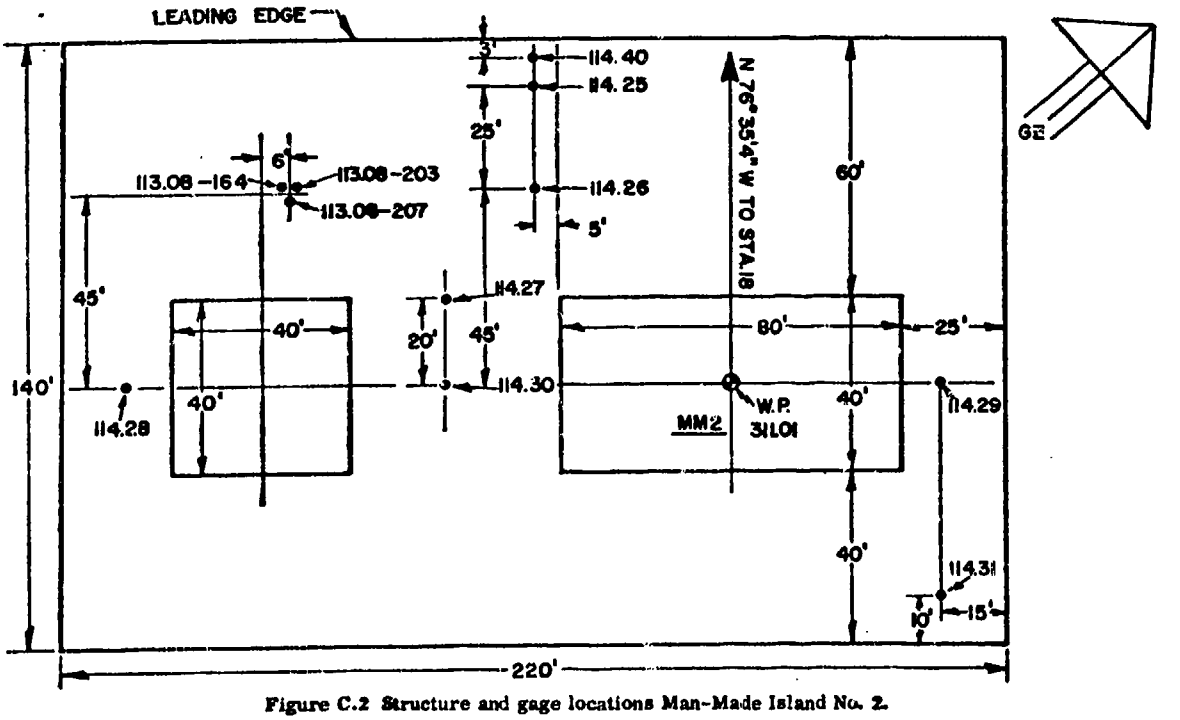


Figure C.2 Structure and gage locations Man-Made Island No. 2.

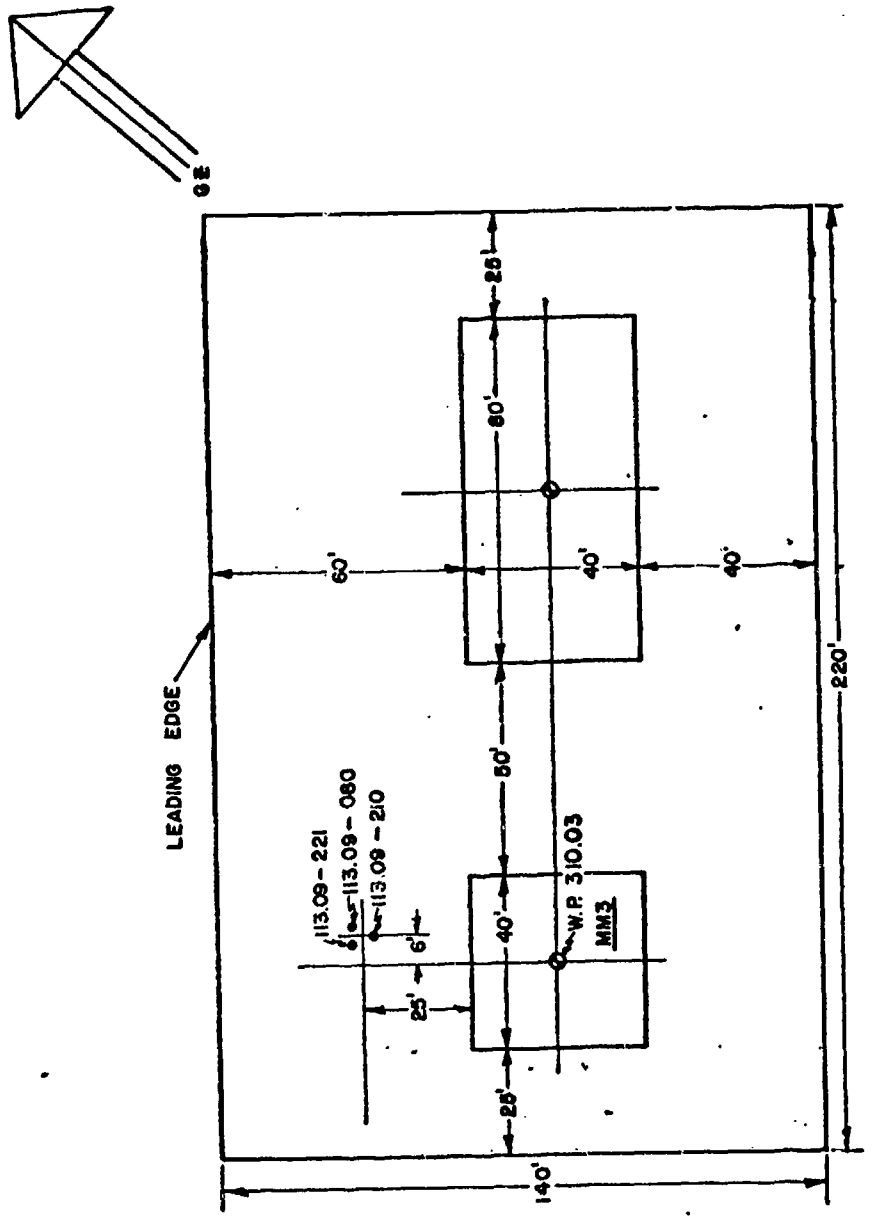


Figure C.3 Structure and gage locations Man-Made Island No. 3.



SECRET

# REFERENCES


1. J.J. Meszaros and C.N. Kingery; "Ground Surface Air Pressure Versus Distance From High Yield Detonations"; Project 1.2b, Operation Castle, WT-905, May 1957; Explosion Kinetics Branch, Terminal Ballistics Laboratory, Ballistic Research Laboratories, Aberdeen Proving Ground, Maryland; Secret Formerly Restricted Data.

2. C.D. Broyles and M.L. Merritt; "Ground Level Pressures from Surface Bursts"; Project 1.2a, Operation Castle, WT-904, October 1957; Sandia Corporation, Albuquerque, New Mexico; Secret Formerly Restricted Data.

3. E.J. Bryant and others; "Measurements of Air-Blast Phenomena with Self-Recording Gages"; Project 1.14b, Operation Teapot, WT-1155, July 1959; Explosion Kinetics Branch, Terminal Ballistics Laboratory, Ballistic Research Laboratories, Aberdeen Proving Ground, Maryland; Confidential Formerly Restricted Data.

4. "Capabilities of Atomic Weapons"; TM 23-200, Department of the Army, Department of the Navy, and Department of the Air Force; Revised Edition, November 1957; Confidential.

5. "Proceedings of the AFSWP Symposium on Air-Blast Phenomena"; AFSWP-898, February 1957.

6. "Summary Report of the Technical Director, Programs 1-9"; Operation Upshot-Knothole, WT-782, March 1955; Armed Forces Special Weapons Project, Sandia Base, Albuquerque, New Mexico; Secret Restricted Data.

# DISTRIBUTION

*Military Distribution Category 12*

ARMY ACTIVITIES

1 Deputy Chief of Staff for Military Operations, D/A, Washington 25, D.C. ATTN: Dir. of SW&R
2 Chief of Research and Development, D/A, Washington 25, D.C. ATTN: Atomic Div.
3 Assistant Chief of Staff, Intelligence, D/A, Washington 25, D.C.
4 Chief of Engineers, D/A, Washington 25, D.C. ATTN: ENGNB
5 Chief of Engineers, D/A, Washington 25, D.C. ATTN: ENGEB
6 Chief of Engineers, D/A, Washington 25, D.C. ATTN: ENGTB
7- 8 Office, Chief of Ordnance, D/A, Washington 25, D.C. ATTN: ORDTN
9- 11 Commanding General, U.S. Continental Army Command, Ft. Monroe, Va.
12 Director of Special Weapons Development Office, Headquarters CONARC, Ft. Bliss, Tex. ATTN: Capt. Chester I. Peterson
13 President, U.S. Army Artillery Board, Ft. Sill, Okla.
14 President, U.S. Army Air Defense Board, Ft. Bliss, Tex.
15 Commandant, U.S. Army Command & General Staff College, Ft. Leavenworth, Kansas. ATTN: ARCHIVES
16 Commandant, U.S. Army Armored School, Ft. Knox, Ky.
17 Commandant, U.S. Army Artillery and Missile School, Ft. Sill, Okla. ATTN: Combat Development Department
18 Commandant, U.S. Army Aviation School, Ft. Rucker, Ala.
19 Commandant, U.S. Army Infantry School, Ft. Benning, Ga. ATTN: C.D.S.
20 Commandant, U.S. Army Ordnance School, Aberdeen Proving Ground, Md.
21 Commandant, U.S. Army Ordnance and Guided Missile School, Redstone Arsenal, Ala.
22 Commanding General, Chemical Corps Training Comd., Ft. McClellan, Ala.
23 Commanding General, The Engineer Center, Ft. Belvoir, Va. ATTN: Asst. Cmdt, Engr. School
24 Director, Armed Forces Institute of Pathology, Walter Reed Army Med. Center, 625 16th St., NW, Washington 25, D.C.
25 Commanding Officer, Army Medical Research Lab., Ft. Knox, Ky.
26 Commandant, Walter Reed Army Inst. of Res., Walter Reed Army Medical Center, Washington 25, D.C.
27- 28 Commanding General, Qm R&D Comd., QM R&D Cntr., Natick, Mass. ATTN: CBR Liaison Officer
29- 30 Commanding Officer, Chemical Warfare Lab., Army Chemical Center, Md. ATTN: Tech. Library
31 Commanding General, Engineer Research and Dev. Lab., Ft. Belvoir, Va. ATTN: Chief, Tech. Support Branch
32 Director, Waterways Experiment Station, P.O. Box 631, Vicksburg, Miss. ATTN: Library
33 Commanding Officer, Picatinny Arsenal, Dover, N.J. ATTN: ORDBB-TK
34 Commanding Officer, Diamond Ord. Fuze Labs., Washington 25, D.C. ATTN: Chief, Nuclear Vulnerability Br. (230)
35- 36 Commanding General, Aberdeen Proving Grounds, Md. ATTN: Director, Ballistics Research Laboratory
37 Commanding General, Frankford Arsenal, Bridge and Tacony St., Philadelphia, Pa.
38 Commanding Officer, Watervliet Arsenal, Watervliet, New York. ATTN: ORDBF-RR
39 Commander, Army Rocket and Guided Missile Agency, Redstone Arsenal, Ala. ATTN: Tech Library
40 Commanding General, White Sands Proving Ground, Las Cruces, N. Mex. ATTN: ORDBS-OM
41 Commander, Army Ballistic Missile Agency, Redstone Arsenal, Ala. ATTN: ORDAB-HT
42 Commanding General, Ordnance Tank Automotive Command, Detroit Arsenal, Centerline, Mich. ATTN: ORDMC-RO
43 Commanding General, Ordnance Weapons Command, Rock Island, Ill.
44 Commanding General, U.S. Army Electronic Proving Ground, Ft. Huachuca, Ariz. ATTN: Tech. Library
45 Commanding General, USA Combat Surveillance Agency, 1124 N. Highland St., Arlington, Va.
46 Director, Operations Research Office, Johns Hopkins University, 6935 Arlington Rd., Bethesda 14, Md.
47 Commanding General, U. S. ORD Special Weapons-Ammunition Command, Dover, N.J.
48 Commander-in-Chief, U.S. Army Europe, APO 403, New York, N.Y. ATTN: Opns. Div., Weapons Br.

NAVY ACTIVITIES

49 Chief of Naval Operations, D/N, Washington 25, D.C. ATTN: OP-03EG
50 Chief of Naval Operations, D/N, Washington 25, D.C. ATTN: OP-75
51- 52 Chief of Naval Research, D/N, Washington 25, D.C. ATTN: Code 811
53- 54 Chief, Bureau of Aeronautics, D/N, Washington 25, D.C.
55- 59 Chief, Bureau of Aeronautics, D/N, Washington 25, D.C. ATTN: AER-AD-41/20
60 Chief, Bureau of Ordnance, D/N, Washington 25, D.C.
61 Chief, Bureau of Ships, D/N, Washington 25, D.C. ATTN: Code 423
62 Chief, Bureau of Yards and Docks, D/N, Washington 25, D.C. ATTN: D-440
63 Director, U.S. Naval Research Laboratory, Washington 25, D.C. ATTN: Mrs. Katherine H. Case
64- 65 Commander, U.S. Naval Ordnance Laboratory, White Oak, Silver Spring 19, Md.
66 Director, Material Lab. (Code 900), New York Naval Shipyard, Brooklyn 1, N.Y.
67 Commanding Officer and Director, Navy Electronics Laboratory, San Diego 52, Calif.
68 Commanding Officer, U.S. Naval Mine Defense Lab., Panama City, Fla.
69- 70 Commanding Officer, U.S. Naval Radiological Defense Laboratory, San Francisco, Calif. ATTN: Tech. Info. Div.
71- 72 Commanding Officer and Director, U.S. Naval Civil Engineering Laboratory, Port Hueneme, Calif. ATTN: Code L31
73 Commanding Officer, U.S. Naval Schools Command, U.S. Naval Station, Treasure Island, San Francisco, Calif.
74 Superintendent, U.S. Naval Postgraduate School, Monterey, Calif.
75 Commanding Officer, U.S. Fleet Sonar School, U.S. Naval Base, Key West, Fla.
76 Commanding Officer, U.S. Fleet Sonar School, San Diego 47, Calif.
77 Officer-in-Charge, U.S. Naval School, CEC Officers, U.S. Naval Construction Bn. Center, Port Hueneme, Calif.
78 Commanding Officer, Nuclear Weapons Training Center, Atlantic, U.S. Naval Base, Norfolk 11, Va. ATTN: Nuclear Warfare Dept.
79 Commanding Officer, Nuclear Weapons Training Center, Pacific, Naval Station, San Diego, Calif.
80 Commanding Officer, U.S. Naval Damage Control Tng. Center, Naval Base, Philadelphia 12, Pa. ATTN: ABC Defense Course
81 Commanding Officer, Air Development Squadron 5, VX-5, China Lake, Calif.
82 Commanding Officer, Naval Air Material Center, Philadelphia 12, Pa. ATTN: Technical Data Br.
83 Commander, Officer U.S. Naval Air Development Center, Johnsville, Pa. ATTN: NAS, Librarian

84 Commanding Officer, U.S. Naval Medical Research Institute, National Naval Medical Center, Bethesda, Md.
85- 86 Commanding Officer and Director, David W. Taylor Model Basin, Washington 7, D.C. ATTN: Library
87 Commanding Officer and Director, U.S. Naval Engineering Experiment Station, Annapolis, Md.
88 Commander, Norfolk Naval Shipyard, Portsmouth, Va. ATTN: Underwater Explosions Research Division
89 Commandant, U.S. Marine Corps, Washington 25, D.C. ATTN: Code A03H
90 Director, Marine Corps Landing Force, Development Center, MCS, Quantico, Va.
91 Commanding Officer, U.S. Naval CIC School, U.S. Naval Air Station, Glynco, Brunswick, Ga.
92- 99 Chief, Bureau of Naval Weapons, Navy Department, Washington 25, D.C. ATTN: RR12

AIR FORCE ACTIVITIES

100 Assistant for Atomic Energy, HQ, USAF, Washington 25, D.C. ATTN: DCS/O
101 Hq. USAF, ATTN: Operations Analysis Office, Office, Vice Chief of Staff, Washington 25, D. C.
102-103 Air Force Intelligence Center, HQ. USAF, ACS/I (AFCIN-3V1) Washington 25, D.C.
104 Director of Research and Development, DCS/D, HQ. USAF, Washington 25, D.C. ATTN: Guidance and Weapons Div.
105 The Surgeon General, HQ. USAF, Washington 25, D.C. ATTN: Bio.-Def. Pre. Med. Division
106 Commander, Tactical Air Command, Langley AFB, Va. ATTN: Doc. Security Branch
107 Commander, Air Defense Command, Ent AFB, Colorado. ATTN: Assistant for Atomic Energy, ADLDC-A
108 Commander, Hq. Air Research and Development Command, Andrews AFB, Washington 25, D.C. ATTN: RDRWA
109 Commander, Air Force Ballistic Missile Div. HQ. ARDC, Air Force Unit Post Office, Los Angeles 45, Calif. ATTN: WDSOT
110-111 Commander, AF Cambridge Research Center, L. G. Hanscom Field, Bedford, Mass. ATTN: CRUST-2
112-116 Commander, Air Force Special Weapons Center, Kirtland AFB, Albuquerque, N. Mex. ATTN: Tech. Info. & Intel. Div.
117-118 Director, Air University Library, Maxwell AFB, Ala.
119 Commander, Lowry Technical Training Center (TW), Lowry AFB, Denver, Colorado.
120 Commandant, School of Aviation Medicine, USAF, Randolph AFB, Tex. ATTN: Research Secretariat
121 Commander, 1009th Sp. Wpns. Squadron, HQ. USAF, Washington 25, D.C.
122-124 Commander, Wright Air Development Center, Wright-Patterson AFB, Dayton, Ohio. ATTN: WCACT (For WCOSI)
125-126 Director, USAF Project RAND, VIA: USAF Liaison Office, The RAND Corp., 1700 Main St., Santa Monica, Calif.
127 Commander, Rome Air Development Center, ARDC, Griffiss AFB, N.Y. ATTN: Documents Library, RCSSL-1
128 Commander, Air Technical Intelligence Center, USAF, Wright-Patterson AFB, Ohio. ATTN: AFCIN-4Bla, Library
129 Assistant Chief of Staff, Intelligence, HQ. USAFE, APO 633, New York, N.Y. ATTN: Directorate of Air Targets
130 Commander-in-Chief, Pacific Air Forces, APO 953, San Francisco, Calif. ATTN: PFCIB-MB, Base Recovery

OTHER DEPARTMENT OF DEFENSE ACTIVITIES

131 Director of Defense Research and Engineering, Washington 25, D.C. ATTN: Tech. Library
132 Chairman, Armed Services Explosives Safety Board, DOD, Building T-7, Gravelly Point, Washington 25, D.C.
133 Director, Weapons Systems Evaluation Group, Room 1E880, The Pentagon, Washington 25, D.C.
134-137 Chief, Defense Atomic Support Agency, Washington 25, D.C. ATTN: Document Library
138 Commander, Field Command, DASA, Sandia Base, Albuquerque, N. Mex.
139 Commander, Field Command, DASA, Sandia Base, Albuquerque, N. Mex. ATTN: FCTG
140-144 Commander, Field Command, DASA, Sandia Base, Albuquerque, N. Mex. ATTN: FCWT
145 Commander, JTF-7, Arlington Hall Station, Arlington 12, Va.
146 Administrator, National Aeronautics and Space Administration, 1520 "H" St., N.W., Washington 25, D.C. ATTN: Mr. R. V. Rhode
147 Commander-in-Chief, Strategic Air Command, Offutt AFB, Neb. ATTN: OAMS
148 Commandant, US Coast Guard, 1300 E. St., N.W., Washington 25, D.C. ATTN: (OIN)
149 Commander-in-Chief, EUCOM, APO 128, New York, N.Y.

ATOMIC ENERGY COMMISSION ACTIVITIES

150-152 U.S. Atomic Energy Commission, Technical Library, Washington 25, D.C. ATTN: For RSA
153-154 Los Alamos Scientific Laboratory, Report Library, P.O. Box 1663, Los Alamos, N. Mex. ATTN: Helen Redman
155-159 Sandia Corporation, Classified Document Division, Sandia Base, Albuquerque, N. Mex. ATTN: H. J. Smyth, Jr.
160-162 University of California Lawrence Radiation Laboratory, P.O. Box 808, Livermore, Calif. ATTN: Clovis G. Craig
163 Essential Operating Records, Division of Information Services for Storage at ERC-H. ATTN: John H. Hane, Chief, Headquarters Records and Mail Service Branch, U.S. AEC, Washington 25, D.C.
164 Weapon Data Section, Technical Information Service Extension, Oak Ridge, Tenn.
165-195 Technical Information Service Extension, Oak Ridge, Tenn. (Surplus)

**Defense Threat Reduction Agency**
8725 John J Kingman Road MS 6201
Ft Belvoir, VA 22060-6201

TDANP/TRC

March 2, 2001

MEMORANDUM TO THE DEFENSE TECHNICAL INFORMATION CENTER
ATTN: OCQ

SUBJECT: DOCUMENT UPDATES

The Defense Threat Reduction Agency Security Office has performed a classification/distribution statement review of the following documents. The documents should be changed to read as follows:

WT-1628, AD-357954, OPERATION HARDTACK, PROJECT 3.4, LOADING AND RESPONSE OF SURFACE-SHIP HULL STRUCTURES FROM UNDERWATER BURSTS, UNCLASSIFIED, DISTRIUBTION STATEMENT A.

WT-1301, AD-341065, OPERATION REDWING, PROJECT 1.1, GROUND SURFACE AIR BLAST PRESSURE VERSUS DISTANCE, UNCLASSIFIED, DISTRIBUTION STATEMENT A.

WT-748, OPERATION UPSHOT KNOTHOLE, PROJECT 5.1, ATOMIC WEAPON EFFECTS ON AD TYPE AIRCRAFT IN FLIGHT. UNCLASSIFIED, DISTRIBUTION STATEMENT A. FORWARD TO YOU FOR YOUR COLLECTION

WT-9001-SAN, GENERAL REPORT ON WEAPONS TESTS, UNCLASSIFIED, DISTRIBUTION STATEMENT A. FORWARD TO YOU FOR YOUR COLLECTION.

POR-2260-SAN, OPERATION SUN BEAM, SHOTS LITTLE FELLER 1 AND 2, PROJECT 1.1, AIRBLAST PHENOMENA FROM SMALL YIELD DEVICES, SANITIZED VERSION. UNCLASSIFIED, DISTRIBUTION STATEMENT A. FORWARD TO YOU FOR YOUR COLLECTION.

If you have any questions, please call me at 703-325-1034.

Ardith Jarrett

ARDITH JARRETT
Chief, Technical Resource Center